AD-A102 622 IIT RESEARCH INST ANNAPOLIS MD F/G 20/14
APACK, A COMBINED ANTENNA AND PROPAGATION MODEL.(U)
JUL 81 S CHANG, H C MADDOCKS F19628-80-C-0042
UNCLASSIFIED ESD-TR-80-102 NL

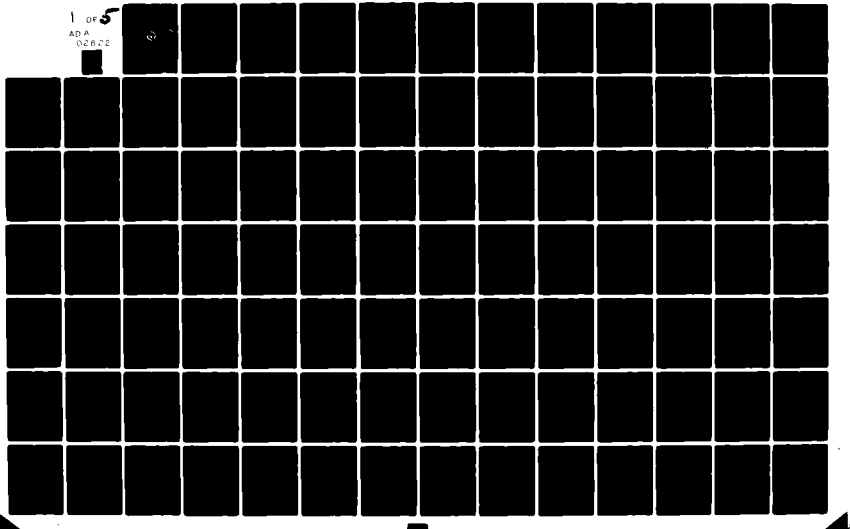

"SD-TR-80-102

APACK, A COMBINED ANTENNA AND PROPAGATION MODEL

Sooyoung Chang, Ph.D.
and
Hugh C. Maddocks, Ph.D.
of
IIT Research Institute
Under Contract to
DEPARTMENT OF DEFENSE
Electromagnetic Compatibility Analysis Center
Annapolis, Maryland 21402

JULY 1981

FINAL REPORT

Prepared for

Electromagnetic Compatibility Analysis Center
Annapolis, MD 21402

ESD-TR-80-102

This report was prepared by the IIT Research Institute under Contract F-19628-80-C-0042 with the Electronic Systems Division of the Air Force Systems Command in support of the DoD Electromagnetic Compatibility Analysis Center, Annapolis, Maryland.

This report has been reviewed and cleared for open publication and/or public release by the appropriate Office of Information [OI] in accordance with AFR 190-17 and DoDD 5230.9. There is no objection to unlimited distribution of this report to the public at large, or by DDC to the National Technical Information Service [NTIS].

Reviewed by:

William D. Stuart

WILLIAM D. STUART
Project Manager, IITRI

James H. Cook

JAMES H. COOK
Assistant Director
Capability Development Department
Engineering Resources Division

Approved by:

Paul T. McEachern

PAUL T. McEACHERN
Colonel, USAF
Director

A. M. Messer

A. M. MESSER
Chief, Plans & Resource
Management Office

UNCLASSIFIED

SECURITY CLASSIFICATION OF THIS PAGE (When Data Entered)

REPORT DOCUMENTATION PAGE	READ INSTRUCTIONS BEFORE COMPLETING FORM
1. REPORT NUMBER: ESD-TR-80-102 ✓	2. GOVT ACCESSION NO.: AD-A102 622
	3. RECIPIENT'S CATALOG NUMBER:
4. TITLE (and Subtitle): APACK, A COMBINED ANTENNA AND PROPAGATION MODEL.	5. TYPE OF REPORT & PERIOD COVERED: FINAL
	6. PERFORMING ORG. REPORT NUMBER:
7. AUTHOR(s): Sooyoung Chang, Ph.D. Hugh C. Maddocks, Ph.D.	8. CONTRACT OR GRANT NUMBER(s): CDRL # 10S F-19628-80-C-0042
9. PERFORMING ORGANIZATION NAME AND ADDRESS: DoD Electromagnetic Compatibility Analysis Center, North Severn, Annapolis, MD 21402	10. PROGRAM ELEMENT, PROJECT, TASK AREA & WORK UNIT NUMBERS:
11. CONTROLLING OFFICE NAME AND ADDRESS: Electromagnetic Compatibility Analysis Center Annapolis, MD 21402	12. REPORT DATE: July 1981
	13. NUMBER OF PAGES: 296
14. MONITORING AGENCY NAME & ADDRESS (if different from Controlling Office)	15. SECURITY CLASS. (of this report): UNCLASSIFIED
	15a. DECLASSIFICATION/DOWNGRADING SCHEDULE:

16. DISTRIBUTION STATEMENT (of this Report)

UNLIMITED

DISTRIBUTION STATEMENT A
Approved for public release;
Distribution Unlimited

17. DISTRIBUTION STATEMENT (of the abstract entered in Block 20, if different from Report)

18. SUPPLEMENTARY NOTES

19. KEY WORDS (Continue on reverse side if necessary and identify by block number)

LINEAR ANTENNAS	ANTENNA PATTERNS	GROUND SCREENS
ANTENNA GAIN	TRANSMISSION LOSS	DIPOLE
DIRECTIVE GAIN	BASIC TRANSMISSION LOSS	
POWER GAIN	GROUND EFFECTS	
RADIATION EFFICIENCY	LOSSY GROUND	

20. ABSTRACT (Continue on reverse side if necessary and identify by block number)

Equations for predicting the electric far-field strengths, directive gains, power gains, and transmission loss for 16 types of linear antennas are presented along with an interview of the methods used to develop the equations. The effects of the radio surface wave including diffraction beyond the horizon as well as the direct and ground reflected waves are included. The equations were programmed in a set of computer subroutines termed the Accessible Antenna Package (APACK). These subroutines may be

DD FORM 1 JAN 73 1473 EDITION OF 1 NOV 65 IS OBSOLETE

UNCLASSIFIED

SECURITY CLASSIFICATION OF THIS PAGE (When Data Entered)

175300

D

19. Continued

MONOPOLE	DOUBLE RHOMBOID
INVERTED-L	ANTENNA FIELD STRENGTH
LONG-WIRE	HF ANTENNAS
SLOPING-V	VHF ANTENNAS
RHOMBIC	UHF ANTENNAS
HALF-RHOMBIC	GROUND WAVE
YAGI	SKY WAVE
YAGI-UDA ARRAY	HFMUFES-4
LOG-PERIODIC	IONCAP
LOG-PERIODIC DIPOLE ARRAY	NEC
CURTAIN ARRAY	NEC-2

20. Continued

called by other programs in order to compute antenna and propagation effects at frequencies between 150 kHz and 500 MHz over lossy earth.

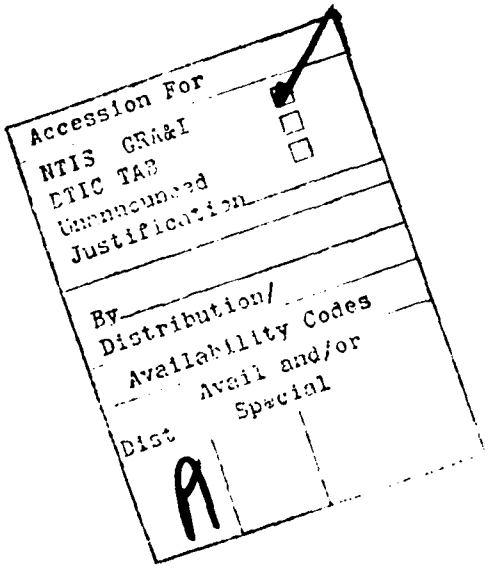

EXECUTIVE SUMMARY

The Accessible Antenna Package (APACK) is a versatile, automated, combined-antenna-and-propagation set of computer subroutines for predicting electric far-field strength, directive gains, power gains, and transmission loss for 16 types of linear antennas that are typically used at frequencies between 150 kHz and 500 MHz. The types of antennas considered are: horizontal dipole, vertical monopole, vertical monopole with radial-wire ground screen, elevated vertical dipole, inverted-L, arbitrarily tilted dipole, sloping long-wire, terminated sloping V, terminated sloping rhombic, terminated horizontal rhombic, side-loaded vertical half-rhombic, horizontal Yagi-Uda array, horizontally polarized log-periodic dipole array, vertically polarized log-periodic dipole array, curtain array, and sloping double rhomboid.

Expressions for fields from these antennas for direct and ground-reflected waves are available in the literature and one form is employed in the ECAC computerized SKYWAVE model. These expressions do not include radio surface wave terms and, therefore, are not applicable to ground-wave analyses. Expressions for the surface waves were developed, combined with the existing expressions, and the combinations included in APACK. Previously available ground-wave propagation models implicitly assume that the antenna is an infinitesimal point source, i.e., a Hertzian dipole, whereas APACK explicitly accounts for the antenna structure.

APACK accounts for the effects of lossy ground under the antennas in three far-field regions: planar earth within the radio horizon (for low antennas), spherical earth within the radio horizon (for high antennas), and the diffraction region beyond the radio horizon. Automated switching criteria are used to determine which of the three regions is appropriate for the analysis.

The current distribution for a resonant antenna is assumed to be sinusoidal, and the current distribution for a traveling-wave antenna is

assumed to be exponential. Comparisons of APACK predictions with various types of data are presented indicating the versatility and reasonableness of APACK. In particular, for an electrical large, sloping, double rhomboid, APACK predicts behavior that is similar to that predicted by the Numerical Electromagnetic Code (NEC). However, one significant advantage of APACK is that it requires only 1/1000th of the computer run time of the NEC analysis. It is found that APACK is applicable except when the antenna employs resonant elements of length very close to integral multiples of a wavelength since the sinusoidal current distribution assumption is not appropriate in this case.

PREFACE

The Electromagentic Compatibility Analysis Center (ECAC) is a Department of Defense facility, established to provide advice and assistance on electromagnetic compatibility matters to the Secretary of Defense, the Joint Chiefs of Staff, the military departments and other DoD components. The center, located at North Severn, Annapolis, Maryland 21402, is under the policy control of the Assistant Secretary of Defense for Communication, Command, Control, and Intelligence and the Chairman, Joint Chiefs of Staff, or their designees, who jointly provide policy guidance, assign projects, and establish priorities. ECAC functions under the executive direction of the Secretary of the Air Force and the management and technical direction of the Center are provided by military and civil service personnel. The technical support function is provided through an Air Force-sponsored contract with the IIT Research Institute (IITRI).

To the extent possible, all abbreviations and symbols used in this report are taken from American National Standard ANSI Y10.19 (1969) "Letter Symbols for Units Used in Science and Technology" issued by the American National Standards Institute, Inc.

Users of this report are invited to submit comments that would be useful in revising or adding to this material to the Director, ECAC, North Severn, Annapolis, Maryland 21402, Attention: XM.

TABLE OF CONTENTS

TABLE OF CONTENTS (Continued)

TABLE OF CONTENTS (Continued)

TABLE OF CONTENTS (Continued)

LIST OF ILLUSTRATIONS

Figure

TABLE OF CONTENTS (Continued)

LIST OF ILLUSTRATIONS (Continued)

TABLE OF CONTENTS (Continued)

LIST OF ILLUSTRATIONS (Continued)

TABLE OF CONTENTS (Continued)

LIST OF ILLUSTRATIONS (Continued)

TABLE OF CONTENTS (Continued)

LIST OF ILLUSTRATIONS (Continued)

LIST OF TABLES

TABLE OF CONTENTS (Continued)

LIST OF APPENDIXES

SECTION 1
INTRODUCTION

BACKGROUND

The Electromagnetic Compatibility Analysis Center (ECAC) is a Department of Defense facility, established to provide advice, assistance, and analyses on electromagnetic compatibility (EMC) matters. Many analyses have been and are being performed in the frequency region between 150 kHz and 500 MHz for both desired and interfering signals that propagate by ground wave as well as sky wave.

The antenna-gain models currently used by ECAC for ionospheric sky-wave analyses are those developed by the Institute for Telecommunication Sciences (ITS) as part of a model for predicting ionospheric propagation (HFMUFES-4).[1] Because the antenna-gain models developed by ITS account for the contributions of the direct and ground-reflected waves of linear antennas mounted over lossy ground but do not consider the contribution of the surface wave, the models are not suitable for use in ground-wave analyses.

For sky-wave calculations, it is proper to neglect the contribution of the surface wave. Also, it is true that the contribution of the surface wave is small for the case of a horizontally polarized wave. However, the contribution of the surface wave is significant for ground-wave calculations involving vertically polarized waves.

The surface wave is guided along the surface of the earth, much as an electromagnetic wave is guided by a transmission line. Since the surface wave

---

[1] Barghausen, A.F., Finney, J.W., Proctor, L.L., and Schultz, L.D., Predicting Long-Term Operational Parameters of High-Frequency SKYWAVE Telecommunication Systems, ESSA Technical Report ERL 110-ITS-78, Institute for Telecommunication Science, Boulder, CO, May 1969.

is affected by losses in the earth, its attenuation is directly affected by the permittivity and conductivity of the earth.

When both the transmitting and receiving antennas are located at the surface of the earth, the direct and ground-reflected waves cancel each other. In this case, the transmitted wave reaches the receiving antenna entirely by means of the surface wave, assuming that there is no sky-wave or tropospheric-scatter propagation.

ECAC has an operational method-of-moments computer program, the Numerical Electromagnetic Code (NEC),[2] that predicts the gain pattern of an antenna in the presence of a lossy ground and includes the surface wave term. NEC requires as input detailed description of the antenna dimensions and location and sizes of conducting obstacles (such as guy wires). In addition, NEC requires considerable computer time to make its predictions.

Other models in use at ECAC[3,4] predict basic transmission loss without calculating field strength for a Hertzian dipole but do not account for the actual antenna configuration. Therefore, an automated model was needed to calculate the gain and field strengths for commonly used linear antennas. This model should be capable of predicting rapidly directive and power gains suitable for both ground-wave and sky-wave analyses in addition to predicting ground-wave transmission loss in the 150 kHz to 500 MHz region. The model was

---

[2] Burke, G. and Poggio, A., Numerical Electromagnetic Code (NEC) -- Method of Moments, Part I: Program Description - Theory, Part II: Program Description - Code, and Part III: User's Guide, Technical Document 116, Naval Ocean Systems Center, San Diego, CA, 18 July 1977 (revised 2 January 1980).

[3] Meidenbauer, R., Chang, S., and Duncan, M., A Status Report on the Integrated Propagation System (IPS), ECAC-TN-78-023, Electromagnetic Compatibility Analysis Center, Annapolis, MD, October 1978.

[4] Maiuzzo, M.A. and Frazier, W.E., A Theoretical Ground Wave Propagation Model - Nλ Model, ESD-TR-68-315, Electromagnetic Compatibility Analysis Center, Annapolis, MD, December 1968.

designed to be modular in the sense that it would be a collection of subroutines to be called by the various other ECAC models as needed. This collection of subroutines is termed APACK.

OBJECTIVES

The objectives of this report are:

1. To document the equations that comprise APACK and provide an overview of the methods used to develop the equations
2. To compare APACK predictions for antenna gain and transmission loss with other available data.

APPROACH

The Hertzian Dipole

The Hertzian dipole is used as a building block in the analysis of linear antennas, because the fields of linear antennas are given in terms of integrals of the current distribution. Since the current distribution of the Hertzian dipole is assumed to be uniform, the integrals describing the fields of a Hertzian dipole are simplified. Actual linear antennas with nonuniform current distributions can then be simplified for the purposes of analysis by considering them to be comprised of a superposition of many Hertzian dipoles, each with a uniform current distribution.

The equations of a Hertzian dipole over lossy planar earth are well known.[5,6] The actual antenna structure was considered as a superposition of Hertzian dipoles giving a sinusoidal current distribution for the antenna.

---

[5] Banos, A., Jr., Dipole Radiation in the Presence of a Conducting Half-Space, Pergamon Press, Oxford, England, 1966.

[6] Weeks, W.L., Antenna Engineering, McGraw-Hill, New York, NY, 1968.

Appropriate formulations were applied to extend the equations for the fields over planar earth to spherical earth within the radio horizon and to the diffraction region beyond the radio horizon.

Even the analysis of the fields of a Hertzian dipole is not simple when it is located over lossy planar earth.[7,8,9] The analysis herein is based on that of Norton.[10] Norton provides practical formulas to calculate the field intensity of electric and magnetic dipoles over lossy ground. Norton also separated his solutions into a space wave and a surface wave. It has been shown that Norton's formulation gives close agreement with the numerical solution of Sommerfeld's equations.[11]

Linear Antennas Over Lossy Planar Earth

APACK predicts basic transmission loss from calculated values of electric field strength. The APACK field strengths account for the actual antenna structure and include the effects of the contributions of the direct, ground-reflected, and surface waves.

---

[7] Sommerfeld, A., "Uber die Ausbreitung der Wellen in der drahtlosen Telegraphic," Ann. Physik, Vol. 28, 1909, pp. 665-736.

[8] Sommerfeld, A., "Uber die Ausbreitung der Wellen in der drahtlosen Telegraphic," Ann. Physik, Vol. 81, 1926, pp. 1135-1153.

[9] Sommerfeld, A., Partial Differential Equations, Academic Press, New York, NY, 1949.

[10] Norton, K.A., "The Propagation of Radio Waves Over the Surface of the Earth and in the Upper Atmosphere": Part I, Proc. IRE, Vol. 24, October 1936, pp. 1369-1389; Part II, Proc. IRE, Vol. 25, September 1937, pp. 1203-1236.

[11] Kuebler, W. and Snyder, S., The Sommerfeld Integral, Its Computer Evaluation and Application to Near Field Problems, ECAC-TN-75-002, Electromagnetic Compatibility Analysis Center, Annapolis, MD, February 1975.

The equations developed for the contributions of the direct and ground-reflected waves from the 16 linear antennas listed in TABLE 1 have been derived previously by others. Laitenen derived formulas for the fields of linear antennas assuming a sinusoidal current distribution.[12] He included only the direct and ground-reflected waves in his calculation. Ma and Walters[13] derived similar formulas, and Ma later extended the results using a more accurate three-term current distribution.[14] However, Laitenen, Ma, and Walters (see References 12, 13, and 14) do not consider the surface wave.

The surface wave formulas used in APACK were formulated in terms of the fields of a current element over lossy planar earth employing Norton's equations. The expressions for directive gain and power gain were derived from the expressions for the far fields.

Thus, the initial steps in the development of the APACK equations were the formulation of the expressions for directive and power gains in terms of the far fields and the formulation of the expressions for the far fields of a current element over lossy planar earth. These formulations are presented in Section 2.

Assumed Antenna Current Distribution

The determination of the fields of the current element requires a knowledge of the current distribution on the element which, in turn, requires a knowledge of the current distribution on the actual antenna structure. The

---

[12] Laitenen, P., Linear Communication Antennas, Technical Report No. 7, U.S. Army Signal Radio Propagation Agency, Fort Monmouth, NJ, 1959.

[13] Ma, M.T. and Walters, L.C., Power Gains for Antennas Over Lossy Plane Ground, Technical Report ERL 104-ITS 74, Institute for Telecommunication Sciences, Boulder, CO, 1969.

[14] Ma, M.T., Theory and Application of Antenna Arrays, Wiley Interscience, New York, NY, 1974.

equations derived for APACK assume that the current distribution for a resonant antenna is sinusoidal and that the current distribution for a traveling-wave antenna is exponential.

TABLE 1

TYPES OF LINEAR ANTENNAS PRESENTLY INCLUDED IN APACK

1.	Horizontal dipole
2.	Vertical monopole
3.	Vertical monopole with radial-wire ground screen
4.	Elevated vertical dipole
5.	Inverted-L
6.	Arbitrarily tilted dipole
7.	Sloping long-wire
8.	Terminated sloping-V
9.	Terminated sloping rhombic
10.	Terminated horizontal rhombic
11.	Side-loaded vertical half-rhombic
12.	Horizontal Yagi-Uda array
13.	Horizontally polarized log-periodic dipole array
14.	Vertically polarized log-periodic dipole array
15.	Curtain array
16.	Sloping double rhomboid

Sinusoidal current distribution was first treated by Pocklington.[15] However, it is well known that sinusoidal current distribution is only an approximation. Schelkunoff and Friis[16] made the following statements on the relationship between the current distribution and the radiation pattern as well as the radiated power.

---

[15]Pocklington, H.E., "Electrical Oscillations in Wires," Comb. Phil. Soc. Proc., 25 October 1897, pp. 324-332.

[16]Schelkunoff, S.A. and Friis, H.T., Antennas, Theory and Practice, John Wiley and Sons, New York, NY, 1952.

> The radiation pattern and power radiated by the antenna are insensitive to errors in the assumed form of current distribution. The antenna current must be known more accurately if we are interested in the minima in the radiation pattern; but it need not be known accurately otherwise. . . .

A primary consideration in the design of APACK was that the resulting model execute in minimal time for each required value of gain or transmission loss. This consideration is due to the fact that hundreds or thousands of values of gain may be necessary for an analysis of one circuit throughout the HF band or thousands of values of transmission loss may be required for analyzing a ground-wave circuit over a wide range of frequencies. The need for large numbers of predictions involving many frequencies precludes the use of method-of-moments models that use matrix techniques to compute the antenna current distribution at each frequency.

Also, because it was important that the model execute in minimal time, a sinusoidal current distribution was assumed for resonant antennas. This distribution is not as accurate or elegant as the three-term current distribution used by Ma (see Reference 14), but it does provide reasonable results except when the lengths of the resonant elements are very close to integral multiples of a wavelength.

The restrictions associated with the sinusoidal current distribution for resonant antennas do not arise with traveling-wave (i.e., nonresonant) antennas when an exponential current distribution is assumed. The use of the exponential current distribution was, therefore, believed to be reasonable without restrictions.

Extension of the Formulation to Spherical Earth

When the antenna is located close to the surface of the earth, the earth can be considered as planar. However, when the feed point of the antenna is located several wavelengths or more above the surface, the earth can no longer be considered as planar for calculations within the radio horizon.

Therefore, the formulation of the fields of a current element over lossy planar earth (presented in Section 2) was extended to account for the curvature of the earth. Although the Bremmer formulation[17] can be used within the radio horizon, many terms of the series for the fields are required to make the series converge in this region.

Norton[18] provided approximate formulas that account for the curvature without resorting to the rigorous Bremmer techniques and are computationally efficient. Norton's formulas were thus used to extend the APACK equations to account for the curvature of the earth within the radio horizon. This extension is presented in Section 3.

Extension of the Formulation to the Diffraction Region

In the diffraction region beyond the radio horizon, the basic formulation presented in Section 2 for the fields of a current element over lossy planar earth was modified by making use of the radiation vector and the Bremmer formulation (see Reference 17). The radiation vector is similar to the formulation presented in Section 2 and accounts for the geometry of the antenna structure. The Bremmer secondary factor accounts for the geometry of the path.

The resulting electric far-field components, presented in Section 4, are in terms of the product of the radiation vector and the Bremmer secondary factor. The advantage of this formulation for APACK calculations in the diffraction region was that the radiation vector and Bremmer secondary factor could be calculated independently, and thus the two routines could be modular.

---

[17] Bremmer, H., Terrestrial Radio Waves, Elsevier Publishing Co., New York, NY, 1949.

[18] Norton, K.A., "The Calculation of Ground Wave Field Intensity Over a Finitely Conducting Spherical Earth," Proc. IRE, Vol. 29, No. 12, December 1941, pp. 623-639.

Resulting Formulas for Field Strength and Gain

The formulation presented in Section 2 with the extensions presented in Sections 3 and 4 was used to derive equations for the electric far-field components, directive gain, and power gain for the 16 types of linear antennas considered (see TABLE 1). Sinusoidal current distribution was assumed for resonant antennas, and exponential current distribution was assumed for traveling-wave (i.e., nonresonant) antennas.

To simplify the use of this report for reference purposes, key equations for determining the field strengths and directive gains of the antennas are listed in TABLE 2 in Section 5. TABLE 2 refers to appropriate equations in APPENDIXES A and D in which the mathematical details for each antenna are provided. In addition to TABLE 2, Section 5 includes a figure showing the geometry of each antenna and a brief introduction to each antenna for the uninitiated reader.

Transmission Loss

Because the basic equations derived for APACK are for the electric far fields of the antennas, calculations of ground-wave transmission loss are also straightforward. The general equations presented in Section 6 were used to derive the transmission loss relative to free-space loss in terms of the power gains of the antennas and the ratio of the actual disturbed field at the observation point to the free-space field at the observation point.

Automated criteria, also presented in Section 6, were used to determine in which of the three regions the far-field observation point lies: planar earth (for low antennas), spherical earth (for high antennas), or the diffraction region beyond the radio horizon. These criteria are based simply on the path length, operating frequency, and heights of the transmitting and receiving antenna feed points above ground. The criteria were also used in conjunction with the equations listed in TABLE 2 of Section 5 so that

calculations of field strength and gain, in addition to transmission loss, would automatically account for the location of the observation point.

Comparisons Between APACK Predictions and Other Data

Gains predicted by APACK were compared with gains obtained from other sources. These comparisons, presented in Section 7, include an example of each of the 16 types of antennas and various ground constants (i.e., conductivities and permittivities). While the comparisons are not exhaustive, they do indicate that APACK gain predictions are reasonable.

Transmission-loss predictions made by APACK were compared with transmission-loss predictions obtained from other sources and are presented in Section 8. Various ground constants, typical of soil and sea water, were used to demonstrate the versatility of the model.

SECTION 2
GENERAL CONSIDERATIONS FOR CALCULATING GAIN AND FIELD INTENSITIES OF A LINEAR ANTENNA

INTRODUCTORY REMARKS

The directive and power gains calculated by APACK use the definitions of gains in terms of the electric far fields of the antenna being considered. Electric far field intensities are calculated from those of a current element located above planar earth. Fresnel reflection coefficients are used to account for the presence of ground both in formulating the electric far fields and in formulating the radiation resistance.

This section presents general expressions for calculating directive and power gain. It also presents the expressions for the electric far fields of a current element located above planar earth. The formulation for the current element is extended in Section 3 to include the effects of spherical earth within the radio horizon by using the divergence factor with the Fresnel reflection coefficients. The radiation vector and Bremmer secondary factor are used in Section 4 to include the diffraction region beyond the radio horizon.

GAIN CALCULATIONS

The directive gain (g_d) of an antenna in a given direction is defined as the ratio of the radiation intensity in that direction to the average power radiated per unit solid angle. Thus:

$$g_d(\theta,\phi) = \frac{\Phi(\theta,\phi)}{\Phi_{av}} = \frac{\Phi(\theta,\phi)}{\frac{W_r}{4\pi}} = \frac{4\pi\,\Phi(\theta,\phi)}{W_r} \qquad (2\text{-}1)$$

where

$g_d(\theta,\phi)$ = directive gain in the direction specified by the spherical-coordinate angles θ and ϕ (numerical ratio)

$\Phi(\theta,\phi)$ = radiation intensity in the direction specified by the spherical-coordinate angles θ and ϕ, in watts/steradian

Φ_{av} = average power radiated per unit solid angle, in watts/steradian

W_r = total power radiated by the antenna, in watts.

The radiation intensity in a given direction can also be defined in terms of electric field intensity by:

$$\Phi(\theta,\phi) = \frac{r^2|\bar{E}(\theta,\phi)|^2}{120\pi} \qquad (2\text{-}2)$$

where

r = spherical-coordinate radial distance, in meters

$\bar{E}(\theta,\phi)$ = electric far field in the direction specified by the spherical-coordinate angles θ and ϕ, in volts/meter.

From Equations 2-1 and 2-2:

$$g_d(\theta,\phi) = \frac{r^2|\bar{E}(\theta,\phi)|^2}{30\ W_r} = \frac{r^2|\bar{E}(\theta,\phi)|^2}{30 I_b^2\ R_{rb}} \qquad (2\text{-}3)$$

where

I_b = current at the antenna feed point (base), in amperes

R_{rb} = radiation resistance referred to the antenna feed point (base), in ohms.

The maximum value of the directive gain is called the directivity. The directivity is sometimes loosely referred to as the "gain," but this usage is depracated.

The power gain (g_ρ) of an antenna in a given direction is defined by:

$$g_\rho(\theta,\phi) = \frac{4\pi\ \Phi(\theta,\phi)}{W_{in}} \qquad (2\text{-}4)$$

where

$g_\rho(\xi,\phi)$ = power gain in the direction specified by the spherical-coordinate angles θ and ϕ (numerical ratio)

W_{in} = power input to the antenna, in watts.

The radiation efficiency (η) is defined by:

$$\eta = \frac{W_r}{W_{in}} \qquad (2\text{-}5)$$

(η is a numerical ratio, $0 \leq \eta \leq 1$.)

From Equations 2-1 and 2-5:

$$\eta\, g_d(\theta,\phi) = \frac{4\pi\, \Phi(\theta,\phi)}{W_{in}} = g_\rho(\theta,\phi) \qquad (2\text{-}6)$$

Since $\eta \leq 1$, $g_\rho \leq g_d$, and the difference between g_ρ and g_d can be significant. The radiation efficiency can also be expressed as:

$$\eta = \frac{R_{rb}}{R_{rb} + R_{loss}} \qquad (2\text{-}7)$$

where

R_{loss} = losses associated with the antenna, in ohms.

From Equations 2-3, 2-6, and 2-7:

$$g_\rho(\theta,\phi) = \frac{r^2\, |\bar{E}(\theta,\phi)|^2}{30\, I_b^2\, (R_{rb} + R_{loss})} \qquad (2\text{-}8)$$

In spherical coordinates r, θ, ϕ:

$$|\bar{E}(\theta,\phi)|^2 = |E_\theta|^2 + |E_\phi|^2 \qquad (2\text{-}9)$$

The power gain in decibels (G_p) is given by:

$$G_p(\theta,\phi) = 10 \log_{10} g_\rho(\theta,\phi) \qquad (2\text{-}10)$$

FIELD-INTENSITY CALCULATIONS

Consider a linear antenna element as shown in Figure 1 with the XY-plane being lossy planar earth. The electric-field components produced by the antenna at a point P (r,θ,ϕ), including the contributions of the direct, ground-reflected, and surface waves are given in spherical coordinates (r,θ,ϕ) by:

$$E_\theta = j30k \frac{e^{-jkr}}{r} \Big[\cos\alpha' \cos(\phi - \phi') \cos\theta \times \int_0^\ell I(s)\, e^{jks\cos\psi} \left(1 - R_v e^{-jskH_s\cos\theta} + \text{surface wave terms}\right) ds - \sin\alpha' \sin\theta \times \int_0^\ell I(s)\, e^{jks\cos\psi} \left(1 + R_v e^{-j2kH_s\cos\theta} + \text{surface-wave terms}\right) ds\Big] \quad (2\text{-}11)$$

$$E_\phi = -j30k \frac{e^{-jkr}}{r} \cos\alpha' \sin(\phi - \phi') \int_0^\ell I(s)\, e^{jks\cos\psi} \times \left(1 + R_h e^{-j2kH_s\cos\theta} + \text{surface-wave terms}\right) ds \quad (2\text{-}12)$$

where

$E_{\theta,\phi}$ = θ-, ϕ- component of the electric far field, in volts/meter

$k = 2\pi/\lambda$

λ = wavelength, in meters

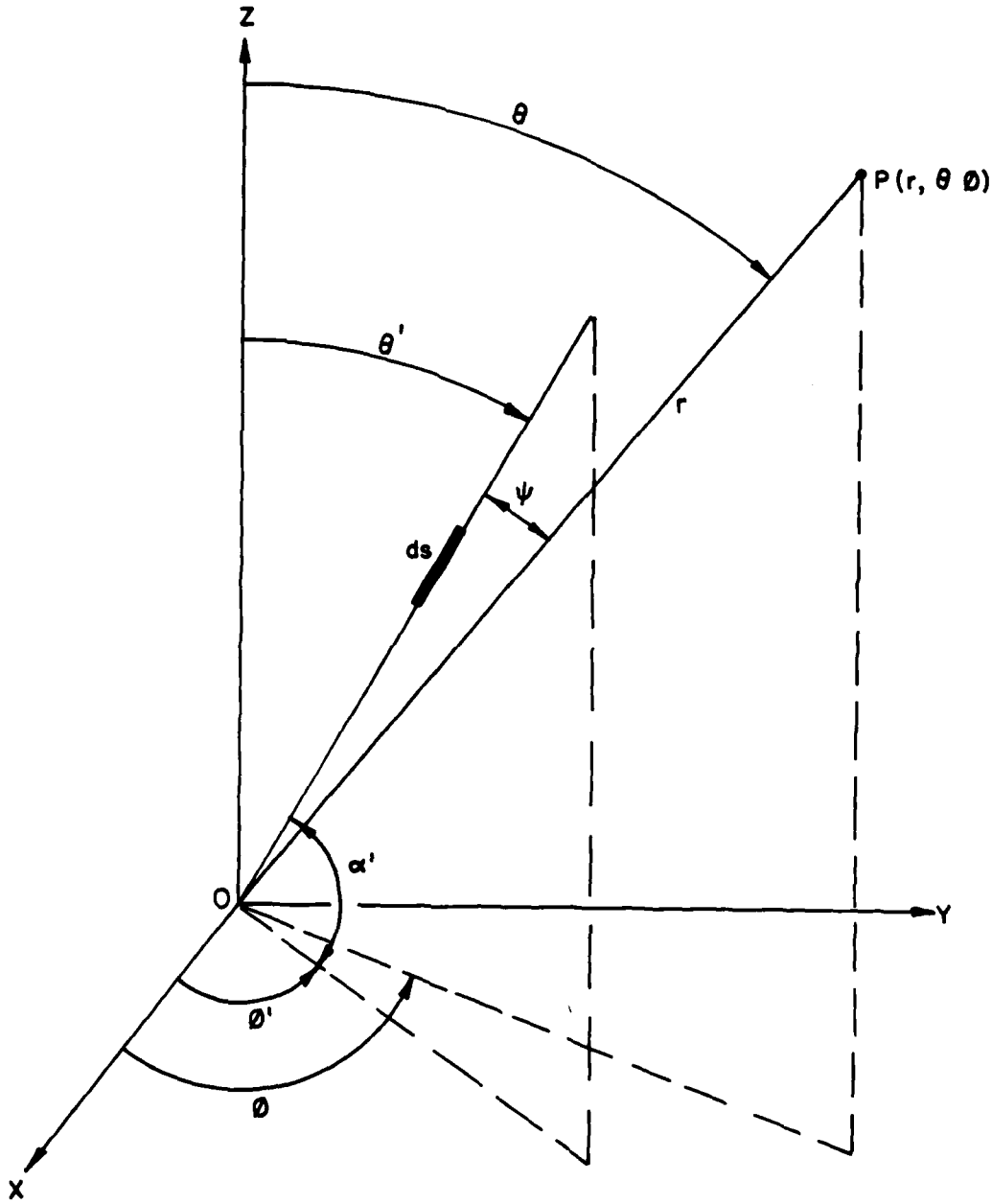

Figure 1. Arbitrarily oriented current element over lossy planar earth.

r = radial distance from the origin to the far-field point $P(r,\theta,\phi)$, in meters

α' = angle between the antenna element and its projection on the XY-plane, in degrees

ϕ' = angle between the X-axis and the projection of the antenna element on the XY-plane, in degrees

ℓ = length of the antenna element, in meters

$I(s)$ = linear current density for the antenna element, in amperes/meters

s = linear coordinate coinciding with the antenna element, in meters

ψ = angle between the antenna element and the line from the origin to the far-field point $P(r,\theta,\phi)$, in degrees

R_v = Fresnel reflection coefficient for the vertically polarized component, defined below

H_s = height of the current element at ds above the XY-plane, in meters

d_s = differential element of length along the antenna element, in meters

R_h = Fresnel reflection coefficient for the horizontally polarized component, defined below

θ' = angle between the Z-axis and the antenna element, in degrees.

The angle ψ can be calculated from:

$$\cos\psi = \cos\theta \cos\theta' + \sin\theta \sin\theta' \cos(\phi-\theta') \qquad (2\text{-}13)$$

where the primed coordinates refer to locations on the antenna element and unprimed coordinates refer to the far-field observation point $P(r,\theta,\phi)$.

The Fresnel reflection coefficients for the vertically and horizontally polarized components of the electric field (R_v and R_h, respectively) are given by:

$$R_v = \frac{n^2 \cos\theta_r - \sqrt{n^2 - \sin^2\theta_r}}{n^2 \cos\theta_r + \sqrt{n^2 - \sin^2\theta_r}} \qquad (2\text{-}14)$$

and

$$R_h = \frac{\cos\theta_r - \sqrt{n^2 - \sin^2\theta_r}}{\cos\theta_r + \sqrt{n^2 - \sin^2\theta_r}} \qquad (2\text{-}15)$$

where

n = refractive index of the medium under the antenna, defined below

θ_r = angle between the line from the image of the current element at ds to the far-field point $P(r,\theta,\phi)$ and the Z-axis, in degrees.

The refractive index of the medium under the antenna (n) is:

$$n^2 = \varepsilon_r - j\frac{18000\sigma}{f_{MHz}} \qquad (2\text{-}16)$$

where

ε_r = relative dielectric constant of the medium (dimensionless)

σ = conductivity of the medium, in mhos/meter

f_{MHz} = frequency, in MHz.

The input resistance of an antenna (R_{in}), including the effects of lossy ground, is calculated from:

$$R_{in} = R_{11} + R_e(CZ_m) \qquad (2\text{-}17)$$

where

R_{in} = input resistance, in ohms

R_{11} = real part of the antenna self-impedance, in ohms

Z_m = mutual impedance between the antenna and its image in perfectly conducting ground, in ohms

C = factor to account for lossy ground, as given below.

$$c = e^{-j\alpha'} (R_h' \cos \alpha' + j R_v' \sin \alpha') \quad (2\text{-}18)$$

R_h' is obtained by evaluating Equation 2-15 at $\theta_r = 0°$ to give:

$$R_h' = \frac{1-n}{1+n} \quad (2\text{-}19)$$

R_v' is obtained by evaluating Equation 2-14 at $\theta_r = 0°$ to give:

$$R_v' = \frac{n-1}{n+1} \quad (2\text{-}20)$$

VARIATION OF ANTENNA GAIN AS A FUNCTION OF FAR-FIELD DISTANCE

The definitions of directive gain and power gain of an antenna are the result of considering the properties of an antenna located in free space. When the fields vary as 1/r, the expressions for directive gain and power gain (see Equations 2-3 and 2-8) are not a function of the distance from the antenna to the observer.

However, when an antenna is deployed over lossy ground, the far fields no longer vary exactly as 1/r. Thus, the presence of lossy ground makes the gain

a function of the far-field distance between an observer and the antenna under consideration. Weeks presents the following discussion of this point (see Reference 6, pp. 346-347).

> The measurements and application of the concepts of power gain, directivity, and radiation efficiency are particularly difficult when the antennas must operate in lossy environments. The definitions of these quantities were conceived initially to provide simplicity in free-space environments; they do not lend simplicity elsewhere. Honest and meaningful evaluation are also clouded by the divergent motives and objectives of the pure antenna engineer and the user. For, if system performance is degraded by an environment over which he has no control, the antenna engineer understandably would like to describe the gain and efficiency of his product as they would be in an ideal environment, since after all "his" part of the system is "working fine."
>
> On the other hand, the systems engineer and user are concerned with overall performance and, understandably, are not kindly disposed toward an antenna that would "work fine" in an ideal environment but fails to provide communication in the actual environment. So to sell his product, the antenna engineer must evaluate his product as it would function in an actual environment.
>
> The most common application in which these difficulties are manifest is that of antennas for operation on or close to the surface of the earth, at frequencies below, say 30 MHz. Here, one of the most basic difficulties is that the definitions of power gain and directive gain have in them inherently the assumption that the fields vary as 1/r and that the power density varies as 1/r. In the actual earth environment, this is not the case; in the direction near the ground, the field falls off faster than this, perhaps much faster. Thus, with a direct application of the usual definition, the gain depends on distance from the antenna. The radiation pattern may also depend on the distance from the antenna structure, even though the distance may be large compared with the free-space distant-field criteria. At large distances, even for vertical antennas, there is usually essentially a null at the horizon.

Since the electric far field due to the surface wave attenuates more rapidly than 1/r the gain obviously is a function of far-field distance when the surface-wave contribution is included in the total field. Less obvious is the fact that gain can be a function of far-field distance even if the surface-wave contribution is not included. This fact will be addressed below.

The objective of the SKYWAVE antenna gain routines (see Reference 1) is to calculate vertical gain patterns for use in ionospheric propagation predictions, so the SKYWAVE gain equations do not include distance at all. APACK calculates both sky-wave and ground-wave field strengths and gains. APACK directive and power gain are calculated from Equations 2-3 and 2-8, respectively, from the electric far fields.

As long as the field strength varies as 1/r, gain is independent of distance. The reason that gain can vary as a function of far-field distance even if the surface-wave contribution is not included is that the Fresnel reflection coefficients depend on the angle θ_r which changes with distance.

SECTION 3
EXTENSION OF THE FORMULATION TO SPHERICAL EARTH WITH THE RADIO HORIZON

INTRODUCTORY REMARKS

The formulation of the far fields of a current element presented in Section 2 assumes that the element is located above planar earth. When the feed point of the antenna is located several wavelengths or more above the surface of the earth, the earth can no longer be considered planar.

For rigorous calculations of electric field intensities over a spherical earth, the Bremmer formulation (see Reference 17) should be used. However, since the Bremmer series requires a large number of terms for convergence within the radio horizon, this formulation is used by APACK only in the diffraction region beyond the radio horizon. Within the radio horizon, the planar earth formulation can be modified to account for the curvature of the earth without resorting to the rigorous Bremmer techniques (see Reference 17).

Strictly speaking, a spherical reflection coefficient should be used to include the effect of earth curvature. APACK uses the Fresnel reflection coefficient within the radio horizon because the difference between the Fresnel coefficient and the spherical coefficient is negligible except near the horizon. The Fresnel coefficient must be appropriately modified, however, by the divergence factor.

CALCULATION OF THE DIVERGENCE FACTOR

The divergence factor (α_{div}), a geometrical quantity independent of frequency, is a measure of the extra divergence acquired by a beam of rays after reflection from a spherical surface as opposed to a planar surface. The divergence factor is defined by:

$$\alpha_{div} \approx \frac{a_e (C+C') \sqrt{\sin \beta \cos\beta}}{b\, b' \sin\theta\, (C\, b' \cos\alpha' + C' b \cos\alpha)} \quad (3\text{-}1)$$

when

$$a_e = 6370 \left[1 - 0.04665 e^{0.005577 N_s} \right]^{-1} \quad (3\text{-}2)$$

$$N_s = N_o e^{-0.1057 h_s} \quad (3\text{-}3)$$

where

a_e = effective earth radius, in kilometers
N_s = surface atmospheric refractivity, in N-units
N_o = surface atmospheric refractivity reduced to sea level, in N-units
h_s = elevation of the surface above mean sea level, in kilometers.

(If N_o and h_s are not given, N_s = 301 is assumed.) The quantities C, C', α, α', β, and θ are as defined in Figure 2. The quantities b, b', and d are defined by:

$$b = a_e + h_2 \quad (3\text{-}4)$$

$$b' = a_e + h_1 \quad (3\text{-}5)$$

$$d = a_e \theta \quad (3\text{-}6)$$

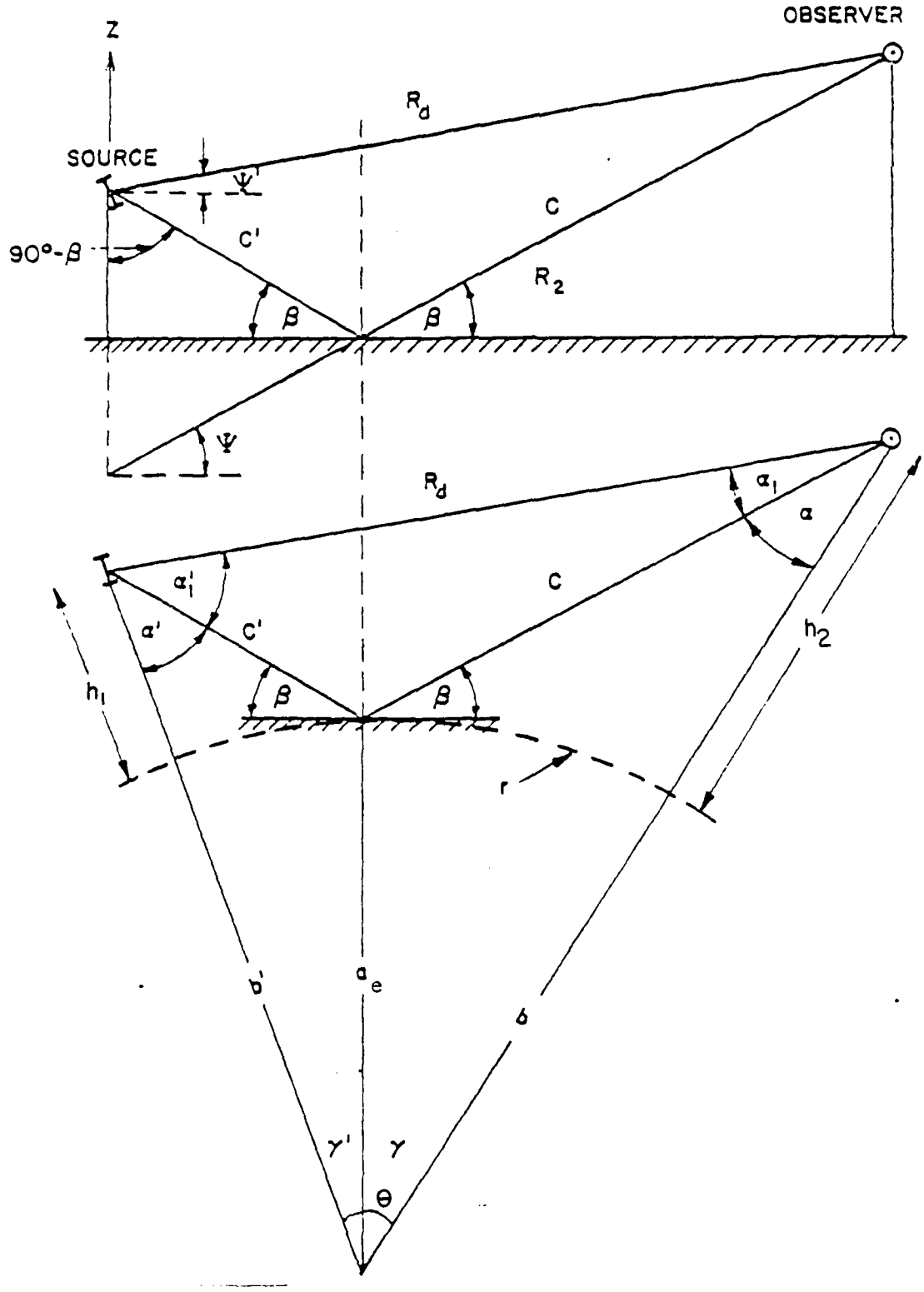

Figure 2. Geometry for divergence-factor calculations.

where

h_1 = height of the transmitting antenna feed point above ground, in kilometers

h_2 = height of the receiving antenna feed point above ground, in kilometers

d = path length (measured along the surface of the spherical earth), in kilometers

The distances C and C' and the angles γ and γ'(as defined in Figure 2) and the angles α, α' and β can be calculated from the antenna height (h_1 and h_2) and the path length (d) by using the nine-step procedure given below.

Step 1

Determine the ratio of the heights (u) from:

$$u = \begin{cases} \frac{h_2}{h_1} = \frac{b - a_e}{b' - a_e}, & \frac{h_2}{h_1} > 1 \\ \text{and let: } \frac{h_1}{h_2} = \frac{b' - a_e}{b - a_e}, & \frac{h_2}{h_1} \leq 1 \end{cases} \tag{3-7}$$

$$v = \frac{d}{\sqrt{2a_e (b' - a_e)}} \tag{3-8}$$

Step 2

Solve for S from:

$$S^3 - \frac{3}{2} S^2 - \frac{S}{2} \frac{1 + u}{v^2} - 1 + \frac{1}{2 v^2} = 0 \tag{3-9}$$

Step 3

Solve for β from:

$$\beta = \tan^{-1}\left[\sqrt{\frac{h_1}{2a_e}}\left|\frac{1}{SV} - SV\right|\right] \quad (3\text{-}10)$$

Step 4

Solve for α and α' from:

$$\alpha = \sin^{-1}\left(\frac{a_e}{b}\cos\beta\right) \quad (3\text{-}11)$$

$$\alpha' = \sin^{-1}\left(\frac{a_e}{b'}\cos\beta\right) \quad (3\text{-}12)$$

Step 5

Calculate γ and γ' from:

$$\gamma = \pi/2 - (\alpha + \beta) \quad (3\text{-}13)$$

$$\gamma' = \pi/2 - (\alpha' + \beta) \quad (3\text{-}14)$$

Step 6

Check to see whether or not:

$$\theta = \pi - 2\beta - (\alpha + \alpha') \quad (3\text{-}15)$$

with θ given by Equation 3-6.

If the equality in Equation 3-15 is not satisfied, assume another value of β and repeat Steps 4, 5, and 6 until the equality in Equation 3-15 is satisfied.

Step 7

Calculate C and C' from:

$$C = a_e \frac{\sin \gamma}{\sin \alpha} \tag{3-16}$$

$$C' = a_e \frac{\sin \gamma'}{\sin \alpha'} \tag{3-17}$$

Step 8

Solve for R_d (needed for the calculation of the field strength due to the direct wave) from:

$$R_d = \sqrt{b^2 + b'^2 - 2\, bb' \cos\theta} \tag{3-18}$$

with b, b', and θ given by Equations 3-4, 3-5, and 3-6, respectively.

Step 9

Solve for α_{div} from Equation 3-1.

SUMMARY

Within the radio horizon, the divergence factor is used by APACK to account for the effects of earth curvature without using the Bremmer

formulation. The contribution of the direct wave at the observation point is calculated using the antenna heights and path length. The contribution of the ground-reflected wave at the observation point is calculated from the antenna heights and path length by using the Fresnel reflection coefficient multiplied by the divergence factor. Since the surface-wave contribution is negligible when the antennas are several wavelengths or more above the ground, the surface wave does not have to be included in this region.

SECTION 4
EXTENSION OF THE FORMULATION TO THE DIFFRACTION REGION BEYOND THE RADIO HORIZON

INTRODUCTORY REMARKS

The formulation presented in Section 2 for the far fields of a current element assumes that the element is located above planar earth. For calculations of field intensities over a spherical earth in the diffraction region beyond the radio horizon, APACK employs the Bremmer formulation (see Reference 17). This formulation gives the far fields of a linear antenna in terms of the radiation vector which accounts for the geometry of the antenna and the Bremmer secondary factor which accounts for the geometry of the path.

The radiation vector is useful not only in describing the far fields in the diffraction region but also for calculating antenna gain. Therefore, the radiation vector will be discussed first, followed by a discussion of the diffraction region far fields.

THE RADIATION VECTOR

The radiation vector $(\bar{N})$ for a linear antenna is defined by:[19,20]

$$\bar{N} = \int_L \bar{I}(s)\, e^{jks\cos\psi}\, ds \qquad (4\text{-}1)$$

---

[19] Foster, D., "Radiation from Rhombic Antenna," Proc. IRE, Vol. 25, No. 10, October 1937, pp. 1327-1353.

[20] Schelkunoff, S.A., "A General Radiation Formula," Proc. IRE, Vol. 27, No. 10, October 1939, pp. 660-666.

where L indicates integration over the current elements comprising the linear antenna and all other terms have been defined in Section 2 following Equations 2-11 and 2-12 (see also Figure 1). In spherical coordinates (r,θ,ϕ), the radiation vector can be written as:

$$n = \bar{a}_r N_r + \bar{a}_\theta N_\theta + \bar{a}_\phi N_\phi \qquad (4\text{-}2)$$

where $\bar{a}_r$, $\bar{a}_\theta$, and $\bar{a}_\phi$ are unit vectors in the r-, θ-, and ϕ-directions, respectively.

The free-space far-field components are then given in terms of the radiation vector by:

$$E_\theta = j30k \frac{e^{-jkr}}{r} N_\theta \qquad (4\text{-}3)$$

$$E_\phi = j30k \frac{e^{-jkr}}{r} N_\phi \qquad (4\text{-}4)$$

$$H_\theta = \frac{j30k}{120\pi} \frac{e^{-jkr}}{r} N_\phi \qquad (4\text{-}5)$$

$$H_\phi = \frac{j30k}{120\pi} \frac{e^{-jkr}}{r} N_\theta \qquad (4\text{-}6)$$

where

$E_{\theta,\phi}$ = θ-, ϕ- component of the electric far field, in volts/meter
$H_{\theta,\phi}$ = θ-, ϕ- component of the magnetic far field, in amperes/meter
$N_{\theta,\phi}$ = θ-, ϕ- component of the radiation vector, in volt-meters
$k = \frac{2\pi}{\lambda}$ where λ is wavelength, in meters
r = radial distance from the origin to the observation point, in meters.

The time-average Poynting vector ($\bar{P}_r$) is found from:

$$\bar{P}_r = \frac{1}{2} \bar{a}_r R_e (\bar{E} \times \bar{H}^*) \quad (4\text{-}7)$$

where

$\bar{P}_r$ = time-average Poynting vector, in watts/square meter
$\bar{a}_r$ = unit vector in the r-direction in spherical coordinates (r, θ, ϕ)
$\bar{E}$ = electric far field, in volts/meter
$\bar{H}$ = magnetic far field, in amperes/meter

(In Equation 4-7, "R_e" denotes the real part of, and "*" denotes complex conjugate.) For the components of $\bar{E}$ and $\bar{H}$ given by Equations 4-3 through 4-6:

$$\bar{P}_r = \frac{1}{2} \bar{a}_r R_e (E_\phi H_\theta^* + E_\theta H_\phi^*) \quad (4\text{-}8)$$

Substituting Equations 4-3 through 4-6 into Equation 4-7, the magnitude of the time average Poynting vector can be written in terms of the radiation vector as:

$$P_r = \frac{1}{2} \frac{(30k)^2}{120\pi r^2} \left[|N_\theta|^2 + |N_\phi|^2 \right] = \frac{15\pi}{r^2\lambda^2} \left[|N_\theta|^2 + |N_\phi|^2 \right] \quad (4\text{-}9)$$

The radiation intensity (Φ) is then given by:

$$\Phi(\theta,\phi) = r^2 P_r = \frac{15\pi}{\lambda^2} |N_\theta|^2 + |N_\phi|^2 \qquad (4\text{-}10)$$

where

$\Phi(\theta,\phi)$ = radiation intensity as a function of the spherical angular coordinates θ and ϕ, in watts/steradian.

Therefore, the antenna power gain (g_p) can be expressed as:

$$g_p(\theta,\phi) = \frac{4\pi\ \Phi(\theta,\phi)}{W_{in}} = \frac{15\ k^2\ [|N_\theta|^2 + |N_\phi|^2]}{W_{in}} \qquad (4\text{-}11)$$

where

$g_p(\theta,\phi)$ = power gain as a function of the spherical angular coordinates θ and ϕ (numerical ratio)

W_{in} = power input to the antenna, in watts.

THE BREMMER FORMULATION

The divergence factor, presented in Section 3, extends the basic formulation for an elementary current element over planar earth to include the effects of spherical earth within the radio horizon. Beyond the radio horizon, diffraction phenomena must be taken into account.

The problem of electromagnetic wave propagation over a lossy homogenous spherical earth was solved by Bremmer (see Reference 17) and others[21,22] many years ago. In this solution, the transmitting antenna is assumed to be a Hertzian dipole.

The assumption of a Hertzian dipole antenna does not fundamentally limit the solution obtained because it is well known that the fields of an antenna of finite length can be obtained by integration from the superposition of Hertzian dipole. The integration is not straightforward, however, because the fields of a Hertzian dipole located above lossy spherical earth are given by an infinite series.

In the spherical-earth theory, the vertical component of the electric far field of a Hertzian dipole is given by:[23]

$$E = \frac{I_o \ell k^2 e^{-jkr}}{4\pi \varepsilon_o \omega d}\left(2F_r\right) = \frac{30k\, I_o \ell}{d} e^{-jkr}\left(2F_r\right) \qquad (4\text{-}12)$$

where

E = vertical component of the electric far field, in volts/meter

I_o = Hertzian dipole current, in amperes

---

[21] Van der Pol, B. and Bremmer, H., "The Diffraction of Electromagnetic Waves from an Electrical Point Source Round a Finitely Conducting Sphere," Phil. Mag.: Ser. 7, 24, 1937, pp. 141-176 and 825-864; 25, 1938, pp. 817-834; and 26, 1939, pp. 261-275.

[22] Fock, V.A., Electromagnetic Diffraction and Propagation Problems, Pergamon Press, New York, NY, 1965.

[23] Johler, J.R., Kellar, W.J., and Walters, L.C., Phase of the Low Radio-Frequency Ground Wave, National Bureau of Standards Circular 573, National Bureau of Standards, Boulder, CO, 26 June 1956.

ℓ = length of the Hertzian dipole, in meters

k = wave number $(\frac{2\pi}{\lambda})$, in meters^{-1}

ε_o = permittivity of free space, in farads/meter

ω = frequency, in radians/second

d = distance along the surface of the spherical earth, in meters

r = radial distance from the origin to the observation point, in meters

F_r = Bremmer secondary factor.

The Bremmer secondary factor (F_r) is used to describe the far fields of linear antennas in the diffraction region when the radiation vector for the antennas is known. F_r is given by:

$$F_r = \sqrt{2\pi\alpha^{\frac{2}{3}} (ka)^{\frac{1}{3}} \frac{d}{a}} \sum_{s=o}^{\infty} \frac{f_s(h_1) f_s(h_2)}{2\tau s - \frac{1}{\delta_2}} \times \exp\left\{ j\left\{ \left[(ka)^{\frac{1}{3}} \tau_s \alpha^{\frac{2}{3}} \frac{d}{a} + \frac{\alpha d}{2a} + \frac{\pi}{4} \right] \right\} \right\} \quad (4\text{-}13a)$$

where

a = radius of the spherical earth, in meters

a_e = effective radius of the spherical earth, in meters

$\alpha = \frac{a}{a_e}$ = parameter associated with the vertical lapse of the permittivity of the atmosphere (dimensionless)

h_1 = height of the transmitting antenna feed point above the surface of the spherical earth, in meters

h_2 = height of the receiving antenna feed point above the surface of the spherical earth, in meters

$f_s(h_1)$ = height gain factor of the transmitting antenna

$f_s(h_2)$ = height gain factor of the receiving antenna

$$\delta_e = K_e e^{j(\frac{3\pi}{4} - \psi_e)} \quad \text{(for a vertical element)} \qquad (4\text{-}13b)$$

$$\delta_m = K_m e^{j(\frac{\pi}{4} + \psi_m)} \quad \text{(for a horizontal element)} \qquad (4\text{-}13c)$$

The factor τ_s is calculated from Riccati's differential equation:

$$\frac{d\delta_e}{d\tau_s} - 2\delta_e{}^2 \tau_s + 1 = 0 \qquad (4\text{-}13d)$$

Computational formulas for evaluating $f_s(h_1)$, $f_s(h_2)$, τ_s, and δ can be found in Reference 23, Appendix I. Although the formulas presented in Reference 23 are not amendable to manual computation, they can be used for automated calculations.

As shown in Reference 20, the free-space field intensities of linear antennas other than the Hertzian dipole can be obtained by replacing the dipole moment in expressions for the field intensities of a Hertzian dipole with the radiation vector. Extending this principle to the diffraction region, the equations for the electric far-field components of a linear antenna in the diffraction region are given by:

$$E_\theta = j30k \frac{e^{-jkd}}{d} N_\theta(2F_r) \qquad (4\text{-}14)$$

$$E_\phi = j30k \frac{e^{-jkd}}{d} N_\phi(2F_r) \qquad (4\text{-}15)$$

(A similar use of this principle was made by Kuebler[24] in the line-of-sight region by substituting the field function for linear antennas for the dipole moment. The field function is identical to the radiation vector except for a constant.)

Equations 4-14 and 4-15 were used to formulate the far fields of the 16 types of linear antennas listed in TABLE 1 for the diffraction region beyond the radio horizon.

[24] Kuebler, W., Ground-Wave Electric Field Intensity Formulas for Linear Antennas, ECAC-TN-74-11, Electromagnetic Compatibility Analysis Center, Annapolis, MD, June 1974.

SECTION 5
CALCULATIONS OF FIELD STRENGTH AND GAIN

The formulation presented in Section 2 for the far fields of a current element above planar earth was used to derive the far-field expressions for the 16 types of antennas considered. The extensions to this formulation, presented in Sections 3 and 4, were utilized to derive the far fields over spherical earth within the radio horizon and in the diffraction region beyond the radio horizon.

This section presents a brief introduction to each of the 16 types of antennas (including a figure of the antenna geometry and a description of the geometrical parameters), TABLE 2 (which refers to appropriate equations in APPENDIXES A and D for calculating the components of the electric far field, directive gain, and radiation efficiency), and supplemental symbols and formulas that are frequently used in the equations listed in TABLE 2. Symbols occurring in the equations in APPENDIX D are described with corresponding equations in APPENDIX A.

TABLE 2 serves as a reference to key equations for calculating the electric far fields, directive gains, and radiation efficiencies of the 16 types of antennas. Summaries of the derivations of these equations are presented in APPENDIX A. The observation point P (r,θ,ϕ) indicated in all figures and referenced to in TABLE 2 is determined by the standard spherical coordinates r, θ, and ϕ.

HORIZONTAL DIPOLE

The horizontal dipole (or doublet) antenna shown in Figure 3 is a basic antenna type commonly used over a wide range of frequencies. The dipole also serves as a building block element for antenna arrays. The fields of the dipole are a function of its length and height above ground. For this antenna, the feed point (i.e., the point at which the antenna is excited by transmission line) is located at the center of the element.

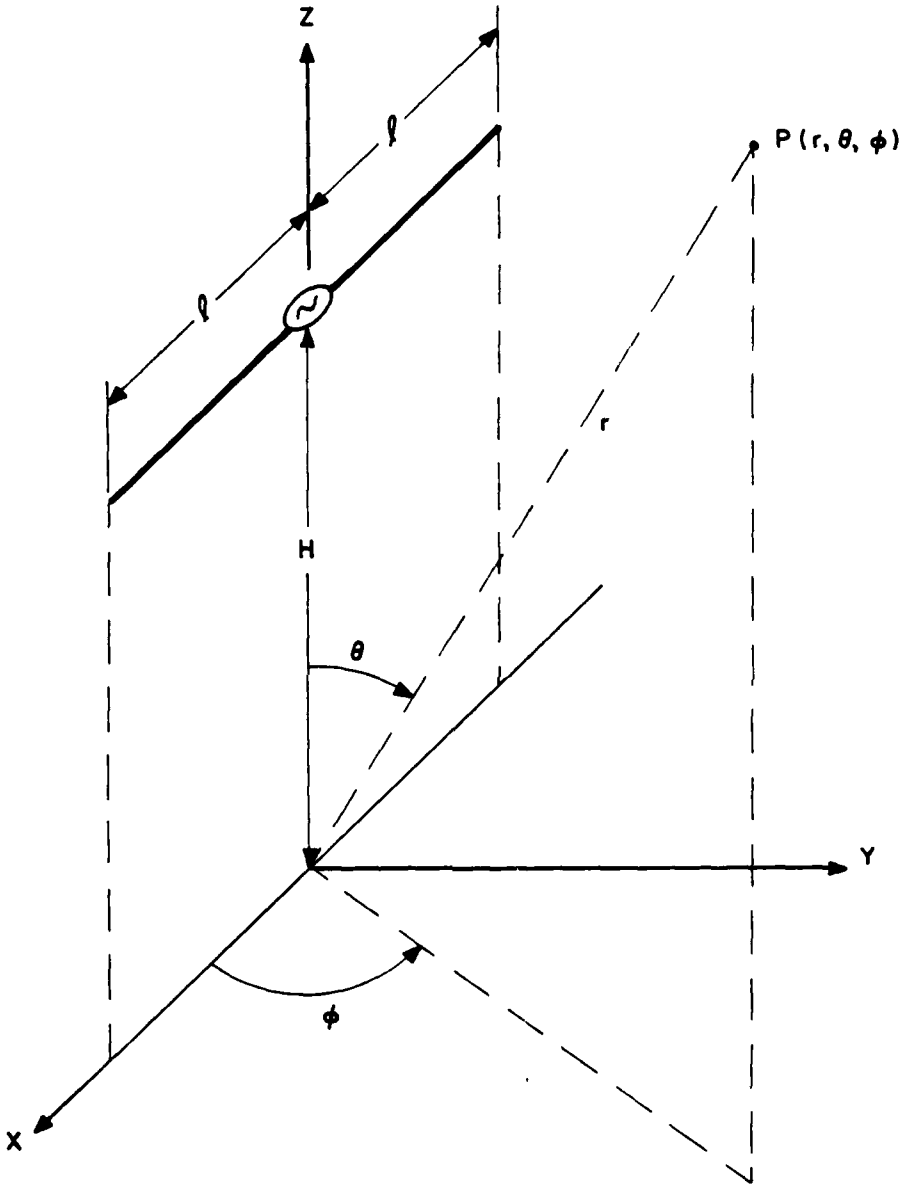

Figure 3. Horizontal dipole.

The geometrical parameters of interest for the horizontal dipole are:

ℓ = half-length of the dipole
H = height of the feed point (i.e., center of the dipole) above ground.

VERTICAL MONOPOLE

The vertical monopole, also known as a "whip," is identical to half of a dipole antenna. The vertical monopole is fed at its base and produces a field that is not a function of the spherical angle ϕ. Since the field is not a function of ϕ, the vertical monopole is referred to as being omnidirectional, often shortened to "omni." The only geometrical parameter needed for the vertical monopole is ℓ, the length of the monopole. Figure 4 shows the geometry of the vertical monopole.

VERTICAL MONOPOLE WITH RADIAL-WIRE GROUND SCREEN

Most vertical monopoles that are permanently installed include a ground screen to improve the radiation resistance and to increase the level of the fields radiated at small values of elevation angle (i.e., values of θ near 90°). One form of ground screen commonly used consists of a group of radial wires placed on the ground that are centered at the base of the monopole and spaced equally in angle.

The geometrical quantities of interest for the vertical monopole with radial-wire ground screen (see Figure 5) are:

ℓ = length of the monopole
C = radius of the wires comprising the ground screen
a = radius of ground screen
N = number of radial wires.

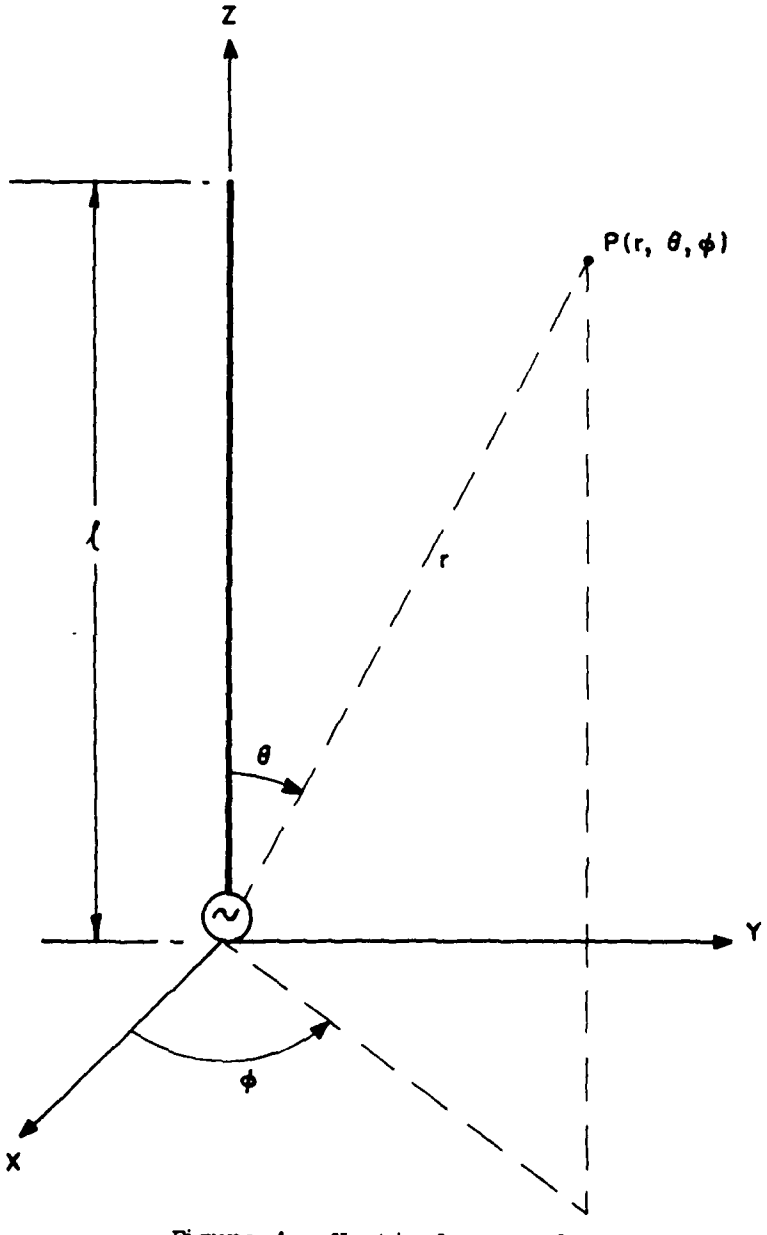

Figure 4. Vertical monopole.

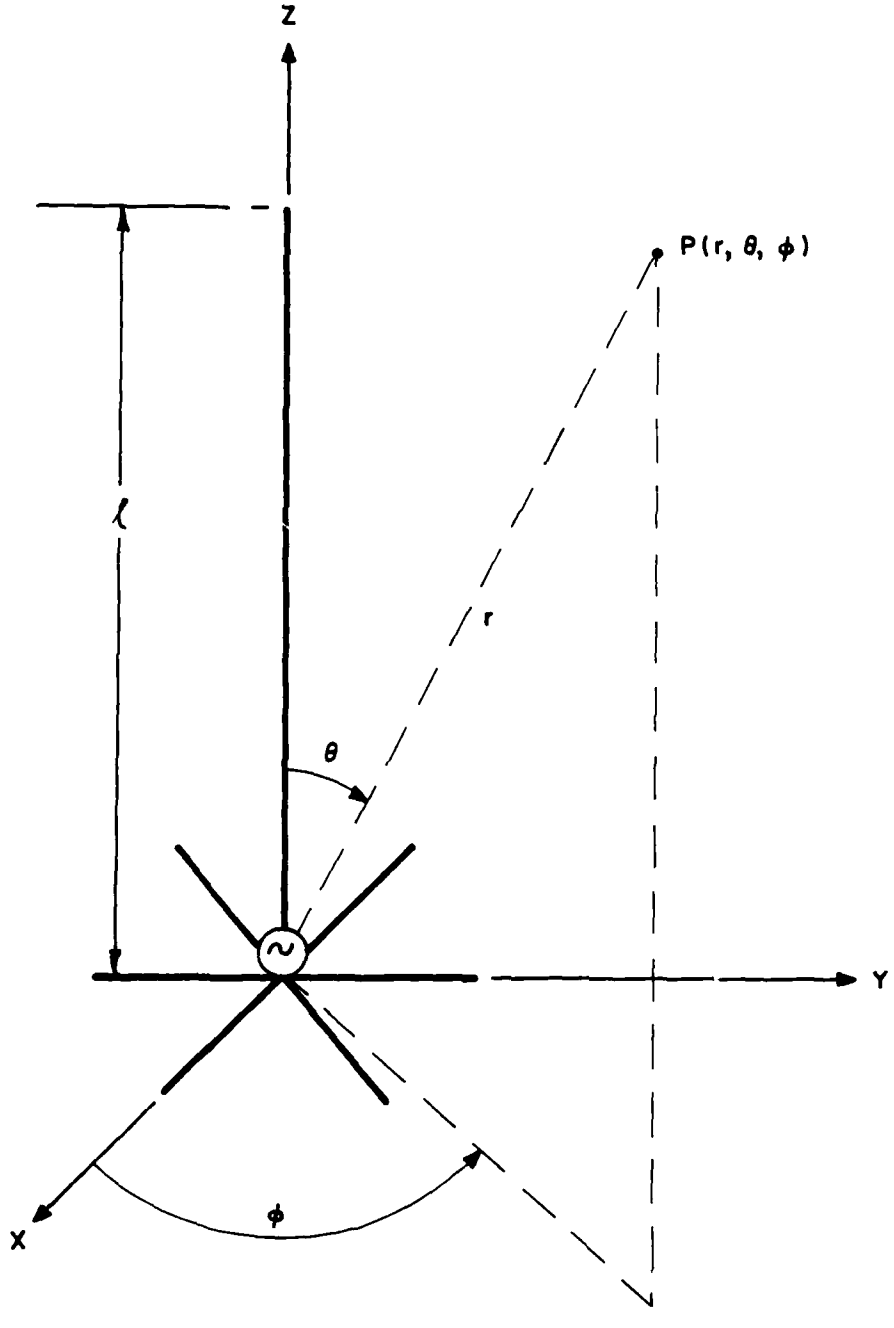

Figure 5. Vertical monopole with radial-wire ground screen.

ELEVATED VERTICAL DIPOLE

The elevated vertical dipole antenna is simply a dipole that is oriented with its axis orthogonal to the ground plane below it. The fields of this antenna are not a function of the spherical angle ϕ, so the elevated vertical dipole is also considered "omni."

The pertinent geometrical quantities shown in Figure 6 are:

ℓ = half-length of the dipole
Z_o = height of the feed point (i.e., center of the dipole) above ground.

INVERTED-L

The inverted-L antenna, shown in Figure 7, consists of both a vertical and a horizontal section. This antenna is fed at the bottom of the vertical section. The inverted-L is often used when a tall vertical monopole is inconvenient to erect, because the horizontal section acts as a "top load" for the vertical section. This effectively increases the length of the vertical section.

The geometrical parameters for the inverted-L are H, the length of the vertical section, and ℓ, the length of the horizontal section.

ARBITRARILY TILTED DIPOLE

The arbitrarily tilted dipole is a dipole that is inclined at an angle with respect to the ground under it. The geometrical parameters as shown in Figure 8 are:

ℓ = half-length of the dipole
H = height of the feed point (i.e., center of the dipole) above ground
α' = angle between the axis of the dipole and the Y-axis.

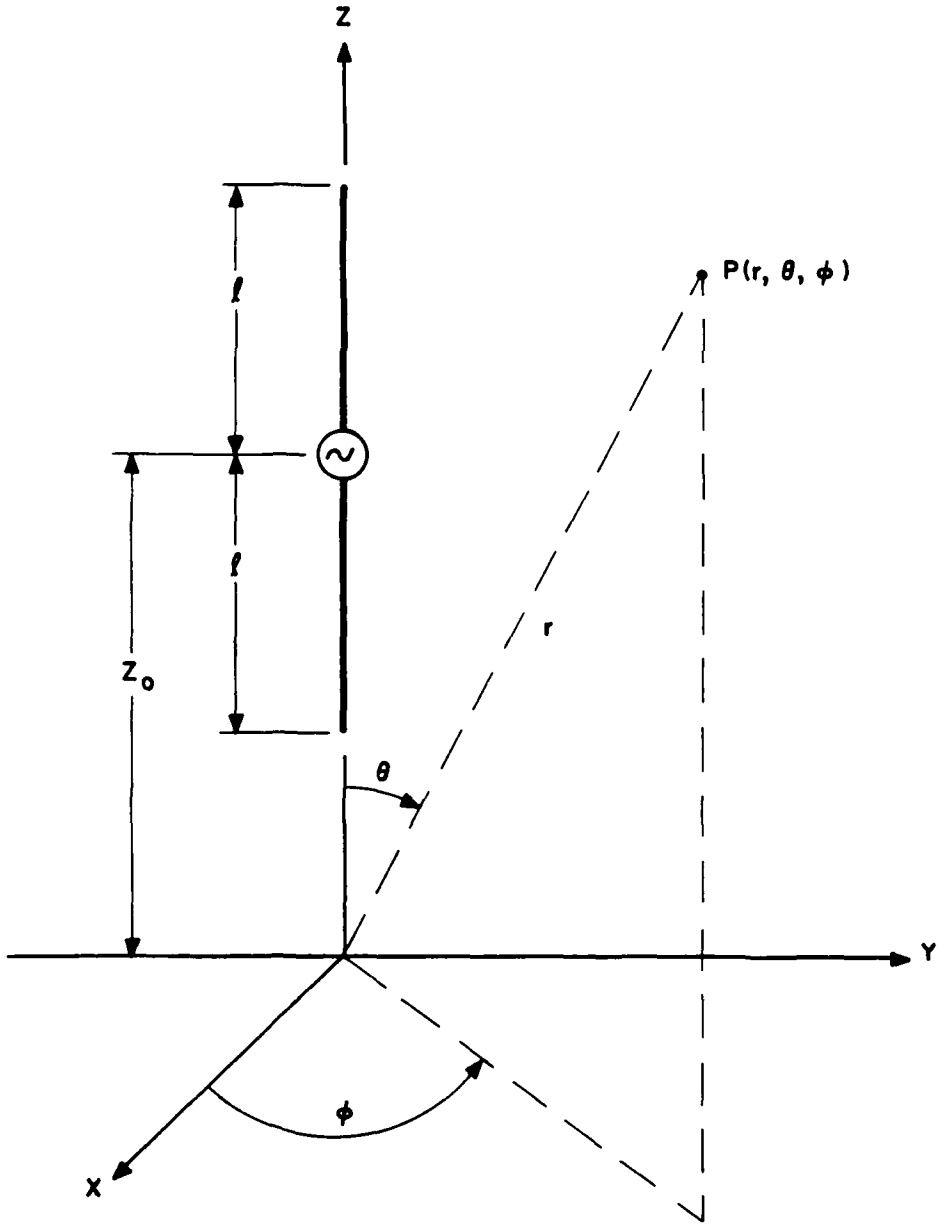

Figure 6. Elevated vertical dipole.

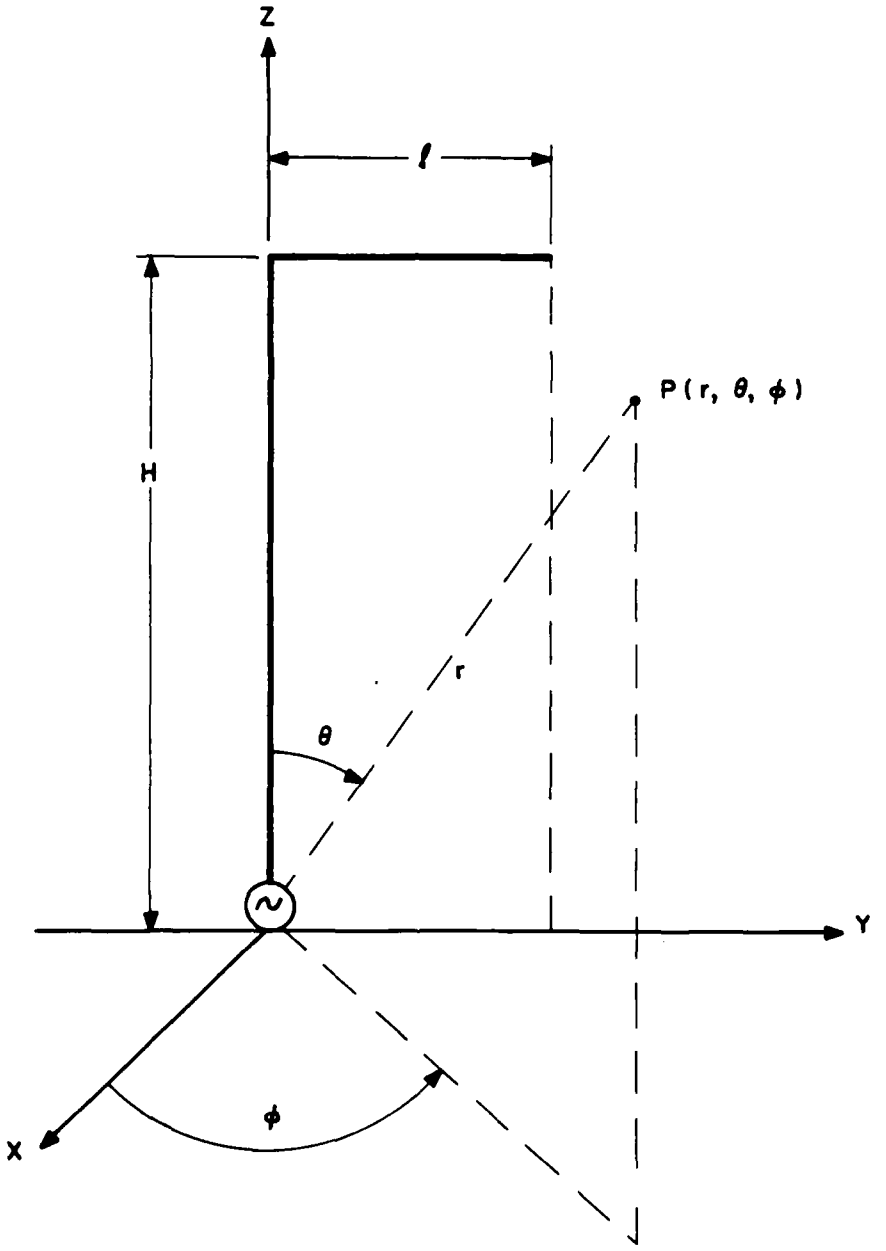

Figure 7. Inverted-L.

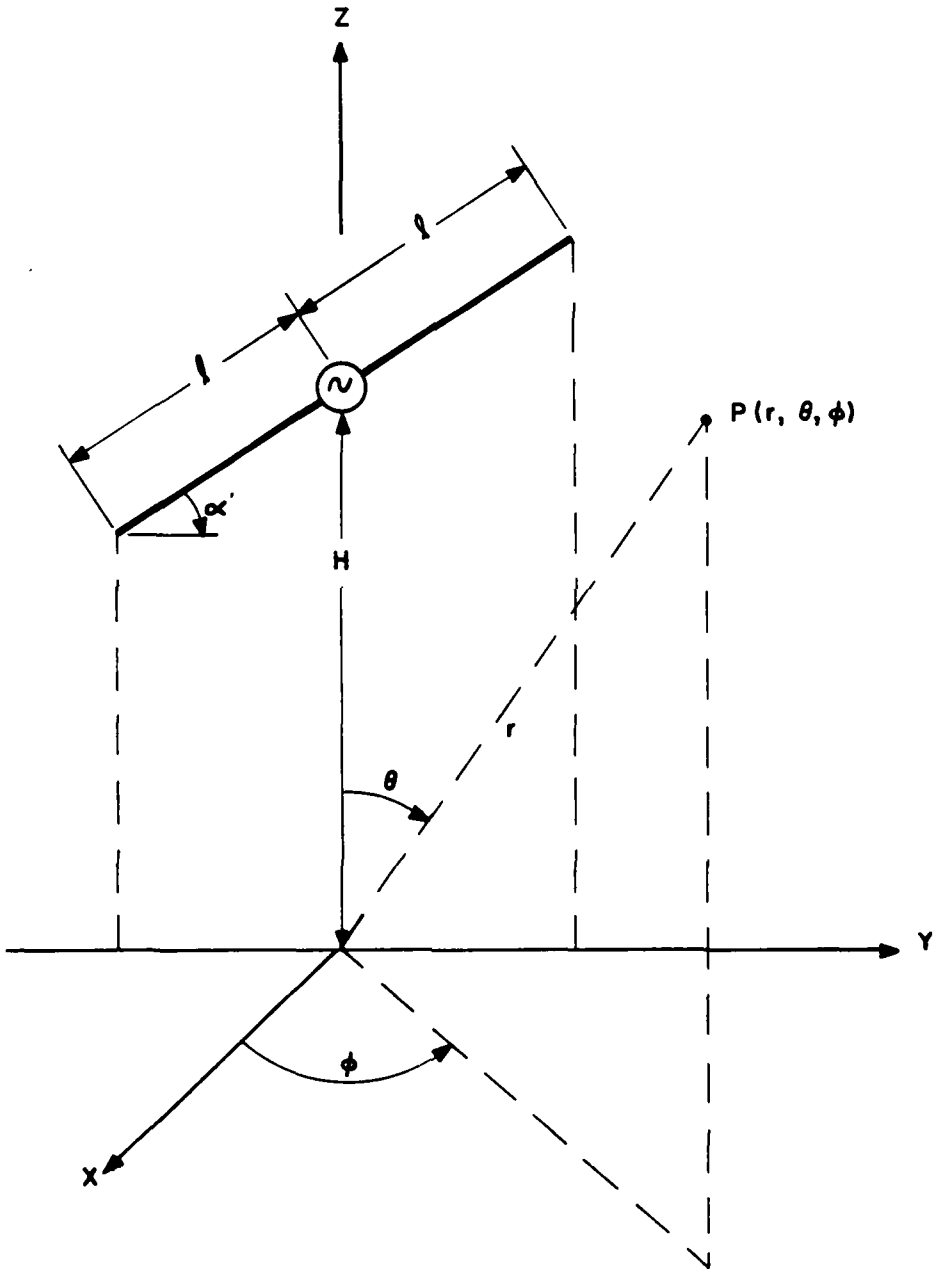

Figure 8. Arbitrarily tilted dipole.

SLOPING LONG-WIRE

The sloping long-wire, shown in Figure 9, is fed at the base and produces both vertically and horizontally polarized field components that depend on the inclination of the wire with respect to the ground plane. The conductivity of the ground beneath the wire can have substantial effects on the radiation characteristics. When the ground has high conductivity, radiation is reflected off the ground in the direction of the high end of the wire. When the ground has low conductivity, radiation directed toward the ground is absorbed, and radiation directed upward and in the direction opposite to the high end predominates.

The geometrical parameters of interest for the sloping long-wire are:

ℓ = length of the wire
α' = angle between the axis of the wire and the Y-axis.

TERMINATED SLOPING-V

The terminted sloping-V, shown in Figure 10, consists of two wires fed at the apex and terminated with appropriate resistances at the ends away from the feed point. The terminating resistances on the wires cause the currents in the wires to result in traveling waves. Thus, the terminated sloping-V is a traveling-wave (i.e., nonresonant) antenna as opposed to other types discussed previously which are resonant antennas. Traveling-wave antennas have the advantage of providing operation over a wide range of frequencies without the need for matching (coupling) networks between the feed point and attached transmission line.

The fields of the terminated sloping-V depend on a number of parameters including the wire lengths, angle between the wires, and heights of the structure. The geometrical parameters are:

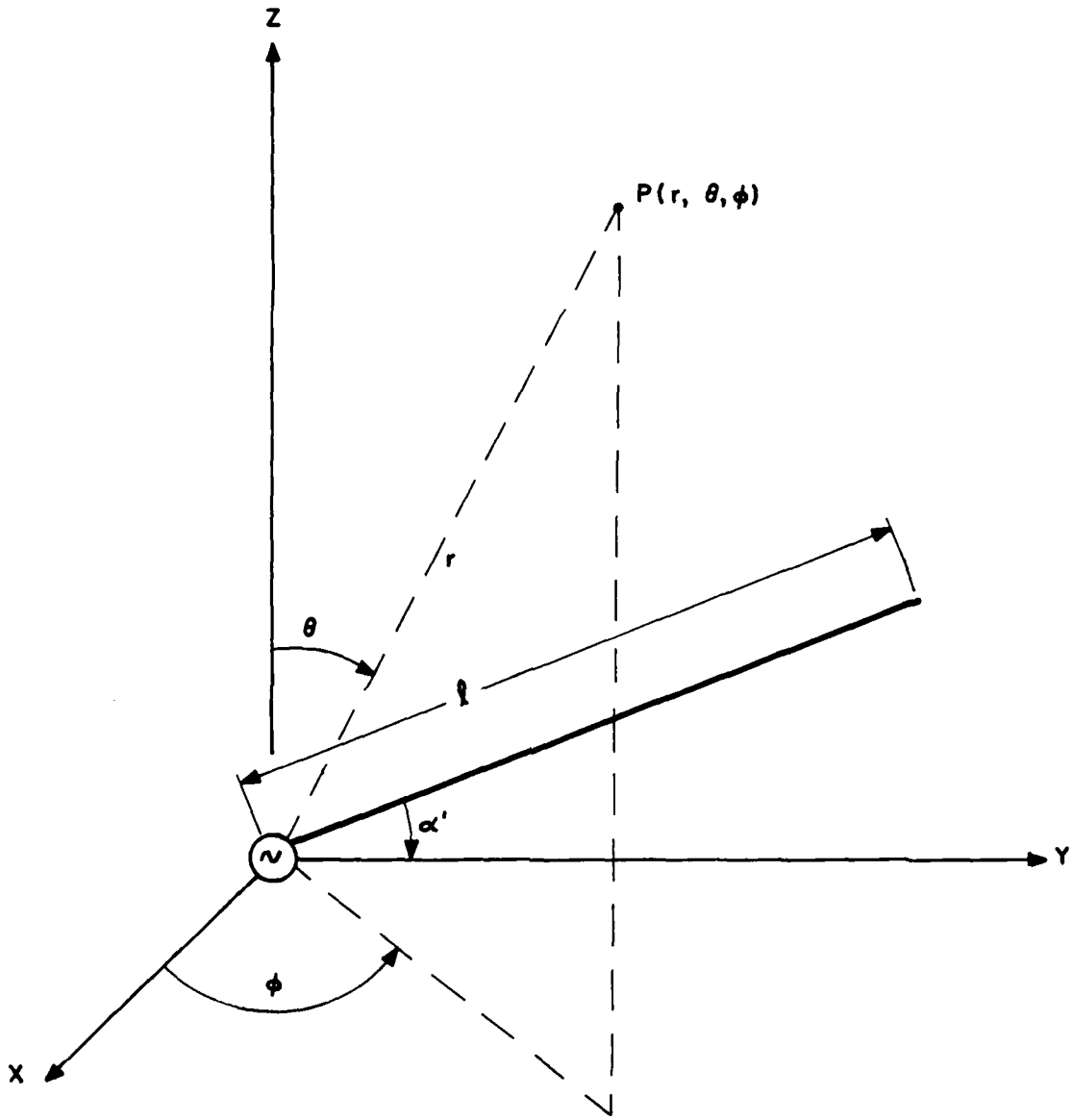

Figure 9. Sloping long-wire.

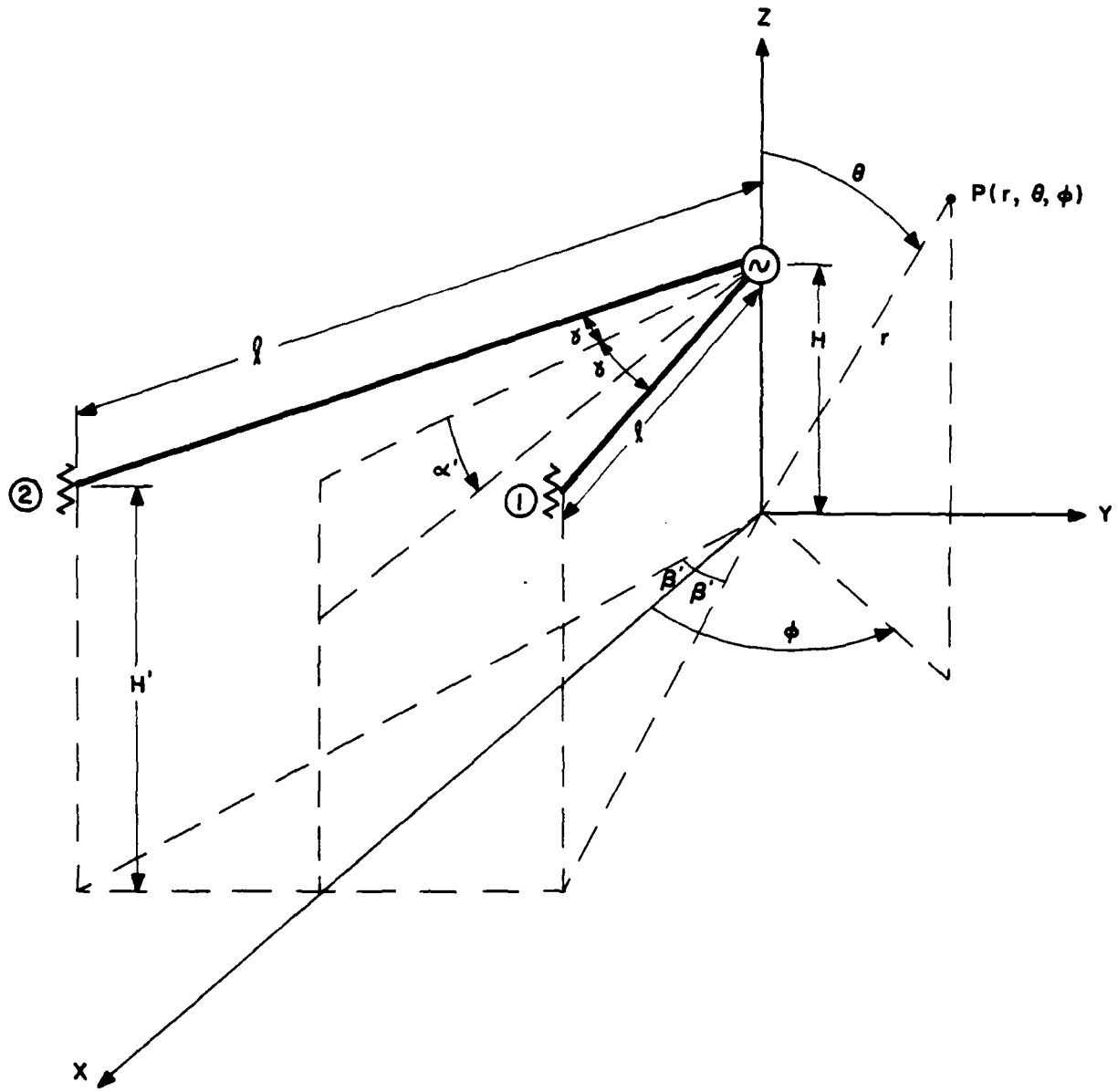

Figure 10. Terminated sloping-V.

ℓ = length of the wire
γ = half-angle between the wires
H = height of the apex (feed point) above ground
H' = height of the terminated end of the wires above ground
α' = angle between the plane containing the wires and the X-axis
β' = angle between the projection of the wires in the XY-plane and the X-axis.

TERMINATED SLOPING RHOMBIC

The terminated sloping rhombic, shown in Figure 11, can be considered as being made up of two sloping-V antennas placed end-to-end. The apex of one of the sloping-V antennas is used as the feed point, and the apex of the other sloping-V antenna is terminated in an appropriate resistance. The terminated rhombic is also a traveling-wave antenna that can be operated over a wide range of frequencies without matching (coupling) networks.

The geometrical parameters are:

ℓ = length of each of the four wires comprising the rhombus
γ = half angle between the wires, the feed point, and the termination
H = height of the feed-point apex above ground
H' = height of the terminated apex above ground
H" = height of the center of the rhombus above ground
α' = angle between the plane containing the rhombus and the x-axis
β' = angle between the projection of the feed-point apex in the XY-plane and the x-axis.

TERMINATED HORIZONTAL RHOMBIC

The terminated horizontal rhombic is identical to the terminated sloping rhombic except that the plane of the rhombus is parallel to the XY-plane. The geometrical parameters for the horizontal rhombic, shown in Figure 12, are identical to those for the sloping rhombic except that H is the height of the rhombus above ground.

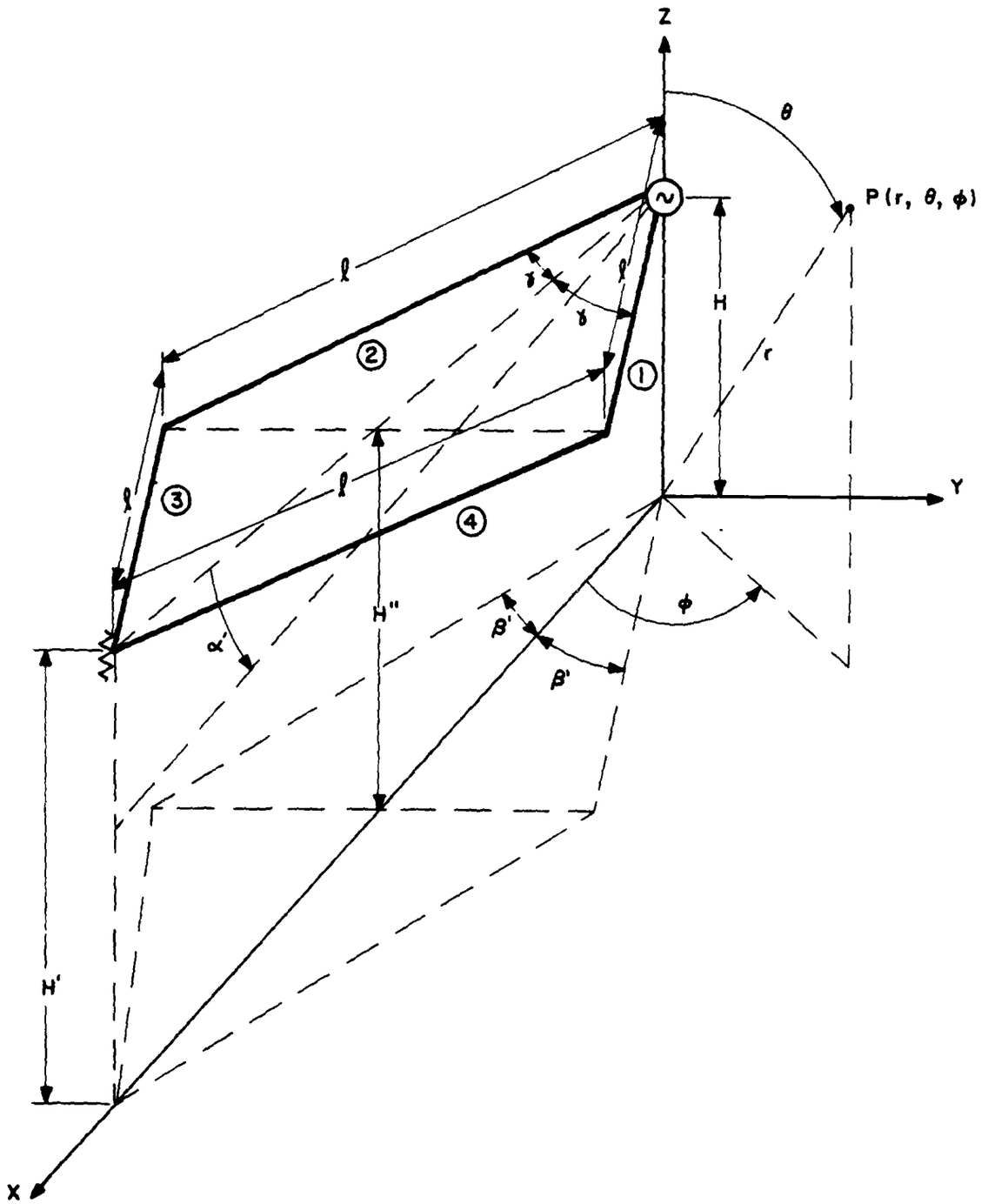

Figure 11. Terminated sloping rhombic.

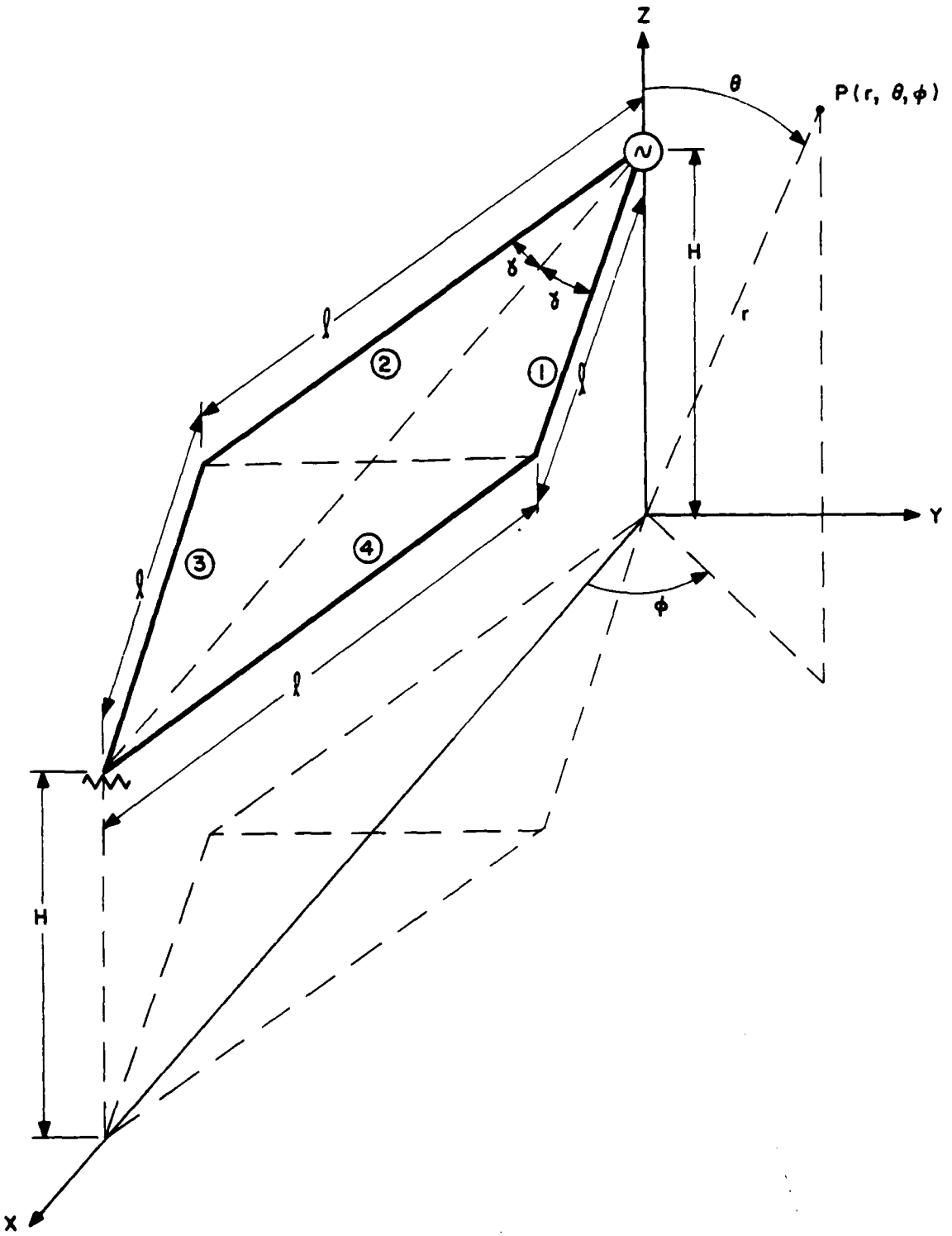

Figure 12. Terminated horizontal rhombic.

SIDE-LOADED VERTICAL HALF-RHOMBIC

The side-loaded vertical half-rhombic, shown in Figure 13, consists of two sectons of wire fed at one end and terminated with an appropriate resistor at the other end. The side-loaded vertical half-rhombic is also a traveling-wave antenna and radiates a combination of vertically and horizontally polarized fields depending on the length of the wires and their inclination with respect to the ground plane. Note that if the ground plane were perfectly conducting, the two wire sections and their images below the ground would form a rhombic antenna in the YZ-plane.

The geometrical parameters of interest for the side-loaded vertical half-rhombic are:

ℓ = length of each of the wire sections

α' = angle between the feed point or termination point of the wires and the Y-axis.

HORIZONTAL YAGI-UDA ARRAY

The horizontal Yagi-Uda array is a coplanar arrangement of dipole elements of different lengths with variable spacing between dipoles. Specifically, a Yagi-Uda array consists of a single driven element and one or more parasitic elements that can function either as reflectors or as directors (see Figure 14).

The director element is directly coupled to the transmission line at the center of the element. The parasitic elements are not coupled directly to the transmission line but are rather coupled through the electromagnetic fields emanating from the driven element. The parasitic reflector element is longer than the driven element and is placed behind the driven element with respect to the desired direction of radiation. The parasitic director elements are shorter than the driven element and are placed in front of the driven element with respect to the desired direction of radiation.

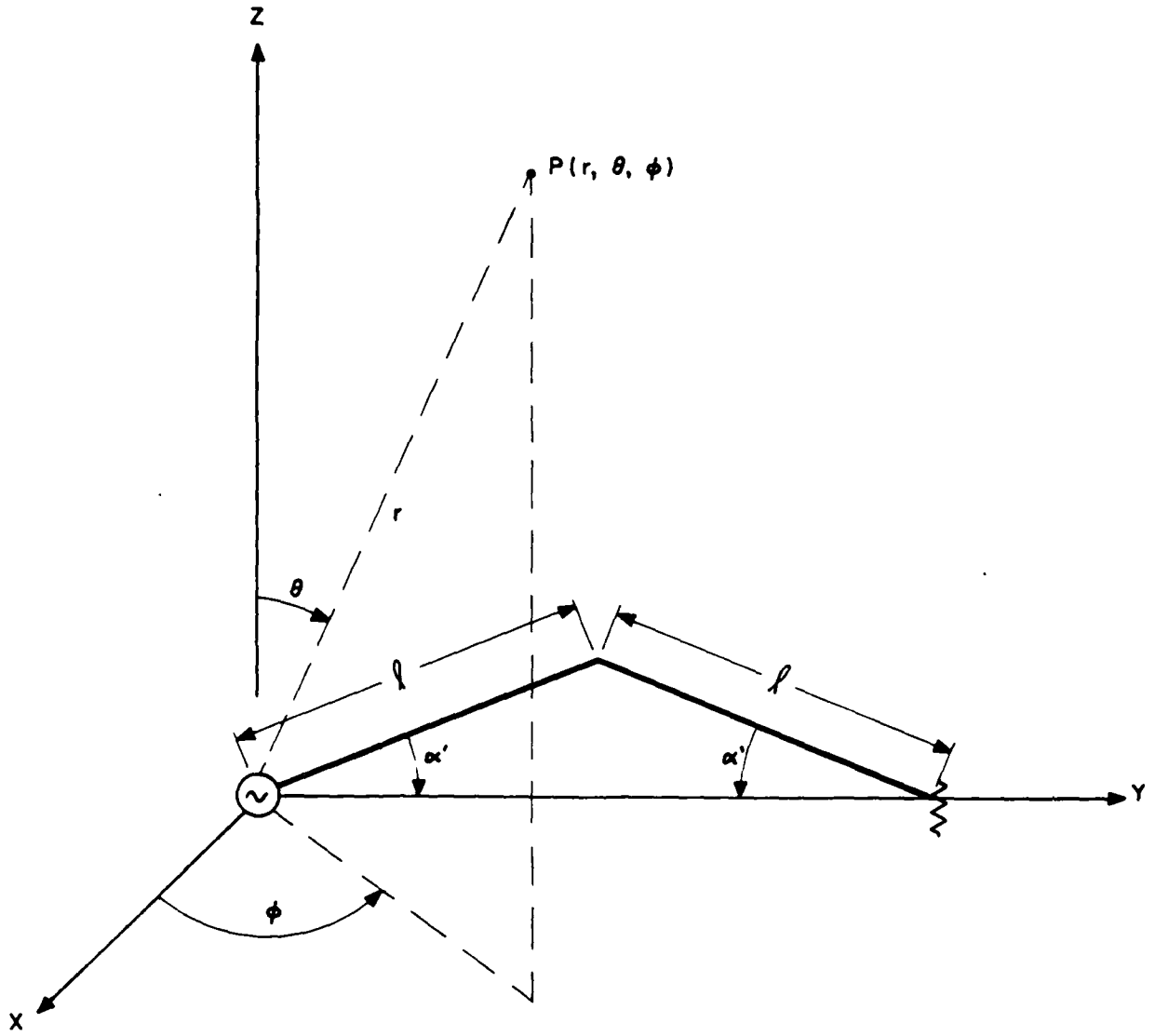

Figure 13. Side-loaded vertical half-rhombic.

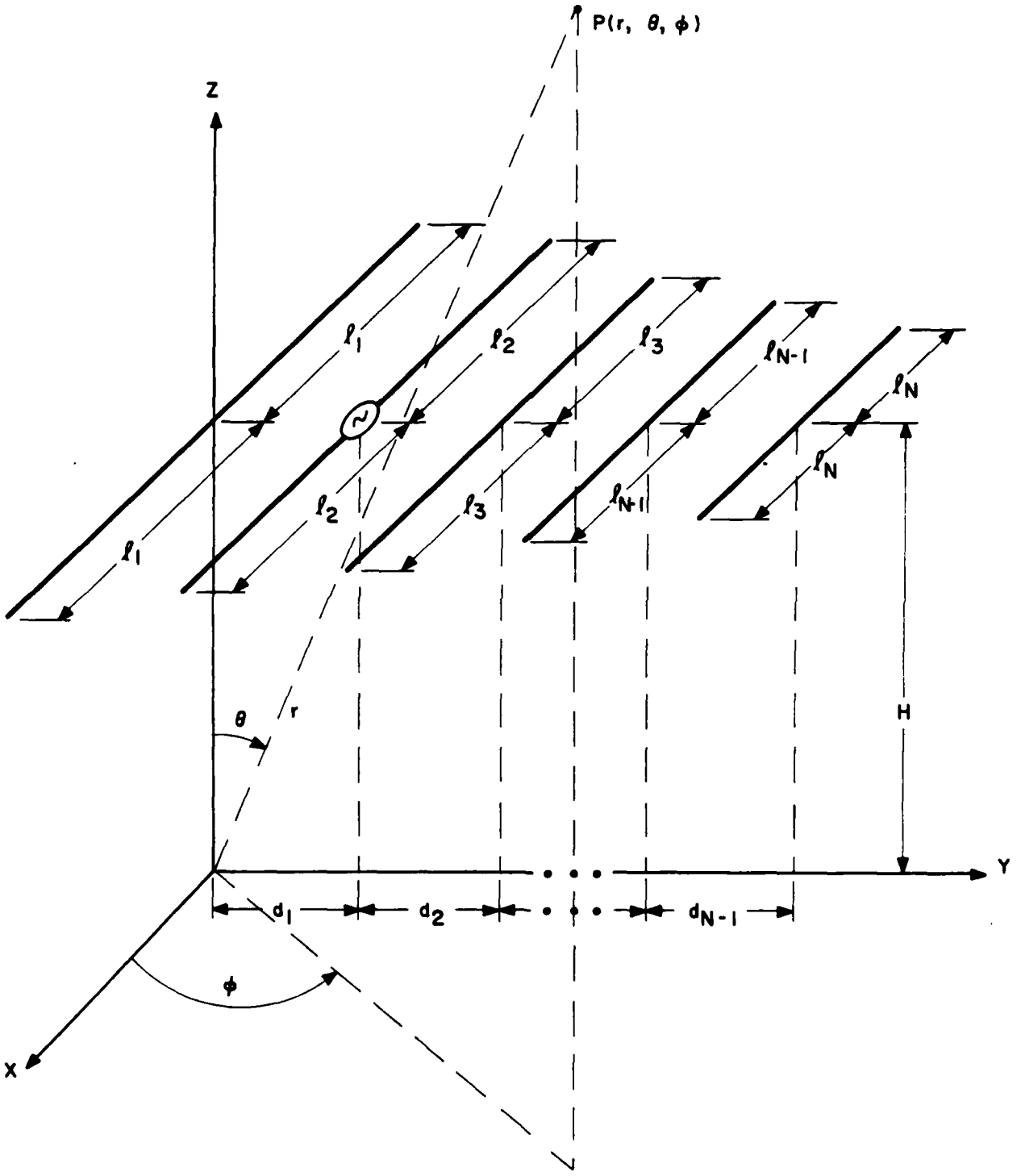

Figure 14. Horizontal Yagi-Uda array.

A common arrangement is for the reflector to be slightly longer than a half-wavelength, the driven element about a half-wavelength, and the directors less than a half-wavelength. Typical spacings between the dipole elements vary from about one-tenth to four-tenths of a wavelength.

The geometrical parameters for a Yagi-Uda array are:

ℓ_i = half-length of the i^{th} element
d_i = spacing between the i^{th} element and the $(i + 1)^{th}$ element
H = height of the array above the ground.

HORIZONTALLY POLARIZED LOG-PERIODIC DIPOLE ARRAY

The horizontally polarized log-periodic dipole array is also a coplanar arrangement of dipole elements with varying lengths and spacing between elements. The log-periodic dipole array differs from the Yagi-Uda array in that the element lengths, spacings, and excitation are designed to provide operation over a wide range of frequencies (typically two or three octaves) without the need for matching (coupling) networks between the feed point and attached transmission line.

The geometrical parameters for the horizontally polarized log-periodic dipole array (see Figure 15) are as follows:

ℓ_i = half-length of the i^{th} element
d_i = spacing between the i^{th} element and the $(i + 1)^{th}$ element
H_1 = height of the shortest element above the Y-axis
H_N = height of the longest element above the Y-axis
α = angle between the array axis and the line connecting the tips of the elements
θ'' = angle between the Z-axis and the array axis.

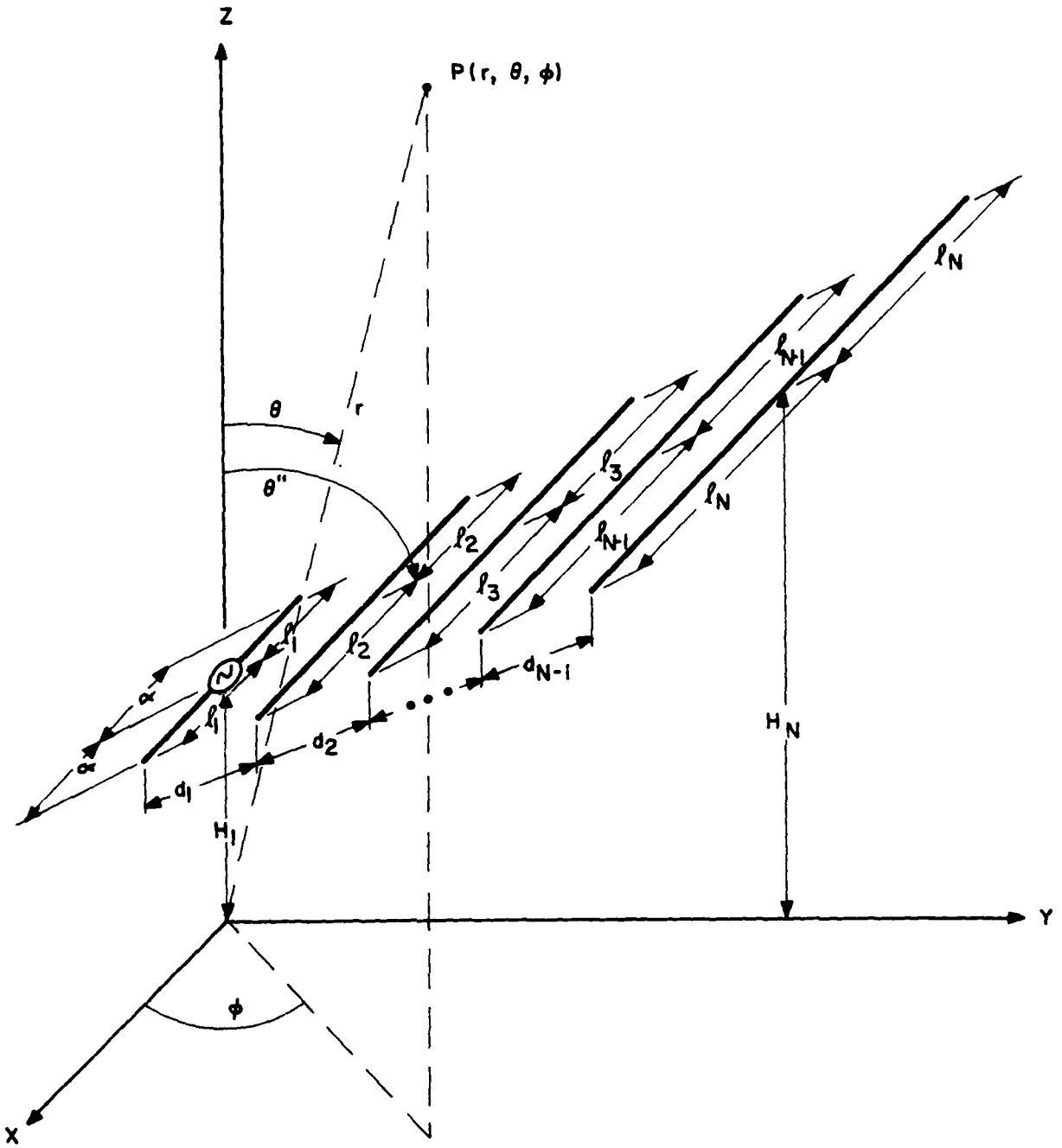

Figure 15. Horizontally polarized log-periodic dipole array.

VERTICALLY POLARIZED LOG-PERIODIC DIPOLE ARRAY

The vertically polarized log-periodic dipole array is the same basic structure as the horizontally polarized log-periodic dipole array except that the plane containing the array is vertical. The geometrical quantities for this antenna, shown in Figure 16, are as follows:

ℓ_i = half-length of the i^{th} element
d_i = spacing between the i^{th} element and the $(i + 1)^{th}$ element
H_1 = height of the center of the shortest element above the Y-axis
H_N = height of the center of the longest element above the Y-axis
α_1 = angle between the array axis and the line connecting the upper tips of the elements
α_2 = angle between the array axis and the line connecting the lower tips of the elements
α_3 = angle between the line connecting the lower tips of the elements and the Y-axis
θ" = angle between the Z-axis and the array axis.

CURTAIN ARRAY

The curtain array, shown in Figure 17, is a coplanar arrangement of dipole elements with spacings and excitations such that the direction of maximum far-field strength can be varied in both the vertical plane (XZ-plane) and the horizontal plane (XY-plane). The array of dipoles is installed in front of a wire screen to provide a unidirectional characteristic. The dipole-to-screen spacing is usually less than a half-wavelength.

The dipoles are arranged in bays of vertically stacked elements with variable spacing. The bays of elements are horizontally separated by variable distances.

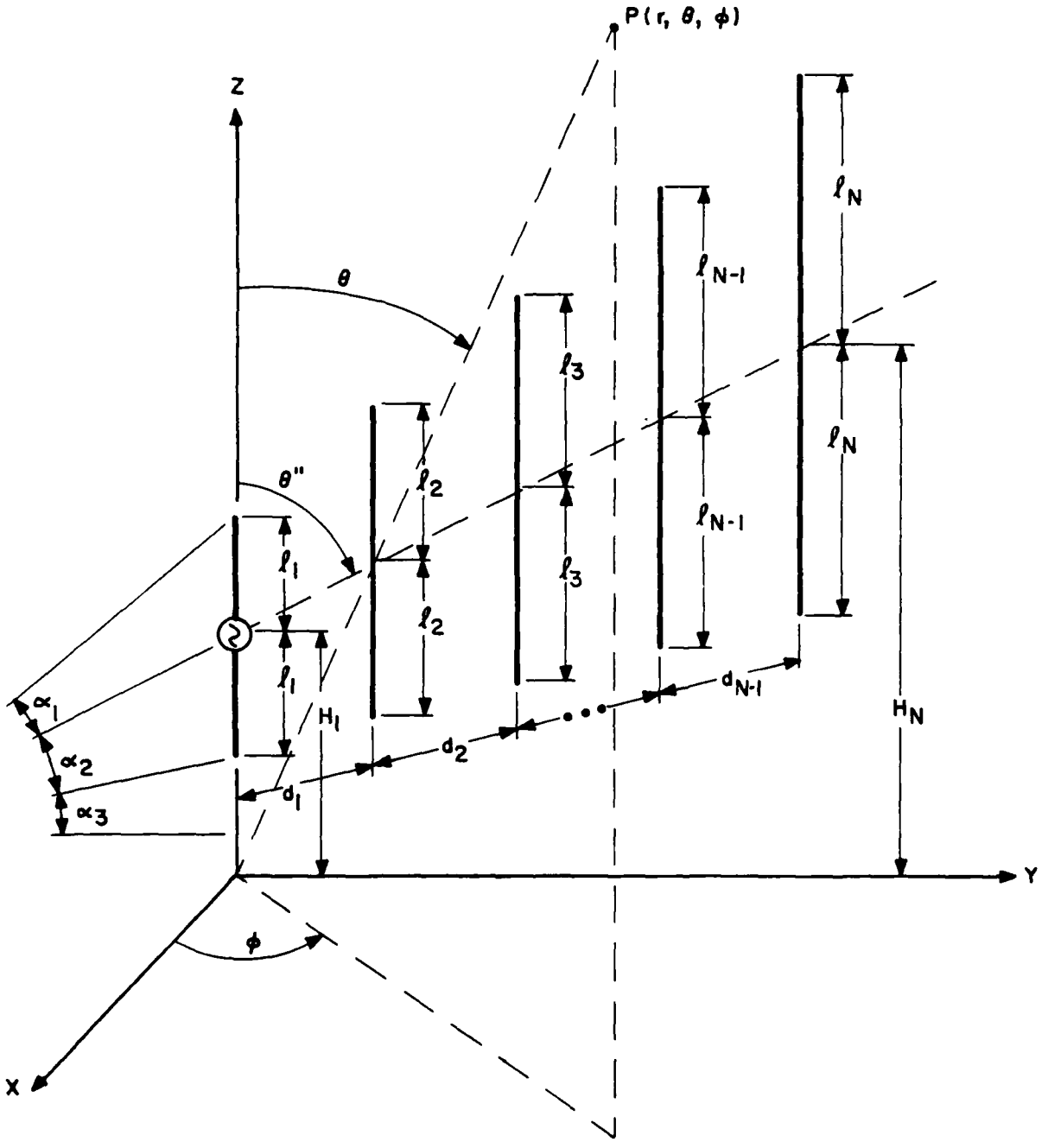

Figure 16. Vertically polarized log-periodic dipole array.

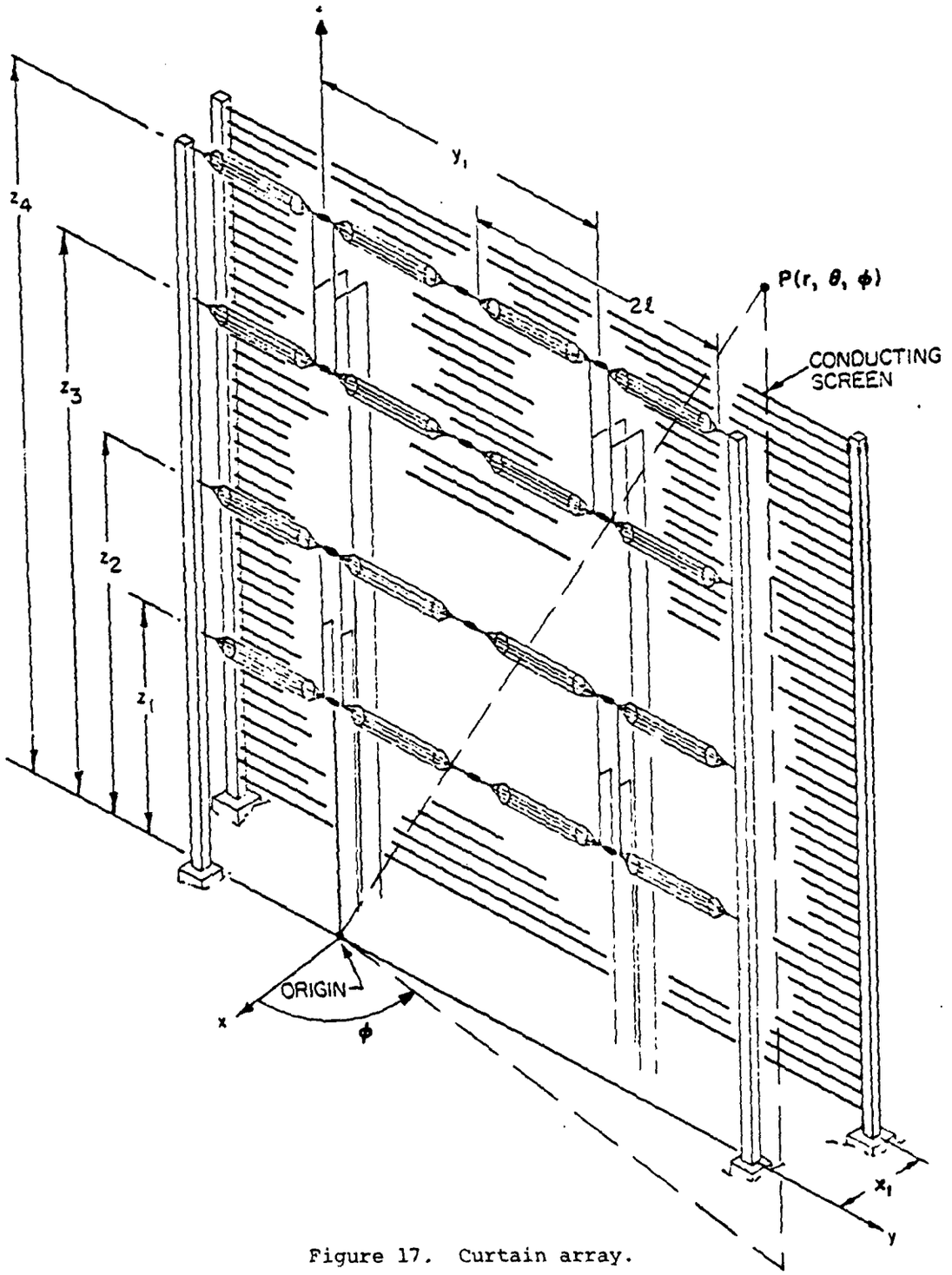

Figure 17. Curtain array.

The geometrical quantities of interest for the curtain array are:

ℓ = half-length of a dipole element
X_1 = spacing between the bays of dipoles and the wire screen
y_i = horizontal position of the center line of the $(i + 1)^{th}$ bay (where $y_o \triangleq 0$)
Z_i = height of the i^{th} element of each bay above ground.
M = number of elements in each bay
N = number of bays.

SLOPING DOUBLE RHOMBOID

The sloping double rhomboid, shown in Figure 18, consists of two sloping rhombics fed at a common apex and terminated at the opposite apexes with appropriate resistors. The sloping double rhomboid is also a traveling-wave antenna that can be used over a wide range of frequencies without the need for matching (coupling) networks between the feed point at the common apex and the attached transmission line. When the geometry for this antenna is carefully chosen, the result is a pattern with higher gain in the mainbeam direction and lower gain in the sidelobe regions that could be realized with a single rhombic.

The geometrical parameters for the sloping double rhombiod are:

ℓ_1 = length of the short legs of each rhombus
ℓ_2 = length of the long legs of each rhombus
α = angle between the principal antenna axis (Y-axis) and the major rhomboid axis
β = angle between the major rhomboid axis and the long leg
γ = angle between the major rhomboid axis and the short leg
H_1 = height of the feed point at the common apexes above the Y-axis
H_2 = height of the apexes at the ends of the short legs emanating from the feed point above the Y-axis

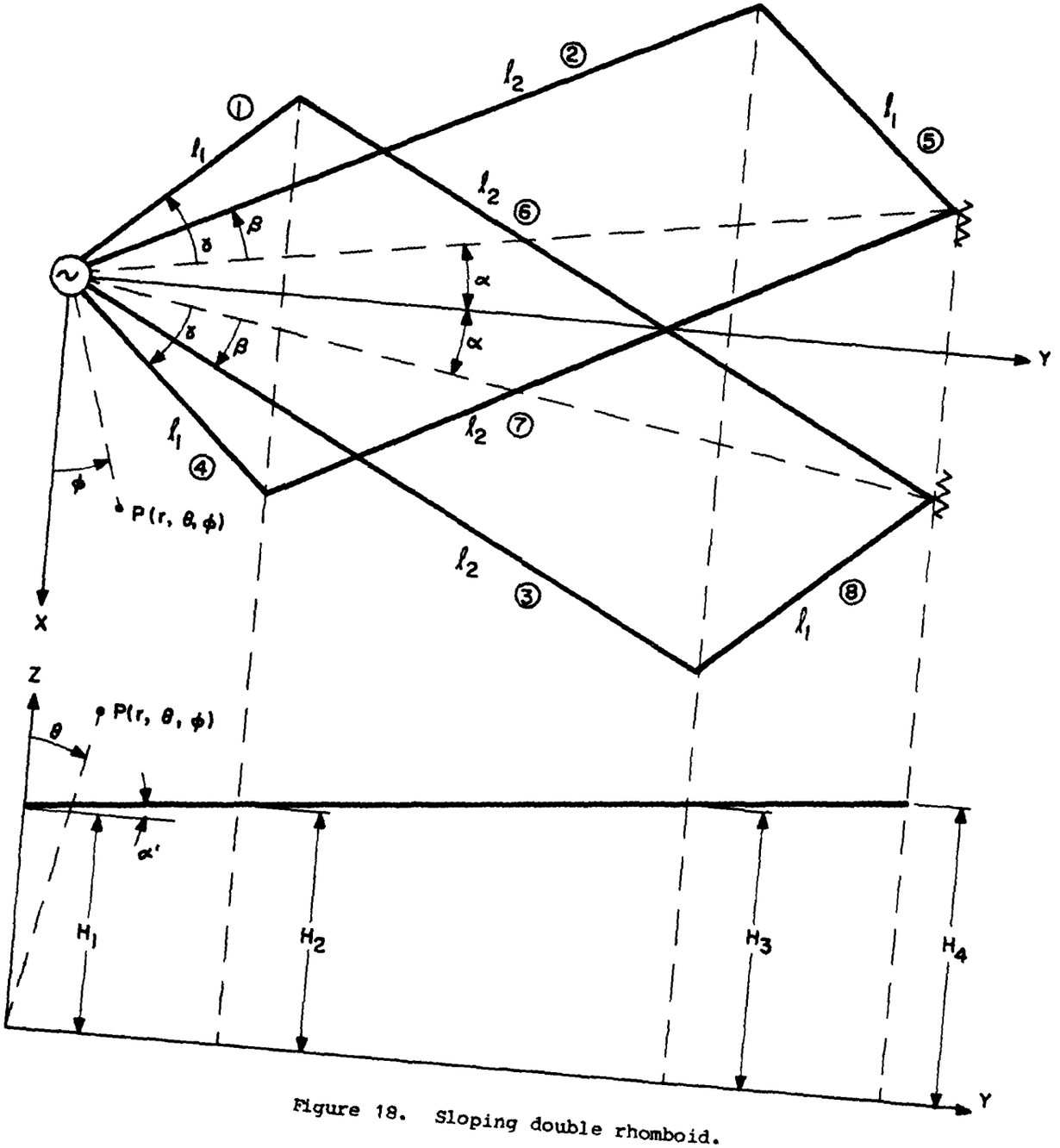

Figure 18. Sloping double rhomboid.

H_3 = height of the apexes at the ends of the long legs emanating from the feed point above the Y-axis

H_4 = height of the terminated apexes above the Y-axis

α' = angle between the plane containing the two rhomboids and the Y-axis.

KEY EQUATIONS

To facilitate the use of this report as a reference for key equations for each of the 16 types of antennas considered, TABLE 2 was prepared. TABLE 2 indicates the appropriate equations in APPENDIXES A and D that give the electric far-field components in each of the three regions considered:

1. Over planar earth
2. Over spherical earth within the radio horizon
3. In the diffraction region beyond the radio horizon.

The criteria used to determine in which of the three regions the observation point is located are given in Section 6 under the subsection, "Changeover Criteria." The equations for the electric far-field components indicated in TABLE 2 together with the changeover criteria given in Section 6 have been used at ECAC to write a computer program that calculates the electric far fields of the 16 types of antennas over lossy ground at any point in the far field.

TABLE 2 also indicates appropriate equations in APPENDIX A for calculating the directive gain of each of the 16 types of antennas as well as appropriate equations or values for radiation efficiency. Note that since the equations given in APPENDIX A for directive gain are expressed as numerical ratios, the directive gain in dB is given by:

$$G_d(\theta,\phi) = 10 \log_{10} g_d(\theta,\phi) \qquad (5\text{-}1)$$

TABLE 2

EQUATIONS FOR ELECTRIC FIELD STRENGTH, DIRECTIVE GAIN, AND RADIATION EFFICIENCY

(Page 1 of 3)

COMPONENT ELECTRIC FIELD STRENGTHS

	Over Planar Earth		Over Spherical Earth Within the Radio Horizon		In the Diffraction Region Beyond the Radio Horizon		Directive Gain	Radiation Efficiency	Figure Showing Geometry
Antenna Type	E_θ	E_ϕ	E_θ	E_ϕ	E_θ	E_ϕ			
Horizontal Dipole	A-17	A-18	D-1	D-2	A-32	A-33	A-23	0 dB	3
Vertical Monopole	A-46	0	D-3	0	A-59	0	A-50	A-53	4
Vertical Monopole with Radial-Wire Ground Screen	A-60 A-61 A-64	0	D-5 D-6	0	A-77	0	A-73	A-53	5
Elevated Vertical Dipole	A-94	0	D-8	0	A-104	0	A-98	0 dB	6
Inverted-L	A-108 A-109	A-110	D-10 D-12	D-13	A-132	A-133	A-119	A-120	7
Arbitrarily Tilted Dipole	A-137	A-138	D-14	D-15	A-155	A-156	A-142	0 dB	8
Sloping Long-Wire	A-160	A-161	D-16	D-17	A-177	A-178	A-167	-1.7 dB	9
Terminated Sloping-V	A-185 A-186 A-192	A-187 A-188 A-193	D-18 D-19 D-22	D-20 D-21 D-23	A-198 A-204	A-199 A-205	A-194	-1.7 dB	10

TABLE 2

(Page 2 of 3)

COMPONENT ELECTRIC FIELD STRENGTHS

Antenna Type	Over Planar Earth		Over Spherical Earth Within the Radio Horizon		In the Diffraction Region Beyond the Radio Horizon		Directive Gain	Radiation Efficiency	Figure Showing Geometry
	E_θ	E_ϕ	E_θ	E_ϕ	E_θ	E_ϕ			
Terminated Sloping Rhombic	A-185 A-186 A-210 A-211 A-214	A-187 A-188 A-212 A-213 A-215	D-18 D-19 D-24 D-26 D-27	D-20 D-21 D-25 D-28 D-29	A-219 A-225	A-220 A-226	A-216	-2.3 dB	11
Terminated Horizontal Rhombic	A-235 A-236 A-237	A-235 A-236 A-238	D-30,D-31 D-32,D-33 D-38	D-34,D-35 D-36,D-37 D-39	A-242 A-248	A-243 A-249	A-239	-1.7 dB	12
Side-loaded Vertical Half-Rhombic	A-263 A-265	A-264 A-266	D-40	D-41	A-270 A-276	A-271 A-277	A-267	-1.7 dB	13
Horizontal Yagi-Uda Array	A-283	A-284	D-42	D-43	A-302	A-303	A-293	-1.8 dB	14
Horizontally Polarized Log-Periodic Dipole Array	A-312 A-314	A-313 A-315	D-44	D-45	A-342 A-343	A-342 A-344	A-317	0 dB	15
Vertically Polarized Log-Periodic Dipole Array	A-349 A-351	0	D-46	0	A-363 A-367	0	A-362	-1.8 dB	16

TABLE 2

(Page 3 of 3)

COMPONENT ELECTRIC FIELD STRENGTHS

	Over Planar Earth		Over Spherical Earth Within the Radio Horizon		In the Diffraction Region Beyond the Radio Horizon		Directive Gain	Radiation Efficiency	Figure Showing Geometry
Antenna Type	E_θ	E_ϕ	E_θ	E_ϕ	E_θ	E_ϕ			
Curtain Array	A-369 A-373 A-374 A-375	A-370 A-373 A-374 A-376	D-48	D-49	A-373 A-374 A-384	A-373 A-374 A-385	A-380	0 dB	17
Sloping Double Rhomboid	A-405 through A-412 and A-427	A-413 through A-420 and A-428	D-50 through D-57 and D-66	D-58 through D-65 and D-67	A-430 through A-437 and A-446, A-452	A-438 through A-445 and A-447, A-453	A-429	-1.7 dB	18

where

$G_d(\theta,\phi)$ = directive gain as a function of the spherical angular coordinates θ and ϕ, in dB

$g_d(\theta,\phi)$ = directive gain as a function of the spherical angular coordiantes θ and ϕ as a numerical ratio (as given by the equations in APPENDIX A).

Also, the power gain is calculated simple from:

$$G_p(\theta,\phi) = G_d(\theta,\phi) + \eta_{dB} \qquad (5\text{-}2)$$

where

$G_p(\theta,\phi)$ = power gain as a function of the spherical angular coordinates θ and ϕ, in dB

η_{dB} = radiation efficiency, in dB.

The formulas for directive gain and radiation efficiency (presented in TABLE 2) and the formulas for transmission loss (presented in Section 6) have also been programmed at ECAC. Thus, APACK provides a versatile automated package for calculating far-field intensity, directive gain, power gain, and transmission loss for 16 types of antennas mounted over lossy ground.

The equations indicated in TABLE 2 are the primary equations used in calculating the various quantities. Secondary equations defining additional geometrical quantities and terms such as the radiation resistance are given in APPENDIX A in the same subsection as the primary equations. Other symbols and formulas that appear often in the primary equations are presented below.

SUPPLEMENTAL SYMBOLS AND FORMULAS

The following supplemental symbols and formulas are used with the equations indicated in TABLE 2 to calculate field intensities and gains.

Symbols frequently used are:

$$k = \frac{2\pi}{\lambda} = \text{free-space wave number, in (meters)}^{-1}$$

where

λ = wavelength, in meters

k_2 = wave number for the lossy medium under the antenna, in $(\text{meters})^{-1}$

α_{div} = divergence factor used for calculations over spherical earth within the radio horizon, given by Equation 3-1

$N_{r,\theta,\phi}$ = r-,θ-, or ϕ-component of the radiation vector used for calculations in the diffraction region beyond the radio horizon

F_r = Bremmer secondary factor used for calculations in the diffraction region beyond the radio horizon, given by Equation 4-13a

d = distance along the surface of a spherical earth between the antenna location and the observation point

R_d = distance from the feed point of the antenna to the observation point

θ_d = angle between the Z-axis and the line between the antenna feed point and the observation point

R_r = distance from the feed point of the image antenna and the observation point

θ_r = angle between the Z-axis and the line between the image antenna feed point and the observation point.

Formulas frequently used are:

$$n = \frac{k_2}{k} = \sqrt{\varepsilon_r - j\frac{18000\sigma}{f_{MHz}}} \qquad (5\text{-}3)$$

where

n = complex index of refraction for the lossy medium under the antenna (dimensionless)

ε_r = relative dielectric constant of the lossy medium under the antenna (dimensionless)

σ = conductivity of the lossy medium under the antenna, in mhos/meter

f_{MHz} = frequency, in MHz.

$$P_e = \frac{-jkR_r}{2 \sin^2 \theta_r} \left(\cos \theta_r + \frac{\sqrt{n^2 - \sin^2 \theta_r}}{n^2} \right)^2 \qquad (5\text{-}4)$$

where

P_e = complex numerical distance for vertical polarization (dimensionless)

and all other terms have been defined previously.

$$P_m = \frac{-jkR_r}{2 \sin^2 \theta_r} \left(\cos\theta_r + \sqrt{n^2 - \sin^2 \theta_r} \right)^2 \qquad (5\text{-}5)$$

where

P_m = complex numerical distance for horizontal polarization (dimensionless)

and all other terms have been defined previously.

$$F_e = 1-j\sqrt{\pi P_e}\, e^{-P_e}\, \mathrm{erfc}\,(j\sqrt{P_e}) \tag{5-6}$$

where

F_e = surface-wave attenuation function for vertical polarization (dimensionless)

and

erfc = complementary error function defined by:

$$\mathrm{erfc}(x) = 1 - \frac{2}{\sqrt{\pi}} \int_0^x e^{-\partial^2}\, dy \tag{5-7}$$

$$F_m = 1-j\sqrt{\pi P_m}\, e^{-P_m}\, \mathrm{erfc}\,(j\sqrt{P_m}) \tag{5-8}$$

where

F_m = surface-wave attenuation function for horizontal polarization (dimensionless)

$$R_v = \frac{n^2 \cos\theta_r - \sqrt{n^2 - \sin^2\theta_r}}{n^2 \cos\theta_r + \sqrt{n^2 - \sin^2\theta_r}} \tag{5-9}$$

where

R_V = Fresnel plane-wave reflection coefficient for vertical polarization (dimensionless)

$$R_H = \frac{\cos \theta_r - \sqrt{n^2 - \sin^2 \theta_r}}{\cos \theta_r + \sqrt{n^2 - \sin^2 \theta_r}} \qquad (5\text{-}10)$$

where

R_H = Fresnel plane-wave reflection coefficient for horizontal polarization (dimensionless).

SECTION 6

CALCULATIONS OF TRANSMISSION LOSS

The basic calculations performed by APACK are those for the electric far fields of a linear antenna over planar earth, over spherical earth within the radio horizon, and over spherical earth in the diffraction region beyond the radio horizon. Since the electric far fields are calculated, APACK can be used to calculate transmission loss as well as directive and power gains.

This section presents expressions used for calculating transmission loss, a discussion of field-strength curves presented by the International Radio Consultative Committee (CCIR), and a discussion of the changeover criteria used to calculate field strengths in different regions.

TRANSMISSION-LOSS EXPRESSIONS

Transmission loss (L) is defined by:[25]

$$L = P_T - P_R \tag{6-1}$$

where

L = transmission loss between the transmitting antenna and the receiving antenna, in dB

P_T = total power radiated from the transmitting antenna, in dBm

P_R = resultant signal power that would be available from an equivalent loss-free antenna, in dBm.

---

[25] Rice, P.L., Longley, A.G., Norton, K.A., and Barsis, A.P., Transmission Loss Predictions for Tropospheric Communication Circuits, NBS Technical Note 101, Vols. I and II, National Bureau of Standards, Boulder, CO, 1967.

Transmission loss can also be expressed as:

$$L = P_T' + P_R' + \eta_T + \eta_R \qquad (6\text{-}2)$$

where

P_T' = power input to the feed point of the transmitting antenna, in dBm
P_R' = resultant signal power available at the feed point of the receiving antenna, in dBm
η_T = radiation efficiency of the transmitting antenna, in dB
η_R = radiation efficiency of the receiving antenna, in dB.

(Note that η_T and η_R are always less than or equal to 0 dB because radiation efficiency is always less than or equal to 100%.)

Basic transmission loss (L_b) which is the loss between two lossless isotropic antennas is defined in Reference 19 as:

$$L_b = L + G_p \qquad (6\text{-}3)$$

where

L_b = basic transmission loss, in dB
G_p = path antenna gain, in dBi.

When multipathing and antenna efficiencies are taken into account, the path antenna gain is not the sum of the directive gains. Thus, in general:

$$G_p \neq G_{Td} + G_{Rd} \quad (6\text{-}4)$$

where

G_{Td} = directive gain of the transmitting antenna, in dBi
G_{Rd} = directive gain of the receiving antenna, in dBi.

The basic transmission loss can also be expressed as:

$$L_b = L_{bf} + ADB \quad (6\text{-}5)$$

where

L_{bf} = basic transmission loss in free space, in dB
ADB = attenuation relative to free-space loss (where all difficult problems in analyzing propagation phenomena are hidden), in dB.

The basic free-space transmissin loss (L_{bf}) can also be expressed as:

$$L_{bf} = 20 \log_{10} \frac{4\pi d}{\lambda} = 32.45 + 20 \log_{10} f_{MHz} + 20 \log_{10} d_{km} \quad (6\text{-}6)$$

where

d = path length, in meters
λ = wavelength, in meters
f_{MHz} = frequency, in MHz
d_{km} = path length, in kilometers.

From the above equations:

$$L = L_{bf} + ADB - G_p$$

$$= 32.45 + 20 \log_{10} f_{MHz} + 20 \log_{10} d_{km} + ADB - G_p \quad (6\text{-}7)$$

where, in this case

$$G_p = G_{Td} + G_{Rd} \quad (6\text{-}8)$$

The resultant signal power available at the feed point of the receiving antenna (P_r') is then given in terms of the power input to the feed point of the transmitting antenna (P_T'), directive gains (G_{Td}, G_{Rd}), and radiation efficiencies (η_T, η_R) by:

$$P_R' = P_T' - 32.45 - 20 \log_{10} f_{MHz} - 20 \log_{10} d_{km} - ADB + G_{Td} + G_{Rd} + \eta_T + \eta_R \quad (6\text{-}9)$$

where

$$ADB = 20 \log_{10} \frac{1}{|A|} \quad (6\text{-}10)$$

with

$$|A| = \frac{|\text{Actual disturbed field at observation point}|}{|\text{Free-space field at observation point}|} \quad (6\text{-}11)$$

In terms of spherical coordinates (r,θ,d), $|A|$ can be expressed as:

$$|A| = \frac{\sqrt{|E_\theta|^2 + |E_\phi|^2}}{\sqrt{|E_{\theta f}|^2 + |E_{\phi f}|^2}} \quad (6\text{-}12)$$

where

$|E_\theta|$ = magnitude of the θ-component of the actual disturbed field at the observation point, in volts/meter

$|E_{\theta f}|$ = magnitude of the θ-component of the free-space field at the observation point, in volts/meter

$|E_{\phi f}|$ = magnitude of the ϕ-component of the free-space field at the observation point, in volts/meter

$|E_\phi|$ = magnitude of the ϕ-component of the actual disturbed field at the observation point, in volts/meter.

Equations 6-9, 6-10, and 6-12 are the expressions used by APACK to calculate transmission loss.

CCIR CURVES

Various propagation models have been used at ECAC to predict ground wave loss over a spherical earth. These models include curves published by the CCIR[26] and other models referred to at ECAC as IPS and Nλ (see References 3

[26] International Radio Consultative Committee (CCIR), Recommendations and Reports of the CCIR, 1978, Propagation in Non-Ionized Media, Vol. V, XIVth Plenary Assembly, Kyoto, Japan, 1978.

and 4, respectively). The CCIR curves which are based on Bremmer's formulation (see Reference 17) assume that both the transmitting and receiving antennas are located on the ground and that both antennas are Hertzian dipoles. The CCIR curves based on these assumptions are presented in terms of field strength which can be converted to basic transmission loss (see Reference 26) by:

$$L(dB) = 132.45 + 20 \log_{10} f_{MHz} - E \qquad (6\text{-}13)$$

where

$L(dB)$ = basic transmission loss, in dB

f_{MHz} = frequency, in MHz

E = electric field strength, in dB, with respect to 1 microvolt/meter (dB (μV/m)).

The other models used at ECAC (see References 3 and 4) predict basic transmission loss without calculating field strength but do account for the heights of the antenna feed points above ground. APACK predicts basic transmission loss from calculated values of electric field strength. The APACK field strengths account for the actual antenna structure and include the effects of the contributions of the direct, ground-reflected, and surface waves.

CHANGEOVER CRITERIA

The calculations of electric far fields made by APACK depend on the region in which the observation point is located. Three regions are considered:

Region 1. The line-of-sight region when the antenna is near the ground so that the earth can be considered as planar.

Region 2. The line-of-sight region when the antenna is well above the ground so that the earth must be considered as spherical.

Region 3. The diffraction region beyond the radio horizon.

The calculations include the surface-wave terms in Region 1 but not in Region 2, because the surface wave is negligible when the antenna is well above the ground. The calculations made for Region 3 (the diffraction region) can be used for all three regions. However, since a large number of terms are required for convergence of the Bremmer series within the radio horizon, APACK uses the Bremmer formulation only in the diffraction region (Region 3).

The APACK criteria for determining the appropriate region for the calculations have been adopted from Reference 22 and are described below. The region in which the observation point is located is determined by the path length, the effective radius of the earth (in terms of atmospheric refractivity), the heights of the feed points of the transmitting and receiving antennas above ground, and frequency.

Four quantities (d, d_c, d_D, and M) are calculated, and the appropriate region is then selected from the following relationships among these quantities.

1. If $d \leq d_c$ and $d_c > Md_D$, then the observation point is in Region 1 (line-of-sight, planar earth).
2. If $d \leq Md_D$ and $d_c \leq Md_D$, then the observation point is in Region 2 (line-of-sight, spherical earth).
3. If ($d > d_c$ and $d_c > Md_D$) or ($d > Md_D$ and $d_c \leq Md_D$), then the observation point is in Region 3 (diffraction region).

The quantities d, d_c, d_D, and M are defined as follows:

d = path length, in kilometers

$$d_c \begin{cases} = 148 \times 10^{-4} \dfrac{a_e^{1.0195}}{f_{MHz}^{0.1194}}, & 0.15 \leq f_{MHz} < 1 \quad (6\text{-}14) \\ = 148 \times 10^{-4} \dfrac{a_e^{1.0195}}{f_{MHz}^{0.5305}}, & 1 \leq f_{MHz} < 100 \quad (6\text{-}15) \\ 59.5 \times 10^{-4} \dfrac{a_e^{1.0195}}{f_{MHz}^{0.3337}}, & 100 \leq f_{MHz} \leq 500 \quad (6\text{-}16) \end{cases}$$

where

$$a_e = 6370 \left[1 - 0.04665 e^{0.005577 N_s}\right]^{-1} \quad (6\text{-}17)$$

$$N_s = N_o e^{-0.1057 h_s} \quad (6\text{-}18)$$

with

a_e = effective earth radius, in kilometers

N_s = surface atmospheric refractivity, in N-units

N_o = surface atmospheric refractivity reduced to sea level, in N-units

h_s = elevation of the surface above mean sea level, in kilometers.

(If N_o and h_s are not given, $N_s = 301$ is assumed.)

$$d_D = \sqrt{-2k + k^2 + 2 a_e h_1 \times 10^{-3}} + \sqrt{k^2 + 2 a_e h_2 \times 10^{-3}} \qquad (6\text{-}19)$$

where

$$k = a_e \left(\frac{\lambda \times 10^{-3}}{2\pi a_e}\right)^{\frac{1}{3}} \qquad (6\text{-}20)$$

h_1 = height of the transmitting antenna feed point above ground, in meters

h_2 = height of the receiving antenna feed point above ground, in meters

λ = wavelength, in meters.

$$m = \begin{cases} 0.75, & f_{MHz} < 3 \qquad (6\text{-}21) \\ 1.0, & f_{MHz} \geq 3 \qquad (6\text{-}22) \end{cases}$$

SECTION 7
COMPARISONS BETWEEN GAINS PREDICTED BY APACK AND OTHER DATA

For each of the 16 types of linear antennas considered in APACK, predictions of APACK power gains as a function of elevation (vertical) and/or azimuth (horizontal) angle were made for antennas mounted over soil with various permittivities and conductivities and/or over sea water. The APACK predictions were compared with other available data, including manufacturer's data, predictions from the SKYWAVE computer model developed by ITS (see Reference 1), and predictions resulting from Ma's three-term current distribution (see Reference 14).

APACK gain predictions were also compared with gain predictions resulting from modeling the antennas with the Numerical Electromagnetic Code (NEC), a method-of-moments computer program developed at the Lawrence Livermore Laboratory under the sponsorship of the Naval Ocean Systems Center (NOSC) and the Air Force Weapons Laboratory (AFWL) (see Reference 2). In most cases, there is reasonable agreement between the APACK predictions and the NEC predictions. This indicates that APACK, based on sinusoidal current distribution for resonant antennas and exponential current distribution for traveling-wave antennas, provides reasonable predictions and at the same time large savings in computer time. For example, the time required to obtain gains for an electrically large antenna using APACK, such as a sloping double rhomboid, can be approximately 1/1000th of the time required by the rigorous NEC method-of-moments program.

The comparisons provided in this section are not exhaustive, but they do provide an indication of the versatility and reasonableness of the APACK model for providing rapid predictions of gains. Comparisons performed for the various types of antennas are described below and shown in the accompanying figures.

AD-A102 622 IIT RESEARCH INST ANNAPOLIS MD F/G 20/14
APACK, A COMBINED ANTENNA AND PROPAGATION MODEL,(U)
JUL 81 S CHANG, H C MADDOCKS F19628-80-C-0042
UNCLASSIFIED ESD-TR-80-102 NL

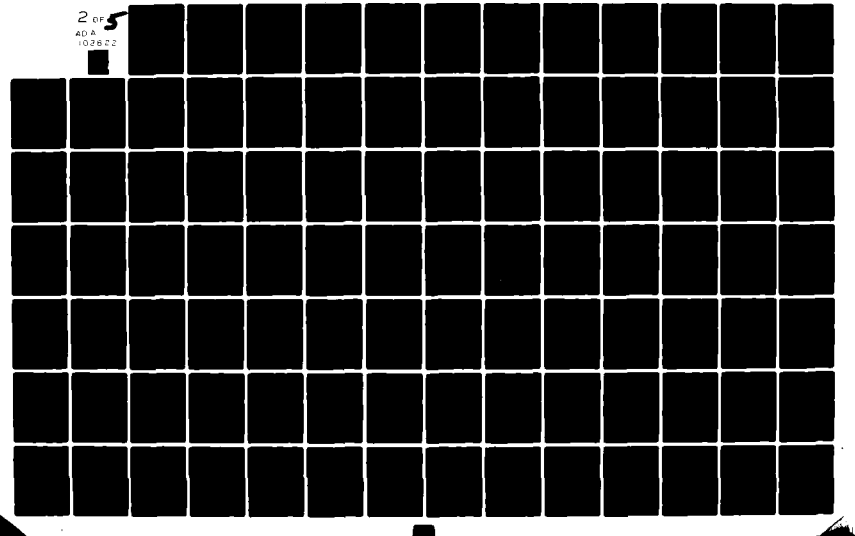

HORIZONTAL DIPOLE

Figures 19 through 22 show comparisons between APACK, NEC, and manufacturer's data for the Collins 637T-1/2 half-wave horizontal dipole mounted above soil for frequencies of 5, 10, 20, and 30 MHz, respectively. In all cases, the gains predicted by APACK differ by less than approximately 2 dB from the other data.

VERTICAL MONOPOLE

Figure 23 shows comparisons between APACK and NEC for a quarter-wave vertical monopole (without a ground screen) mounted above soil. The gains predicted by APACK differ from those predicted by NEC by less than approximately 1 dB. The APACK predictions shown in Figure 23 are identical to those of the ITS SKYWAVE program (see Reference 1).

VERTICAL MONOPOLE WITH RADIAL-WIRE GROUND SCREEN

Figure 24 shows comparisons between APACK, NEC, and Ma's three-term current-distribution predictions for a vertical monopole with radial-wire ground screen mounted above soil and sea water at an operating frequency of 10 MHz. The differences between APACK predictions and Ma's predictions are less than approximately 1 dB for both soil and sea water. The NEC predictions are identical to Ma's for the monopole mounted over sea water. When the monopole is mounted over soil, the NEC predictions of gain are considerably higher (as much as about 3 dB) than either APACK or Ma. The reason for the higher gains predicted by NEC has not been determined.

ELEVATED VERTICAL DIPOLE

Figure 25 shows comparisons of predictions made by APACK, NEC, and the ITS SKYWAVE program for a vertical half-wave dipole with its feed point located 2.5 meters above soil at a frequency of 30 MHz. The differences between the APACK predictions and the NEC predictions are less than 5 dB for

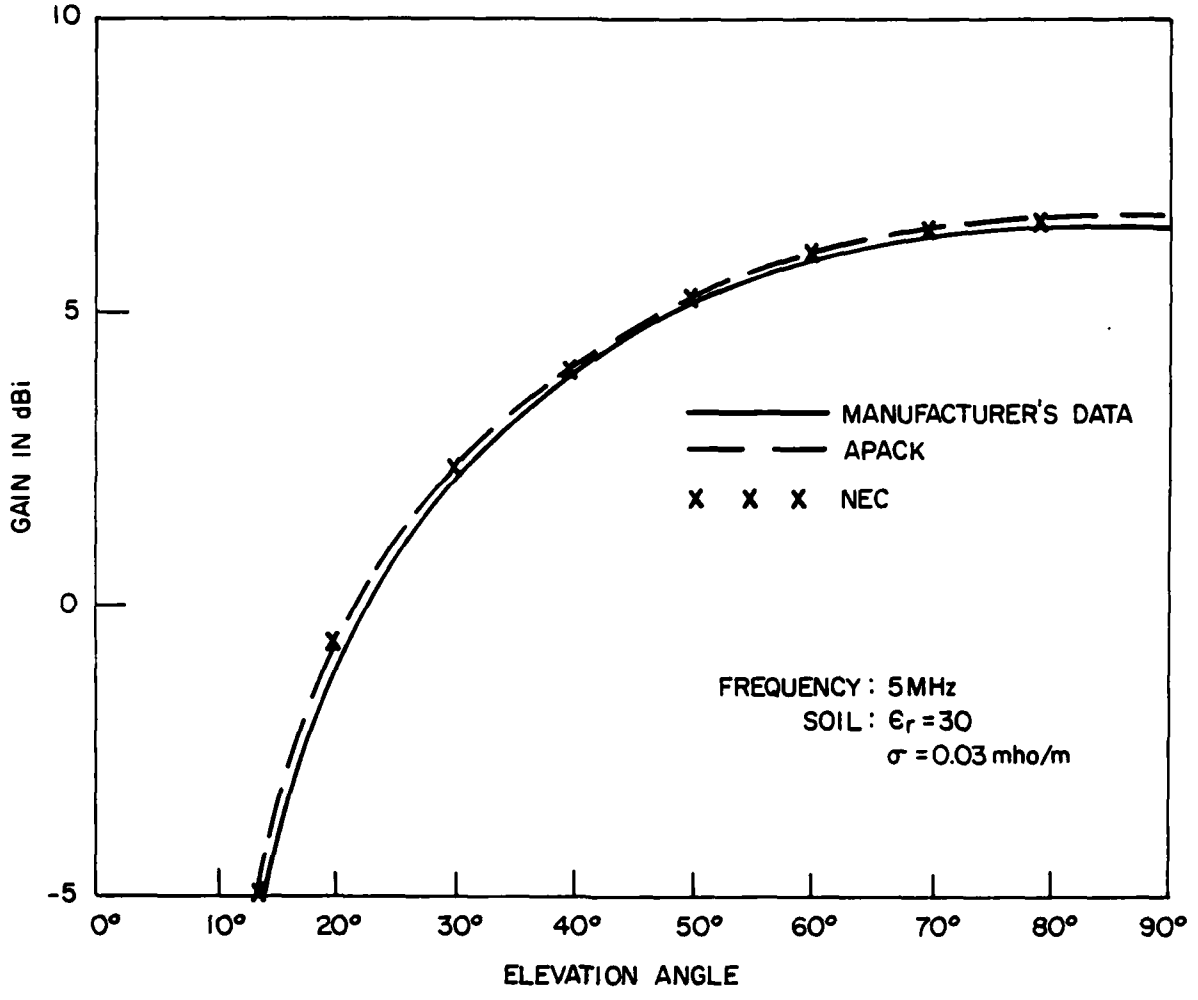

Figure 19. Elevation patterns of a Collins 637T-1/2 half-wave horizontal dipole mounted 7.6 m above soil (5 MHz).

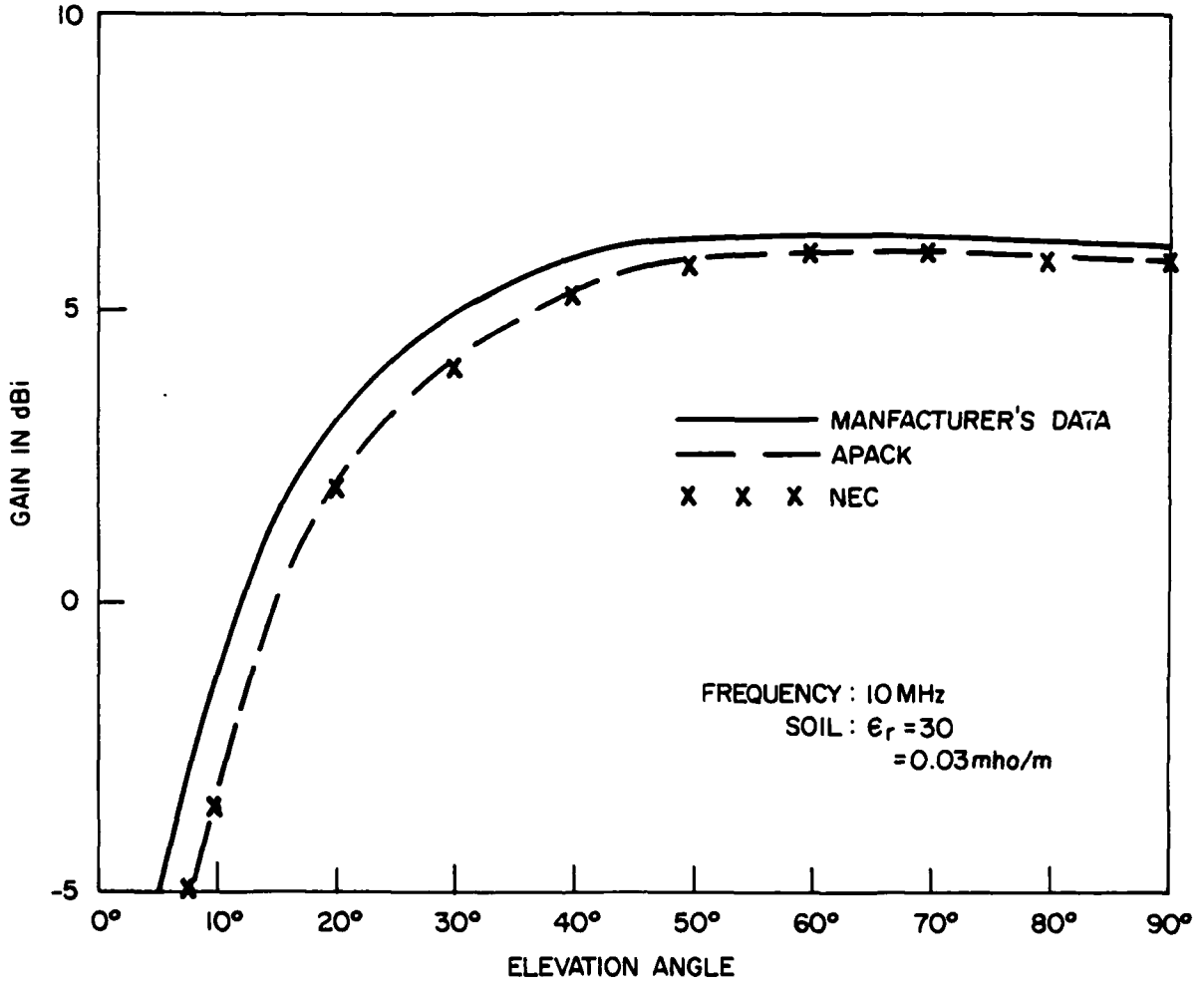

Figure 20. Elevation patterns of a Collins 637T-1/2 half-wave horizontal dipole mounted 7.6 m above soil (10 MHz).

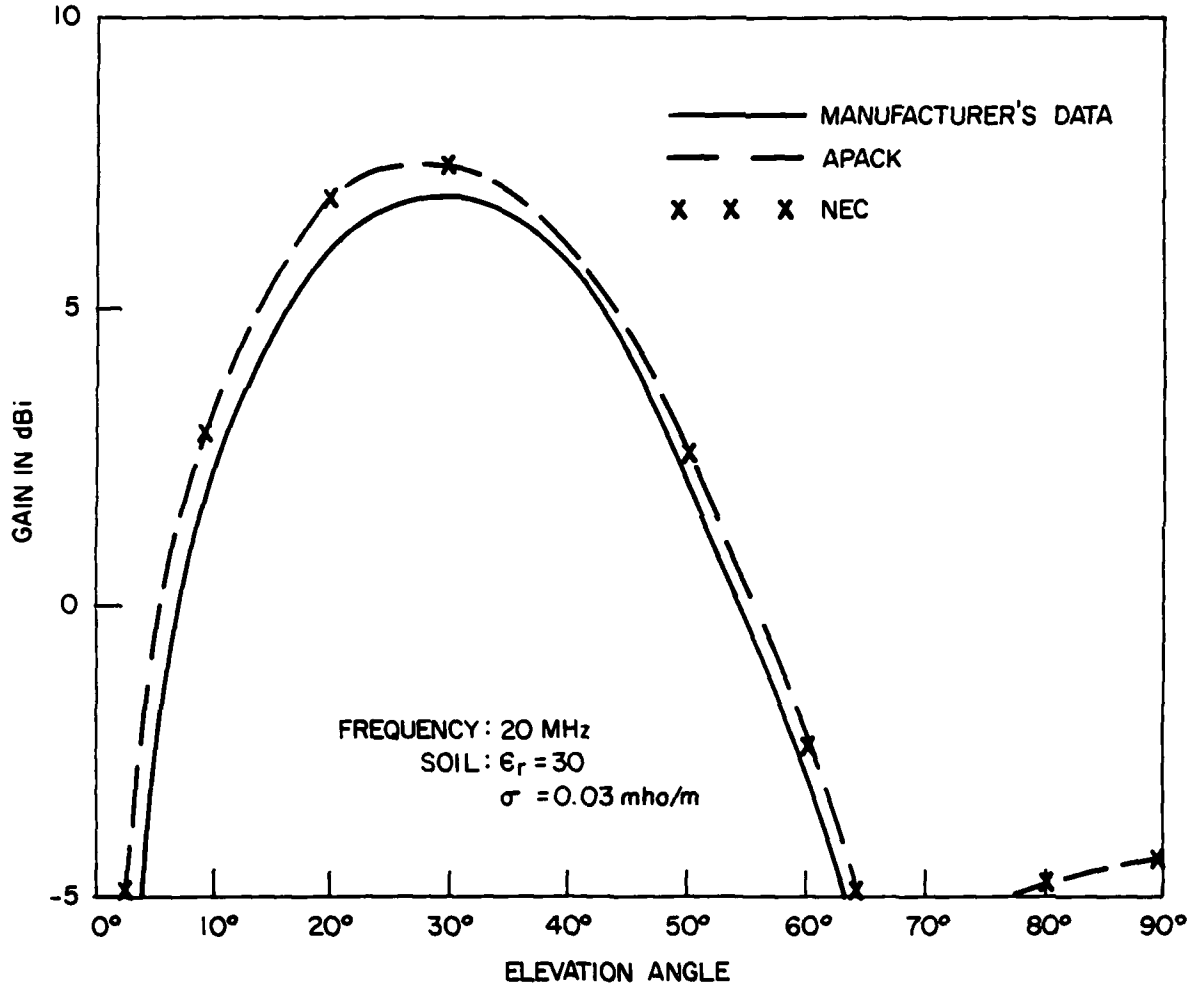

Figure 21. Elevation patterns of a Collins 637T-1/2 half-wave horizontal dipole mounted 7.6 m above soil (20 MHz).

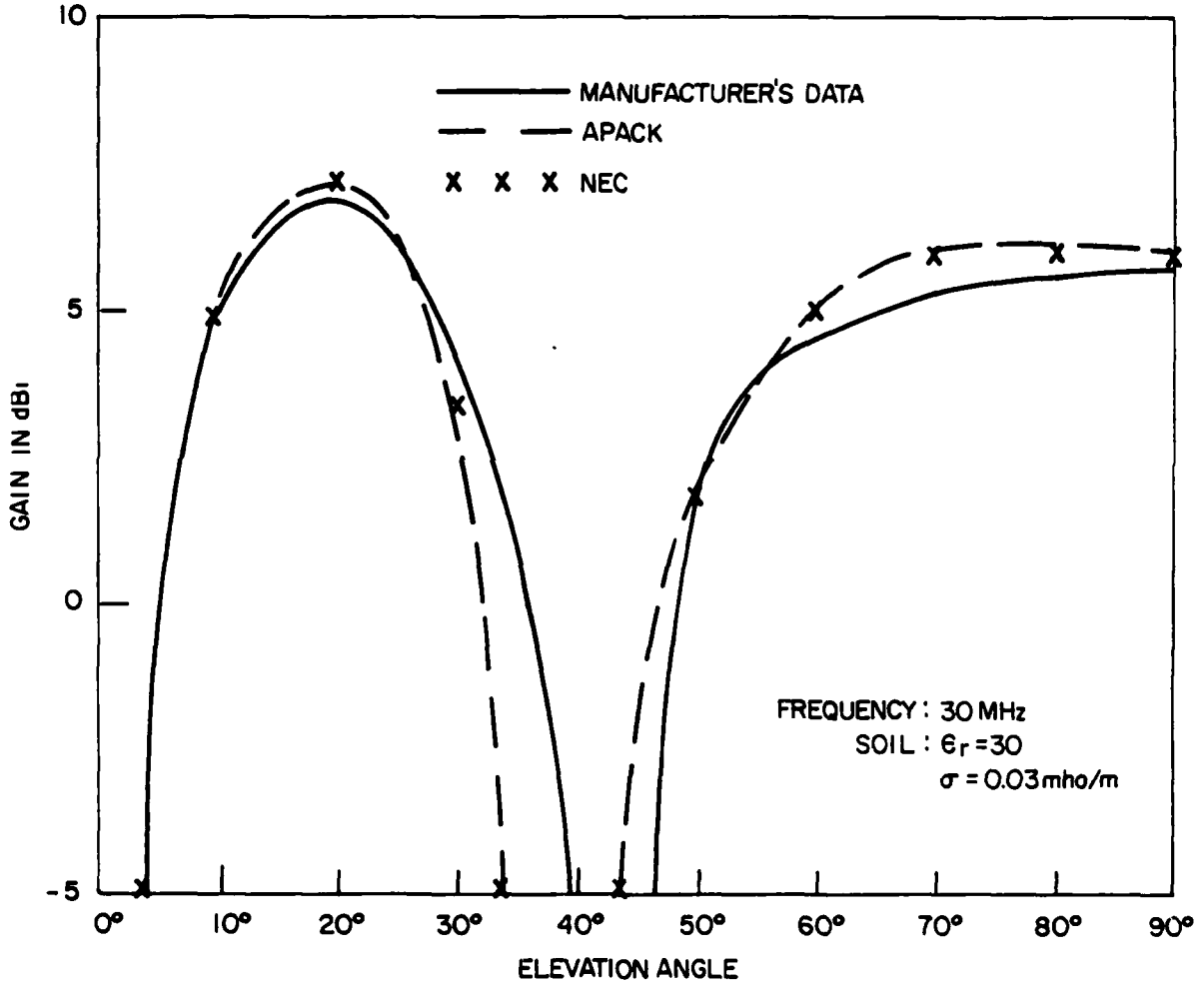

Figure 22. Elevation patterns of a Collins 637T-1/2 half-wave horizontal dipole mounted 7.6 m above soil (30 MHz).

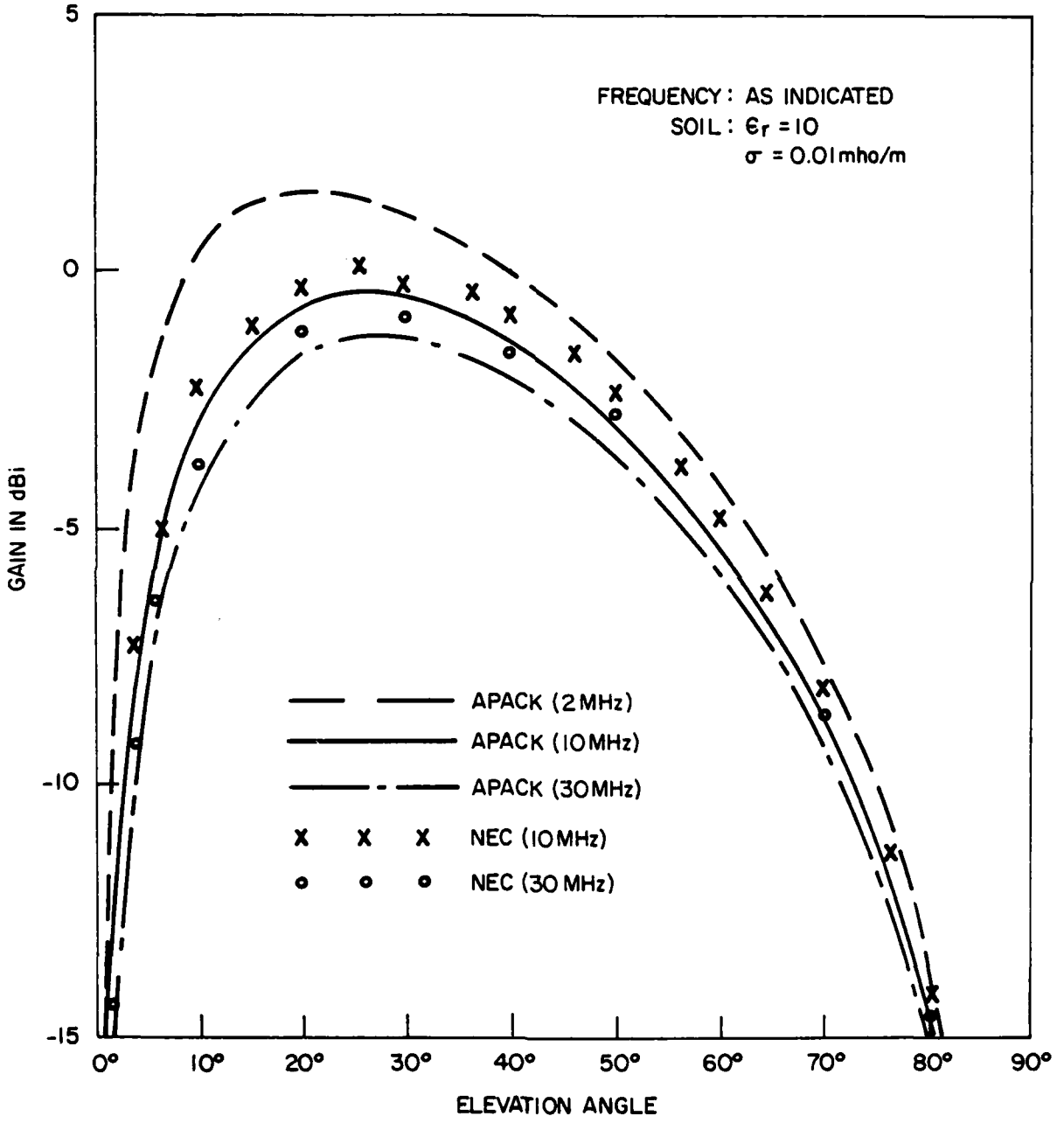

Figure 23. Elevation patterns of a quarter-wave vertical monopole mounted above soil.

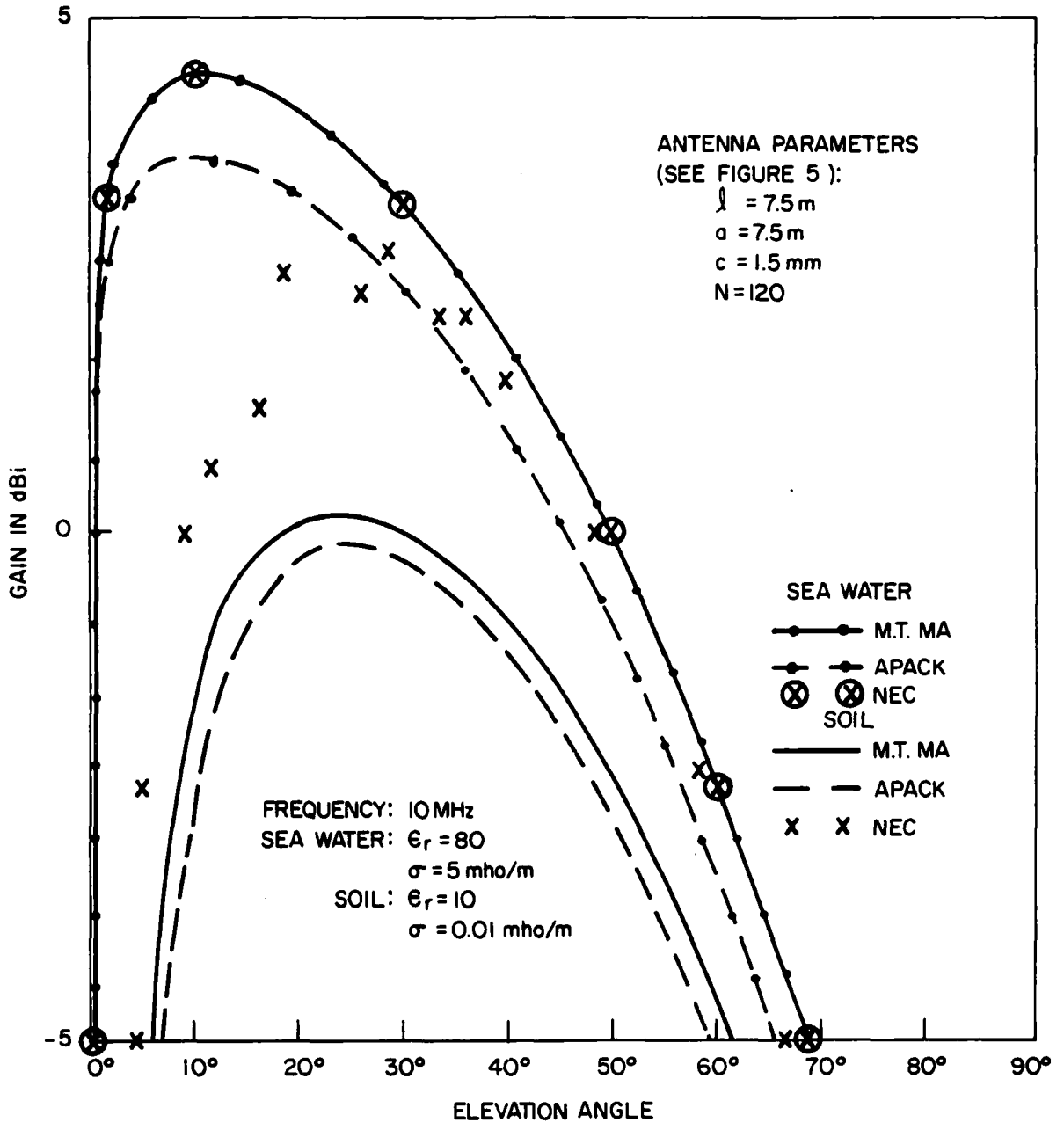

Figure 24. Elevation patterns of a vertical monopole with radial-wire ground screen mounted above sea water and soil.

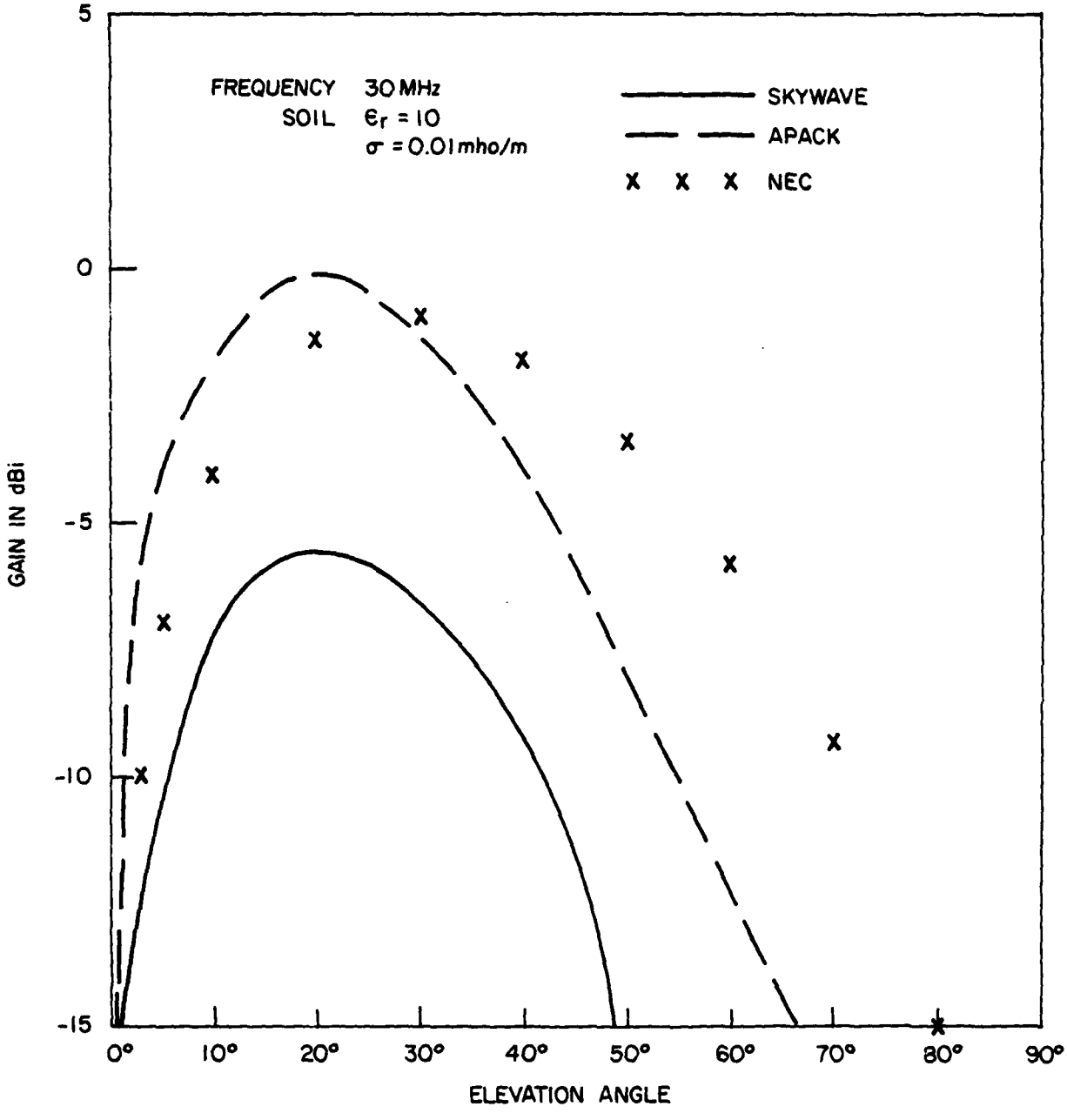

Figure 25. Elevation patterns of a half-wave vertical dipole mounted with feed point 2.5 m above soil.

low elevation angles and approach 7 dB near the zenith. The gains predicted by the ITS SKYWAVE program are considerably less than those predicted by either APACK or NEC. The low values of SKYWAVE gains are due to the fact that SKYWAVE uses the free-space value of radiation resistance in computing gain.

INVERTED-L

Figures 26, 27, and 28 show comparisons between APACK, NEC, and ITS SKYWAVE for an inverted-L (mounted above soil) operating at frequencies of 10, 20, and 30 MHz, respectively. The differences between the predicted gains (as much as 7 dB) are believed to be due mainly to differences in the values used for the radiation resistance. The reason for the high values of gain predicted by NEC at 30 MHz, as compared with the APACK and SKYWAVE values, has not been explained.

ARBITRARILY TILTED DIPOLE

The horizontal dipole and elevated vertical dipole are both special cases of the arbitrarily oriented dipole. Since comparisons of APACK predictions with other data for both horizontal and vertical orientations indicated reasonable agreement, comparisons for other orientations were not made.

SLOPING LONG-WIRE

Figure 29 shows comparisons between APACK, NEC, and ITS SKYWAVE predictions for a sloping long-wire (mounted over soil) operating at 10 MHz. The predictions of APACK and SKYWAVE in this case are identical, but both APACK and SKYWAVE predict lower gains than NEC. The difference in gains, varying from as much as 3 dB at low elevation angles to as much as 5 dB near the zenith is believed to be due to the approximations made by APACK SKYWAVE for the radiation resistance.

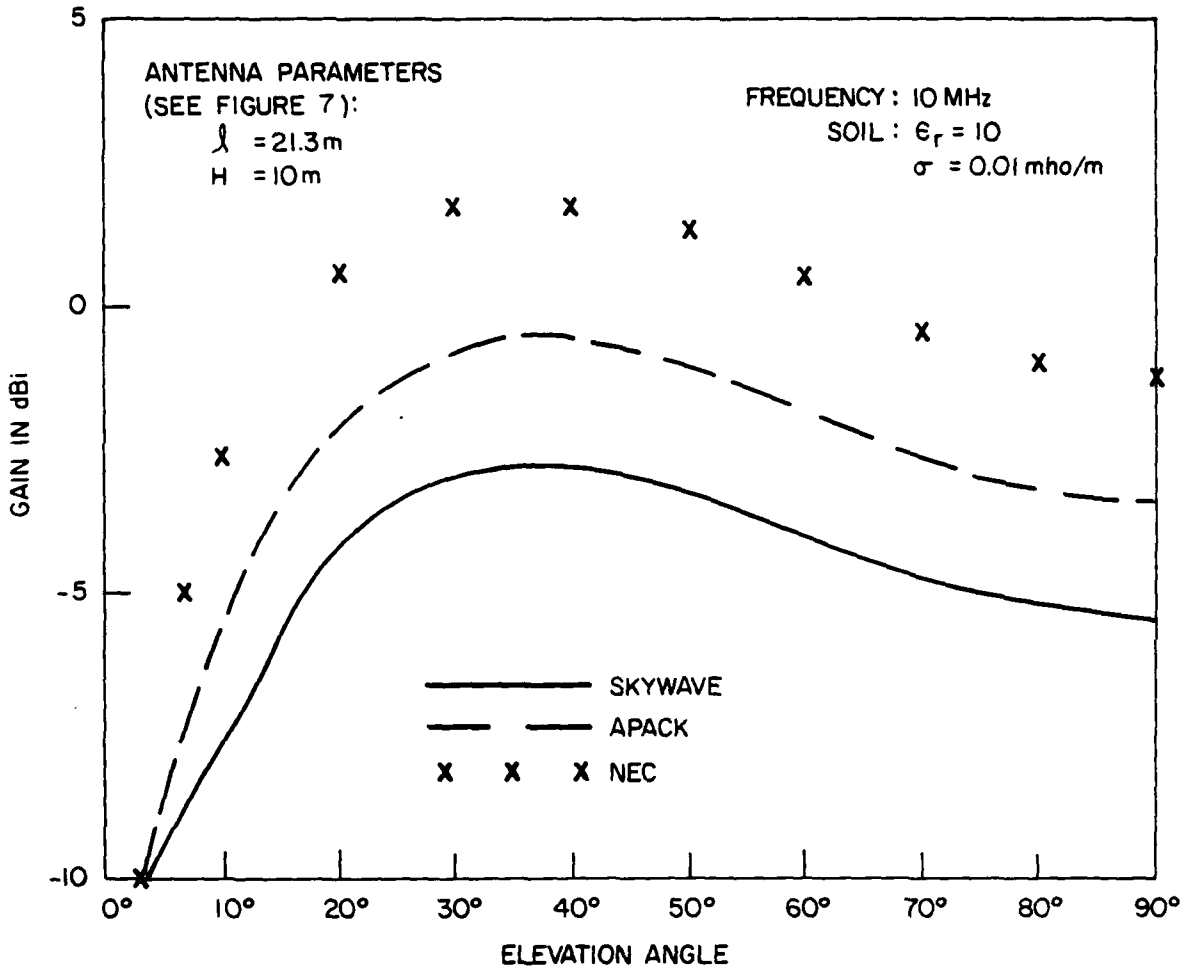

Figure 26. Elevation patterns of an inverted-L mounted above soil (10 MHz).

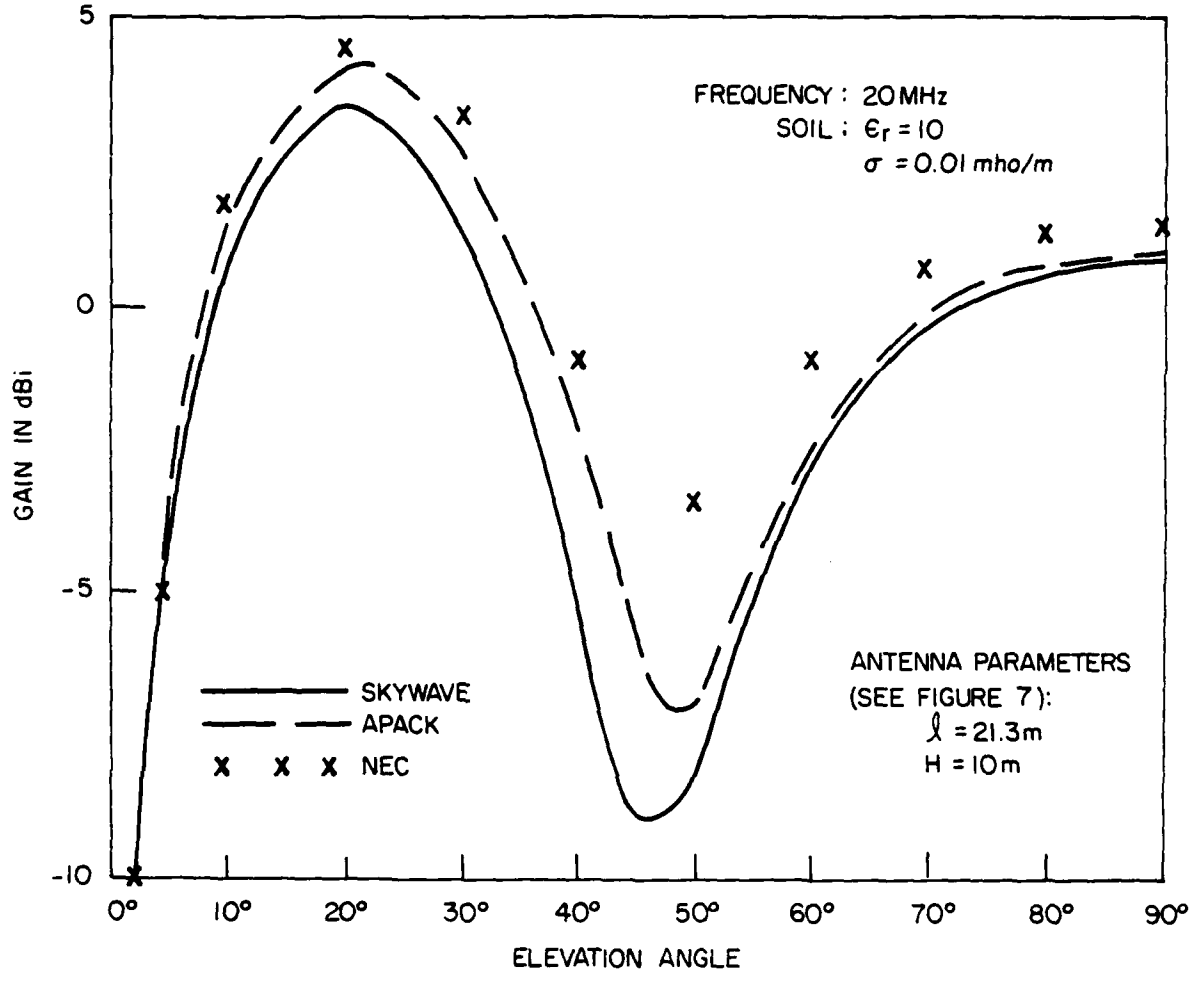

Figure 27. Elevation patterns of an inverted-L mounted above soil (20 MHz).

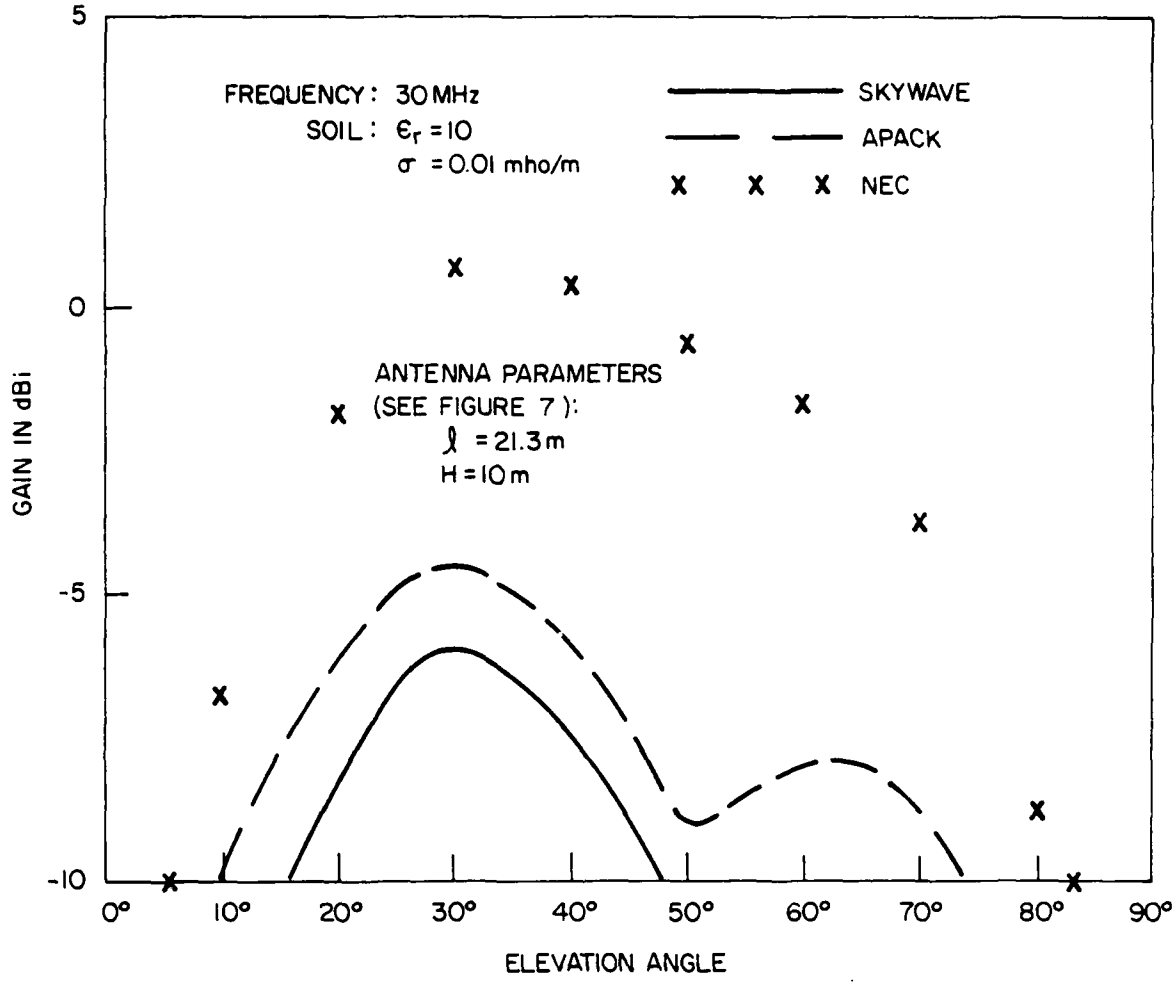

Figure 28. Elevation patterns of an inverted-L mounted above soil (30 MHz).

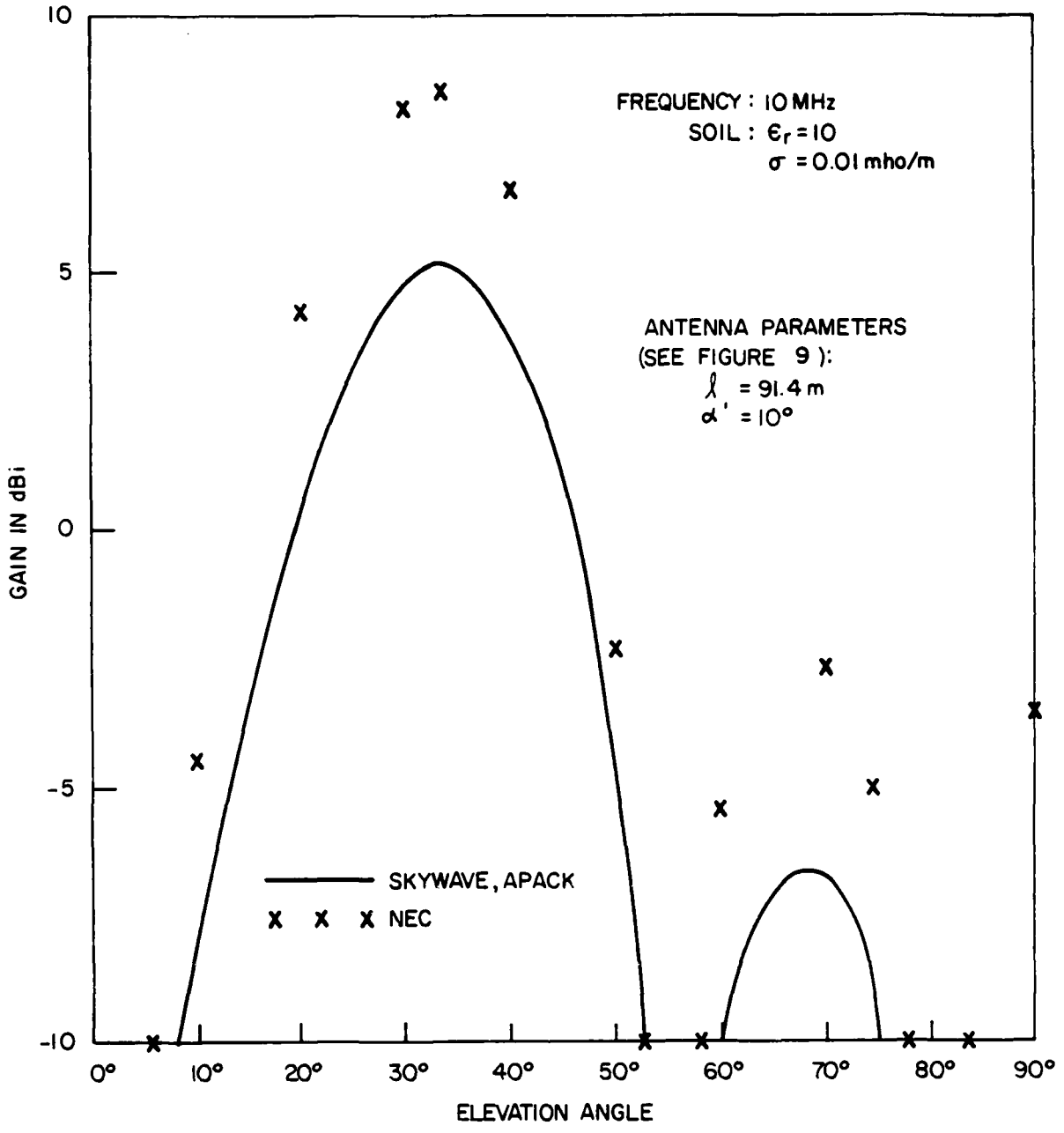

Figure 29. Elevation patterns of a sloping long-wire mounted above soil.

TERMINATED SLOPING-V

Figure 30 shows comparisons between APACK, NEC, and Ma's three-term current-distribution model for a terminated sloping-V (mounted over soil) operating at a frequency of 10 MHz. Figure 30 gives gains as a function of elevation angle, and Figure 31 gives gains as a function of azimuth angle for the same antenna and operating frequency. The gains shown in Figure 31 are for an elevation angle of 14 degrees.

Figure 30 indicates excellent agreement in the elevation pattern, with gains predicted by APACK differing from other data by about 1 dB or less. The agreement indicated in Figure 31 for the azimuth pattern is also very good, with gains predicted by APACK differing from other data by 3 dB or less.

TERMINATED SLOPING RHOMBIC

Figures 32 and 33 show comparisons between APACK, NEC, and Ma's predictions for a terminated sloping rhombic over sea water for an operating frequency of 10 MHz. Figure 32, comparing elevation patterns, indicates agreement between APACK and other data within 5 dB at most, with 3 dB being typical. Figure 33, comparing azimuth patterns at an elevation angle of 20 degrees, indicates agreement between APACK and other data within approximately 3 dB.

TERMINATED HORIZONTAL RHOMBIC

Figure 34 shows comparisons between APACK, NEC, and SKYWAVE for a terminated horizontal rhombic operating at 10 MHz mounted over soil. The elevation gains shown in Figure 34 indicate that APACK predictions differ from other data by not more than 2 dB at low elevation angles and by not more than 5 dB near the zenith.

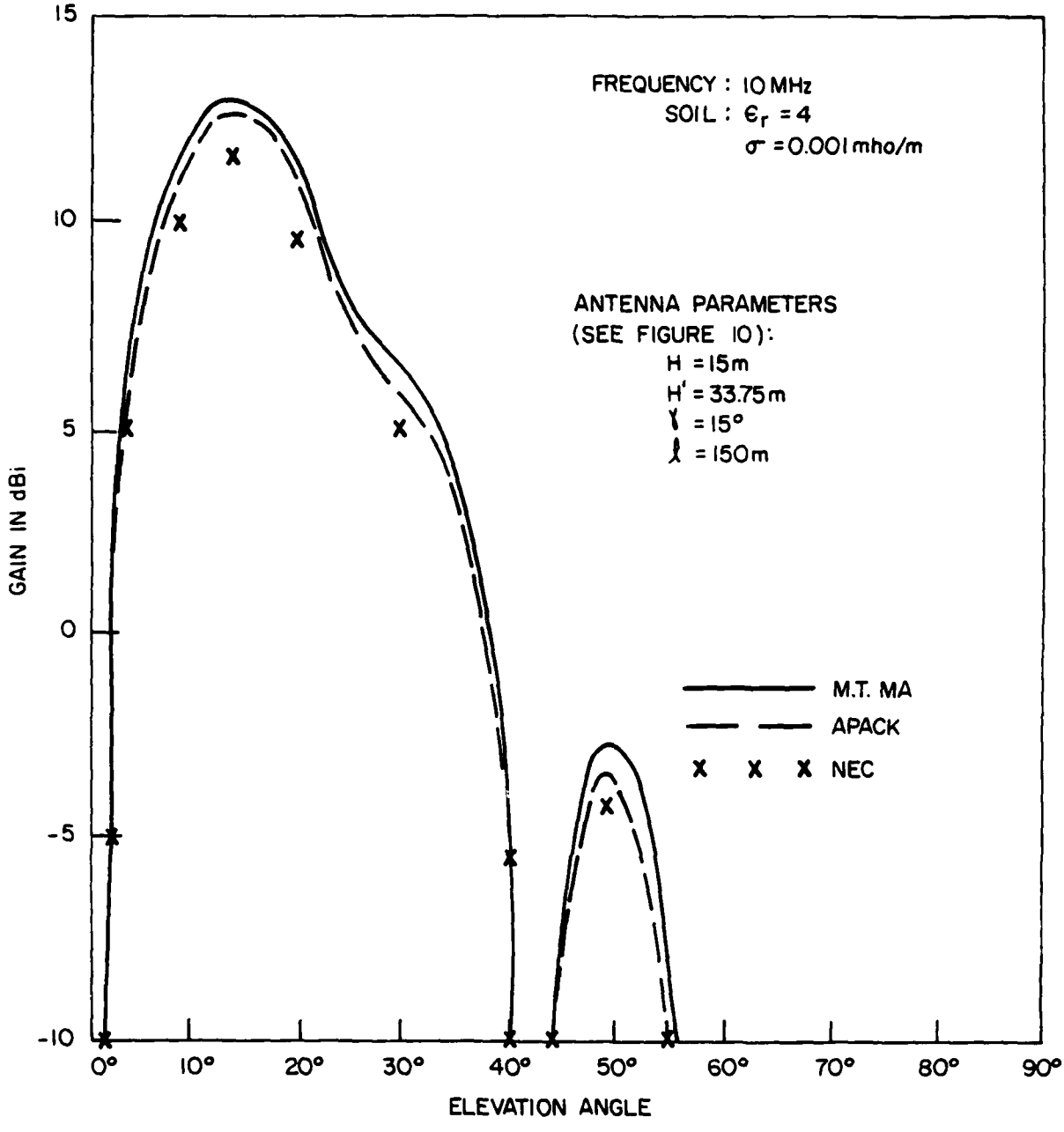

Figure 30. Elevation patterns of a terminated sloping-V mounted above soil.

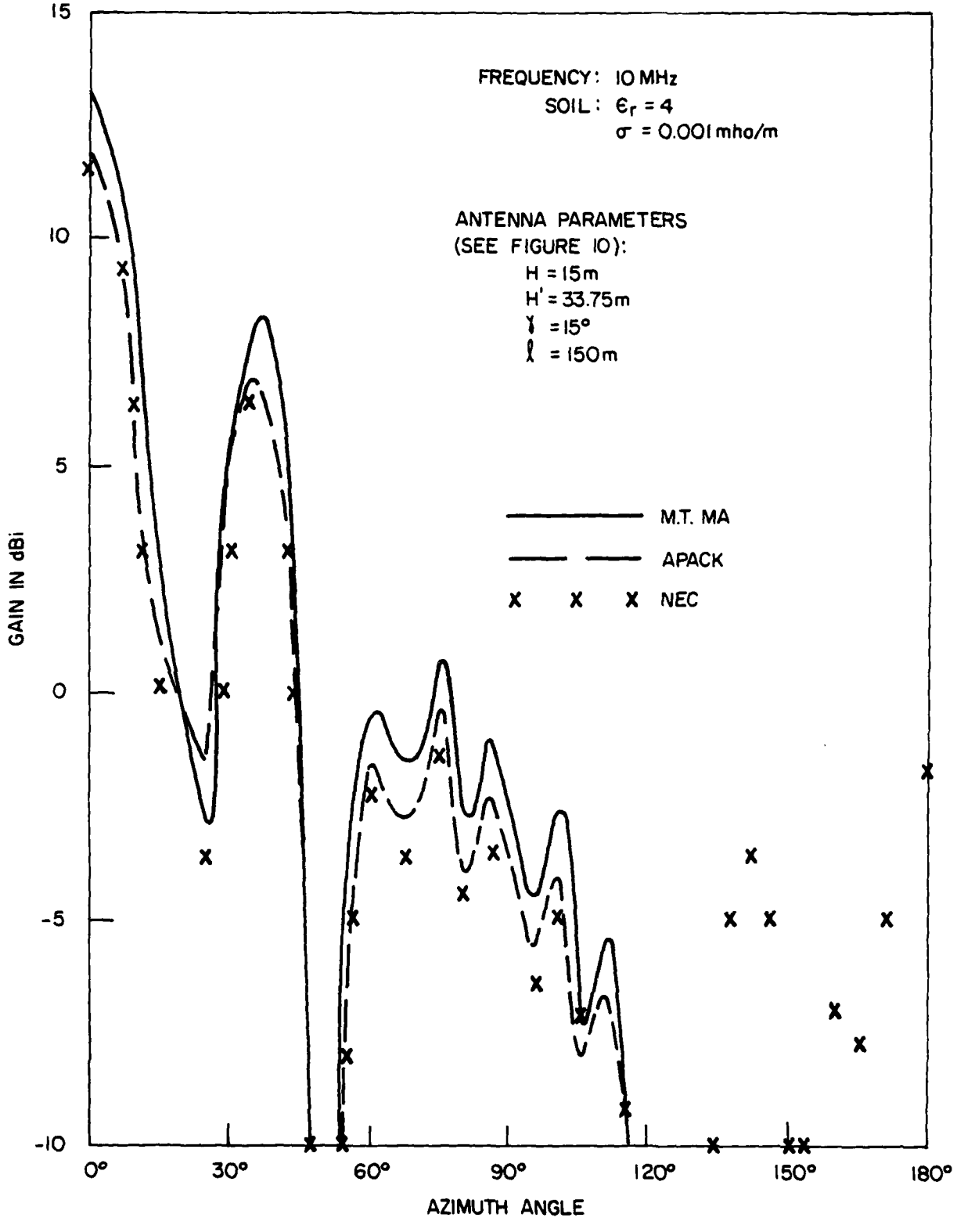

Figure 31. Azimuth patterns of a terminated sloping-V (mounted above soil) at an elevation angle of 14°.

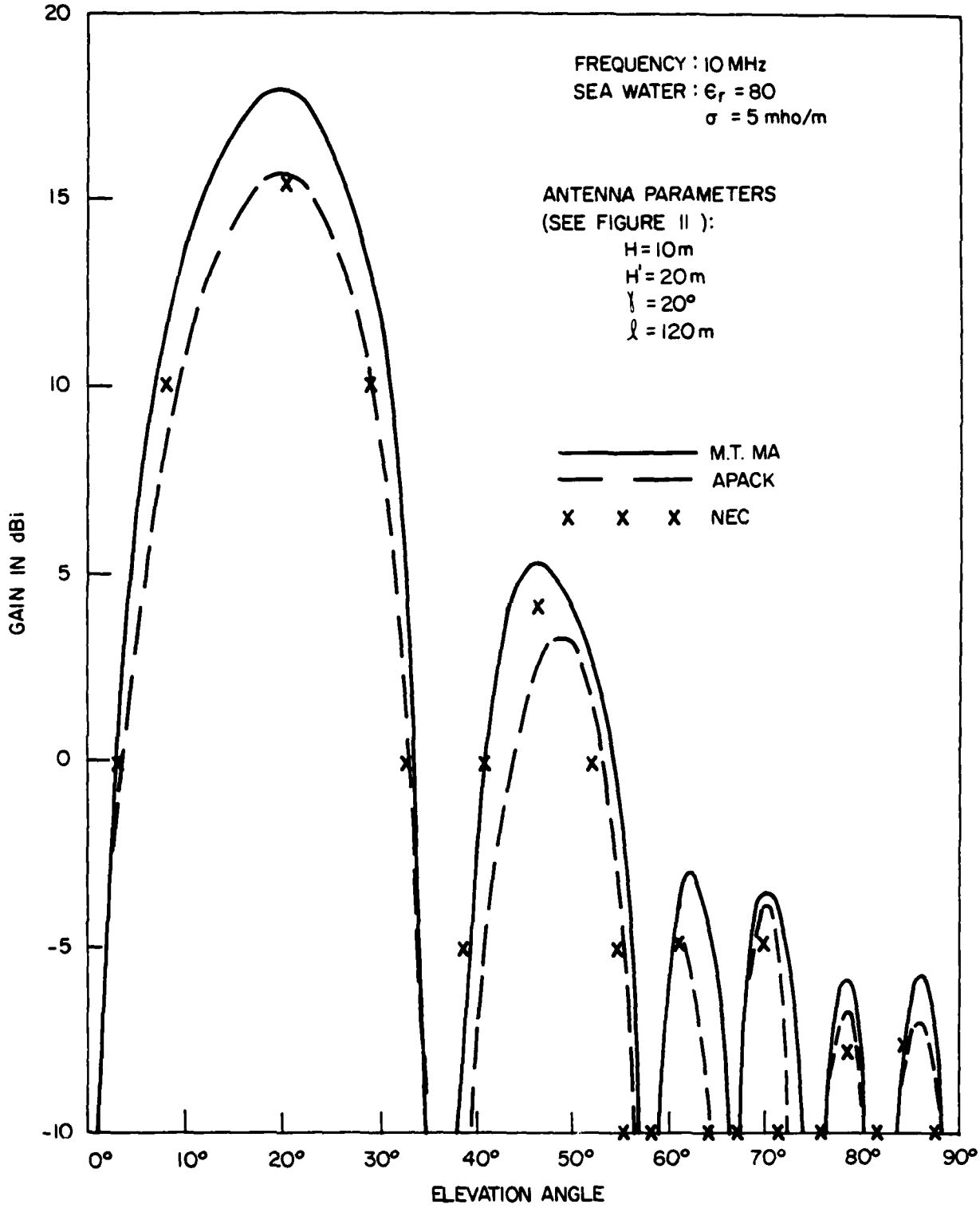

Figure 32. Elevation patterns of a terminated sloping rhombic mounted above sea water.

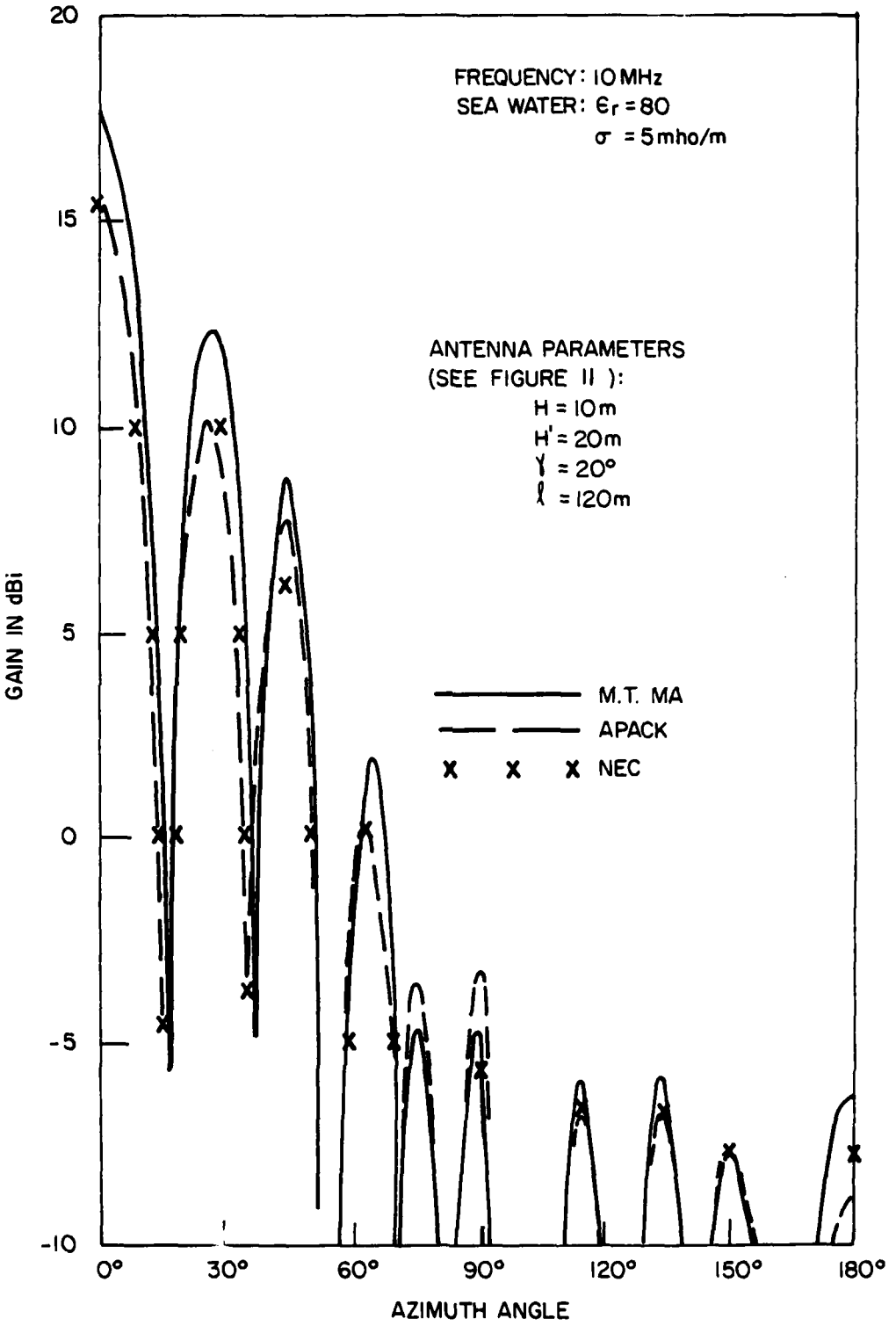

Figure 33. Azimuth patterns of a terminated sloping rhombic (mounted above sea water) at an elevation angle of 20°.

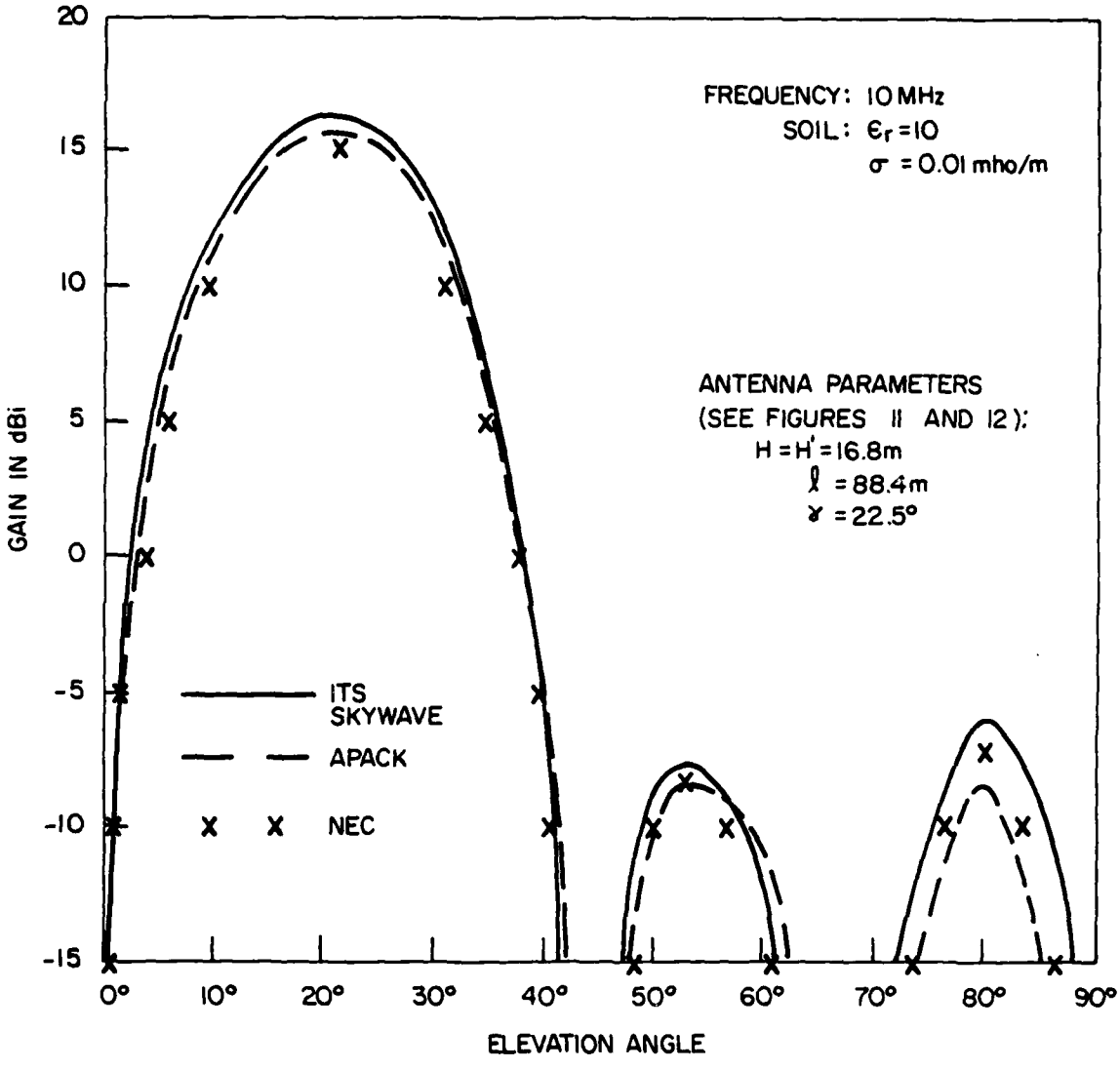

Figure 34. Elevation patterns of a terminated horizontal rhombic mounted above soil.

SIDE-LOADED VERTICAL HALF-RHOMBIC

Figure 35 gives comparisons between APACK, NEC, and SKYWAVE predictions for the elevation patterns of a side-loaded vertical half-rhombic mounted over soil and operating at a frequency of 10 MHz. In this case, the gains predicted by APACK differ from other data by 3 dB or less.

Figures 36 and 37 show elevation and azimuth patterns, respectively, of a side-loaded vertical half-rhombic operting at 10 MHz mounted over sea water. The comparisons between APACK, NEC, and Ma's model for elevation patterns (see Figure 36) indicate agreement generally within 3 dB. The comparisons for azimuth patterns at an elevation angle of 2 degrees (see Figure 37) indicate similar agreement.

HORIZONTAL YAGI-UDA ARRAY

Figure 38 gives comparisons between APACK, NEC, and Ma's predictions for gains of a horizontal Yagi-Uda array operating at 10 MHz over soil and sea water. Excellent agreement is indicated with APACK gains differing from other data by 1 dB or less for all elevation angles above 10 degrees.

HORIZONTALLY POLARIZED LOG-PERIODIC DIPOLE ARRAY

Figures 39 and 40 compare APACK predictions with Ma's predictions for gains of a horizontally polarized log-periodic dipole array operating at. 12 MHz mounted over both soil and sea water. The elevation-pattern comparisons in Figure 39 indicate excellent agreement for soil (within 1 dB) and good agreement for sea water (within 2 dB) for all elevation angles above 10 degrees. The azimuth-plane comparisons made at an elevation angle of 36 degrees (see Figure 40) indicate agreement within 3 dB for all azimuth angles.

Figures 41, 42, and 43 show comparisons between APACK, NEC, and manufacturer's data for the Collins 237B-3 horizontally polarized log-periodic dipole array (above soil) operating at frequencies of 8, 12, and 20 MHz,

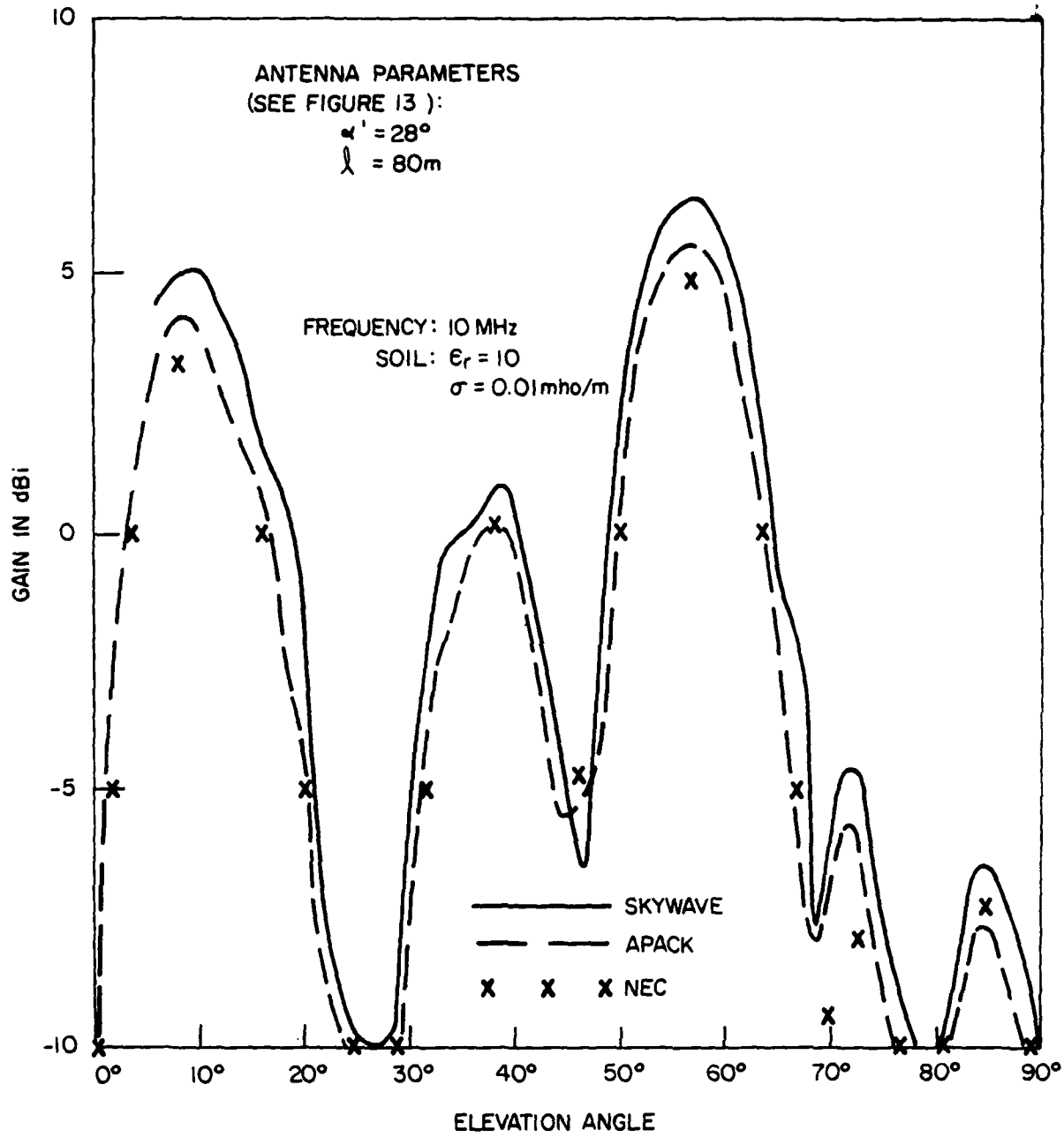

Figure 35. Elevation patterns of a side-loaded vertical half-rhombic mounted above soil.

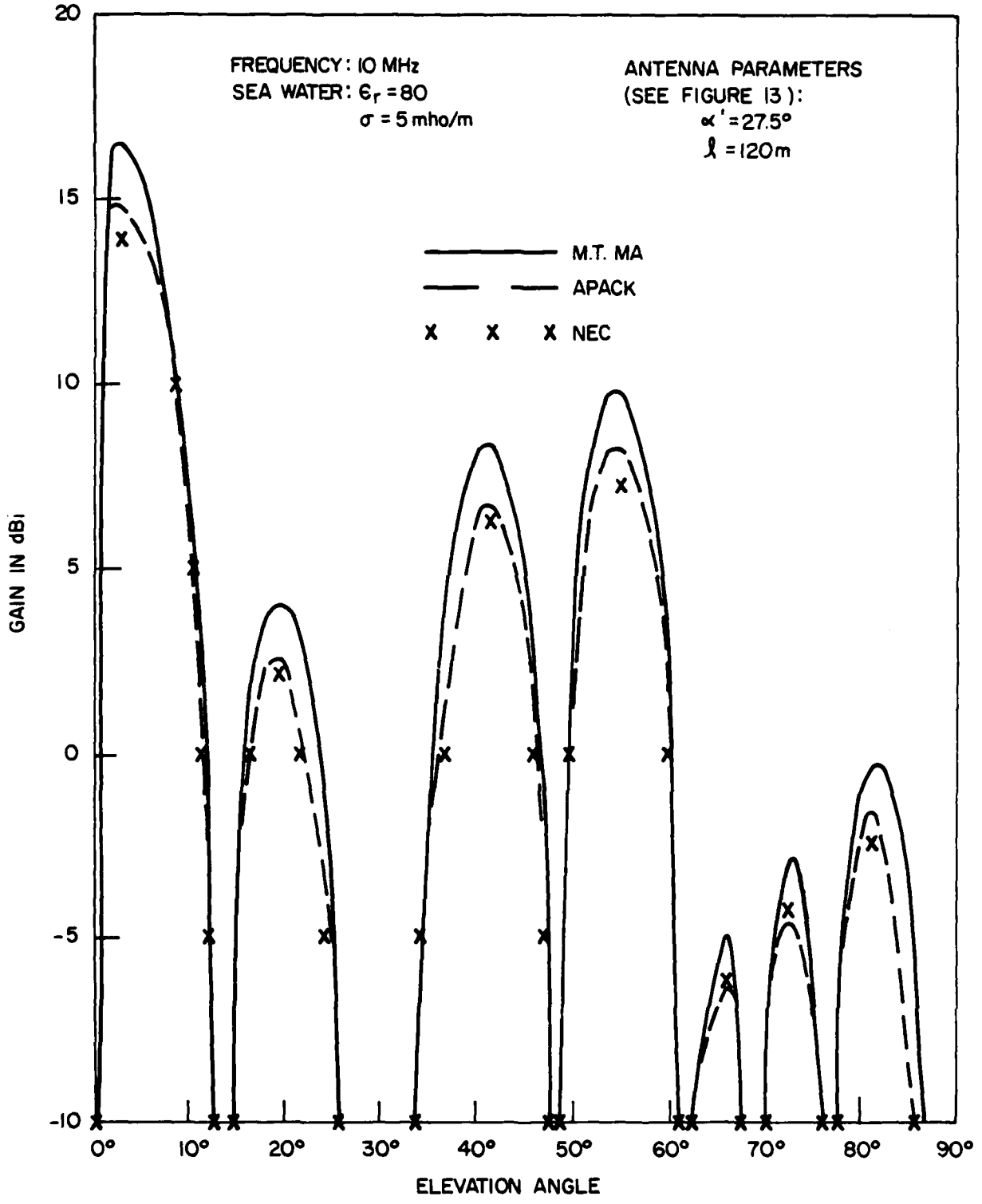

Figure 36. Elevation patterns of a side-loaded vertical half-rhombic mounted above sea water.

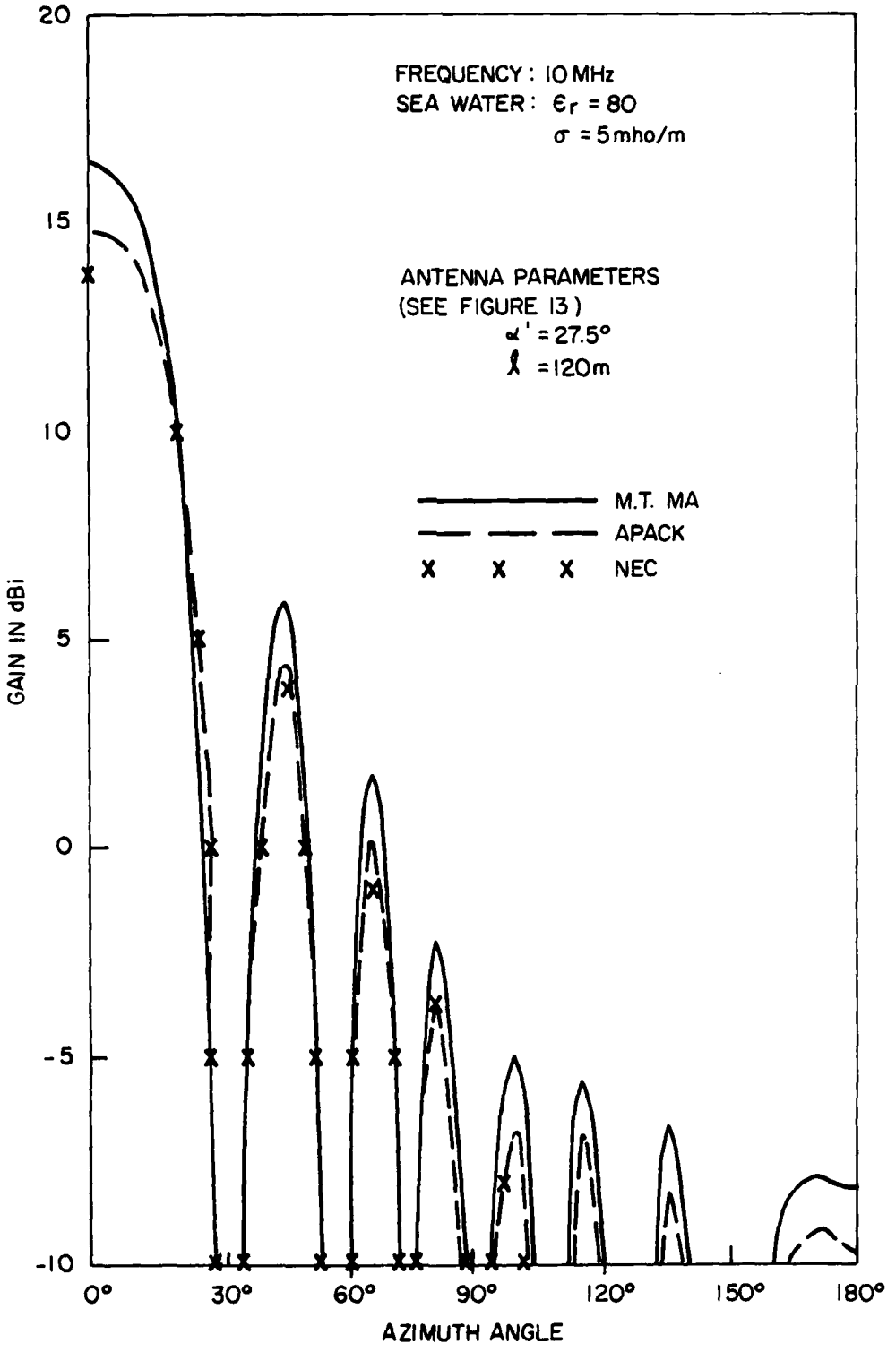

Figure 37. Azimuth patterns of a side-loaded vertical half-rhombic (mounted above sea water) at an elevation angle of 2°.

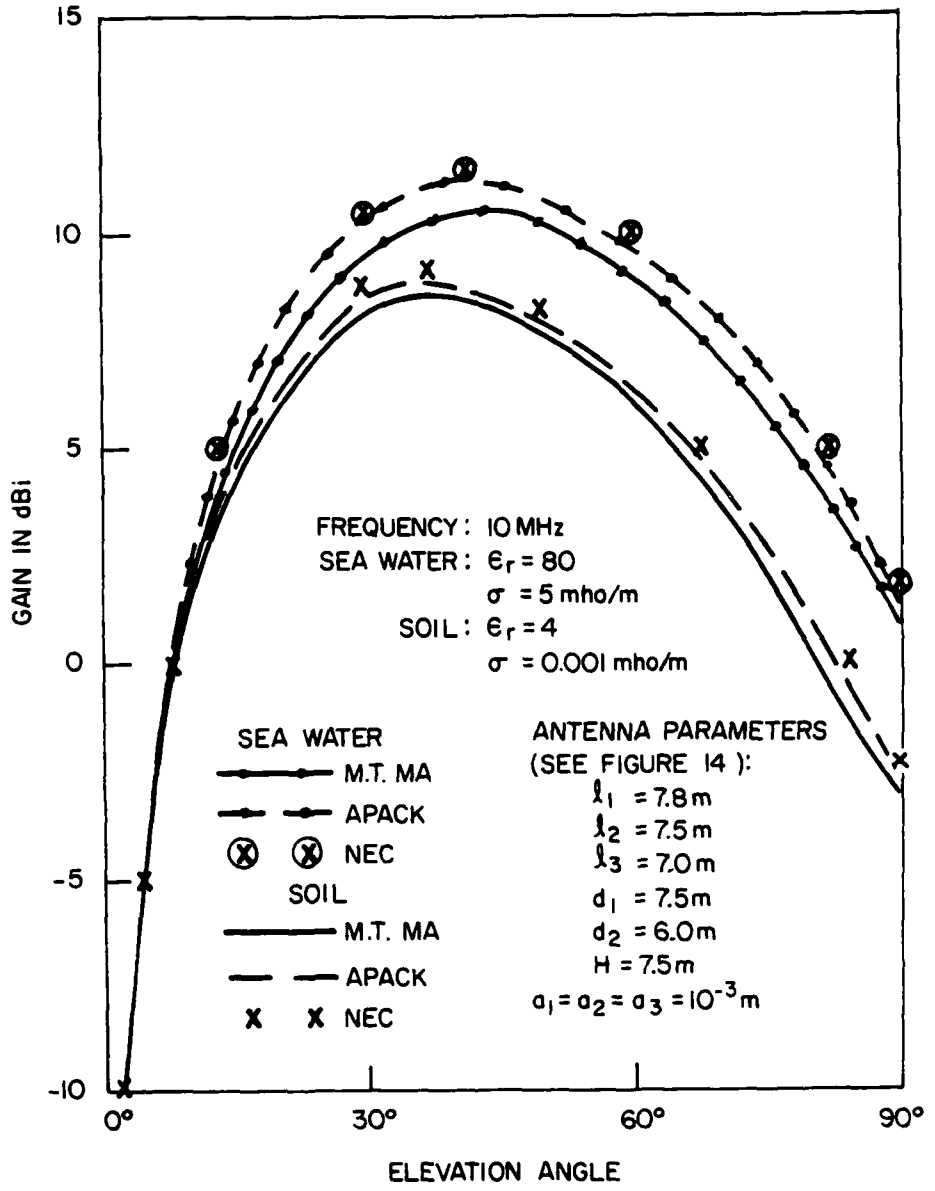

Figure 38. Elevation patterns of a three-element horizontal Yagi-Uda array mounted above sea water and soil.

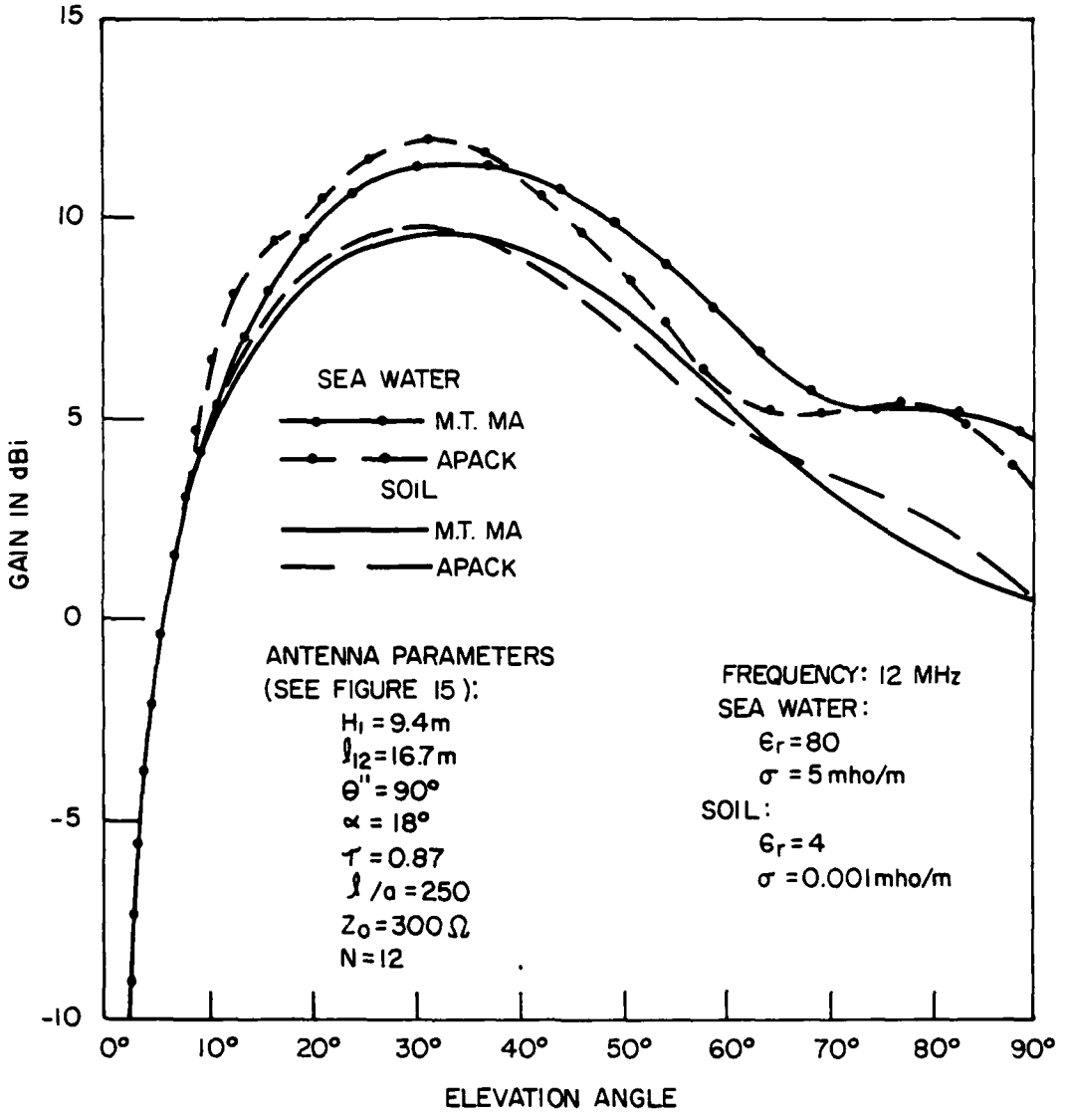

Figure 39. Elevation patterns of a horizontally polarized log-periodic dipole array mounted above sea water and soil.

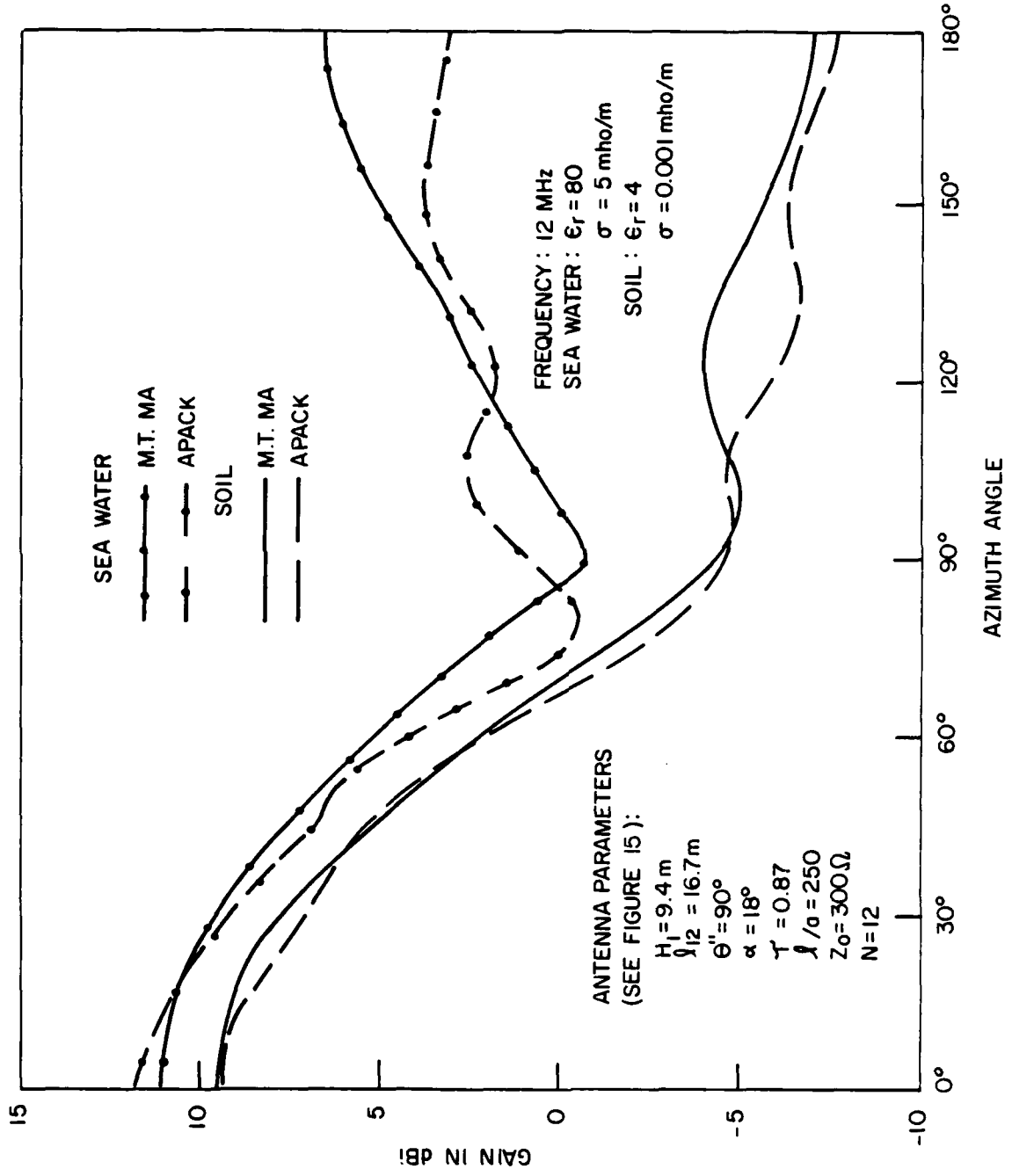

Figure 40. Azimuth patterns of a horizontally polarized array (mounted above sea water and soil) at an elevation angle of 36°.

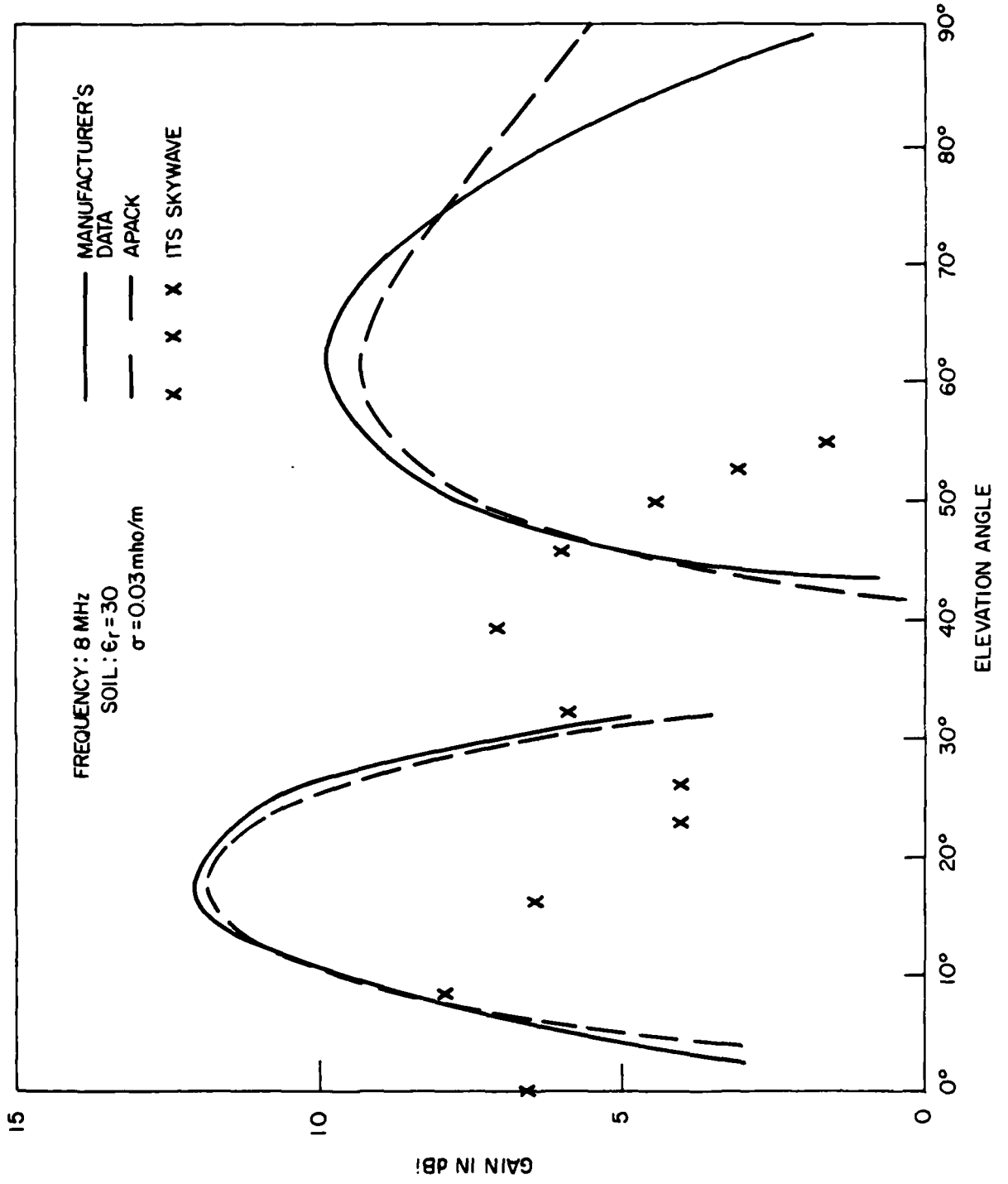

Figure 41. Elevation patterns of a Collins 237B-3 horizontally polarized log-periodic dipole array mounted above soil (8 MHz).

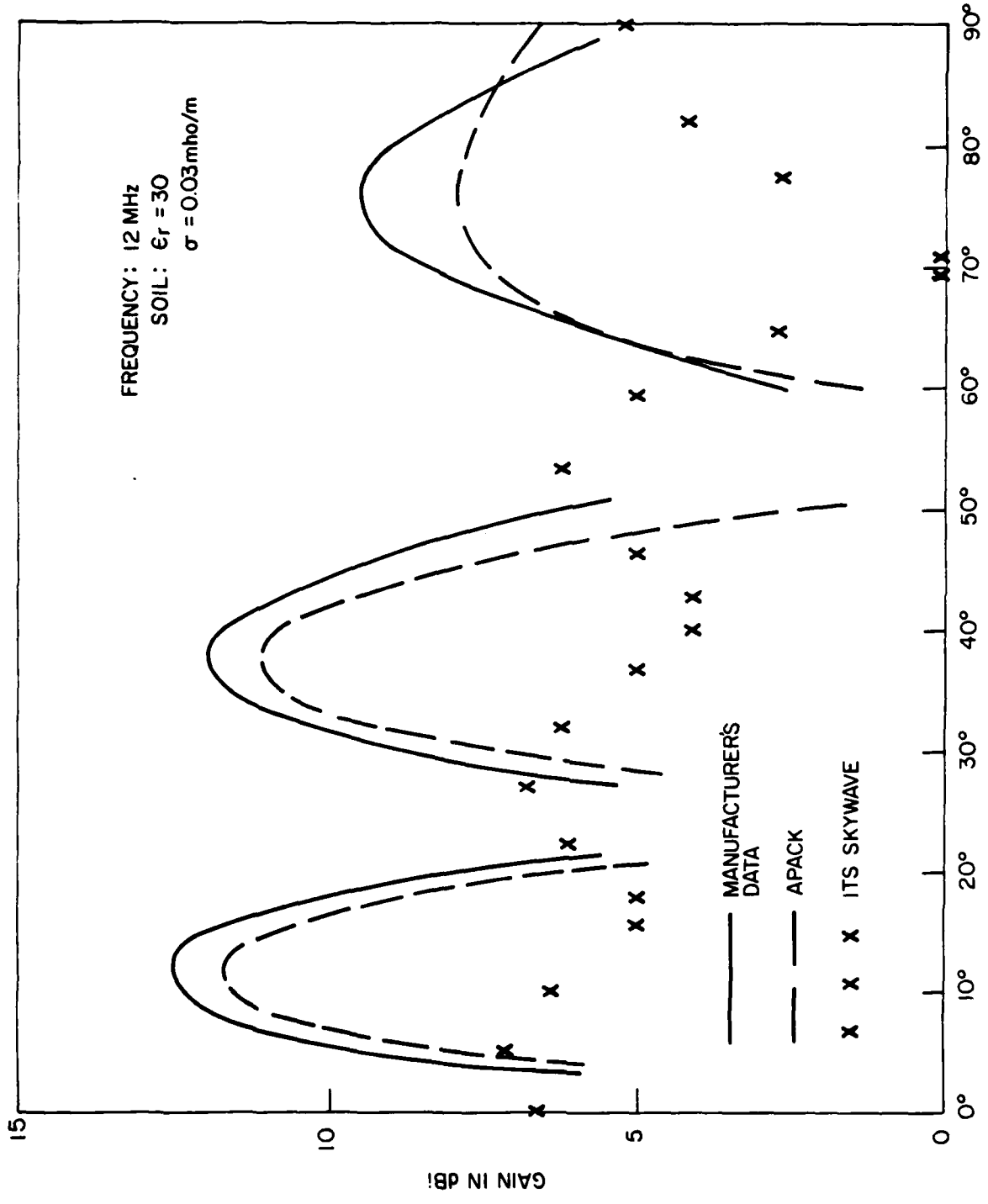

Figure 42. Elevation patterns of a Collins 237B-3 horizontally polarized log-periodic dipole array mounted above soil (12 MHz).

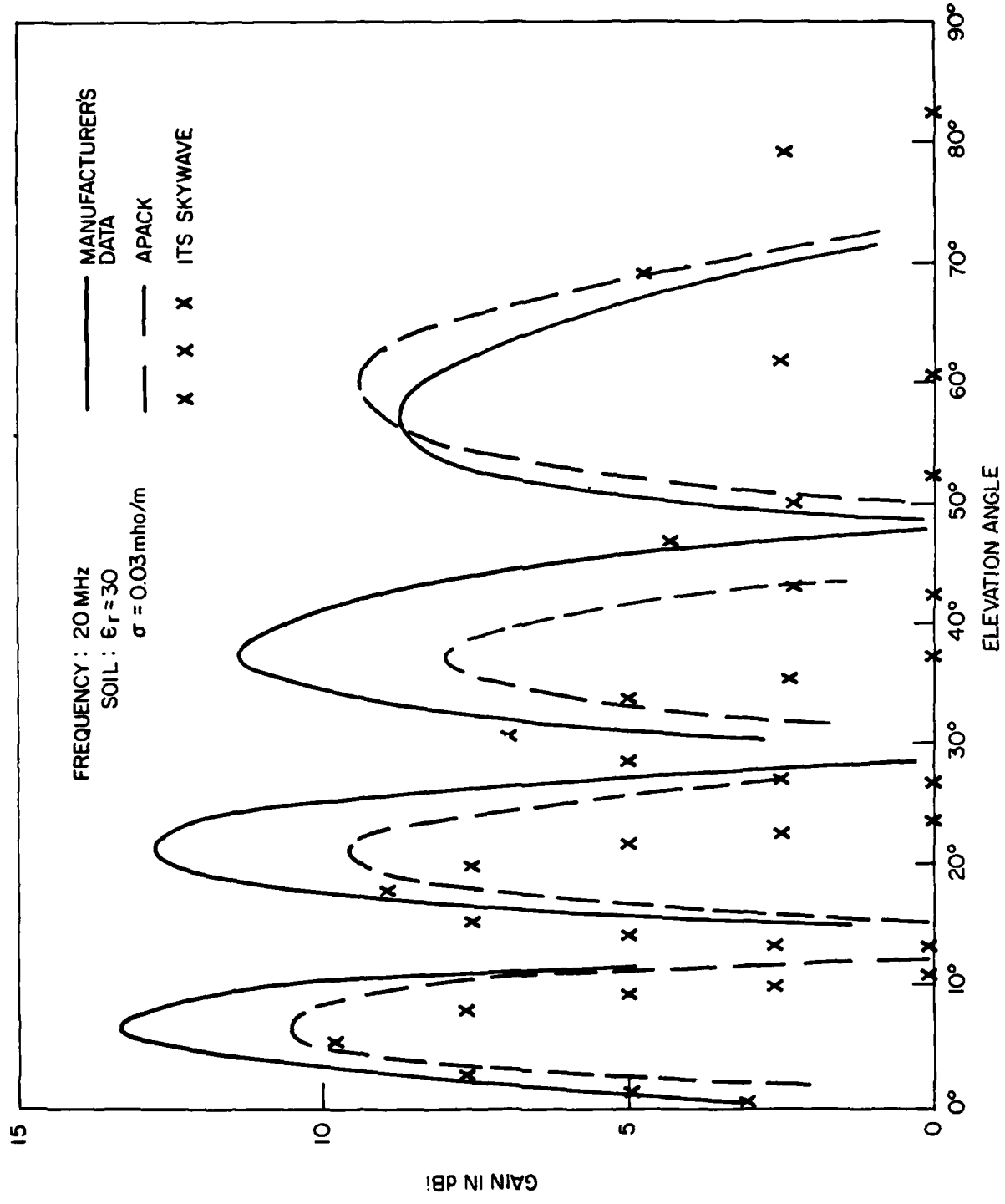

Figure 43. Elevation patterns of a Collins 237B-3 horizontally polarized log-periodic dipole array mounted above soil (20 MHz).

respectively. The predictions of APACK agree with the manufacturer's data within 5 dB or less in general, but the predicted gains of the SKYWAVE program are much lower.

Not only are the SKYWAVE gain values much lower than those predicted by APACK and the manufacturer, but the peaks and nulls of the SKYWAVE patterns do not coincide with the other predictions. The inaccuracy of the SKYWAVE predictions is believed to be due not to the theory on which SKYWAVE is based, but rather due to coding errors in the horizontal log-periodic routine that have not been corrected by ITS.

VERTICALLY POLARIZED LOG-PERIODIC

Figure 44 compares elevation-pattern predictions by APACK and Ma's model for a vertically polarized log-periodic dipole array mounted over sea water at frequencies of 6 and 18 MHz. The comparisons at 6 MHz show agreement between the two models to less than 2 dB, while the comparisons at 18 MHz show agreement to within 5 dB.

CURTAIN ARRAY

Figure 45 shows the elevation pattern predicted by APACK for a two-bay, four-stack curtain array operating at 10 MHz over soil. The APACK predictions shown in Figure 45 are essentially identical to those obtained by Barghausen et al. (see Reference 1, p. 230).

Figure 46 compares elevation-plane patterns predicted by APACK and Ma's model for a one-bay, two-stack curtain array operating at 10 MHz over sea water. The predictions agree within 2 dB for all elevation angles above 5 degrees. The predictions are identical for elevation angles above about 60 degrees.

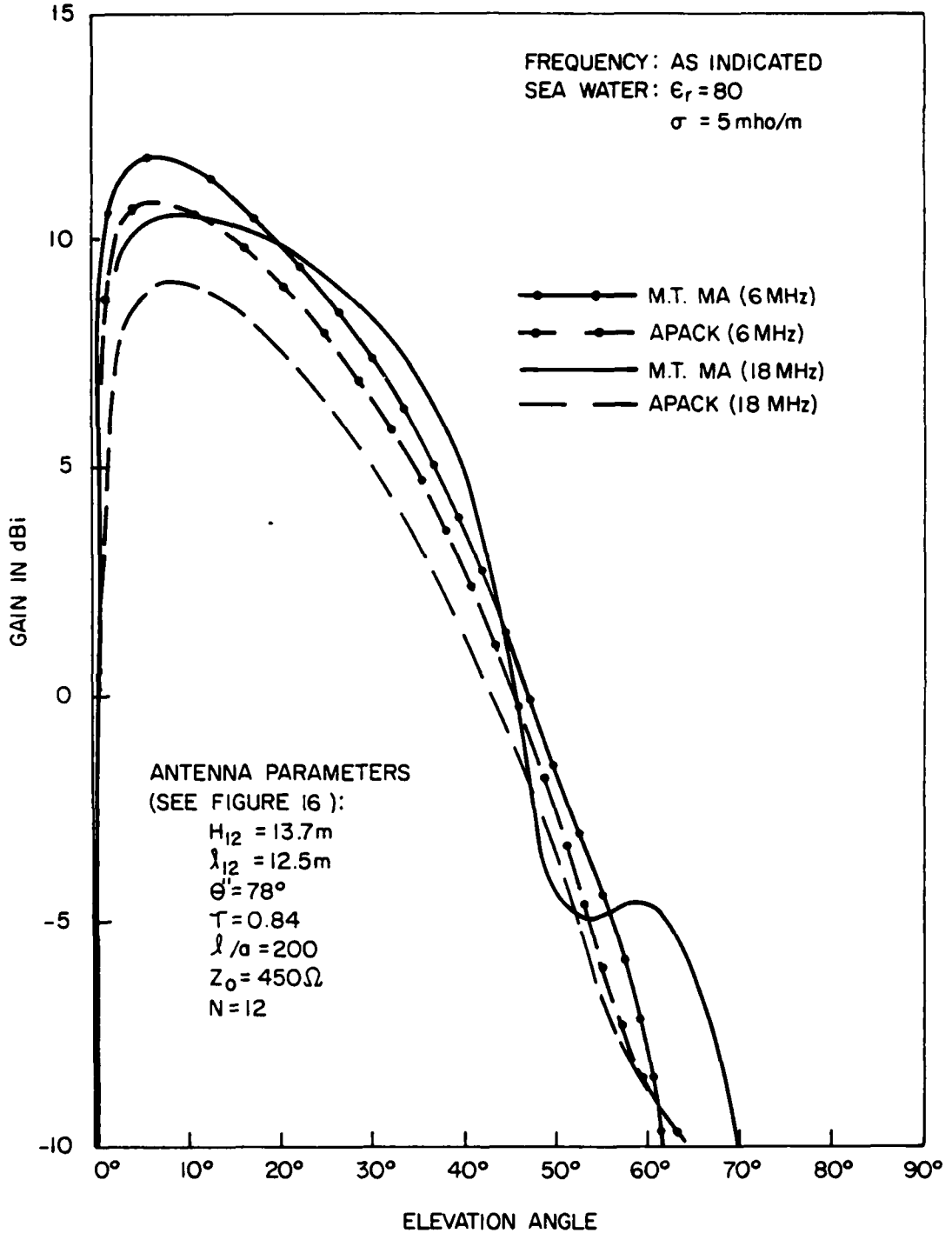

Figure 44. Elevation patterns of a vertically polarized log-periodic dipole array mounted above sea water.

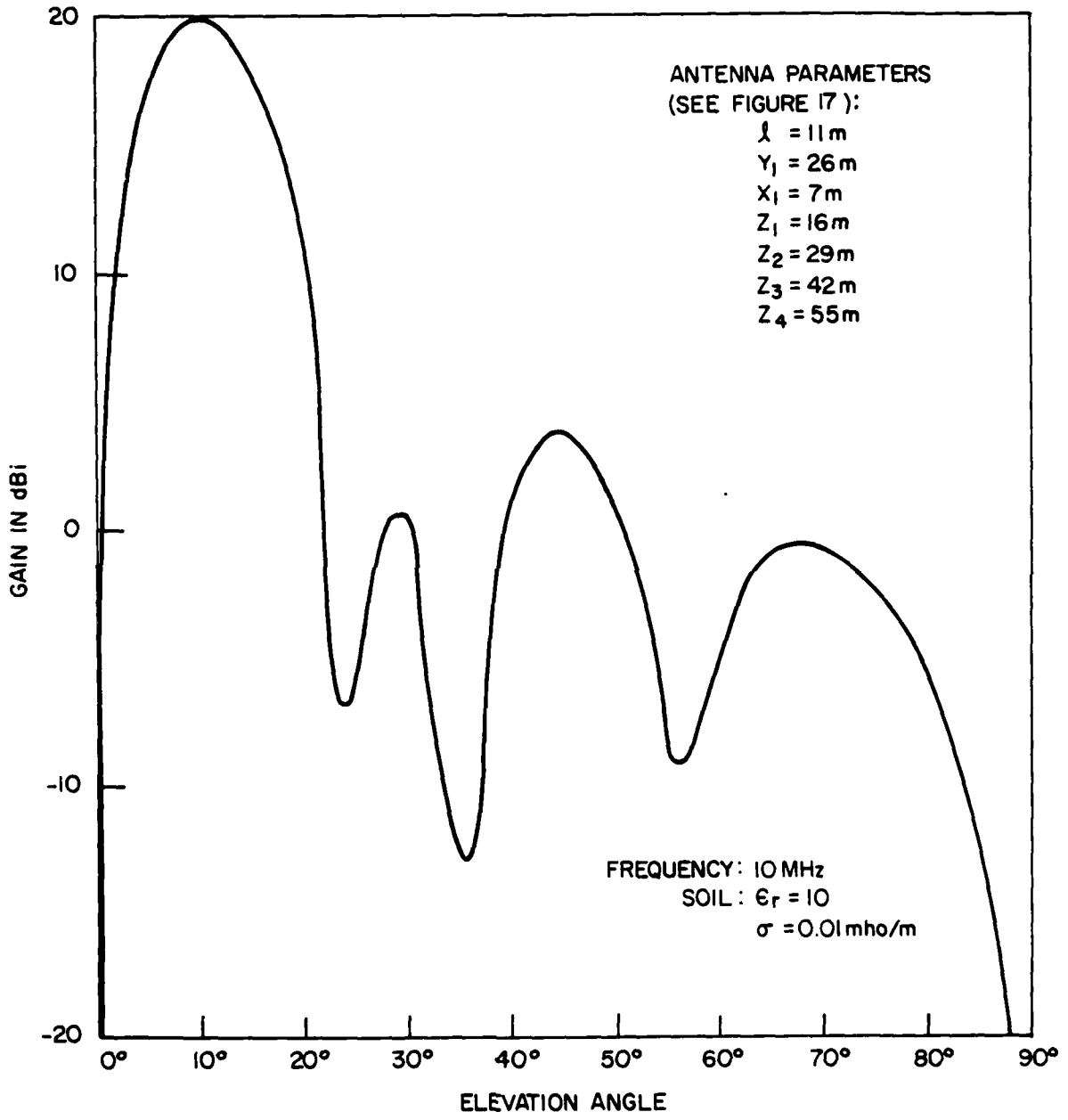

Figure 45. Elevation pattern predicted by APACK for a two-bay, four-stack curtain array mounted above soil.

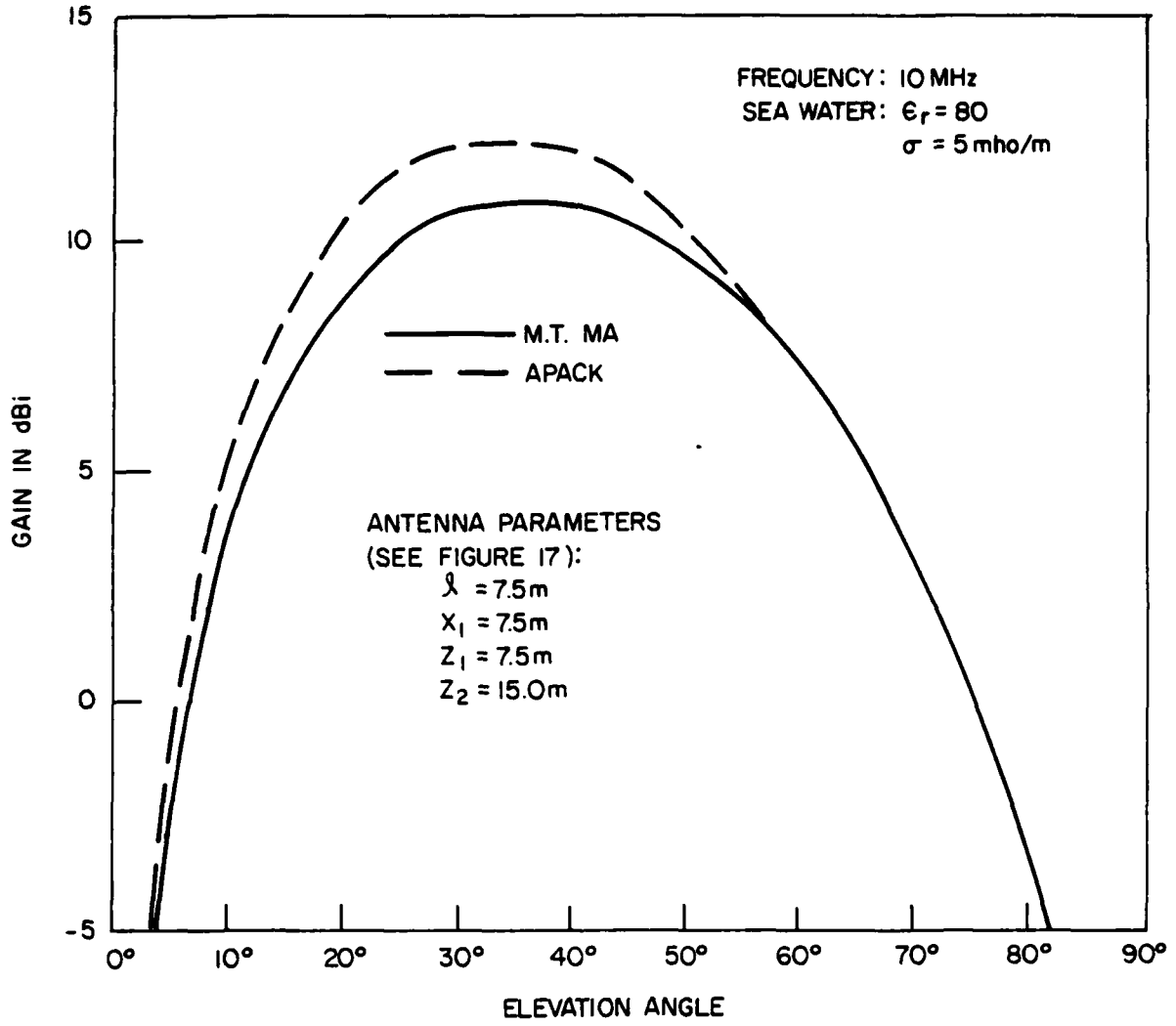

Figure 46. Elevation patterns of a one-bay, two-stack curtain array mounted above sea water.

SLOPING DOUBLE RHOMBOID

Figure 47 shows the azimuth pattern at an elevation angle of 20 degrees predicted by APACK for a sloping double rhomboid mounted over soil and operating at 10 MHz. This pattern is essentially identical to that predicted by the ITS SKYWAVE program.

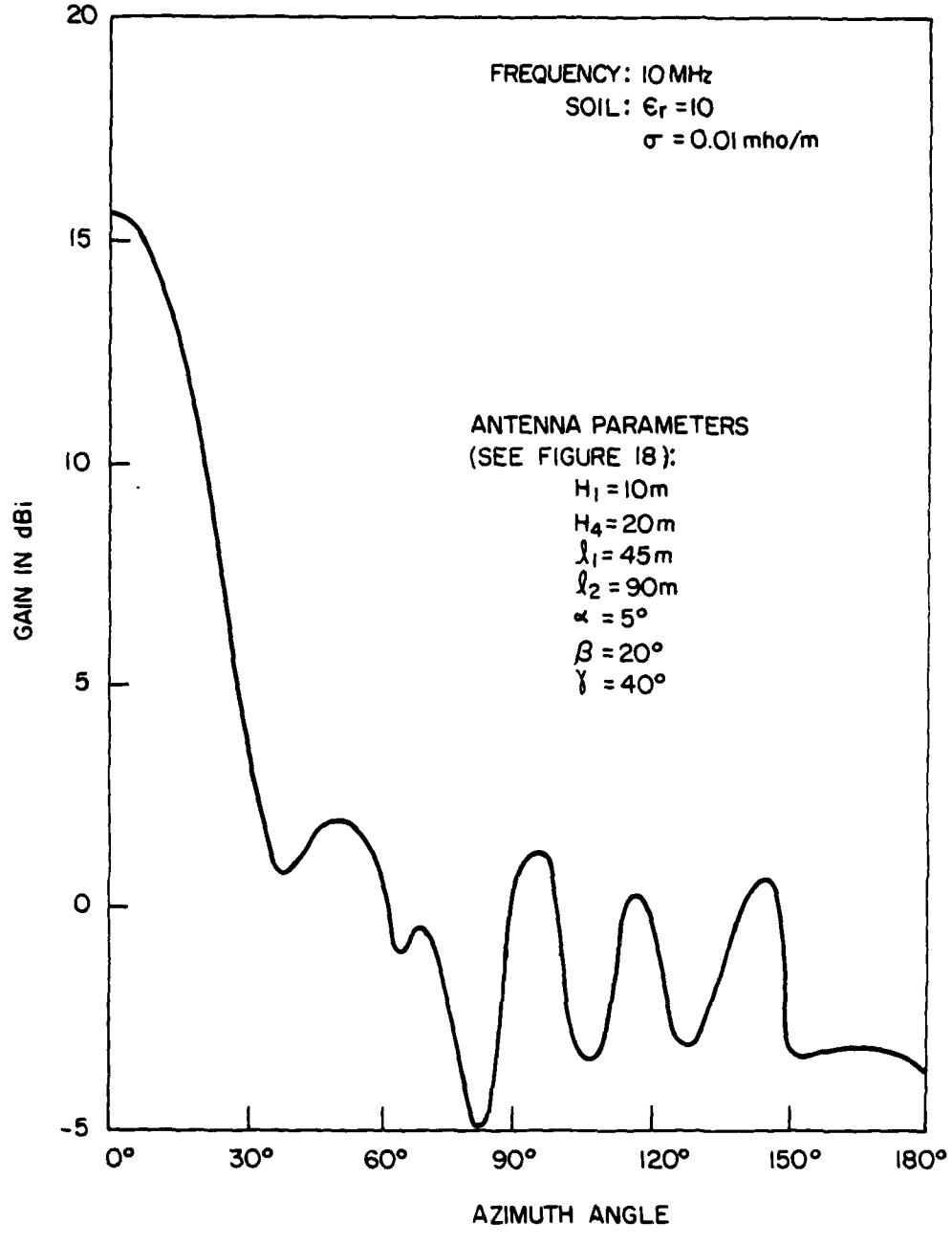

Figure 47. Azimuth pattern predicted by APACK for a sloping double rhomboid (mounted over soil) at an elevation angle of 20°.

SECTION 8
COMPARISONS BETWEEN TRANSMISSION LOSS PREDICTED BY APACK AND OTHER DATA

A number of comparisons were made between transmission loss predicted by APACK and transmission loss predicted by other data. In all cases, comparisons are made with respect to basic transmission loss, i.e., the path loss that would result if the two actual antennas were replaced by lossless isotropic antennas.

The data with which APACK transmission-loss predictions were compared are field-strength curves given by the CCIR (see Reference 26) and results obtained from two other ground-wave propagation models used at ECAC, referred to as the IPS model (see Reference 3) and the Nλ models (see Reference 4). The CCIR curves were converted to basic transmission loss using Equation 6-12. The IPS and Nλ models predict basic transmission loss directly.

The CCIR curves which are based on Bremmer's formulation (see Reference 17) assume that both the transmitting and receiving antennas are located on the ground and that both antennas are Hertzian dipoles. The IPS and Nλ models account for the heights of the antenna feed points above ground. The APACK predictions of transmission loss account for the actual antenna structure.

The comparisons predicted below are made to indicate the accuracy and versatility of APACK for predicting transmission loss for frequencies between 150 kHz and 500 MHz. The comparisons include ground-wave propagation over both average soil and sea water. The differences indicated between the various predictions shown in the figures are not meant to represent either the "best" or "worst" case. Rather, the differences should be considered typical.

Figures 48, 49, and 50 show the basic transmission loss predicted by APACK, CCIR curves, and the IPS model at 1, 3, and 10 MHz, respectively over soil for vertical polarization. Typical differences between losses predicted by APACK and the other models are 5 dB or less.

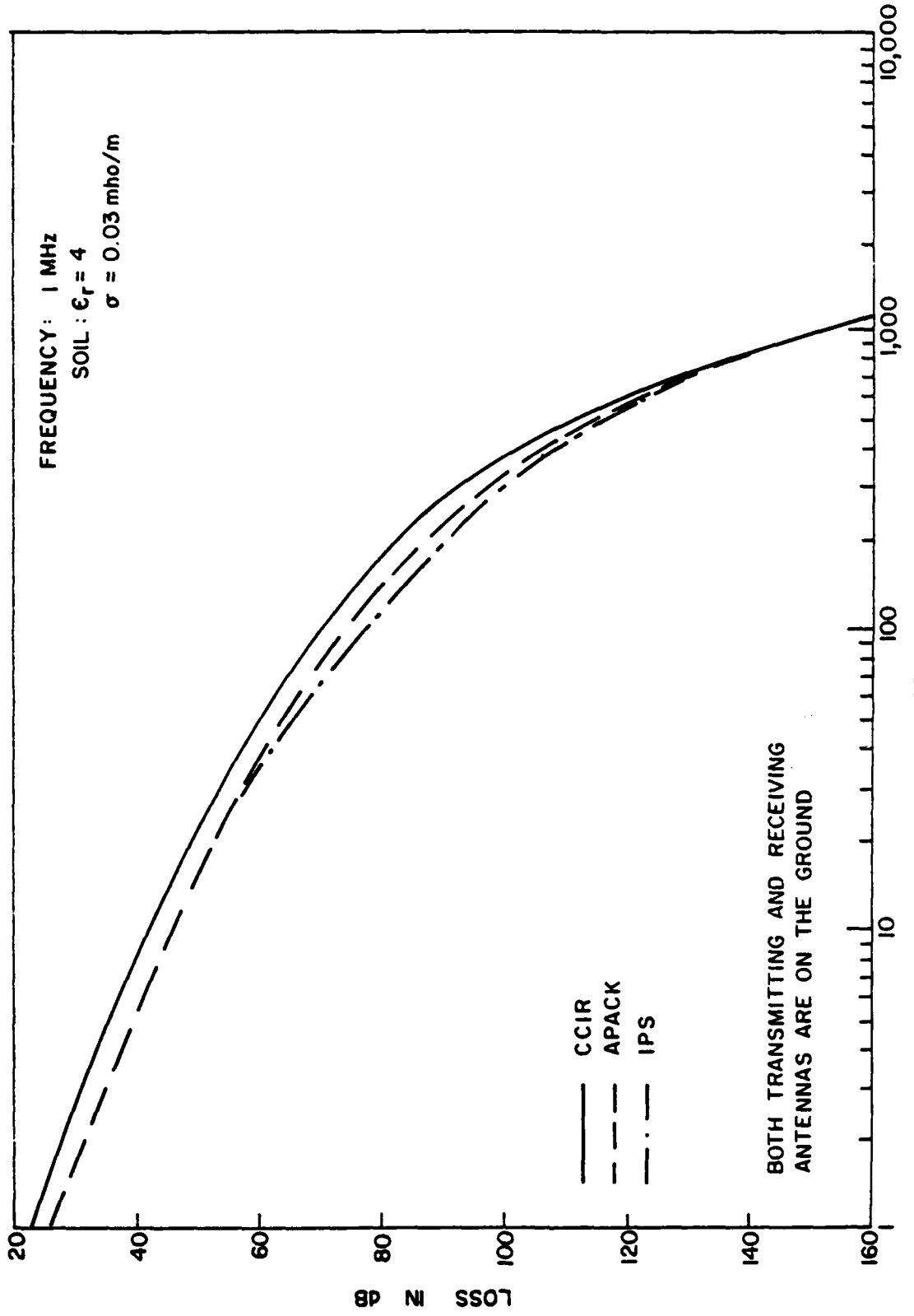

Figure 48. Comparisons between basic transmission loss predicted by APACK, CCIR, and IPS for ground-wave propagation over soil at 1 MHz (vertical polarization).

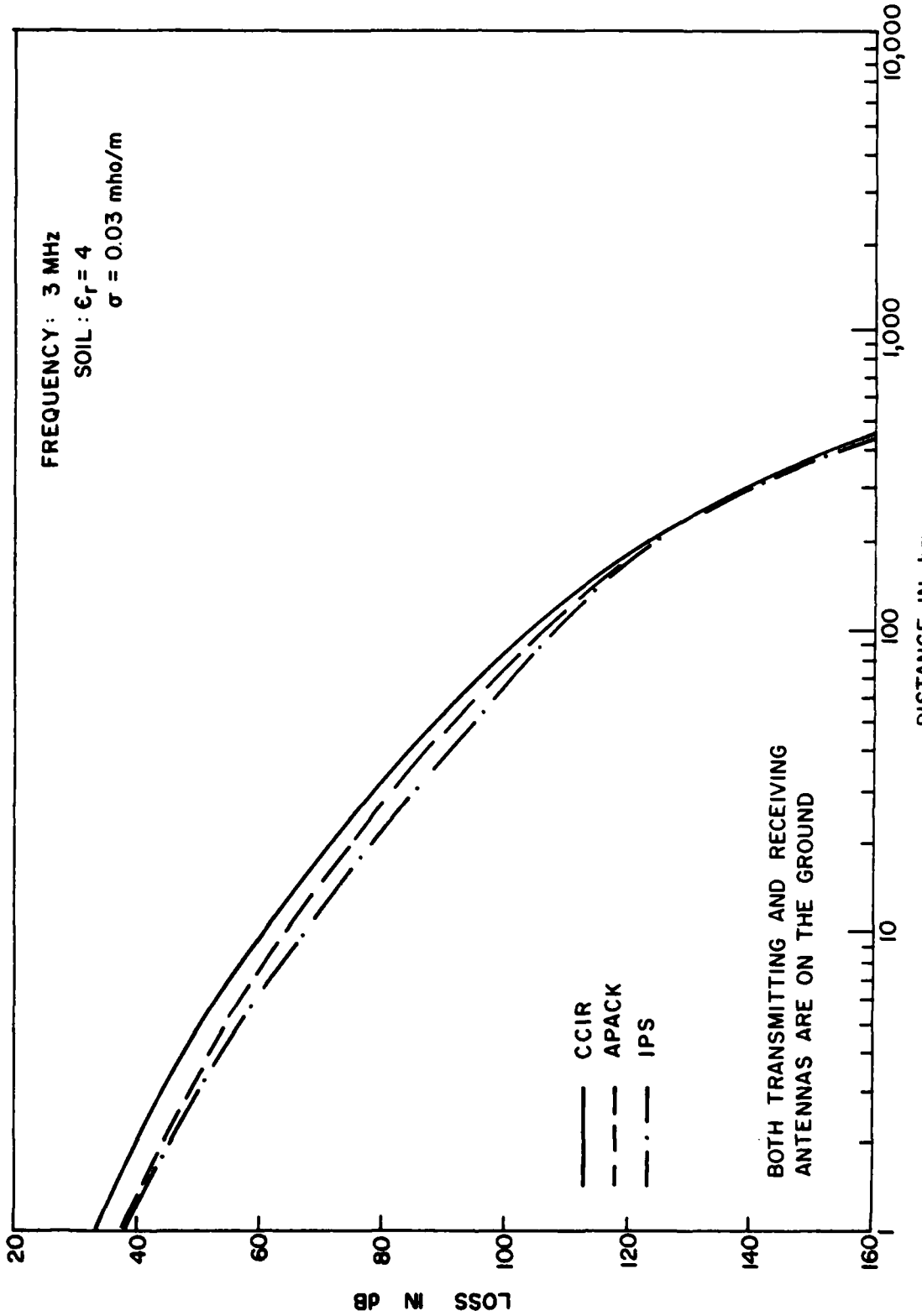

Figure 49. Comparisons between basic transmission loss predicted by APACK, CCIR, and IPS for ground-wave propagation over soil at 3 MHz (vertical polarization).

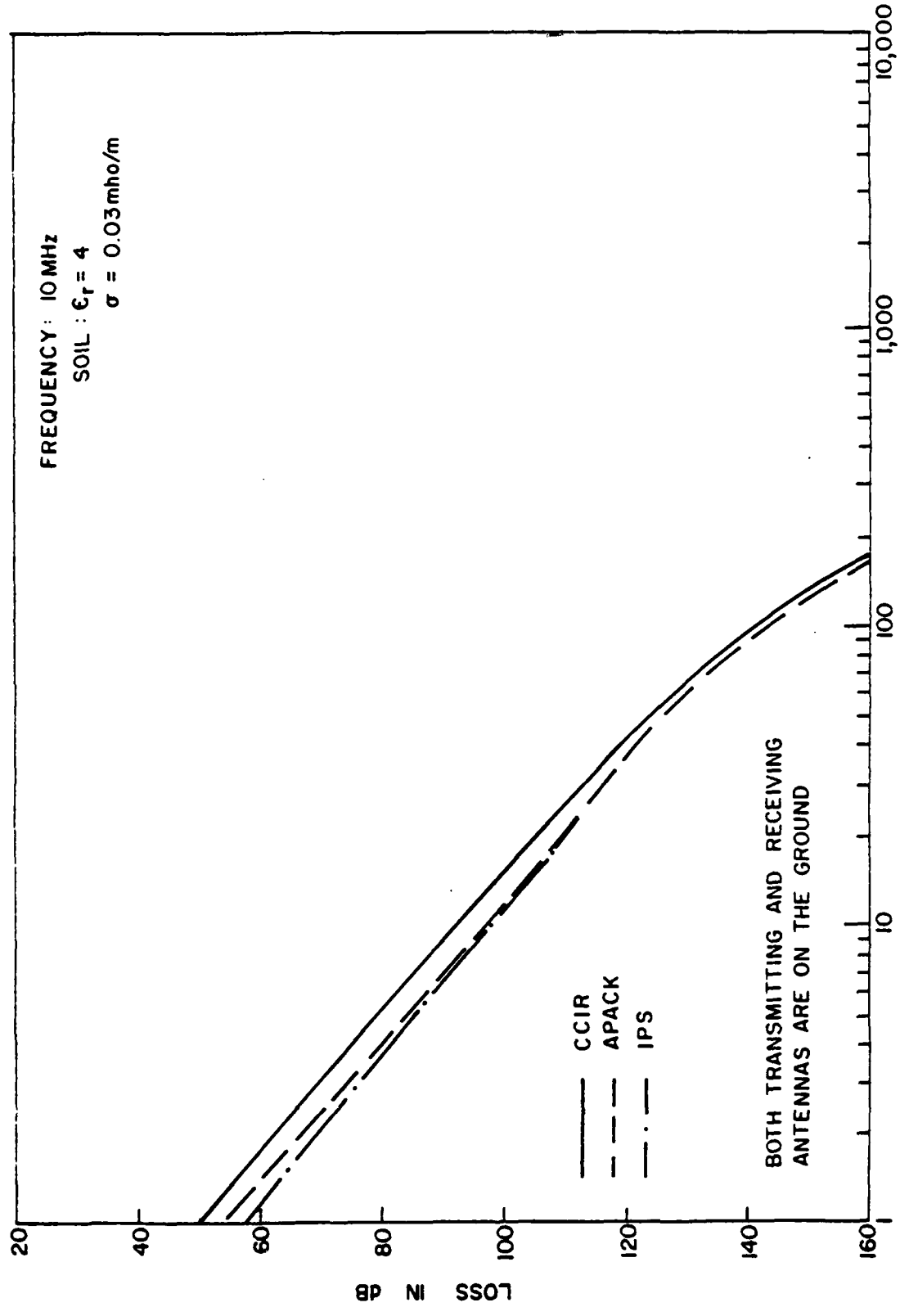

Figure 50. Comparisons between basic transmission loss predicted by APACK, CCIR, and IPS for ground-wave propagation over soil at 10 MHz (vertical polarization).

Figures 51, 52, and 53 show the basic transmission loss predicted by APACK, CCIR curves, and the IPS model at 1, 3, and 10 MHz, respectively, over sea water for vertical polarization. Typical differences between losses predicted by APACK and the other models are again 5 dB or less.

Figures 54 and 55 compare APACK predictions with the CCIR curves at 150 kHz and 10 MHz, respectively, for soil with slightly different constants than used in previous comparisons. Vertical polarization is assumed. The differences at 150 kHz, shown in Figure 54, are 10 dB or less. The differences at 10 MHz, shown in Figure 55, are 5 dB or less.

Figures 56 and 57 compare APACK predictions with those of the Nλ model at frequencies of 42.9 and 100 MHz, respectively, for vertically polarized propagation over soil. For these comparisons, the transmitting antenna is an elevated vertical dipole with its feed point located 10 meters above ground, and the height of the feed point of the receiving antenna is as indicated. In general, the APACK predictions are within 2 dB of the Nλ predictions. The reason for the large discrepancies at distances exceeding approximately 100 kilometers is that Nλ includes a model for tropospheric-scatter predictions, whereas APACK does not.

Figure 58 compares APACK and Nλ predictions at 500 MHz with both antennas located on the ground for propagation over average soil. APACK values are generally within 2-3 dB of the Nλ values except at distances above 10 kilometers where troposcatter propagation is dominant. In Figure 58, the term "Yeh" refers to the tropospheric-scatter model included in Nλ. When Nλ predictions are made without accounting for troposcatter, the results are essentially identical to those obtained with APACK for large distances.

Figures 59 and 60 compare APACK and Nλ predictions for vertically and horizontally polarized propagation, respectively, over sea water at a frequency of 2 MHz. For Figure 59, the transmitting antenna is an elevated vertical dipole 70 meters long with its feed point located 35 meters above the surface, and the height of the receiving antenna feed point is varied. For

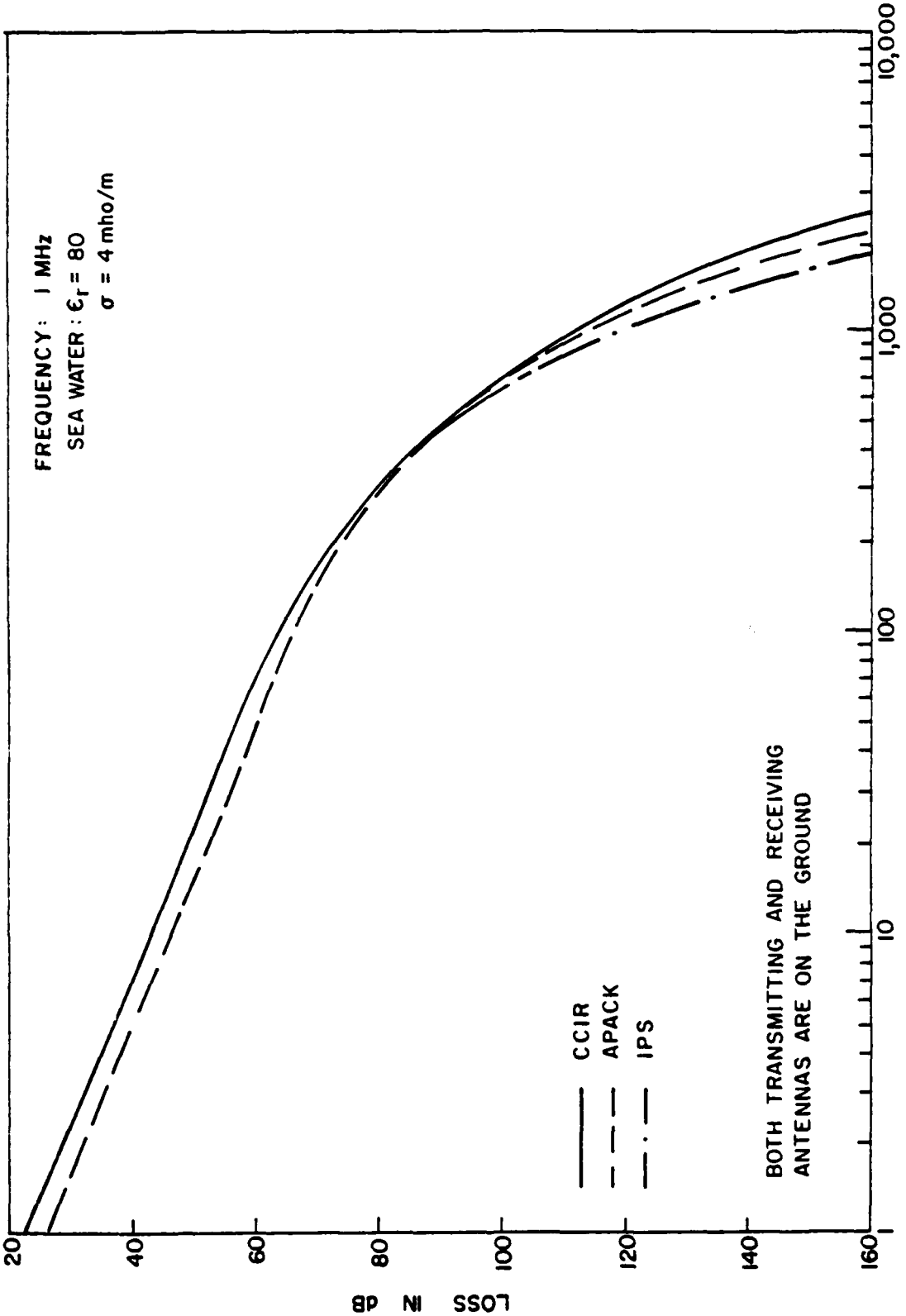

Figure 51. Comparisons between basic transmission loss predicted by APACK, CCIR, and IPS for ground-wave propagation over sea water at 1 MHz (vertical polarization).

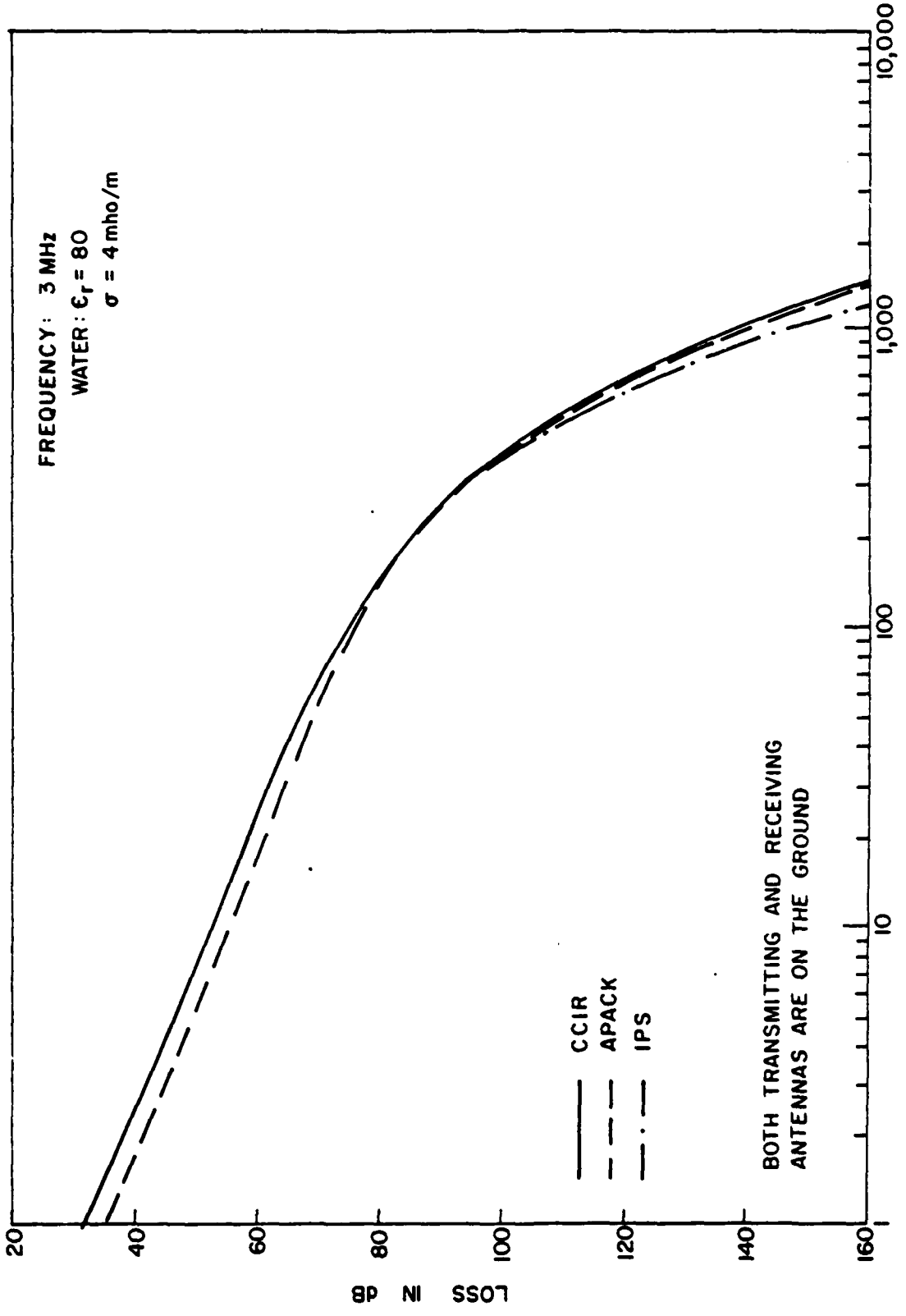

Figure 52. Comparisons between basic transmission loss predicted by APACK, CCIR, and IPS for ground-wave propagation over sea water at 3 MHz (vertical polarization).

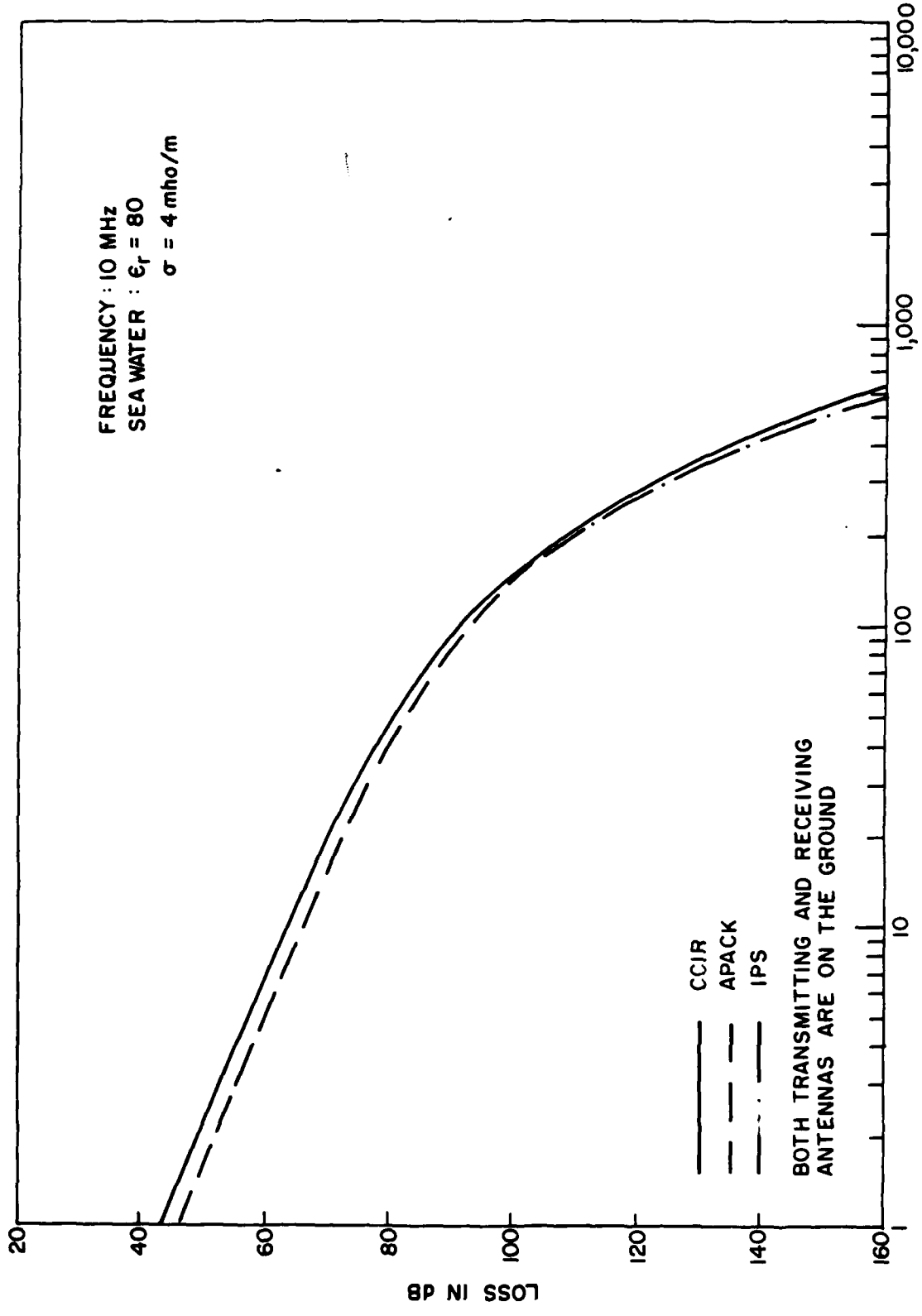

Figure 53. Comparisons between basic transmission loss predicted by APACK, CCIR, and IPS for ground-wave propagation over sea water at 10 MHz (vertical polarization).

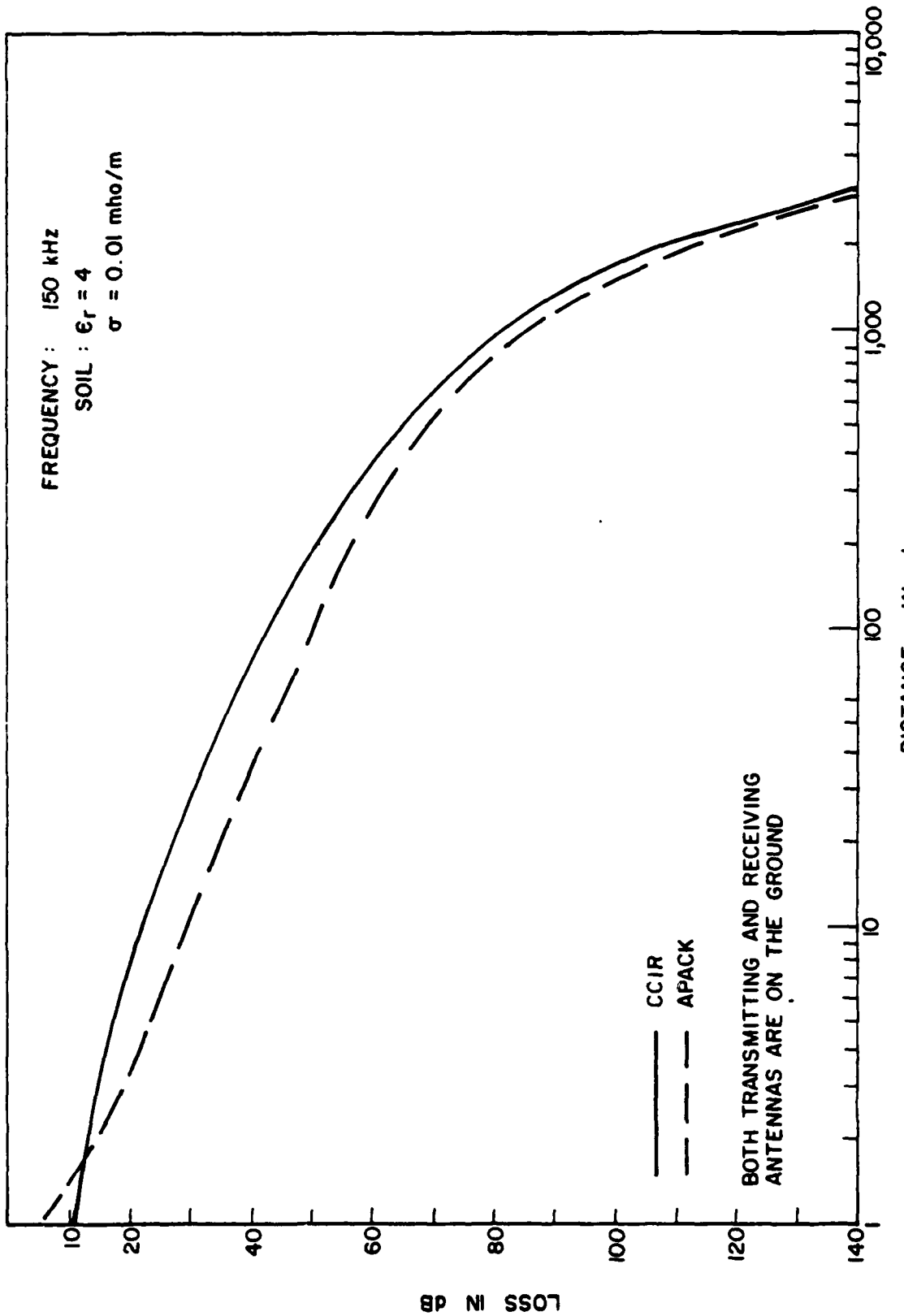

Figure 54. Comparisons between basic transmission loss predicted by APACK and CCIR for ground-wave propagation over soil at 150 kHz (vertical polarization).

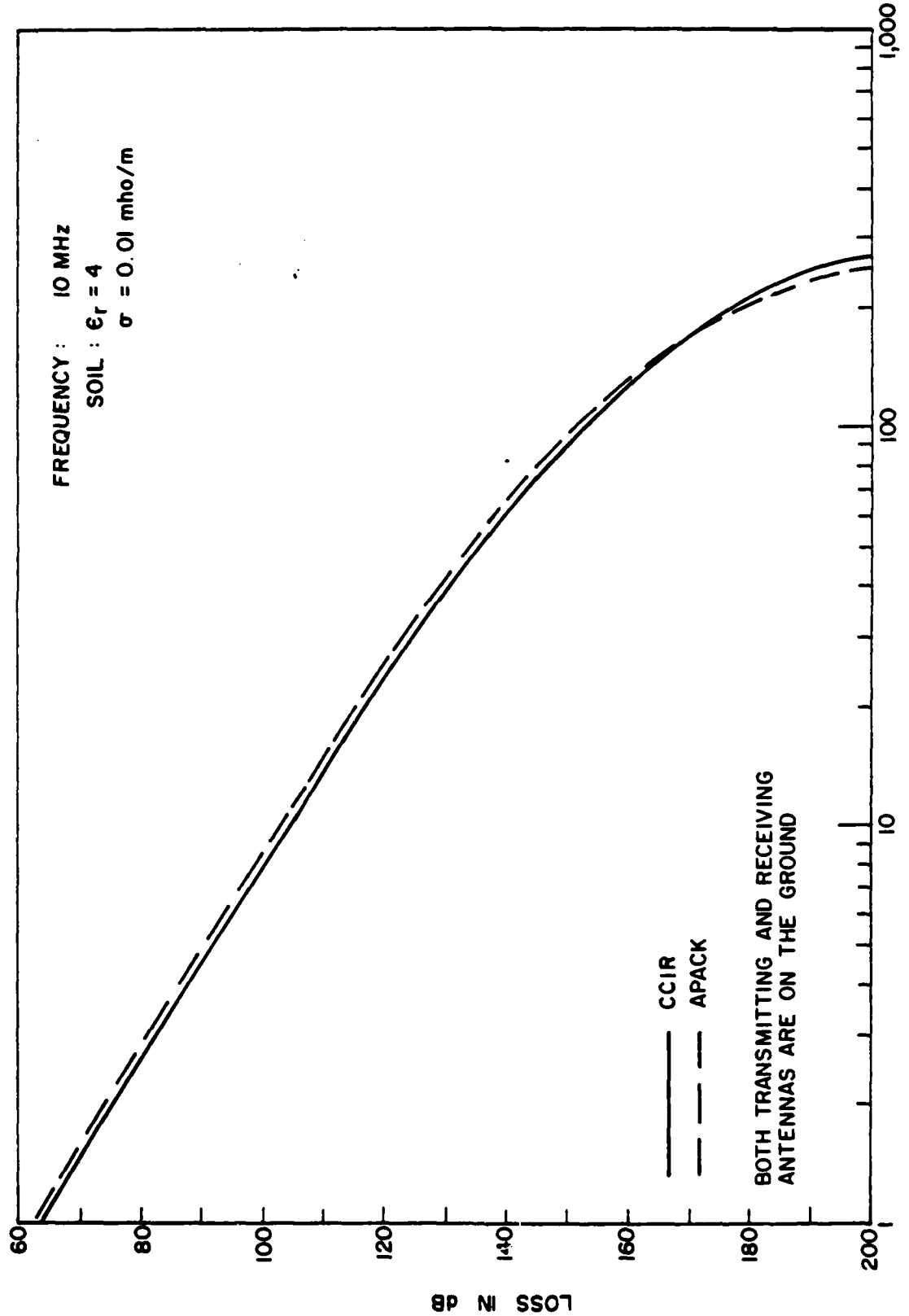

Figure 55. Comparisons between basic transmission loss predicted by APACK and CCIR for ground-wave propagation over soil at 10 MHz (vertical polarization).

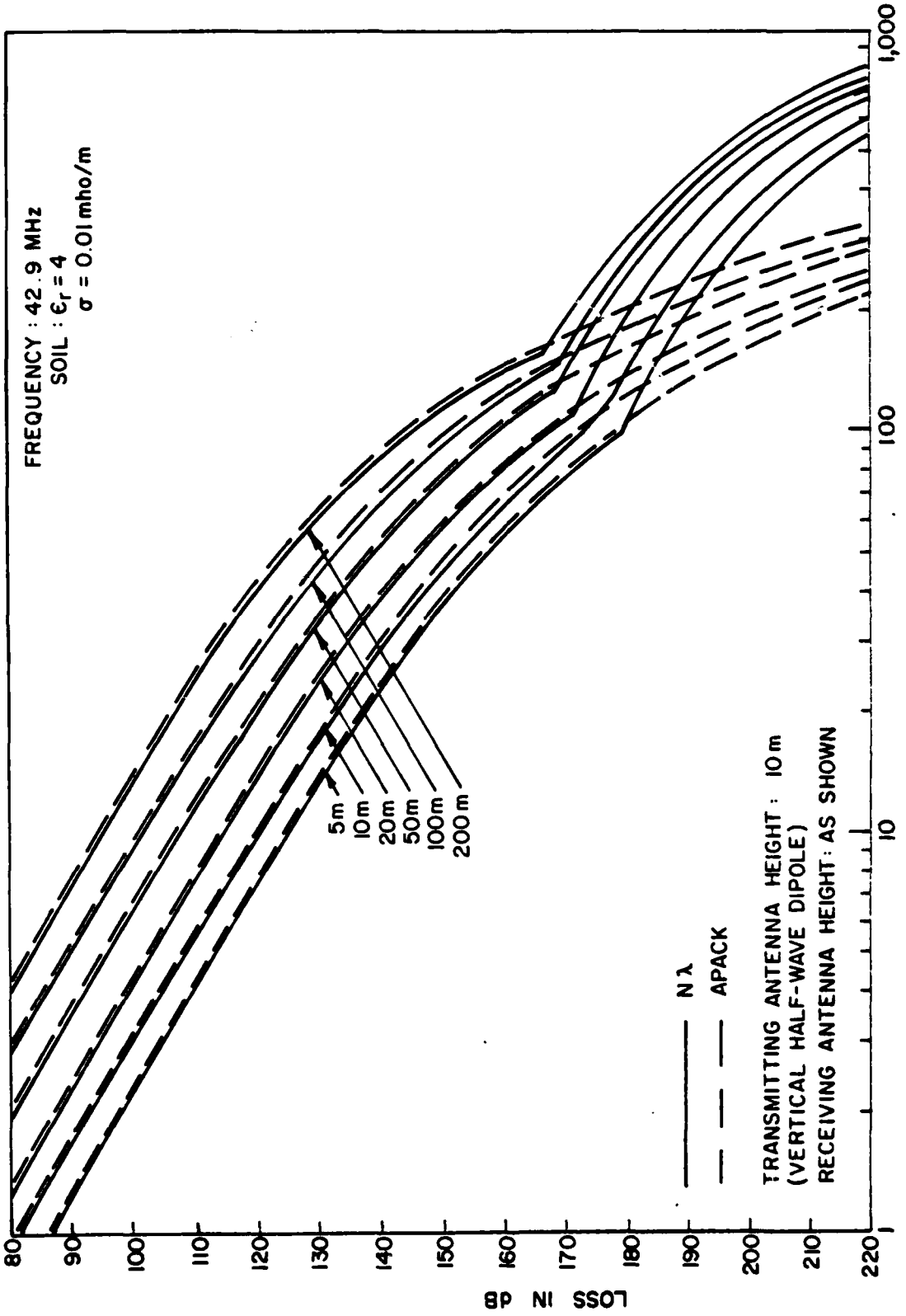

Figure 56. Comparisons between basic transmission loss predicted by APACK and NA for ground-wave propagation over soil at 42.9 MHz (vertical polarization).

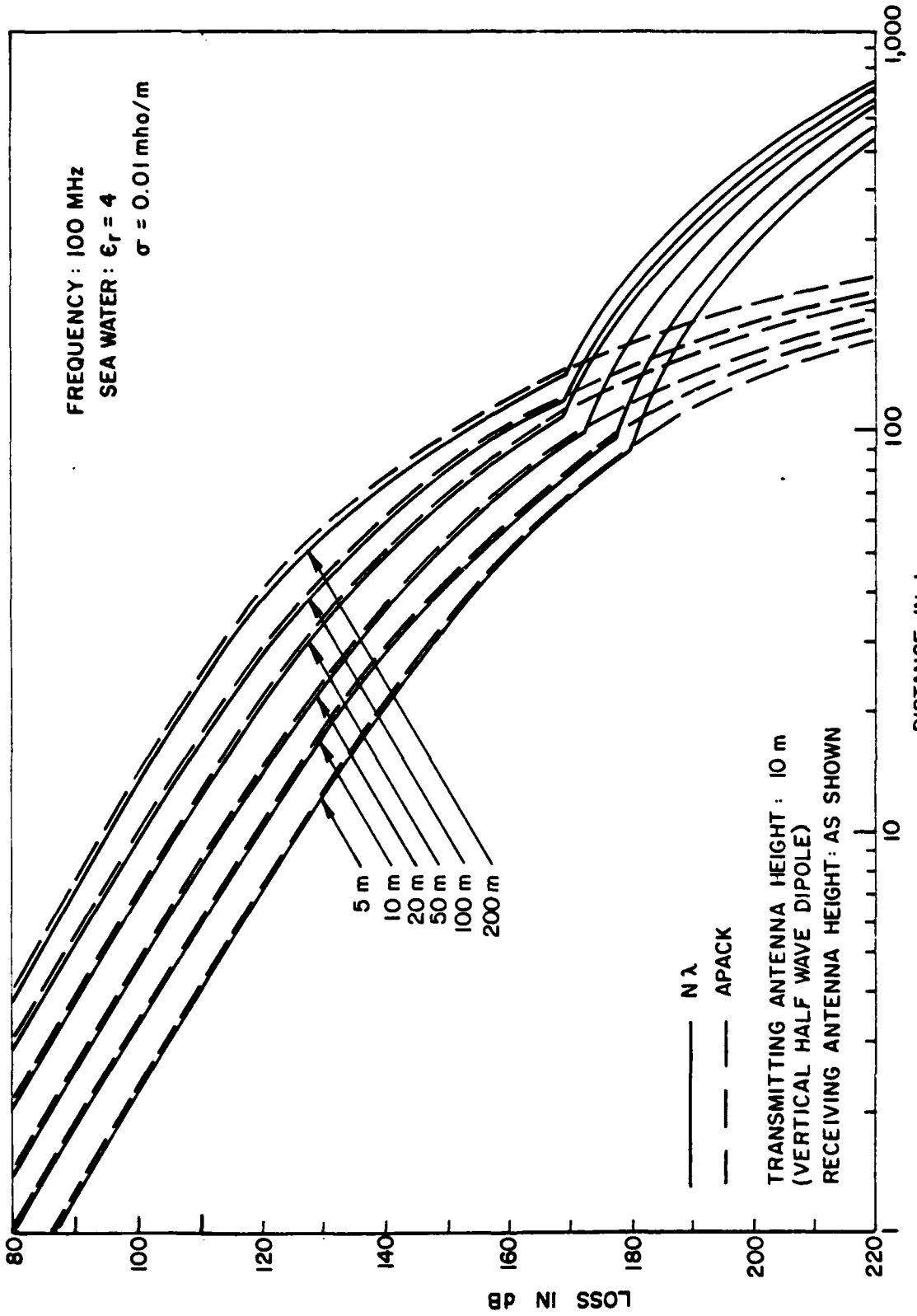

Figure 57. Comparisons between basic transmission loss predicted by APACK and Nλ for ground-wave propagation over soil at 100 MHz (vertical polarization).

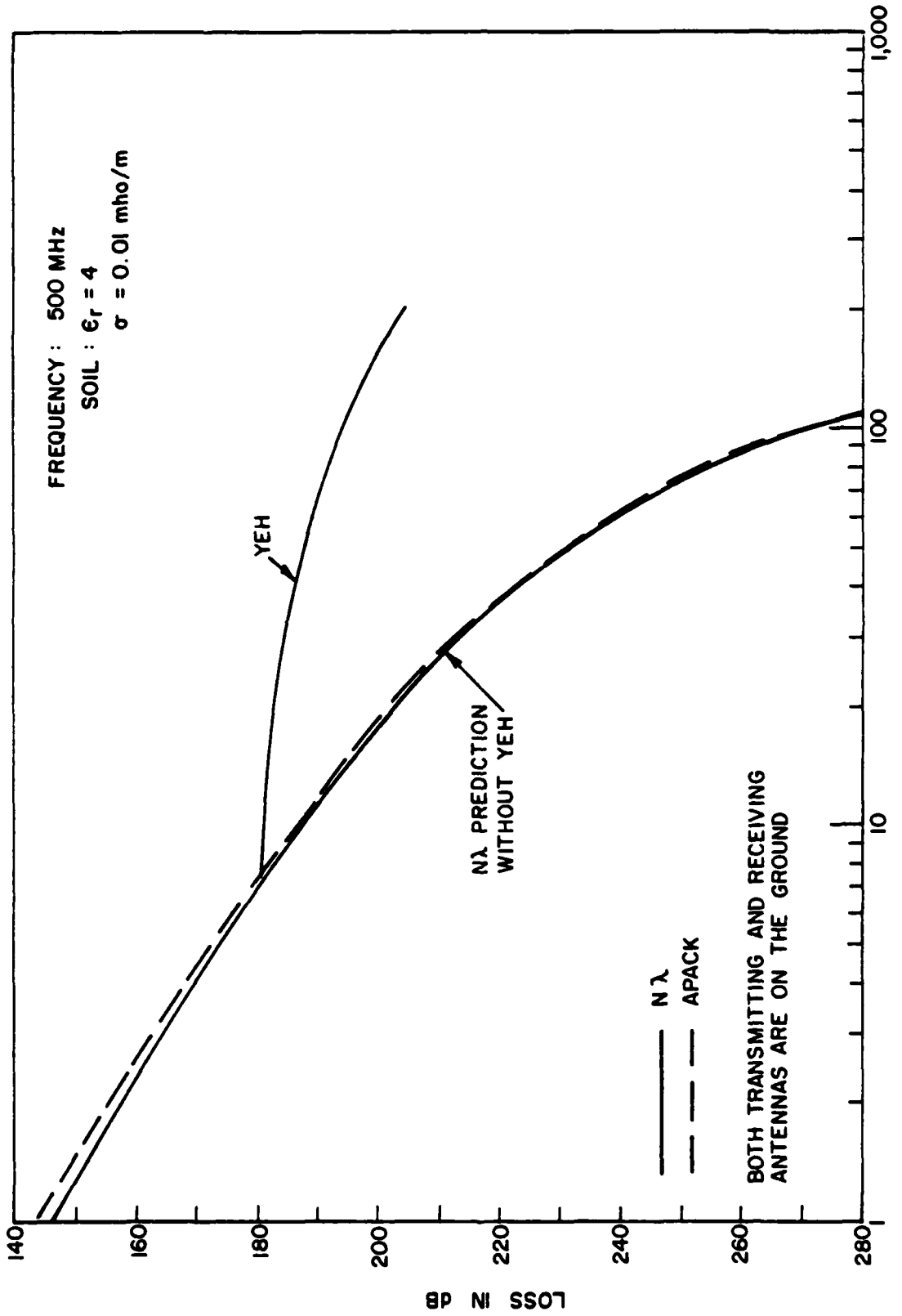

Figure 58. Comparisons between basic transmission loss predicted by APACK and Nλ for ground-wave propagation over soil at 500 MHz (vertical polarization).

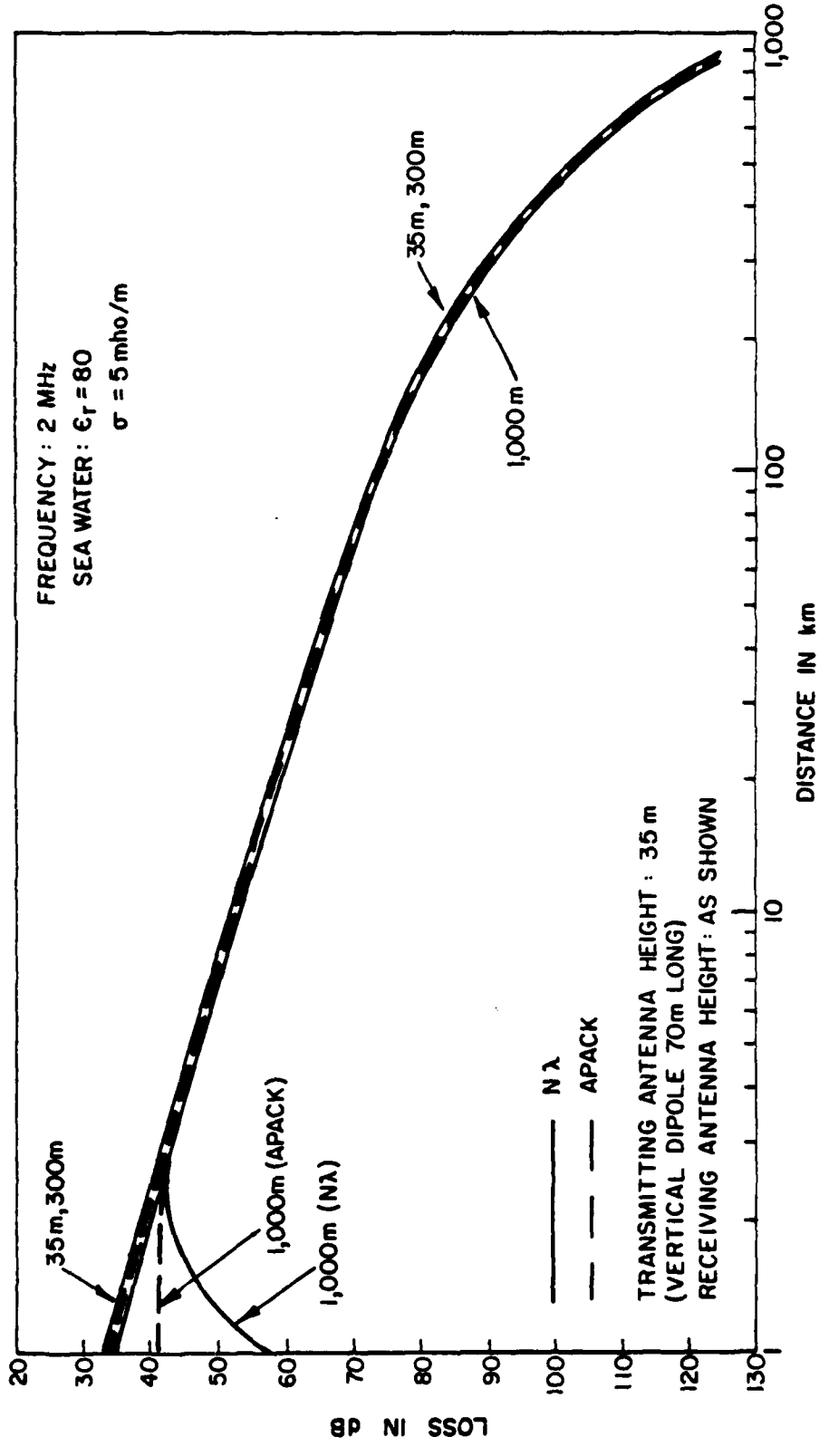

Figure 59. Comparisons between basic transmission loss predicted by APACK and Nλ for ground-wave propagation over sea water at 2 MHz (vertical polarization).

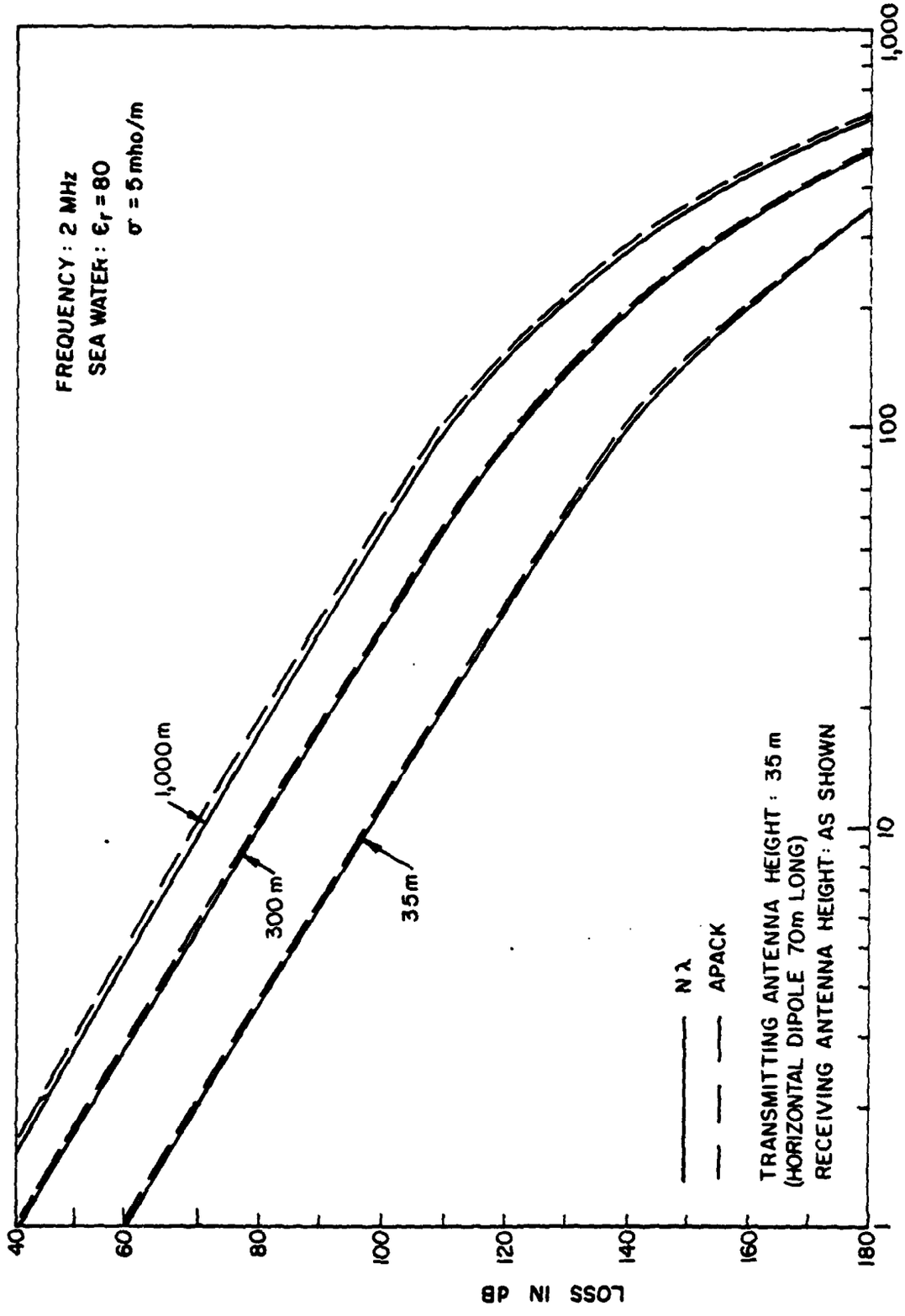

Figure 60. Comparisons between basic transmission loss predicted by APACK and NA for ground-wave propagation over sea water at 2 MHz (horizontal polarization).

Figure 60, the transmitting antenna is a horizontal dipole 70 meters long located 35 meters above the surface, and the height of the receiving antenna feed point is varied. By comparing Figures 59 and 60, it is seen that the horizontally polarized wave is attenuated more rapidly than the vertically polarized wave.

Figure 61 is included to show direct comparisons of field strengths produced by different transmitting antennas with the same feed-point height (10 meters) and polarization at a fixed frequency and receiving-antenna feed-point height (200 meters). The three transmitting antennas compared are the Hertzian dipole used by Bremmer (see Reference 17), a short vertical dipole (1.6 meters long), and a half-wave vertical dipole.

As shown in Figure 61, the field strengths produced by the Hertzian dipole are lower than the fields produced by the short dipole. The significant difference between the fields of the short dipole and the fields of the half-wave dipole (both predicted by APACK) is due to the fact that APACK considers the actual antenna structure.

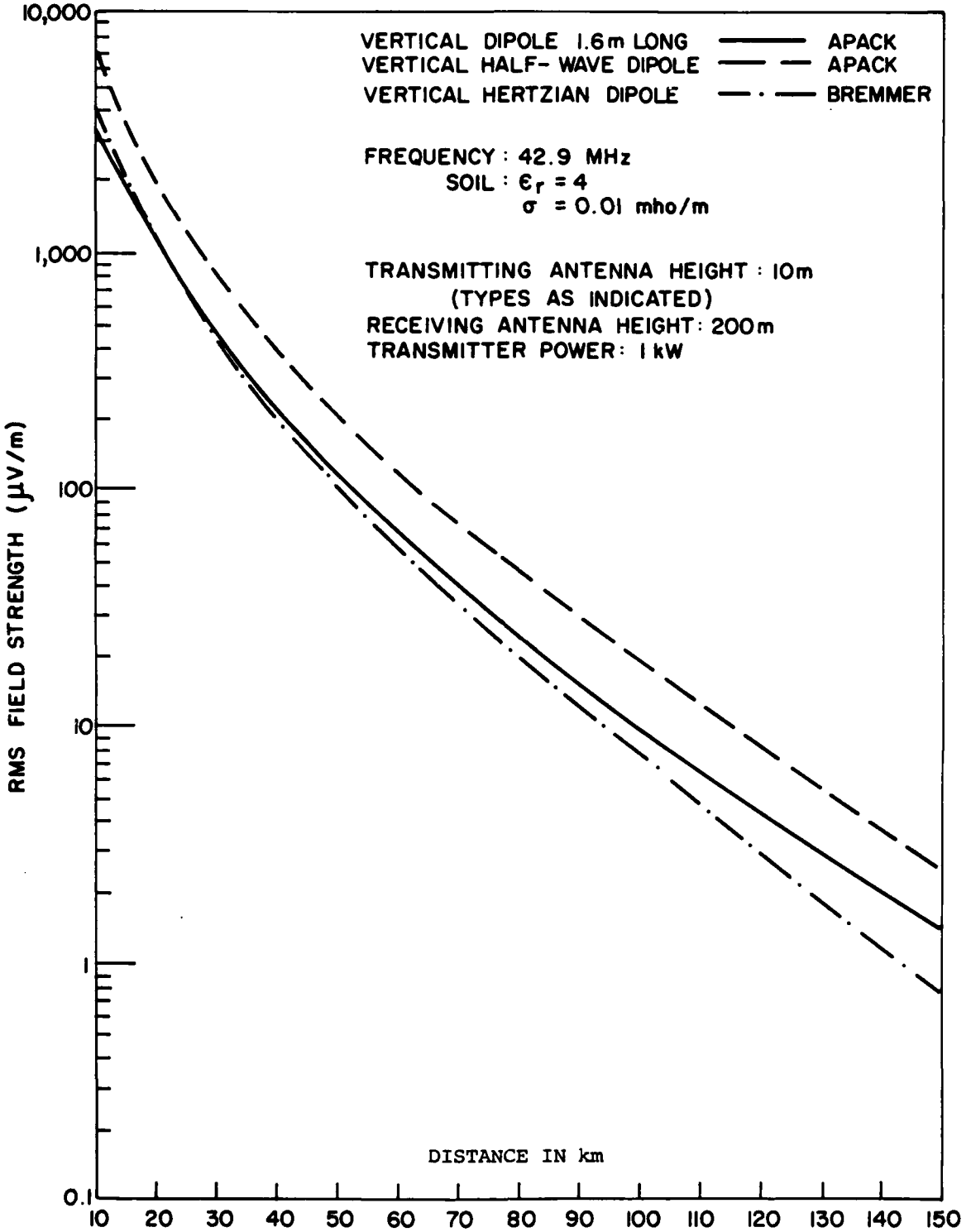

Figure 61. Comparisons between rms field strength predicted by APACK and Bremmer for ground-wave propagation over soil at 42.9 MHz (vertical polarization.)

SECTION 9
RESULTS

Equations have been developed to predict electric far-field strengths, directive gains, power gains, and transmission losses for 16 types of linear antennas used at frequencies between 150 kHz and 500 MHz. The antennas for which equations were developed are: horizontal dipole, vertical monopole, vertical monopole with radial-wire ground screen, elevated vertical dipole, inverted-L, arbitrarily tilted dipole, sloping long-wire, terminated sloping-V, terminated sloping rhombic, terminated horizontal rhombic, side-loaded vertical half-rhombic, horizontal Yagi-Uda array, horizontally polarized log-periodic dipole array, vertically polarized log-periodic dipole array, curtain array, and sloping double rhomboid (see Figures 3 through 18).

The equations include the contributions of the surface wave in addition to the contributions of the direct and ground-reflected waves so that gain predictions for ground-wave as well as sky-wave analyses can be made directly. The inclusion of the surface wave also allows predictions of ground-wave transmission loss accounting for the actual antenna structures.

The basic formulation of the APACK equations is for current elements located over lossy planar earth (see Figure 1). This formulation was extended to consider spherical earth within the radio horizon by making use of the divergence factor (see Figure 2). In the diffraction region beyond the radio horizon, the basic formulation was modified by using the radiation vector and the Bremmer secondary factor. APACK includes criteria to determine in which region the far-field observation point lies so that appropriate equations are used.

Comparisons have been made between APACK predictions of antenna gain and other available data (see Figures 19 through 47). Reasonable agreement is indicated.

Comparisons have also been made between APACK predictions of transmission loss and other available data (see Figures 48 through 61). Reasonable agreement is again indicated.

The APACK equations documented in this report have been automated at ECAC to provide a rapidly executing model for predicting gains and transmission loss for the 16 antennas considered. APACK allows the antennas to be described in terms of simple geometrical parameters, as opposed to the detailed structure description required by rigorous method-of-moments programs, to simplify the use of the model by EMC engineers.

The analytic expressions for the direct and ground-reflected waves have been derived by others. However, the analytic expressions for the surface wave represent new contributions to the antenna and propagation literature.

APPENDIX A

FORMULAS FOR CALCULATING FIELD STRENGTH AND GAIN OVER PLANAR EARTH AND IN THE DIFFRACTION REGION BEYOND THE RADIO HORIZON

HORIZONTAL DIPLOLE

The field intensities for a horizontal dipole are derived from those for a Hertzian dipole by using the principle of superposition. Therefore, consider a Hertzian dipole located H above planar earth with its axis in the same direction as the X-axis. The electric field intensities in cylindrical coordinates (ρ, ϕ, Z) are given as follows:[27]

$$E_\rho = -j \frac{k^2 Idx}{4\pi\varepsilon_1\omega} \cos\phi \left[\cos^2\theta_d \frac{e^{-jkR_d}}{R_d} - R_v \cos^2\theta_r \frac{e^{-jkR_r}}{R_r} - (1 - R_v) F_e \frac{n^2 - \sin^2\theta_r}{n^4} \frac{e^{-jkR_r}}{R_r} \right] \quad \text{(A-1)}$$

$$E_0 = j \frac{k^2 Idx}{4\pi\varepsilon_1\omega} \sin\phi \left[\frac{e^{-jkR_d}}{R_d} + R_h \frac{e^{-jkR_r}}{R_r} + (1 - R_h) F_m \frac{e^{-jkR_r}}{R_r} \right] \quad \text{(A-2)}$$

$$E_z = j \frac{k^2 Idx}{4\pi\varepsilon_1\omega} \cos\phi \left[\cos\theta_d \sin\theta_d \frac{e^{-jkR_d}}{R_d} - R_v \cos\theta_r \sin\theta_r \frac{e^{-jkR_r}}{R_r} + (1 - R_v) F_e \sin\theta_r \frac{\sqrt{n^2 - \sin^2\theta_r}}{n^2} \frac{e^{-jkR_r}}{R_r} \right] \quad \text{(A-3)}$$

---

[27] King, R.W.P., The Theory of Linear Antennas, Harvard University Press, Cambridge, MA, 1956.

E_ρ and E_z can be converted into the component E_θ in spherical coordinates (r, θ,0) as:

$$E_\theta = E_\rho \cos\theta - E_z \sin\theta \tag{A-4}$$

$$\begin{aligned} E_\theta = -j\frac{k^2 Idx}{4\pi\varepsilon_1\omega}\cos\phi\cos\theta\Bigg[&\cos^2\theta_d\frac{e^{-jkR_d}}{R_d} - R_v\cos^2\theta_r\frac{e^{-jkR_r}}{R_r} \\ &-(1-R_v)\,F_e\frac{n^2-\sin^2\theta_r}{n^4}\,\frac{e^{-jkR_r}}{R_r}\Bigg] - j\frac{k^2Idx}{4\pi\varepsilon_1\omega}\cos\phi\sin\theta \\ &\times\Bigg[\cos\theta_d\sin\theta_d\frac{e^{-jkR_d}}{R_d} - \sin\theta_r\cos\theta_r R_v\frac{e^{-jkR_r}}{R_r} \\ &+(1-R_v)\,F_e\sin\theta_r\frac{\sqrt{n^2-\sin^2\theta_r}}{n^2}\frac{e^{-jkR_r}}{R_r}\Bigg] \end{aligned} \tag{A-5}$$

Assuming $\theta_d = \theta_r = \theta$:

$$\begin{aligned} E_\theta = \frac{-jk^2Idx}{4\pi\varepsilon_1\omega}\cos\phi\Bigg[&\cos\theta\frac{e^{-jkR_d}}{R_d} - R_v\cos\theta\frac{e^{-jkR_r}}{R_r} \\ &+(1-R_v)\,F_e\frac{\sqrt{n^2-\sin^2\theta_r}}{n^2}\frac{e^{-jkR_r}}{R_r}\left\{\sin^2\theta - \frac{\sqrt{n^2-\sin^2\theta}}{n^2}\cos\theta\right\}\Bigg] \end{aligned} \tag{A-6}$$

$$E_\phi = \frac{jk^2Idx}{4\pi\varepsilon_1\omega}\sin\phi\left[\frac{e^{-jkR_d}}{R_d} + R_h\frac{e^{-jkR_r}}{R_r} + (1-R_h)\,F_m\frac{e^{-jkR_r}}{R_r}\right] \tag{A-7}$$

where

$$\frac{k^2}{4\pi\varepsilon_1\omega} = 30\ k,\ \varepsilon_1 = \varepsilon_o = \frac{10^{-9}}{36\pi}$$

In the far field, let:

$$R_r = R_d = r \text{ in amplitude terms}$$
$$\left.\begin{aligned} R_d &= r - H\cos\theta \\ R_r &= r + H\cos\theta \end{aligned}\right\} \text{ in exponent terms}$$

Then:

$$E_\theta = -j30kIdx\cos\phi\,\frac{e^{-jkr}}{r}\left[\cos\theta\ e^{jkH\cos\theta} - R_v e^{-jkH\cos\theta} + (1 - R_v)\,F_e\,\frac{\sqrt{n^2 - \sin^2\theta}}{n^2}r\sin^2\theta - \frac{\sqrt{n^2 - \sin^2\theta}}{n^2}\cos\theta \right. \quad \text{(A-8)}$$
$$\left. \times\ e^{-jkH\cos\theta}\right]$$

$$E_\phi = j30kIdx\sin\phi\,\frac{e^{-jkr}}{r}\left[e^{jkH\cos\theta} + R_h e^{-jkH\cos\theta} + (1 - R_h)\,F_m\,e^{-jkH\cos\theta}\right] \quad \text{(A-9)}$$

For the horizontal dipole:

$$\alpha' = 0,\ \theta' = \pi/2,\ \phi' = 0$$

and

$$\cos \psi = \sin \theta \cos \phi \tag{A-10}$$

Assume that the current distribution on the antenna is given by:

$$I = \begin{matrix} I_m \sin k (\ell - x), & x > 0 \\ I_m \sin k (\ell + x), & x < 0 \end{matrix} \tag{A-11}$$

and that the length of antenna is 2ℓ. Then:

$$E_\theta = -j30kI_m \cos \phi \frac{e^{-jkr}}{r} \left[\int_0^\ell \sin k (\ell - x) \, e^{jkx \cos \psi} \cos \theta \right.$$

$$\times \left\{ e^{jkH \cos \theta} - R_v e^{-jkH \cos \theta} + (1 - R_v) F_e \frac{\sqrt{n^2 - \sin^2 \theta}}{n^2 \cos \theta} \right.$$

$$\left. \left. \times e^{-jkH \cos \theta} \left(\sin^2 \theta - \frac{n^2 - \sin^2 \theta}{n^2} \cos \theta \right) \right\} dx \right. \tag{A-12}$$

$$+ \int_{-\ell}^0 \sin k (\ell + x) \, e^{jkx \cos \psi} \cos \theta \left\{ e^{jkH \cos \theta} - R_v e^{-jkH \cos \theta} \right.$$

$$\left. + (1 - R_v) F_e \frac{\sqrt{n^2 - \sin^2 \theta}}{n^2 \cos \theta} \left(\sin^2 \theta - \frac{\sqrt{n^2 - \sin^2 \theta}}{n^2} \cos \theta \right) \right.$$

$$\left. \left. \times e^{-jkH \cos \theta} \right\} dx \right]$$

where $e^{jkx \cos \psi}$ is the phase advance of the current element dx located at x.

$$\int_0^{\ell} e^{jkx \cos \psi} \sin k(\ell - x)\, dx = \frac{\{\cos(k\ell \cos\psi) - \cos k\ell\} + j\{\sin(k\ell \cos\psi) - \cos\psi \sin k\ell\}}{k \sin^2 \psi} \quad \text{(A-13)}$$

$$\int_{-1}^{0} e^{jkx \cos \psi} \sin k(\ell + x)\, dx = \frac{\{\cos(k\ell \cos\psi) - \cos k\ell\} - j\{\sin(k\ell \cos\psi) - \cos\psi \sin k\ell\}}{k \sin^2 \psi} \quad \text{(A-14)}$$

F_e is not a function of x in this case. Thus:

$$E_\theta = -j60I_m \frac{e^{-jkr}}{r} e^{jkH \cos\theta} \frac{\cos(k\ell \cos\psi) - \cos k\ell}{\sin^2 \psi} \cos\phi \times \left[\cos\theta \left(1 - R_v e^{-j2kH \cos\theta}\right) + (1 - R_v) F_e \frac{\sqrt{n^2 - \sin^2\theta}}{n^2} \times \left(\sin^2\theta - \frac{\sqrt{n^2 - \sin^2\theta}}{n^2} \cos\theta\right) e^{-j2kH \cos\theta}\right] \quad \text{(A-15)}$$

Similarly:

$$E_\phi = j60I_m \frac{e^{-jkr}}{r} e^{jkH \cos\theta} \frac{\cos(k\ell \cos\psi) - \cos k\ell}{\sin^2 \psi} \sin\phi \times \left[1 + R_h e^{-jkH \cos\theta} + (1 - R_h) F_m e^{-j2kH \cos\theta}\right] \quad \text{(A-16)}$$

Equations A-15 and A-16 are identical to Equations 65 and 66 of Reference 8 if the surface-wave terms are neglected. For ground-wave calculations, these equations may be written as follows:

$$E_\theta = -j60I_m \frac{\cos(k\ell\cos\psi) - \cos k\ell}{\sin^2\psi} \cos\phi \Bigg[\cos\theta \left(\frac{e^{-jkR_d}}{R_d} - R_v \frac{e^{-jkR_r}}{R_r} + (1 - R_v) \frac{\sqrt{n^2 - \sin^2\theta}}{n^2} \frac{e^{-jkR_r}}{R_r} \left(\sin^2\theta - \frac{\sqrt{n^2 - \sin^2\theta}}{n^2} \cos\theta \right) F_e \right) \Bigg] \quad \text{(A-17)}$$

$$E_\phi = j60I_m \frac{\cos(k\ell\cos\psi) - \cos k\ell}{\sin^2\psi} \sin\phi \left[\frac{e^{-jkR_d}}{R_d} + R_h \frac{e^{-jkR_r}}{R_r} + (1 - R_h) F_m \frac{e^{-jkR_r}}{R_r} \right] \quad \text{(A-18)}$$

where

$R_d = \sqrt{d^2 + (h - H)^2}$

$R_r = \sqrt{d^2 + (h + H)^2}$

d = horizontal distance from the transmitter to the receiver

h = height of the receiving antenna

H = height of the transmitting antenna.

Equations A-17 and A-18 are identical to Equations 10, 11, and 12 of Reference 20 if $\theta_d = \theta_r = \theta$.

The mutual impedance, referred to the dipole base, can be calculated from Reference 8 as:

$$Z_m = \frac{60}{1 - \cos 2k\ell} \left\{ e^{-j2k\ell} \left[K(U_o) - 2K(U_1) \right] + e^{j2k\ell} \left[K(V_o) - 2K(V_1) \right] + 2 \left[K(U_o') - K(U_1) \right] - K(V_1) + 2K(U_o') \right\} \times (1 + \cos 2k\ell) \qquad \text{(A-19)}$$

where

$$K(x) = Ci(x) - jSi(x) = \int_{\infty}^{x} \frac{\cos y}{y}\, dy - j \int_{\infty}^{x} \frac{\sin y}{y}\, dy$$

$$U_o = k\left[\sqrt{d^2 + 4\ell^2} - 2\ell\right] \qquad \text{(A-20)}$$

$$V_o = k\left[\sqrt{d^2 + 4\ell^2} + 2\ell\right]$$

$$U_o' = kd$$

$$U_1 = k\left[\sqrt{d^2 + \ell^2} - \ell\right]$$

$$V_1 = k\left[\sqrt{d^2 + \ell^2} + \ell\right]$$

$$d = 2H$$

The self-impedance, obtained from Equation A-19 if d = 2a, where a is the radius of the dipole, is given by:

$$Z_{11} = 2m\Big|_{d = \sqrt{2a}} \qquad \text{(A-21)}$$

Equation A-19 is not valid when ℓ is an integral multiple of a half-wavelength. In these cases, the impedances should be calculated based on the assumption of a more accurate form of current distribution (see Reference 9). The total input resistance is:

$$R_{in} = \mathrm{Re}\,(Z_{11} + R_h' Z_m) \tag{A-22}$$

R_h' is given by Equation 2-19.

The directive gain can be found using Equations A-1A, A-16, and A-22 as:

$$g_d = \frac{r^2 \left[|E_\theta|^2 + |E_\phi|^2\right]}{30\, I_m^2 \sin^2\left(k\ell\right) R_{in}} \tag{A-23}$$

The radiation vectors are given by:

$$N_\theta = \cos\theta \cos\phi\, e^{jkH\cos\theta} \left[\int_0^\ell I_m \sin k\,(\ell - x)\, e^{jkx\cos\psi}\, dx + \int_{-\ell}^0 I_m \sin k\,(\ell + x)\, e^{jkx\cos\psi}\, dx\right]$$

or

$$N_\theta = -\cos\theta\cos\phi\, e^{jkH\cos\theta}\left(\frac{2\, I_m}{k}\,\frac{\cos\,(KL\cos\psi) - \cos KL}{\sin^2\psi}\right) \tag{A-24}$$

$$N_\phi = \sin\phi\, e^{jkH\cos\theta}\left[\int_0^{\ell} I_m \sin k(\ell-x)\, e^{jkx\cos\psi}\, dx + \int_{-\ell}^{0} I_m \sin k(\ell+x)\, e^{jkx\cos\psi}\, dx\right] \quad \text{(A-25)}$$

or

$$N_\phi = \sin\phi\, e^{jkH\cos\theta}\left(\frac{2I_m}{k}\,\frac{\cos(k\ell\cos\psi) - \cos k\ell}{\sin^2\psi}\right)$$

The free-space field intensities are given by:

$$E_{\theta f} = \frac{-j60\, I_m\, e^{-jkr}}{r}\cos\theta\cos\phi\,\frac{\cos(k\ell\cos\psi) - \cos k\ell}{\sin^2\psi} \quad \text{(A-26)}$$

$$E_{\phi f} = \frac{j\,60\, I_m\, e^{-jkr}}{r}\sin\phi\,\frac{\cos(k\ell\cos\psi) - \cos k\ell}{\sin^2\psi} \quad \text{(A-27)}$$

Then:

$$|E_f| = \sqrt{|E_{\theta f}|^2 + |E_{\phi f}|^2} \quad \text{(A-28)}$$

$$|E| = \sqrt{|E_\theta|^2 + |E_\phi|^2} \quad \text{(A-29)}$$

where E_θ and E_ϕ are given by Equations A-15 and A-16. The attenuation relative to free space is:

$$|A| = \sqrt{\frac{|E_\theta|^2 + |E_\phi|^2}{|E_{\theta f}|^2 + |E_{\phi f}|^2}} \qquad \text{(A-30)}$$

$$ADB = 20 \log \frac{1}{|A|} \qquad \text{(A-31)}$$

The electric field intensities in the diffraction region are given by:

$$E_\theta = \frac{-j\ 60\ I_m e^{-jkd}}{d} \cos\phi \cos\theta \frac{\cos(k\ell \cos\psi) - \cos k\ell}{\sin^2\psi} (2F_r) \qquad \text{(A-32)}$$

$$E_\phi = \frac{j\ 60\ I_m e^{-jkd}}{d} \sin\phi \frac{\cos(k\ell \cos\psi) - \cos k\ell}{\sin^2\psi} (2F_r) \qquad \text{(A-33)}$$

VERTICAL MONOPOLE

The field intensities for the vertical monopole are also derived from those for a Hertzian dipole. The vertical and radial components of electric field intensity due to a vertical Hertzian dipole (see Reference 27) are given by:

$$E_z = -j30k\,IdZ \left| \sin^2\theta_d \frac{e^{-jkR_d}}{R_d} + R_V \sin^2\theta_r \frac{e^{-jkR_r}}{R_r} + (1-R_V) \right.$$
$$\left. \times F_e \sin^2\theta_r \frac{e^{-jkR_r}}{R_r} \right| \qquad \text{(A-34)}$$

$$E_r = j30K\ IdZ \left| \sin\theta_d \cos\theta_d \frac{e^{-jkR_d}}{R_d} + R_V \sin\theta_r \cos\theta_r \right.$$
$$\left. \times \frac{e^{-jkR_r}}{R_r} - (1-R_V)\ F_e \sin\theta_r \frac{\sqrt{n^2-\sin^2\theta_r}}{n^2} \frac{e^{-jkR_r}}{R_r} \right| \qquad \text{(A-35)}$$

Due to symmetry, $E_\phi = 0$.

In spherical coordinates (r, θ, ϕ):

$$E_\theta = E_r \cos\theta - E_Z \sin\theta$$

$$= j30kIdZ \cos\theta \left\{ \sin\theta_d \cos\theta_d \frac{e^{-jkR_d}}{R_d} + R_v \sin\theta_r \cos\theta_r \right. \tag{A-36}$$

$$\left. \times \frac{e^{-jkR_r}}{R_r} - (1-R_v) F_e \sin\theta_r \frac{\sqrt{n^2 - \sin^2\theta_r}}{n^2} \frac{e^{-jkR_r}}{R_r} \right\} + j30kIdZ \sin\theta$$

$$\times \left\{ \sin^2\theta_d \frac{e^{-jkR_d}}{R_d} + R_v \sin^2\theta_r \frac{e^{-jkR_r}}{R_r} + \left(1-R_v\right) F_e \sin^2\theta_r \frac{e^{-jkR_r}}{R_r} \right\}$$

Again, the following approximations are made:

$$\left.\begin{aligned} R_d &= R_r = r \text{ in amplitude terms} \\ \theta_d &= \theta_r = \theta \\ R_d &= r - z\cos\theta \\ R_r &= r + z\cos\theta \end{aligned}\right\} \text{ in exponent terms}$$

Now assume that the current distribution is given by:

$$I = I_m \sin k(\ell - z) \tag{A-37}$$

Then:

$$E_\theta = j30k\ Idz\ \frac{e^{-jkr}}{r}\ \sin\theta \left\{ e^{jkz\cos\theta} + R_V\, e^{-jkz\cos\theta} + (1-R_V) \right.$$
$$\left. x\ F_e\ e^{-jkz\cos\theta}\ \left(\sin^2\theta - \frac{\sqrt{n^2-\sin^2\theta}}{n^2}\ \cos\theta\right)\right\} \qquad \text{(A-38)}$$

Substituting Equation A-37 into A-38 and integrating:

$$E_\theta = j30kI_m\ \frac{e^{-jkr}}{r}\ \sin\theta \int_0^{\ell} \sin k\,(\ell-z) \left\{ e^{jkz\cos\theta} + R_V e^{-jkz\cos\theta} \right.$$
$$\left. + (1-R_V)\ F_e\ e^{-jkz\cos\theta}\ \left(\sin^2\theta - \frac{\sqrt{n^2-\sin^2\theta}}{n^2}\ \cos\theta\right)\right\} dz \qquad \text{(A-39)}$$

where

$$F_e = 1 - j\ \sqrt{\pi P_e}\ e^{-P_e}\ \text{erfc}\ (j\sqrt{P_e})$$

and,

$$\text{erfc}(x) = 1 - \frac{2}{\sqrt{\pi}} \int_0^x e^{-y^2}\, dy$$

Then:

$$E_\theta = j30kI_m \frac{e^{-jkr}}{r} \sin\theta \left[J_1 + \left\{ R_V + (1-R_V)\left(\sin^2\theta - \frac{\sqrt{n^2-\sin^2\theta}}{n^2} \cos\theta\right)\right\} \right.$$
$$\left. x\, J_2 - (1-R_V)\left(\sin^2\theta - \frac{\sqrt{n^2-\sin^2\theta}}{n^2} \cos\theta\right) J_3 \right] \quad \text{(A-40)}$$

where

$$J_1 = \int_0^\ell e^{jkz\cos\theta} \sin k(\ell - z)\, dz \quad \text{(A-41)}$$
$$= \frac{[\cos(k\ell\cos\theta) - \cos k\ell] + j[\sin(k\ell\cos\theta) - \cos\theta \sin k\ell]}{k\sin^2\theta}$$

$$J_2 = \int_0^\ell e^{-jkz\cos\theta} \sin k(\ell - z)\, dz \quad \text{(A-42)}$$
$$= \frac{[\cos(k\ell\cos\theta) - \cos k\ell] - j[\sin(k\ell\cos\theta) - \cos\theta \sin k\ell]}{k\sin^2\theta}$$

$$J_e = \int_0^\ell e^{-jkz\cos\theta} \sin k(\ell - z)\, j\sqrt{\pi P_e}\, e^{-P_e} \operatorname{erfc}(j\sqrt{P_e})\, dz \quad \text{(A-43)}$$

Equation A-43 is evaluated in APPENDIX B as:

$$J_e = \frac{1}{1-R_V}\frac{\sqrt{n^2-\sin^2\theta}}{n^2}\left[\sqrt{\frac{j2\pi r}{k}}\, e^{-P_e}\,\mathrm{erfc}\,(j\sqrt{P_e})\right. \quad \text{(A-44)}$$

$$\times \frac{\{\cos(k\ell\cos\theta) - \cos k\ell\} - j\{\sin(k\ell\cos\theta) - \sin k\ell\cos\theta\}}{\sin\theta}$$

$$\left. + \frac{j2F_e \sin k\ell}{k\sin^2\theta}\right]$$

Then:

$$E_\theta = j30I_m \frac{e^{-jkr}}{r}\left[\frac{A_2+jB_2}{\sin\theta} + R_V\frac{A_2-jB_2}{\sin\theta} + (1-R_v)\left(\sin^2\theta\sqrt{\frac{n^2-\sin^2\theta}{n^2}}\cos\theta\right)\right.$$

$$\times \frac{A_2-jB_2}{\sin_\theta} - (1-R_V)\left(\sin^2\theta - \sqrt{\frac{n^2-\sin^2\theta}{n^2}}\cos\theta\right)\frac{\sin\theta}{1-R_V}\sqrt{\frac{n^2-\sin^2\theta}{n^2}}$$

$$\left.\times\left\{j2\pi kr\; e^{-P_e}\,\mathrm{erfc}\,(j\sqrt{P_e})\,\frac{A_{2-j}B_2}{\sin\theta} + \frac{j2F_e}{\sin^2\theta}\sin k\ell\right\}\right] \quad \text{(A-45)}$$

Simplifying further:

$$E_\theta = j30I_m \frac{e^{-jkr}}{r}\left[\frac{A_2+jB_2}{\sin\theta} + R_V\frac{A_2-jB_2}{\sin\theta} + (1-R_V)\left(\sin^2\theta - \sqrt{\frac{n^2-\sin^2\theta}{n^2}}\cos\theta\right)\right.$$

$$\times \frac{A_2-jB_2}{\sin\theta}\left\{1 - j\sqrt{\pi P_e}\sin^2\theta\, e^{-P_e}\,\mathrm{erfc}\,(j\sqrt{P_e})\right\} - j2F_e\left(\sin^2\theta\right. \quad \text{(A-46)}$$

$$\left.\left. - \sqrt{\frac{n^2-\sin^2\theta}{n^2}}\cos\theta\right)\sqrt{\frac{n^2-\sin^2\theta}{n^2\sin\theta}}\sin k\ell\right]$$

where

$$A_2 = \cos(k\ell \cos\theta) - \cos k\ell \quad \text{(A-47)}$$

$$B_2 = \sin(k\ell \cos\theta) - \cos\theta \sin k\ell \quad \text{(A-48)}$$

The first two terms of Equation A-46 (direct and ground-reflected wave contributions) are identical to Equation 29 in Reference 8. The last two terms represent the surface-wave contribution to the field.

The radiation resistance of a vertical monopole over lossy earth is very difficult to calculate. In fact, no accurate representation is available in the literature.

The method of Sommerfeld and Renner[28,29] cannot be used here because it is not applicable when the dipole touches the ground. Thus, the expression for a perfectly conducting ground will be used here. The input resistance for perfectly conducting ground is:

$$R_{in} = \frac{30}{\sin^2 k\ell}\left[(1+\underset{-}{\text{Cin}}\ 2\ k\ell)\ \text{Cin}\ (2\ k\ell) - \frac{1}{2}\cos 2k\ell\ \text{Cin}\ (4k\ell) + \frac{1}{2}\sin 2\ k\ell\ \text{Si}(4k\ell) - \sin 2k\ell\ \text{Si}\ (2k\ell)\right] \quad \text{(A-49)}$$

---

[28] Sommerfeld, A. and Renner, F., "Strahlungsenergie und Erdabsorption bei Dipolantennen," Ann. Physik, Vol. 41, pp. 1-36, 1942.

[29] Kuebler, W. and Karwath, A., Program RENNER: Normalized Radiation Resistance of a Hertzian Dipole over Arbitrary Ground, ECAC-TN-75-024, Electromagnetic Compatibility Analysis Center, Annapolis, MD, January 1976.

where

$$Cin(x) = 0.577 + \ln x - Ci(x)$$

$$Si(x) = \int_0^x \frac{\sin u}{u}\, du$$

$$Ci(x) = \int_\infty^x \frac{\cos u}{u}\, du$$

(0.577 is Euler's constant)

The directive gain of the dipole is given by:

$$g_d = \frac{r^2 |E_\theta|^2}{30 I_m^2 \sin^2 (k\ell) R_{in}} \qquad (A-50)$$

Since $g_p = \eta g_d$, the power gain of the dipole is given by:

$$g_p = \frac{\eta r^2 |E_\theta|^2}{30 I_m^2 \sin^2 (k\ell) R_{in}} \qquad (A-51)$$

where

$$\eta = 10^{\left[\frac{\eta(dB)}{10}\right]} \qquad (A-52)$$

The radiation efficiency is given in Reference 14 as:

$$n(dB) = 6416.702 \left(\frac{\ell}{\lambda}\right)^4 + 6091.33 \left(\frac{\ell^3}{\lambda}\right) - 2179.89 \left(\frac{\ell^2}{\lambda}\right) + 364.817 \left(\frac{\ell}{\lambda}\right) - 25.646 \quad \text{(A-53)}$$

The radiation vector is obtained by:

$$N_z = -\int_0^{\ell} I_m \sin k(\ell - z)\, e^{jkz\cos\theta}\, dz \quad \text{(A-54)}$$

$$= \frac{I_m}{k} \frac{\{\cos(k\ell\cos\theta) - \cos k\ell\} + j\{\sin(k\ell\cos\theta) - \cos\theta \sin k\ell\}}{\sin^2\theta}$$

$$N_\theta = N_z \sin\theta = -\frac{I_m}{k} \frac{A_2 + j B_2}{\sin\theta} \quad \text{(A-55)}$$

The free-space field intensity is given by:

$$E_{\theta f} = \frac{j 30 I_m e^{-jkr}}{r} \frac{A_2 + j B_2}{\sin\theta} \quad \text{(A-56)}$$

The attenuation relative to free space is:

$$A = \frac{|E_\theta|}{|E_{\theta f}|} \quad \text{(A-57)}$$

$$ADB = 20 \log \frac{1}{|A|} \quad \text{(A-58)}$$

The electric field intensity in the diffraction region is given by:

$$E_\theta = \frac{j30\ I_m\ e^{-jkd}}{d} \quad \frac{A_2 + j\ B_2}{\sin\theta}\ 2\ F_r \qquad \text{(A-59)}$$

VERTICAL MONOPOLE WITH RADIAL-WIRE GROUND SCREEN

Most permanent monopole installations include a ground screen. The presence of a ground screen has been studied by Wait and Pope,[30] Wait and Surtees,[31] Wait,[32] and Maley and King.[33]

The presence of a ground screen will modify the field in the absence of the screen by a correction factor ΔE_θ given by:

$$E'_\theta = E_\theta + \Delta E_\theta \qquad \text{(A-60)}$$

when E_θ (the field without the screen) is given by:

---

[30] Wait, J.R. and Pope, W.A., "The Characteristics of a Vertical Antenna With a Radial Conductor Ground System," Appl. Sci. Res., Section B.4, 1954 pp. 177-185.

[31] Wait, J.R. and Surtees, W.J., "Impedance of a Top-loaded Antenna of Arbitrary Length Over a Circular Grounded Screen," J. Appl. Physics, Vol. 25, 1954, pp. 553-555.

[32] Wait, J.R., "Effect of the Ground Screen on the Field Radiated from a Monopole," IRE Trans. Antennas and Propagation, Vol. AP-4, No. 2, 1956, pp. 179-181.

[33] Maley, S.W. and King, R.J., "The Impedance of a Monopole Antenna With a Circular Conducting-Disk Ground System on the Surface of a Lossy Half-space," J. Research NBS, 65D (Radio Propagation) No. 2, 1961, pp. 183-188.

$$E_\theta = \frac{j30\ I_m e^{-jkr}}{r} \left[\frac{A_2 + jB_2}{\sin\theta} + R_v \frac{A_2 - jB_2}{\sin\theta} + (1-R_v)\left(\sin^2\theta - \frac{\sqrt{n^2 - \sin^2\theta}}{n^2}\cos\theta\right) \right. \quad \text{(A-61)}$$

$$\left. \times \frac{A_2 - jb_2}{\sin\theta} \left\{1 - j\sqrt{\pi P_e}\, e^{-P_e} \sin^2\theta\ \text{erfc}\left(j\sqrt{P_e}\right)\right\} - j2\ F_e \left(\sin^2\theta - \frac{\sqrt{n^2 - \sin^2\theta}}{n^2}\cos\theta\right) \frac{\sqrt{n^2 - \sin^2\theta}}{n^2 \sin\theta} \sin k\ell \right]$$

where

$$A_2 = \cos(k\ell\cos\theta) - \cos k\ell \quad \text{(A-62)}$$

$$B_2 = \sin(k\ell\cos\theta) - \cos\theta \sin k\ell \quad \text{(A-63)}$$

$$\Delta E_\theta = -E_\theta \left[\frac{\eta \sin\theta \int_o^{ka} \left[e^{-j\sqrt{x^2 + k^2\ell^2}} - e^{-jx}\cos k\ell\right] J_1(x\sin\theta)\, dx}{120\,\pi \sin k\ell \left[\cos(k\ell\cos\theta) - \cos k\ell\right]} \right] \quad \text{(A-64)}$$

$$\frac{E'_\theta}{E_\theta} = 1 - \left[\frac{\eta \sin\theta \int_o^{ka} \left[e^{-j\sqrt{x^2 + k^2\ell^2}} - e^{-jx}\cos k\ell\right] J_1(x\sin\theta)\, dx}{120\pi \sin k\ell \left[\cos(k\ell\cos\theta) - \cos k\ell\right]} \right] \quad \text{(A-65)}$$

where

J_1 = Bessel function of the first kind

$$\eta = \frac{j\omega\mu_o}{\sigma + j\omega\varepsilon_o\varepsilon_r}$$, the characteristic impedance of the ground

μ_o = $4\pi x10^{-7}$, the permeability of free space

ε_o = $8.854x10^{-12}$, the permittivity of free space

ε_r = relative dielectric constant of the ground

σ = conductivity of the ground

ω = angular frequency.

If $\sigma = o$, $\eta = \sqrt{\frac{\mu_o}{\varepsilon_o}} = 120\,\pi$ (free-space value)

If $\sigma >> \omega\varepsilon_o\varepsilon_r$, $\eta = \sqrt{\frac{\mu_o\omega}{\sigma}}\ e^{\frac{j\pi}{4}}$ (perfectly conducting ground)

Wait and Pope (Reference 30) have shown that the effect on the radiation resistance caused by the ground screen can be expressed as:

$$R_{in}' = R_{in} + Re\ (\Delta Z_1 + \Delta Z_2) \qquad (A\text{-}66)$$

where

$$R_{in} = \frac{30}{\sin^2 k\ell}\left[(1 + \cos 2k\ell)\ Cin\ (2k\ell) - \frac{1}{2}\cos 2k\ell\ Cin\ (4k\ell)\right.$$
$$\left. - \sin 2k\ell\ Si\ (2k\ell) + \frac{1}{2}\sin 2k\ell\ Si\ (4k\ell)\right] \qquad (A\text{-}67)$$

and ΔZ_1 corresponds to the self-impedance of the monopole over a perfectly conducting discoid. ΔZ_1 can be expressed as:

$$\begin{aligned}\Delta Z_1 = \frac{\eta}{4\pi \sin^2 k\ell} \Bigg\{ & e^{j2k\ell} \left[Ci\,(2k\,(r_o + \ell)) + j\,(\tfrac{\pi}{2} - Si\,(2k\,(r_o + \ell))) \right] \\ & + e^{-j2k\ell} \left[Ci\,(2k\,(r_o - \ell)) + j\,(\tfrac{\pi}{2} - Si\,(2k\,(r_o - \ell))) \right] \\ & + 2\cos^2 k\ell \left[Ci\,(2\,ka) + j\,(\tfrac{\pi}{2} - Si(2ka)) \right] \\ & + 4\cos k\ell \left[Ci\,(kr_1) + j\,(\tfrac{\pi}{2} - Si\,(kr_1)) \right] \\ & - 4\cos k\ell\, e^{-jk\ell} \left[Ci\,(k(r_1 - \ell)) + j\,(\tfrac{\pi}{2} - Si\,(k(r_1 - \ell))) \right] \\ & - 4\cos k\ell\, e^{jk\ell} \left[Ci\,(k(r_1 + \ell)) + j\,(\tfrac{\pi}{2} - Si(k(r_1 + \ell))) \right] \end{aligned} \qquad \text{(A-68)}$$

where

$$r_o = \sqrt{a^2 + \ell^2} \qquad \text{(A-69)}$$

$$r_1 = a + \sqrt{a^2 + \ell^2} \qquad \text{(A-70)}$$

ΔZ_2 accounts for the finite surface impedance of the radial-conductor system and is given by:

$$\Delta Z_2 = -\int_0^a \frac{\eta_s \eta}{\eta_s + \eta} \frac{[e^{-jk\sqrt{\rho^2 + \ell^2}} - e^{-jk\rho} \cos k\ell]^2}{2\pi\rho \sin^2 k\ell} d\rho \quad \text{(A-71)}$$

where

$$\eta_s = j \frac{240\pi^2 \rho}{N\lambda} \ell n \frac{\rho}{NC} \quad \text{(A-72)}$$

C = radius of the conducting screen

N = number of radial conductors

The directive gain for the monopole over a radial-wire ground screen becomes:

$$g_d = \frac{r^2 |E_\theta'|^2}{30 I_m^2 \sin^2(k\ell) R_{in}} \quad \text{(A-73)}$$

(The radiation efficiency is still given by Equation A-53.)

The free-space field intensity is given by:

$$E_{\theta f} = \frac{j30 I_m e^{-jkr}}{r} \frac{A_2 + jB_2}{\sin\theta} \quad \text{(A-74)}$$

The attenuation relative to free space is:

$$A = \frac{|E_\theta'|}{|E_{\theta f}|} \quad \text{(A-75)}$$

$$ADB = 20 \log \frac{1}{|A|} \qquad (A-76)$$

The electric field intensity in the diffraction region is given by:

$$E_\theta = \frac{j30\, I_m\, e^{-jkd}}{d} \frac{A_2 + j\, B_2}{\sin \theta} 2\, F_r \qquad (A-77)$$

ELEVATED VERTICAL DIPOLE

The current distribution assumed for the elevated vertical dipole is:[34]

$$I = \begin{cases} I_m \sin k\,(\ell + z_o - z), & z_o \leq z \leq z_o + \ell \qquad (A-78) \\ I_m \sin k\,(\ell - z_o + z), & z_o - \ell \leq z \leq z_o \qquad (A-79) \end{cases}$$

The coordinate system is identical to that considered for the vertical monopole. From Equation A-38:

[34] Jordan, E.C. and Balmain, K.G., Electromagnetic Waves and Radiating Systems, Prentice Hall, Englewood Cliffs, NJ, 1968.

$$E_\theta = j30\, kI_m dz \frac{e^{-jkr}}{r} \sin\theta \left\{ e^{jkz\cos\theta} + R_v e^{-jkz\cos\theta} + (1-R_v) F_e e^{-jkz\cos\theta} \left(\sin^2\theta - \frac{\sqrt{n^2-\sin^2\theta}}{n^2}\cos\theta\right)\right\}$$

With the current distribution as given by Equations A-78 and A-79:

$$E_\theta = j30\, kI_m \frac{e^{-jkr}}{r} \sin\theta \int_{Z_o-\ell}^{Z_o} \sin k(\ell - Z_\rho + z) \left\{ e^{jkz\cos\theta} + R_v e^{-jkz\cos\theta} + (1-R_v)\left(\sin^2\theta - \frac{\sqrt{n^2-\sin^2\theta}}{n^2}\cos\theta\right) F_e e^{-jkz\cos\theta}\right\}$$

$$+ \int_{Z_o}^{Z_o+\ell} \sin k\,(\ell + Z_o - z) \left\{ e^{jkz\cos\theta} + R_v e^{-jkz\cos\theta} + (1-R_v)\left(\sin^2\theta - \frac{\sqrt{n^2-\sin^2\theta}}{n^2}\cos\theta\right) F_e e^{-jkz\cos\theta}\right\} dz \qquad \text{(A-80)}$$

Equation A-81 is rewritten as:

$$E_\theta = j30\, kI_m \frac{e^{-jkr}}{r} \sin\theta \left[(J_1+J_1') + R_v (J_2+J_2') + (1-R_v)\left(\sin^2\theta - \frac{\sqrt{n^2-\sin^2\theta}}{n^2}\cos\theta\right)(J_3 + J_3')\right] \qquad \text{(A-81)}$$

where

$$J_1 = \int_{Z_o-\ell}^{Z_o} e^{jkz\cos\theta} \sin k(\ell - z_o + z)\, dz$$

$$= \frac{e^{jk(Z_o-\ell)\cos\theta} - e^{jkZ_o\cos\theta}(\cos k\ell - j\cos\theta \sin k\ell)}{k\sin^2\theta} \quad \text{(A-82)}$$

$$J_1' = \int_{Z_o}^{Z_o+\ell} e^{jkz\cos\theta} \sin k(\ell + Z_o - z)\, dz$$

$$= \frac{e^{jk(Z_o+\ell)\cos\theta} - e^{jkZ_o\cos\theta}(\cos k\ell + j\cos\theta \sin k\ell)}{k\sin^2\theta} \quad \text{(A-83)}$$

$$J_1 + J_1' = 2e^{jkZ_o\cos\theta} \frac{\cos(k\ell\cos\theta) - \cos k\ell}{k\sin^2\theta} \quad \text{(A-84)}$$

$$J_2 = \int_{Z_o-\ell}^{Z_o} e^{-jkz\cos\theta} \sin k(\ell - Z_o + z)\, dz$$

$$= \frac{e^{-jk(Z_o-\ell)\cos\theta} - e^{-jkZ_o\cos\theta}(\cos k\ell + j\cos\theta \sin k\ell)}{k\sin^2\theta} \quad \text{(A-85)}$$

$$J_2' = \int_{Z_o}^{Z_o+\ell} e^{-jkZ_o\cos\theta} \sin k(\ell + Z_o - z)\, dz$$

$$= \frac{e^{-jk(Z_o+\ell)\cos\theta} - e^{-jkZ_o\cos\theta}(\cos k\ell - j\cos\theta \sin k\ell)}{k\sin^2\theta} \quad \text{(A-86)}$$

$$J_2 + J_2' = 2\, e^{-jkZ_o\cos\theta}\, \frac{\cos(k\ell\cos\theta) - \cos k\ell}{k\sin^2\theta} \qquad \text{(A-87)}$$

$$J_3 = \int_{Z_o-\ell}^{Z_o} e^{-jkz\cos\theta} \sin k(\ell - Z_o + z)\,[1 - j\sqrt{\pi P_e}\, e^{-P_e}\, \mathrm{erfc}(j\sqrt{P_e})]\, dz \qquad \text{(A-88)}$$

$$J_3' = \int_{Z_o}^{Z_o+\ell} e^{-jkz\cos\theta} \sin k(\ell + Z_o - z)\,[1 - j\sqrt{\pi P_e}\, e^{-P_e}\, \mathrm{erfc}(j\sqrt{P_e})]\, dz \qquad \text{(A-89)}$$

$$J_3 + J_3' = 2\, e^{-jkz_o\cos\theta}\, \frac{\cos(k\ell\cos\theta) - \cos k\ell}{k\sin^2\theta} - \frac{2e^{-jkz_o\cos\theta}}{1 - R_v}\, \sqrt{\frac{n^2 - \sin^2\theta}{n^2\sin\theta}}$$

$$\times\, [\cos(k\ell\cos\theta) - \cos k\ell]\, e^{-P_e}\, \mathrm{erfc}\left(j\sqrt{P_e}\sqrt{\frac{j2\pi r}{k}}\right) \qquad \text{(A-90)}$$

Substituting Equations A-84, A-87, and A-90 into Equation A-81:

$$E_\theta = j60I_m \frac{e^{-jkr}}{r} \frac{\cos(k\ell\cos\theta) - \cos k\ell}{\sin\theta} \left[e^{jkZ_o\cos\theta} + R_v e^{-jkZ_o\cos\theta} + (1-R_v)(\sin^2\theta - \frac{\sqrt{n^2 - \sin^2\theta}}{n^2}\cos\theta) \right. \quad \text{(A-91)}$$

$$\left. \times e^{-jkZ_o\cos\theta} \{1 - j\sqrt{\pi P_e}\sin^2\theta\ e^{-P_e}\ \text{erfc}(j\sqrt{P_e})\} \right]$$

$$E_\phi = j60\, I_m \frac{e^{-jkr}e^{jkZ_o\cos\theta}}{r} \frac{\cos(k\ell\cos\theta) - \cos k\ell}{\sin\theta} \quad \text{(A-92)}$$

Equation A-91 has been derived previously in the literature for the case $Z_o = 0$.[35] The second and third terms of Equation A-91 represent the ground-reflected wave and surface wave, respectively.

If:

$$R_d = r - Z_o\cos\theta$$
$$R_r = r + Z_o\cos\theta \quad \text{(A-93)}$$

Equation A-91 may be written as:

---

[35] Ramo, S., Whinnery, J.R., and Van Duzer, T., Fields and Waves in Communication Electronics, John Wiley and Sons, New York, NY, 1965.

$$E_\theta = j60I_m \frac{\cos(k\ell\cos\theta) - \cos k\ell}{\sin\theta} \left[\frac{e^{-jkR_d}}{R_d} + R_v \frac{e^{-jkR_r}}{R_r} \right.$$

$$+ (1-R_v)\left(\sin^2\theta - \frac{\sqrt{n^2 - \sin^2\theta}}{n^2}\cos\theta\right) \qquad \text{(A-94)}$$

$$\left. \times \frac{e^{-jkR_r}}{R_r} \left\{1 - j\sqrt{\pi P_e}\ \sin^2\theta\ e^{-P_e}\ \text{erfc}\ (j\sqrt{P_e})\right\} \right]$$

For calculation of the ground-wave field intensity, Equation A-94 may be used for better accuracy. It can be obtained from Equations 1 and 2 in Reference 20 if $\theta_r = \theta_d = \theta$ and $\sin^2\theta = 1$ inside the braces.

An analysis of the impedance of an antenna of length 2ℓ and a small radius a at a height $z_o > \ell$ over a lossy ground is an intricate problem and has not been solved completely (Reference 27). An approximate solution is given by Sommerfield and Renner (Reference 28). For a Hertizan dipole or for a very short end-loaded antenna of length 2ℓ with uniform current distribution, Sommerfeld and Renner obtain:

$$R_r^v = 120\,(k\ell)^2 \left[\frac{2}{3} + 2\left[\frac{\sin 2kZ_o - 2kZ_o\cos 2kZ_o}{(2kZ_o)^3}\right]\right.$$

$$+ 2\left|\frac{k}{k_2}\right| \left[\frac{\cos(2kZ_o - \gamma) + 2kZ_o \sin(2kZ_o - \gamma)}{(2kZ_o)^2}\right. \qquad \text{(A-95)}$$

$$\left. \left. - \cos\gamma\ \text{Ci}\ (2kZ_o) - \sin\gamma\left\{\text{Si}\ (2kZ_o) - \frac{\pi}{2}\right\}\right]\right]$$

where

$$\frac{k_2}{k} = \left|\frac{k_2}{k}\right| e^{-j\gamma} \qquad \text{(A-96)}$$

Equation A-95 is multiplied by the factor $(\frac{2}{\pi})^2$ for sinusoidal current distribution as discussed in Reference 28 to give:

$$R_r = (\frac{2}{\pi})^2 R_r^v$$

The directive gain is given by: (A-97)

$$g_d = \frac{r^2 |E_\theta|^2}{30\ I_m^2\ \sin^2(k\ell)\ R_r} \qquad \text{(A-98)}$$

The radiation vector is given by:

$$N_z = \frac{-2\ I_m}{k} \frac{\cos(k\ell\cos\theta) - \cos k\ell}{\sin^2\theta} e^{jkZ_o\cos\theta} \qquad \text{(A-99)}$$

$$N_\theta = \frac{2\ I_m}{k} \frac{\cos(k\ell\cos\theta) - \cos k\ell}{\sin\theta} e^{jkZ_o\cos\theta} \qquad \text{(A-100)}$$

The free-space field intensity is given by:

$$E_{\theta f} = \frac{j60\ I_m e^{-jkr}}{r} \frac{\cos(k\ell\cos\theta) - \cos k\ell}{\sin\theta} \qquad \text{(A-101)}$$

The attenuation relative to free-space is:

$$A = \left| \frac{E_\theta}{E_{\theta f}} \right| \qquad \text{(A-102)}$$

and

$$ADB = 20 \log \frac{1}{|A|} \qquad \text{(A-103)}$$

The electric field intensity in the diffraction region is given by:

$$E_\theta = \frac{j60\ I_m e^{-jkd}}{d} \frac{\cos(k\ell \cos\theta) - \cos k\ell}{\sin\theta} (2\ F_r) \qquad \text{(A-104)}$$

INVERTED-L

The inverted-L is analyzed by considering the vertical and horizontal sections separately and then combining the results.

For the vertical portion:

$$\alpha' = \pi/2$$

$$r' = 0$$

$$H_s = z$$

$$s = z$$

$$\cos \psi'_v = \cos\theta$$

$$I_v(S) = I_m \sin k(H+\ell-z) \quad z > 0 \qquad \text{(A-105)}$$

$$\cos \psi_h' = \sin\theta \sin\phi \qquad \text{(A-106)}$$

$$I_h(s) = I_m \sin k(\ell - y), \quad y > 0 \qquad \text{(A-107)}$$

Following the approach used in the previous subsections:

$$E_{\theta,v} = j30\, I_m \frac{e^{-jkr}}{r}\left[\frac{A_4 + jB_4}{\sin\theta} + R_v \frac{A_4 - jB_4}{\sin\theta}\right.$$

$$+ (1 - R_v)\left(\sin^2\theta - \frac{\sqrt{n^2 - \sin^2\theta}}{n^2}\cos\theta\right)\frac{A_4 - jB_4}{\sin\theta}$$

$$\times \left\{1 - j\sqrt{\pi P_e}\, e^{-P_e} \sin^2\theta\, \operatorname{erfc}(j\sqrt{P_e})\right\}$$

$$\left. - j\left(\sin^2\theta - \frac{\sqrt{n^2 - \sin^2\theta}}{n^2}\cos\theta\right)\frac{\sqrt{n^2 - \sin^2\theta}}{n^2}\frac{2F_e}{\sin\theta}\right] \qquad \text{(A-108)}$$

$$\times \left\{\sin k(H+\ell) - \sin k\ell \cos(kH\cos\theta) + j \sin k\ell \sin(kH\cos\theta)\right\}$$

For the horizontal portion:

$$E_{\theta,h} = -j30 I_m \frac{\sin\phi\cos\theta}{\sin^2\psi_h'} \frac{e^{-jkr}}{r}\sqrt{A_5^2 + B_5^2}\, e^{jb''}\left[1 - R_v e^{-j2kh\cos\theta}\right. \qquad \text{(A-109)}$$

$$\left. + (1 - R_v) F_e \times \frac{\sqrt{n^2 - \sin^2\theta}}{n^2\cos\theta}\left(\sin^2\theta - \frac{\sqrt{n^2 - \sin^2\theta}}{n^2}\cos\theta\right) e^{-j2kH\cos\theta}\right.$$

$$E_{\phi,h} = j30 I_m \frac{e^{-jkr}}{r} \frac{\cos\phi}{\sin^2\psi_h'} \sqrt{A_5^2 + B_5^2}\, e^{jb''} \qquad \text{(A-110)}$$

$$\left[\times\ 1 + R_h e^{-j2kH\cos\theta} + (1 - R_h) F_m e^{-j2kH\cos\theta}\right]$$

where

$$A_4 = \cos(kH\cos\theta)\cos k\ell - \sin(kH\cos\theta)\cos\theta\sin k\ell - \cos(k(H+\ell)) \quad \text{(A-111)}$$

$$B_4 = \cos(kH\cos\theta)\cos\theta\sin k\ell + \sin(kH\cos\theta)\cos k\ell - \cos\theta\sin k(H+\ell) \quad \text{(A-112)}$$

$$A_5 = \cos(k\ell\cos\psi_h') - \cos k\ell \quad \text{(A-113)}$$

$$B_5 = \sin(k\ell\cos\psi_h') - \cos\psi_h'\sin k\ell \quad \text{(A-114)}$$

$$b'' = \tan^{-1}\frac{B_5}{A_5} \quad \text{(A-115)}$$

$$E_\theta = E_{\theta,v} + E_{\theta,h} \quad \text{(A-116)}$$

$$E_\phi = E_{\phi,h}. \quad \text{(A-117)}$$

The radiation resistance is given by:

$$R_{in} = R_{inv} + R_{inh}$$

where R_{inv} is given by Equation A-49 except that ℓ is replaced by $(H + \ell)$.

R_{inh} is given by:

$$R_{inh} = 60 \left[1.415 + \ell n \left(\frac{k\ell}{\pi}\right) - Ci\,(2k\ell) + \frac{\sin 2\,k\ell}{2\,k\ell}\right] \quad \text{(A-118)}$$

The directive gain is given by:

$$g_d = \frac{r^2\,(\,|E_\theta|^2 + |E_\phi|^2)}{30\,I_m^{\,2}\sin^2[k\,(H+\ell)]\,R_{in}} \quad \text{(A-119)}$$

The radiation efficiency η is given for $\frac{H}{\lambda} \leq 0.2$ (Reference 14) by:

$$\eta(dB) = 20\log_{10}\left[6.335\left(\frac{H}{\lambda}\right) + 67.95\left(\frac{H}{\lambda}\right)^2 - 693\left(\frac{H}{\lambda}\right)^3 + 1600\left(\frac{H}{\lambda}\right)^4\right] \quad \text{(A-120)}$$

The power gain is given in dB by:

$$G_p(dB) = \eta(dB) + 10\log_{10} g_d \quad \text{(A-121)}$$

The radiation vectors are:

$$N_{\theta,v} = \sin\theta \int_0^H I_m \sin k\,(H + \ell - z)\, e^{jkz\cos\theta}\, dz = \frac{Im}{k}\,\frac{A_4 + jB_4}{\sin\theta} \quad \text{(A-122)}$$

$$N_{\phi,v} = 0 \quad \text{(A-123)}$$

$$N_{\theta,h} = -\cos\theta \sin\phi \int_0^{\ell} I_m \sin(k(\ell-y)) e^{jky\cos\psi_h'} dy$$

$$= -\cos\theta \sin\phi \frac{I_m}{k} \frac{A_5 + jB_5}{\sin^2\psi_h'} \quad \text{(A-124)}$$

$$N_{\phi,h} = \cos\phi \int_o^{\ell} I_m \sin(k(\ell-y)) e^{jky\cos\psi_h'} dy$$

$$= \cos\phi \frac{I_m}{k} \frac{A_5 + j B_5}{\sin^2 \psi_h'} \quad \text{(A-125)}$$

where A_4, B_4, A_5, and B_5 are given by Equation A-111, A-112, A-113, and A-114, respectively.

$$N_\theta = N_{\theta,v} + N_{\theta,h}$$

$$= \frac{I_m}{k} \left[\frac{A_4 + jB_4}{\sin\theta} - \frac{A_5 + jB_5}{\sin^2 \psi_h'} \cos\theta \sin\phi \right] \quad \text{(A-126)}$$

$$N_\phi = N_{\phi,h} = \frac{I_m}{k} \frac{A_5 + jB_5}{\sin^2 \psi_h'} \cos\phi \quad \text{(A-127)}$$

The free-space field intensities are:

$$E_{\theta f} = \frac{j30 I_m e^{-jkr}}{r} \left[\frac{A_4 + jB_4}{\sin\theta} - \frac{A_5 + jB_5}{\sin^2 \psi_h'} \cos\theta \sin\phi \right] \quad \text{(A-128)}$$

$$E_{\phi f} = \frac{j30\ I_m e^{-jkr}}{r} \frac{A_5 + jB_5}{\sin^2 \psi_h'} \cos\phi \qquad \text{(A-129)}$$

The attenuation relative to free space is given by:

$$A = \sqrt{\frac{|E_\theta|^2 + |E_\phi|^2}{|E_{\theta f}|^2 + |E_{\phi f}|^2}} \qquad \text{(A-130)}$$

where E_θ and E_ϕ are given by Equations A-116 and A-117, respectively.

$$ADB = 20 \log \frac{1}{|A|} \qquad \text{(A-131)}$$

The electric field intensities in the diffraction region are given by:

$$E_\theta = \frac{j30 I_m e^{-jkr}}{r} \left[\frac{A_4 + jB_4}{\sin\theta} - \frac{A_5 + jB_5}{\sin^2 \psi_h'} \cos\theta \sin\phi \right] 2 F_r \qquad \text{(A-132)}$$

$$E_\phi = \frac{j30\ I_m e^{-jkr}}{r} \frac{A_5 + jB_5}{\sin^2 \psi_h'} \cos\phi\ 2\ F_r \qquad \text{(A-133)}$$

ARBITRARILY TILTED DIPOLE

For this antenna:

$$\theta' = \pi/2 - \alpha', \quad \phi' = \pi/2, \quad H_s = Z = H + s \sin\alpha' \tag{A-134}$$

$$\cos\psi = \cos\theta \sin\alpha' + \sin\theta \cos\alpha' \sin\phi \tag{A-135}$$

$$I = \begin{cases} I_m \sin k(\ell + s), & -\ell \leq s < 0 \\ I_m \sin k(\ell - s), & 0 < s \leq \ell \end{cases} \tag{A-136}$$

Using the same approach as in the previous subsections, the field intensities are given by:

$$E_\theta = -j60I_m \frac{e^{-jkr}}{r} e^{jkH\cos\theta} \left[\frac{A_6}{\sin^2\psi} (\cos\alpha' \sin\phi \cos\theta - \sin\alpha' \sin\theta) \right. \tag{A-137}$$

$$-R_v \frac{A_7}{\sin^2\psi'} (\cos\alpha' \sin\phi \cos\theta + \sin\alpha' \sin\theta) e^{-j2kH\cos\theta}$$

$$+ \frac{A_7}{\sin^2\psi'} e^{-j2kH\cos\theta} (1-R_v) F_e$$

$$\left. x \ (\sin^2\theta - \frac{\sqrt{n^2-\sin^2\theta}}{n^2} \cos\theta) (\cos\alpha' \sin\phi \frac{\sqrt{n^2 - \sin^2\theta}}{n^2} - \sin\alpha' \sin\theta) \right.$$

$$E_\phi = j60I_m \frac{e^{-jkr}}{r} e^{jkH\cos\theta} \cos\alpha' \cos\theta \left[\frac{A_6}{\sin^2\psi} + R_h e^{-jZkH\cos\theta} \frac{A_7}{\sin^2\psi'} \right. \tag{A-138}$$

$$\left. + (1-R_h) F_m \frac{A_7}{\sin^2\psi'} e^{-j2kH\cos\theta} \right]$$

where

$$A_6 = \cos(k\ell\cos\psi) - \cos k\ell \tag{A-139}$$

$$A_7 = \cos(k\ell\cos\psi') - \cos k\ell \tag{A-140}$$

$$\cos\psi' = \cos\psi - 2\sin\alpha'\cos\theta = -\cos\theta\sin\alpha' + \sin\theta\cos\alpha'\sin\phi \tag{A-141}$$

The field equations for a horizontal dipole are obtained if $\alpha' = 0$ is substituted in Equations A-137 and A-138. The substitution $\alpha' = \pi/2$ gives the field equations for the vertical dipole, except for a slightly different surface-wave term (because F_e was assumed constant in evaluating the integrals).

The directive gain is obtained from:

$$g_d = \frac{120\,(|F_\theta|^2 + |F_\phi|^2)}{R_{in}} \tag{A-142}$$

where

$$\begin{aligned} F_\theta = \Bigg[& \frac{A_6}{\sin^2\psi}(\cos\alpha'\sin\phi\cos\theta - \sin\alpha'\sin\theta) \\ & - R_v\frac{A_7}{\sin^2\psi}(\cos\alpha'\sin\phi\cos\theta + \sin\alpha'\sin\theta)\, e^{-j2kH\cos\theta} \\ & + \frac{A_7}{\sin^2\psi'} e^{-j2kH\cos\theta}(1-R_v) F_e\left(\sin^2\theta - \frac{\sqrt{n^2-\sin^2\theta}}{n^2}\cos\theta\right) \\ & \times\left(\cos\alpha'\sin\phi\frac{\sqrt{n^2-\sin^2\theta}}{n^2} - \sin\alpha'\sin\theta\right)\Bigg] \end{aligned} \tag{A-143}$$

$$F_\phi = \left[\frac{A_6}{\sin^2\psi} + R_h \frac{A_7}{\sin^2\psi'} e^{-j2kH\cos\theta} + (1-R_h) F_m \frac{A_7}{\sin^2\psi'} e^{-j2kH\cos\theta} \right] \cos\alpha' \cos\phi \quad \text{(A-144)}$$

$$R_{in} = R_{11} + \text{Re}\,[Z_{21} (\cos\alpha' - j \sin\alpha') (R_h' \cos\alpha' + j R_v' \sin\alpha')] \quad \text{(A-145)}$$

where R_h' and R_v' are given by Equations 2-19 and 2-20. The self impedance R_{11} can be calculated from R_{21} by replacing the element separation by 2a, where a is the radius of the element, to give:

$$R_{21} = -30 \int_{-\frac{1}{2}\ell_2}^{\frac{1}{2}\ell_2} \Bigg\{ \left[\frac{1}{\rho^2} \left(\sin 2\pi r_1 \frac{S_z + Z_o + \frac{\ell_1}{2}}{r_1}\right.\right. \quad \text{(A-146)}$$

$$+ \sin 2\pi r_2 \frac{S_z + Z_o - \frac{\ell_1}{2}}{r_2} - 2 \cos \pi\ell_1 \sin 2\pi r \frac{S_z + Z_o}{r}$$

$$\left. \times (S_x^2 + Y_o S_y + S_y^2)\right]$$

$$+ \left[2 \frac{\sin 2\pi r \cos \pi\ell_1}{r} - \frac{\sin 2\pi r_1}{r_1} - \frac{\sin 2\pi r_2}{r_2}\right] S_z \Bigg\} \frac{\sin\left[2\pi\left(\frac{\ell_2}{2} - |s|\right)\right]}{s} ds$$

$$X_{21} = -30 \int_{-\frac{1}{2}\ell_2}^{\frac{1}{2}\ell_2} \left\{ \frac{1}{\rho^2} \left(\cos 2\pi r_1 \frac{S_z + Z_o + \frac{\ell_1}{2}}{r_1}\right.\right. \quad \text{(A-147)}$$

$$+ \cos 2\pi r_2 \frac{S_z + Z_o - \frac{\ell_1}{2}}{r_2} - 2 \cos \pi \ell_1 \cos 2\pi r \frac{S_z + Z_o}{r})$$

$$x \ (S_x^2 + Y_o S_y + S_y^2)\Big] \Bigg\}$$

$$+ \ [2\frac{\cos 2\pi r \cos \pi \ell_1}{r} - \frac{\cos 2\pi r_1}{r_1} - \frac{\cos 2\pi r_2}{r_2}] \ S_z \Bigg\}$$

$$\frac{\sin [2\pi (\frac{\ell_2}{2} - |s|)]}{s} \ ds$$

As can be derived from Figure A-1:

$$S_z = s \cos\theta, \ S_y = s \sin\theta \sin\phi, \ S_x = s \sin\theta \cos\phi$$

$$\rho = \sqrt{S_x^2 + (Y_o + S_y)^2}, \qquad r = \sqrt{\rho^2 + (Z_o + S_z)^2} \tag{A-148}$$

$$r_1 = \sqrt{\rho^2 + (Z_o + S_z + \frac{\ell_1}{2})^2}, \qquad r_2 = \sqrt{\rho^2 + (Z_o + S_z - \frac{\ell_1}{2})^2}$$

$$\cos \alpha = \frac{S_z + Z_o}{r}, \qquad \cos \alpha_1 = \frac{S_z + Z_o + \frac{\ell_1}{2}}{r_1}$$

$$\cos \alpha_2 = \frac{S_z + Z_o - \frac{\ell_1}{2}}{r_2}$$

The radiation vectors are given by:

$$N_\theta = \frac{2 I_m}{k} \frac{\cos (k\ell \cos \psi) - \cos k\ell}{\sin^2 \psi} (-\cos \alpha' \sin\phi \cos\theta + \sin\alpha' \sin\theta) \tag{A-149}$$

$$N_\phi = \frac{2 I_m}{k} \frac{\cos (k\ell \cos\psi) - \cos k\ell}{\sin^2 \psi} \cos\alpha' \cos\phi \tag{A-150}$$

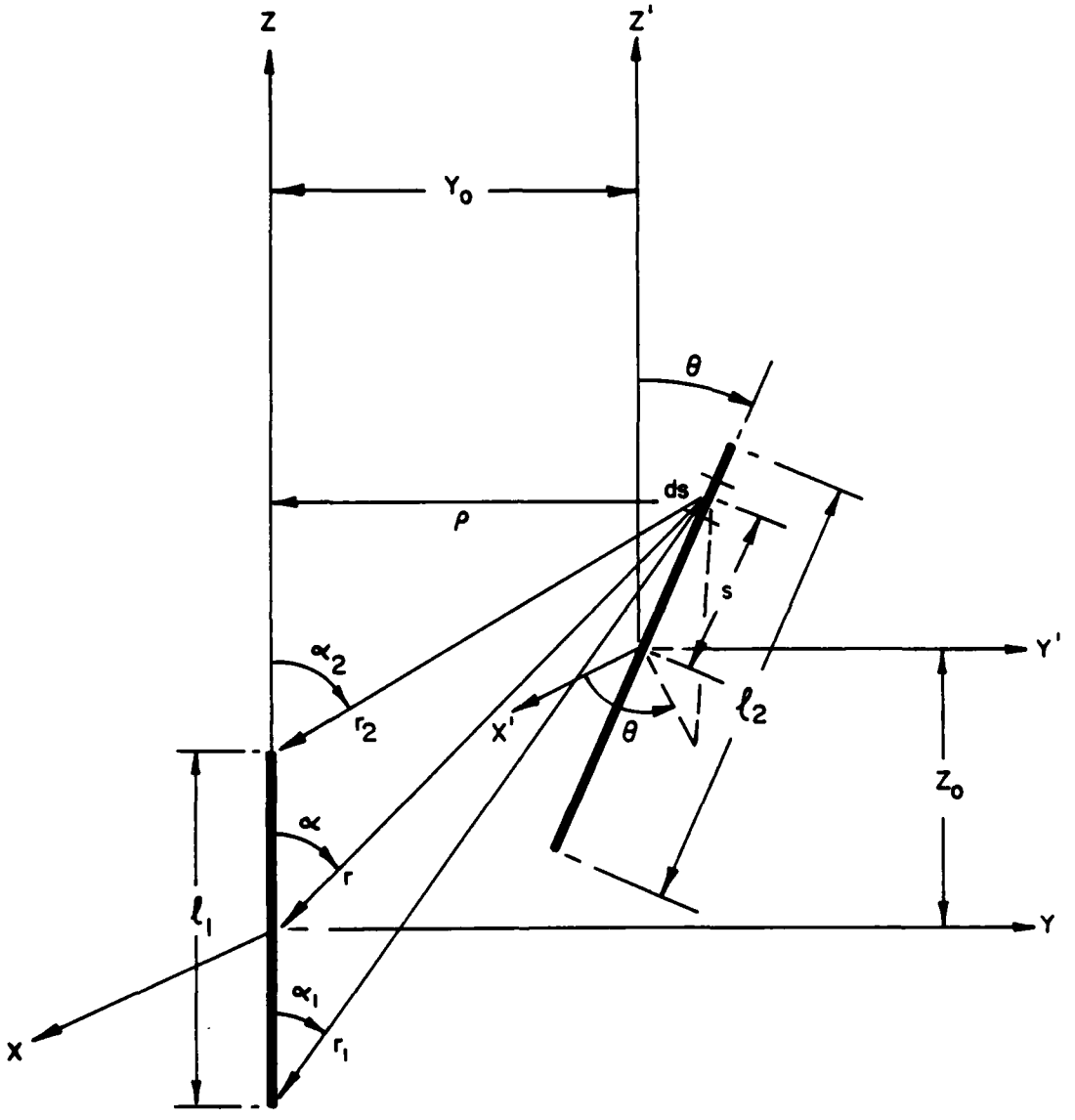

Figure A-1. Geometrical relationships between two thin wires.[36]

[36]Baker, H.C. and LaGrone, A.H., "Digital Computation of the Mutual Impedance Between Thin Dipoles," IRE Trans. Antennas and Propagation, Vol. AP-10, No. 2, pp. 172-178, March 1962.

The free-space field intensities are given by:

$$E_{\theta f} = \frac{60\, I_m e^{-jkr}}{r} \frac{\cos(k\ell\cos\psi) - \cos k\ell}{\sin^2\psi} (-\cos\alpha' \sin\phi \cos\theta + \sin\alpha' \sin\theta) \quad \text{(A-151)}$$

$$E_{\phi f} = \frac{60\, I_m e^{-jkr}}{r} \frac{\cos(k\ell\cos\psi) - \cos k\ell}{\sin^2\psi} \cos\alpha' \cos\phi \quad \text{(A-152)}$$

The attenuation relative to free space is:

$$A = \frac{\sin^2\psi \sqrt{|F_\theta|^2 + |F_\phi|^2}}{[\cos(k\ell\cos\psi) - \cos k\ell] \sqrt{(-\cos\alpha'\sin\phi\cos\theta + \sin\alpha'\sin\theta)^2 + (\cos\alpha'\cos\phi)^2}} \quad \text{(A-153)}$$

$$ADB = 20 \log \frac{1}{|A|} \quad \text{(A-154)}$$

The electric field intensities in the diffraction region are:

$$E_\theta = \frac{60\, I_m e^{-jkd}}{d} \frac{\cos(k\ell\cos\psi) - \cos k\ell}{\sin^2\psi} \quad \text{(A-155)}$$

$$\times (-\cos\alpha' \sin\phi \cos\theta + \sin\alpha' \sin\theta)\left(2\ F_r\right)$$

$$E_\phi = \frac{60\, I_m e^{-jkd}}{d} \frac{\cos(k\ell\cos\psi) - \cos k\ell}{\sin^2\psi} \quad \text{(A-156)}$$

$$\times (\cos\alpha' \cos\phi)\left(2\ F_r\right)$$

SLOPING LONG-WIRE

For this antenna:

$$\theta' = \pi/2 - \alpha', \ \phi = \pi/2, \ H_s = z = s \sin\alpha' \tag{A-157}$$

$$\cos\psi = \cos\theta \sin\alpha' + \sin\theta \cos\alpha' \sin\phi \tag{A-158}$$

The current distribution is given by:

$$I_s = I_m \sin k(\ell - s), \quad s > 0 \tag{A-159}$$

The final expressions for the field strength are:

$$\begin{aligned} E_\theta = -j30 \, I_m \frac{e^{-jkr}}{r} \Bigg[& \frac{A_6 + jB_6}{\sin^2\psi} (\cos\alpha' \sin\phi \cos\theta - \sin\alpha' \sin\theta) \\ & - R_v \frac{A_7 + jB_7}{\sin^2\psi'} (\cos\alpha' \sin\phi \cos\theta + \sin\alpha' \sin\theta) \\ & + \frac{A_7 + jB_7}{\sin^2\psi'} (1 - R_v) F_e \left(\sin^2\theta - \frac{\sqrt{n^2 - \sin^2\theta}}{n^2} \cos\theta\right) \\ & \times \left(\cos\alpha' \sin\phi \frac{\sqrt{n^2 - \sin^2\theta}}{n^2} - \sin\alpha' \sin\theta\right) \Bigg] \end{aligned} \tag{A-160}$$

The first two terms of Equation A-160 are identical to Equation 54 of Reference 8, and the third term represents the surface wave.

AD-A102 622 IIT RESEARCH INST ANNAPOLIS MD F/G 20/14
APACK, A COMBINED ANTENNA AND PROPAGATION MODEL.(U)
JUL 81 S CHANG, H C MADDOCKS F19628-80-C-0042
UNCLASSIFIED ESD-TR-80-102 NL

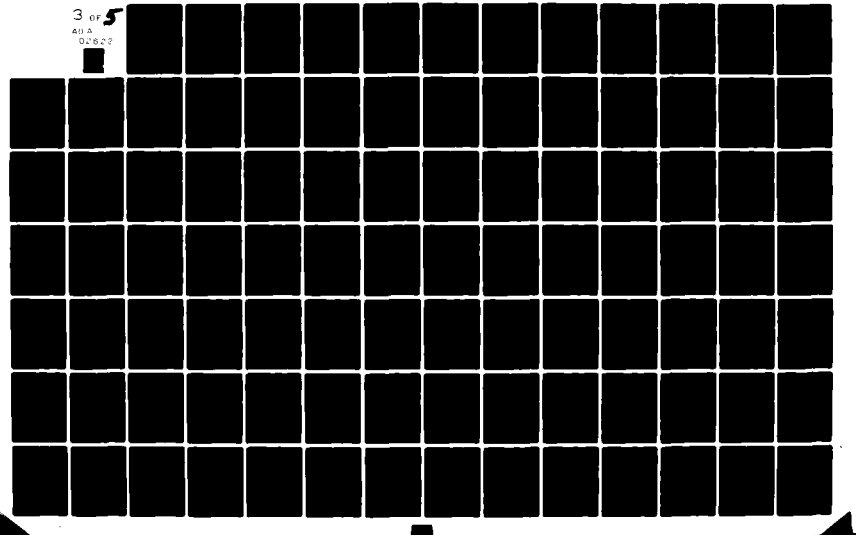

$$E_\phi = j30I_m \frac{e^{-jkr}}{r} \cos\alpha' \cos\phi \left[\frac{A_6 + jB_6}{\sin^2\psi} + R_h \frac{A_7 + jB_7}{\sin^2\psi'} + (1-R_v) F_m \frac{A_7 + jB_7}{\sin^2\psi'} \right] \quad \text{(A-161)}$$

The first two terms of Equation A-161 are identical to Equation 55 of Reference 8, and the third term represents the surface wave. In Equations A-160 and A-161:

$$A_6 = \cos(k\ell\cos\psi) - \cos k\ell \quad \text{(A-162)}$$

$$B_6 = \sin(k\ell\cos\psi) - \sin k\ell\cos\psi \quad \text{(A-163)}$$

$$A_7 = \cos(k\ell\cos\psi') - \cos k\ell \quad \text{(A-164)}$$

$$B_7 = \sin(k\ell\cos\psi') - \sin k\ell\cos\psi' \quad \text{(A-165)}$$

$$\cos\psi' = \cos\psi - 2\sin\alpha'\cos\theta = -\cos\theta\sin\alpha' + \sin\theta\cos\alpha'\sin\phi \quad \text{(A-166)}$$

The directive gain is :

$$g_d = \frac{r^2(|E_\theta|^2 + E_\phi|^2)}{30\, I_m^2 \sin^2(k\ell)\, R_{in}} \quad \text{(A-167)}$$

where

$$R_{in} = R_{11} + R_e (CZ_m) \quad \text{(A-168)}$$

$$R_{11} = 60 \left[\ell n\, k\ell - C_i (2\, k\ell) + \frac{\sin 2k\ell}{2\, k\ell} - 0.423\right] \quad \text{(A-169)}$$

$$Z_m = 120 \left(\ell n \frac{\lambda}{2\pi a} - 0.60 + \ell n \sin\alpha'\right) - j170 \quad \text{(A-170)}$$

with a = wire radius.

The radiation vectors are given by:

$$N_\theta = -(\cos\alpha' \sin\phi \cos\theta - \sin\alpha' \sin\theta) \frac{I_m}{k} \frac{A_6 + jB_6}{\sin^2\psi} \quad \text{(A-171)}$$

$$N_\phi = \cos\alpha' \cos\phi \frac{I_m}{k} \frac{A_6 + jB_6}{\sin^2\psi} \quad \text{(A-172)}$$

The free-space field intensities are given by:

$$E_{\theta f} = \frac{30\, I_m e^{-jkr}}{r} \frac{A_6 + jB_6}{\sin^2\psi} (\cos\alpha' \sin\phi \cos\theta - \sin\alpha' \sin\theta) \quad \text{(A-173)}$$

$$E_{\phi f} = \frac{30\, I_m e^{-jkr}}{r} \frac{A_6 + jB_6}{\sin^2\psi} \cos\alpha' \cos\phi \quad \text{(A-174)}$$

The attenuation relative to free space is:

$$A = \sqrt{\frac{|E_\theta|^2 + |E_\phi|^2}{|E_{\theta f}|^2 + |E_{\phi f}|^2}} \quad \text{(A-175)}$$

where E_θ and E_ϕ are given by Equations A-160 and A-161, respectively.

$$ADB = 20 \log \frac{1}{|A|} \qquad (A\text{-}176)$$

The electric field intensities in the diffraction region are:

$$E_\theta = -\frac{30\, I_m e^{-jkd}}{d} \frac{A_6 + jB_6}{\sin^2\psi} (\cos\alpha' \sin\phi \cos\theta - \sin\alpha' \sin\theta)\left(2\, F_r\right) \qquad (A\text{-}177)$$

$$E_\phi = \frac{30\, I_m e^{-jkd}}{d} \frac{A_6 + jB_6}{\sin^2\psi} (\cos\alpha' \cos\phi)\left(2\, F_r\right) \qquad (A\text{-}178)$$

TERMINATED SLOPING-V

Let the angle between the antenna wires be 2γ, and the angle between the antenna wires and the ground plane be α'. The projection of the two wires on the ground surface makes an angle β' with the X-axis. The length of each wire is ℓ meters.

For wire # 1:

$\theta' = \pi/2 - \alpha$, $\phi' = \beta'$

$$\cos\psi_1 = \cos\theta \sin\alpha' + \sin\theta \cos\alpha' \cos(\phi - \beta') \qquad (A\text{-}179)$$

For wire #2:

$\theta' = \pi/2 - \alpha'$, $\phi' = -\beta'$

$$\cos \psi_2 = \cos\theta \sin\alpha' + \sin\theta \cos\alpha' \cos(\phi + \beta') \quad \text{(A-180)}$$

where

$$\alpha' = \sin^{-1}\left(\frac{H' - H}{\ell}\right), \quad -(\pi/2 - \gamma) \leq \alpha' \leq \pi/2 - \gamma \quad \text{(A-181)}$$

$$\beta' = \sin^{-1}\left(\frac{\sin\gamma}{\cos\alpha'}\right) \quad \text{(A-182)}$$

The height of the current element *ds* above ground is:

$$H_s = z = H + s \sin\alpha' \quad \text{(A-183)}$$

The current distribution is:

$$I_1(s) = -I_m e^{-jks}$$
$$I_2(s) = I_m e^{-jks} \quad \text{(A-184)}$$

With the above current distribution, the components of the electric field become:

$$E_{\theta 1} = 30\, I_m \frac{e^{-jkr}}{r} \left\{ \cos\alpha' \cos\theta \cos(\phi-\beta') \left[\frac{1-e^{-jk\ell u_1}}{U_1} \right.\right. \tag{A-185}$$

$$- R_v e^{-j2kH\cos\theta} \frac{1-e^{-jk\ell U_3}}{U_3} + (1-R_v)$$

$$\left. \times F_e e^{-j2kH\cos\theta} \frac{\sqrt{n^2 - \sin^2\theta}}{n^2 \cos\theta} \left(\sin^2\theta - \frac{\sqrt{n^2-\sin^2\theta}}{n^2}\cos\theta\right) \frac{1-e^{-jk\ell U_3}}{U_3} \right]$$

$$- \sin\alpha' \sin\theta \left[\frac{1-e^{-jk\ell U_1}}{U_1} + R_v\, e^{-j2kH\cos\theta} \frac{1-e^{-jk\ell U_3}}{U_3} \right.$$

$$\left.\left. + (1-R_v)\, F_e\, e^{-j2kH\cos\theta} \left(\sin^2\theta - \frac{\sqrt{n^2 - \sin^2\theta}}{n^2}\cos\theta\right) \frac{1-e^{-jk\ell U_3}}{U_3} \right] \right\}$$

$$E_{\theta 2} = 30\, I_m \frac{e^{-jkr}}{r} \left\{ -\cos\alpha' \cos\theta \cos(\phi + \beta') \left[\frac{1-e^{-jk\ell U_2}}{U_2} \right.\right. \tag{A-186}$$

$$- R_v e^{-j2kH\cos\theta} \frac{1-e^{-jk\ell U_4}}{U_4} + (1-R_v)$$

$$\left. \times F_e\, e^{-j2kH\cos\theta} \frac{\sqrt{n^2 - \sin^2\theta}}{n^2 \cos\theta} \left(\sin^2\theta - \frac{\sqrt{n^2 - \sin^2\theta}}{n^2}\cos\theta\right) \frac{1-e^{-jk\ell U_4}}{U_4} \right]$$

$$+ \sin\alpha' \sin\theta \left[\frac{1-e^{-jk\ell U_2}}{U_2} + R_v e^{-j2kH\cos\theta} \frac{1-e^{-jk\ell U_4}}{U_4} \right.$$

$$\left.\left. + (1-R_v)\, F_e\, e^{-j2kH\cos\theta} \left(\sin^2\theta - \frac{\sqrt{n^2 - \sin^2\theta}}{n^2}\cos\theta\right) \frac{1-e^{-jk\ell U_4}}{U_4} \right] \right\}$$

$$E_{\phi 1} = 30\, I_m \frac{e^{-jkr}}{r} \cos\alpha' \sin(\phi-\beta') \left[\frac{1-e^{-jk\ell U_1}}{U_1} \right. \tag{A-187}$$

$$\left. + R_h e^{-j2kH\cos\theta} \frac{1-e^{-jk\ell U_3}}{U_3} \right.$$

$$+ \quad (1-R_h)\ F_m\ e^{-j2kH\cos\theta}\ \frac{1-e^{-jk\ell U_3}}{U_3}\Bigg]$$

$$E_{\phi 2} = -30\ I_m\ \frac{e^{-jkr}}{r}\ \cos\alpha'\ \sin(\phi+\beta')\Bigg[\frac{1-e^{-jk\ell U_2}}{U_2} \tag{A-188}$$

$$+ R_h\ e^{-j2kH\cos\theta}\ \frac{1-e^{-jk\ell U_4}}{U_4}$$

$$+ \quad (1-R_h)\ F_m\ e^{-j2kH\cos\theta}\ \frac{1-e^{-jk\ell U_4}}{U_4}\Bigg]$$

where

$$U_i = 1-\cos\psi_i\ , \quad i = 1,2,3,4 \tag{A-189}$$

$$\cos\psi_3 = \cos\theta\ \sin\alpha' + \sin\theta\ \cos\alpha'\ \cos\ (\phi - \beta') \tag{A-190}$$

$$\cos\psi_4 = -\cos\theta\ \sin\alpha' + \sin\theta\ \cos\alpha'\ \cos\ (\phi + \beta') \tag{A-191}$$

The total field components become:

$$E_\theta = E_{\theta 1} + E_{\theta 2} \tag{A-192}$$

$$E_\phi = E_{\phi 1} + E_{\phi 2} \tag{A-193}$$

The directive gain is given by:

$$g_d = \frac{r^2 (|E_\theta|^2 + |E_\phi|^2)}{30 I_m^2 R_{in}} \tag{A-194}$$

$$R_{in} = 120 \left(\ell n \frac{\lambda}{2\pi a} + \ell n \sin \gamma - 0.60\right) \tag{A-195}$$

(This is a free-space approximation where a is the wire radius.)

In practice, R_{in} =600 Ω is used.

The radiation efficiency of the terminated sloping-V is:

$$\eta = -2.7 \text{ dB or } (54\%) \tag{A-196}$$

The power gain in decibels is given by:

$$G_p(dB) = -2.7 + 10 \log_{10} g_d \tag{A-197}$$

$$N_\theta = \frac{I_m}{jk}\left[\frac{1-e^{-jk\ell U_1}}{U_1}\left\{\cos\alpha' \cos\theta \cos(\phi - \beta') - \sin\alpha' \sin\theta\right\} + \frac{1-e^{-jk\ell U_2}}{U_2}\left\{-\cos\alpha' \cos\theta \cos(\phi + \beta') + \sin\alpha' \sin\theta\right\}\right] \tag{A-198}$$

$$N_\phi = \frac{I_m}{jk}\left[\frac{1-e^{-jk\ell U_1}}{U_1}\sin(\phi-\beta')\right.$$
$$\left.-\frac{1-e^{-jk\ell U_2}}{U_2}\sin(\phi+\beta')\right]\cos\alpha' \qquad \text{(A-199)}$$

The free-space field intensities are given by:

$$E_{\theta f} = jk\ 30\ \frac{e^{-jkr}}{r}\ N_\theta \qquad \text{(A-200)}$$

$$E_{\phi f} = jk\ 30\ \frac{e^{-jkr}}{r}\ N_\phi \qquad \text{(A-201)}$$

The attenuation relative to free space is:

$$A = \sqrt{\frac{|E_\theta|^2 + |E_\phi|^2}{|E_{\theta f}|^2 + |E_{\phi f}|^2}} \qquad \text{(A-202)}$$

$$ADB = 20\log_{10}\frac{1}{|A|} \qquad \text{(A-203)}$$

The electric field intensities in the diffraction region are:

$$E_\theta = jk\ 30\ \frac{e^{-jkd}}{d}\ (N_\theta)\ (2\ F_r) \qquad \text{(A-204)}$$

$$E_\phi = jk\ 30\ \frac{e^{-jkd}}{d}\ (N_\phi)\ (2\ F_r) \qquad \text{(A-205)}$$

TERMINATED SLOPING RHOMBIC[37,38]

Equations A-185, A-186, A-187, and A-188 still apply for wires #1 and #2, with the understanding that:

$$\alpha' = \sin^{-1} \frac{H'' - H}{\ell} = \sin^{-1} \frac{H' - H}{2\ell} \qquad \text{(A-206)}$$

where

H' = height of the termination
H = height of the feed
H'' = height of the other two vertexes.

For wires #3 and #4:

$$H_s = H'' + s \sin\alpha' \qquad \text{(A-207)}$$

$$I_3(s) = I_m e^{-jk\ell} e^{-jks} \qquad \text{(A-208)}$$

$$I_4(s) = -I_m e^{-jk\ell} e^{-jks} \qquad \text{(A-209)}$$

Since one end of wires #3 and #4 are not located at the origin, the radial distance for these wires ($r' = r - \ell \cos \psi_2$) must be used in the exponent. Assume $r' = r$ in the denominator. These approximations yield the following expressions for the fields from wires #3 and #4:

---

[37]Bruce, E., "Developments in Short-Wave Directional Antennas," Proc. IRE, Vol. 19, No. 8, pp. 1406-1433, August 1931.

[38]Bruce, E., Beck, A.C. and Lowry, L.R., "Horizontal Rhombic Antennas," Proc. IRE, Vol. 23, No. 1, pp. 24-46, January 1935.

$$E_{\theta 3} = 30\, I_m \frac{e^{-jkr}}{r} e^{-jk\ell U_2} \left\{-\cos\alpha' \cos\theta \cos(\phi+\beta') \left[\frac{1-e^{-jk\ell U_1}}{U_1}\right.\right. \tag{A-210}$$

$$- \frac{1-e^{-jk\ell U_3}}{U_3} R_v e^{-j2kH''\cos\theta}$$

$$+ \frac{1-e^{-jk\ell U_3}}{U_3} e^{-j2kH''\cos\theta} (1-R_v) F_e \frac{\sqrt{n^2-\sin^2\theta}}{n^2\cos\theta} (\sin^2\theta$$

$$\left. - \frac{\sqrt{n^2-\sin^2\theta}}{n^2}\cos\theta)\right] + \sin\alpha' \sin\theta$$

$$\times \left[\frac{1-e^{-jk\ell U_1}}{U_1} + \frac{1-e^{-jk\ell U_3}}{U_3} R_v e^{-j2kH''\cos\theta}\right.$$

$$\left.\left. + \frac{1-e^{-jk\ell U_3}}{U_3} (1-R_v) F_e e^{-j2kH''\cos\theta} (\sin^2\theta - \frac{\sqrt{n^2-\sin^2\theta}}{n^2}\cos\theta)\right]\right\}$$

$$E_{\theta 4} = 30\, I_m \frac{e^{-jkr}}{r} e^{-jk\ell U_1} \left\{\cos\alpha' \cos\theta \cos(\phi+\beta') \left[\frac{1-e^{-jk\ell U_2}}{U_2}\right.\right. \tag{A-211}$$

$$- \frac{1-e^{-jk\ell U_4}}{U_4} R_v e^{-j2kH''\cos\theta}$$

$$+ \frac{1-e^{-jk\ell U_4}}{U_4} e^{-j2kH''\cos\theta} (1-R_v) F_e \frac{\sqrt{n^2-\sin^2\theta}}{n^2\cos\theta} (\sin^2\theta - \frac{\sqrt{n^2-\sin^2\theta}}{n^2}\cos\theta)$$

$$- \sin\alpha' \sin\theta \left[\frac{1-e^{-jk\ell U_2}}{U_2} + \frac{1-e^{-jk\ell U_4}}{U_4} R_v e^{-j2kH''\cos\theta}\right.$$

$$\left.\left. + \frac{1-e^{-jk\ell U_4}}{U_4} (1-R_v) F_e e^{-j2kH''\cos\theta} (\sin^2\theta - \frac{\sqrt{n^2-\sin^2\theta}}{n^2}\cos\theta)\right]\right\}$$

$$E_{\phi 3} = -30\, I_m \frac{e^{-jkr}}{r} e^{-jk\ell U_2} \cos\alpha' \sin(\phi-\beta') \left[\frac{1-e^{-jk\ell U_1}}{U_1}\right. \tag{A-212}$$
$$\left. + \frac{1-e^{-jk\ell U_3}}{U_3} R_h e^{-j2kH''\cos\theta} + \frac{1-e^{-jk\ell U_3}}{U_3} (1-R_h) F_m e^{-j2kH''\cos\theta}\right]$$

$$E_{\phi 4} = 30\, I_m \frac{e^{-jkr}}{r} e^{-jk\ell U_1} \cos\alpha' \sin(\phi+\beta') \left[\frac{1-e^{-jk\ell U_2}}{U_2}\right. \tag{A-213}$$
$$+ \frac{1-e^{-jk\ell U_4}}{U_4} R_h e^{-j2kH''\cos\theta}$$
$$\left. + \frac{1-e^{-jk\ell U_4}}{U_4} (1-R_h) F_m e^{-j2kH''\cos\theta}\right]$$

The total field components are:

$$E_\theta = E_{\theta 1} + E_{\theta 2} + E_{\theta 3} + E_{\theta 4} \tag{A-214}$$

$$E_\phi = E_{\phi 1} + E_{\phi 2} + E_{\phi 3} + E_{\phi 4} \tag{A-215}$$

The expression for directive gain is:

$$g_d = \frac{r^2 (|E_\theta|^2 + |E_\phi|^2)}{30\, I_m^2 R_{in}} \tag{A-216}$$

If the rhombic antenna is properly terminated, R_{in} may be taken as the termination resistance. In practice, R_{in} = 600 ohms is used. The radiation efficiency is given by:

$$\eta = -2.3 \text{ dB } (59\%) \tag{A-217}$$

and the power gain is given by:

$$G_p(\text{dB}) = -2.3 + 10 \log_{10} g_d \tag{A-218}$$

The total radiation vectors are:

$$N_\theta = \frac{I_m}{jk} (1-e^{-jk\ell U_1}) (1-e^{-jk\ell U_2}) \left[- \frac{\cos\alpha' \cos\theta \cos(\phi+\beta') - \sin\alpha' \sin\theta}{U_2} + \frac{\cos\alpha' \cos\theta \cos(\phi-\beta') - \sin\alpha' \sin\theta}{U_1} \right] \tag{A-219}$$

$$N_\phi = \frac{I_m}{jk} (1-e^{-jk\ell U_1}) (1-e^{-jk\ell U_2}) \cos\alpha' \left[\frac{\sin(\phi-\beta')}{U_1} - \frac{\sin(\phi+\beta')}{U_2} \right] \tag{A-220}$$

The free-space field intensities are given by:

$$E_{\theta f} = j30k \frac{e^{-jkr}}{r} N_\theta \tag{A-221}$$

$$E_{\phi f} = j30\, k \frac{e^{-jkr}}{r} N_\phi \tag{A-222}$$

The attenuation relative to free-space is:

$$A = \sqrt{\frac{|E_\theta|^2 + |E_\phi|^2}{|E_{\theta f}|^2 + |E_{\phi f}|^2}} \qquad \text{(A-223)}$$

and

$$ADB = 20 \log \frac{1}{|A|} \qquad \text{(A-224)}$$

The electric field intensities in the diffraction region are:

$$E_\theta = j30k \frac{e^{-jkd}}{d} (N_\theta) (2 F_r) \qquad \text{(A-225)}$$

$$E_\phi = j30k \frac{e^{-jkd}}{d} (N_\phi) (2 F_r) \qquad \text{(A-226)}$$

TERMINATED HORIZONTAL RHOMBIC

The following equations can be obtained from those for the terminated sloping rhombic by letting $\alpha' = 0$ and $\beta' = \gamma$.

The θ - components are given by:

$$E_{\theta 1} = 30 I_m \frac{e^{-jkr}}{r} \frac{1-e^{-jk\ell U_1}}{U_1} \cos\theta \cos(\phi-\gamma) \left[1 - R_v e^{-j2kH\cos\theta} + (1-R_v) F_e e^{-j2kH\cos\theta} \frac{\sqrt{n^2 - \sin^2\theta}}{n^2 \cos\theta} \left(\sin^2\theta - \sqrt{\frac{n^2-\sin^2\theta}{n^2}} \cos\theta\right)\right] \qquad \text{(A-227)}$$

$$E_{\theta 2} = -30 I_m \frac{e^{-jkr}}{r} \frac{1-e^{-jk\ell U_2}}{U_2} \cos\theta \cos(\phi+\gamma) \left[1-R_v e^{-j2kH\cos\theta} + (1-R_v) F_e e^{-j2kH\cos\theta} \frac{\sqrt{n^2 - \sin^2\theta}}{n^2 \cos\theta} \left(\sin^2\theta - \sqrt{\frac{n^2 - \sin^2\theta}{n^2}} \cos\theta\right)\right] \qquad \text{(A-228)}$$

$$E_{\theta 3} = -30\, I_m \frac{e^{-jkr}}{r} e^{-jk\ell U_2} \frac{1-e^{-jk\ell U_1}}{U_1} \cos\theta \cos(\phi-\gamma) \left[1-R_v e^{-j2kH\cos\theta} + (1-R_v) F_e e^{-j2kH\cos\theta} \frac{\sqrt{n^2-\sin^2\theta}}{n^2\cos\theta} \left(\sin^2\theta - \sqrt{n^2-\sin^2\theta}\cos\theta\right)\right] \quad \text{(A-229)}$$

$$E_{\theta 4} = 30\, I_m \frac{e^{-jkr}}{r} e^{-jk\ell U_1} \frac{1-e^{-jk\ell U_2}}{U_2} \cos\theta \cos(\phi+\gamma) \left[1-R_v e^{-j2kH\cos\theta} + (1-R_v) F_e e^{-j2kH\cos\theta} \frac{\sqrt{n^2-\sin^2\theta}}{n^2\cos\theta} \left(\sin^2\theta - \frac{\sqrt{n^2-\sin^2\theta}}{n^2}\cos\theta\right)\right] \quad \text{(A-230)}$$

The ϕ-components are given by:

$$E_{\phi 1} = 30\, I_m \frac{e^{-jkr}}{r} \frac{1-e^{-jk\ell U_1}}{U_1} \sin(\phi-\gamma) \left[1 + R_h e^{-j2kH\cos\theta} + (1-R_h) F_m e^{-j2kH\cos\theta}\right] \quad \text{(A-231)}$$

$$E_{\phi 2} = -30\, I_m \frac{e^{-jkr}}{r} \frac{1-e^{-jk\ell U_2}}{U_2} \sin(\phi+\gamma) \left[1 + R_h e^{-j2kH\cos\theta} + (1-R_h) F_m e^{-j2kH\cos\theta}\right] \quad \text{(A-232)}$$

$$E_{\phi 3} = -30\, I_m \frac{e^{-jkr}}{r} \frac{1-e^{-jk\ell U_1}}{U_1} e^{-jk\ell U_2} \sin(\phi-\gamma) \left[1 + R_h e^{-j2kH\cos\theta} + (1-R_h) F_m e^{-j2kH\cos\theta}\right] \quad \text{(A-233)}$$

$$E_{\phi 4} = 30\, I_m \frac{e^{-jkr}}{r} \frac{1-e^{-jk\ell U_2}}{U_2} e^{-jk\ell U_1} \sin(\phi+\gamma) \left[1 + R_h e^{-j2kH\cos\theta} + (1-R_h) F_m e^{-j2kH\cos\theta}\right] \quad \text{(A-234)}$$

where

$$U_1 = 1 - \sin\theta \cos(\phi - \gamma) \tag{A-235}$$

$$U_2 = 1 - \sin\theta \cos(\phi + \gamma) \tag{A-236}$$

Summing the θ- and ϕ- components:

$$E_\theta = -30 I_m \frac{e^{-jkr}}{r} \frac{4e^{\frac{-jk\ell U_2}{2}} e^{\frac{-jk\ell U_2}{2}} \sin\frac{k\ell U_1}{2} \sin\frac{k\ell U_2}{2}}{U_1 U_2} \tag{A-237}$$

$$\times 2\cos\theta \sin\phi \sin\gamma \left[1 - R_v e^{-j2kH\cos\theta} + (1-R_v) F_e e^{-j2kH\cos\theta} \frac{\sqrt{n^2 - \sin^2\theta}}{n^2\cos\theta} \left(\sin^2\theta - \frac{\sqrt{n^2 - \sin^2\theta}}{n^2}\cos\theta\right)\right]$$

$$E_\phi = -30 I_m \frac{e^{-jkr}}{r} \frac{4e^{\frac{-jk\ell U_1}{2}} e^{\frac{-jk\ell U_2}{2}} \sin\frac{k\ell U_1}{2} \sin\frac{k\ell U_2}{2}}{U_1 U_2} \tag{A-238}$$

$$\times 2\sin\gamma \left[\sin\theta\cos\gamma(\cos^2\phi - \sin^2\phi) - \cos\phi\right]$$

$$\times \left[1 + R_h e^{-j2kH\cos\theta} + (1-R_h) F_m e^{-j2kH\cos\theta}\right]$$

The directive gain is given by:

$$g_d = \frac{r^2 \left(|E_\theta|^2 + |E_\phi|^2\right)}{30\, I_m^2\, R_{in}} \qquad \text{(A-239)}$$

where $R_{in} = 600\ \Omega$ in practice.

The radiation efficiency is:

$$\eta = -2.3\ \text{dB}\ (59\%) \qquad \text{(A-240)}$$

The power gain in decibels is given by:

$$G_p = -2.3 + 10 \log_{10} g_d \qquad \text{(A-241)}$$

The radiation vectors are:

$$N_\theta = -\frac{8\, I_m}{jk} \frac{e^{\frac{-jk\ell U_1}{2}}\, e^{\frac{-jk\ell U_2}{2}} \sin\frac{k\ell U_1}{2} \sin\frac{k\ell U_2}{2}}{U_1\, U_2} \cos\theta \sin\phi \sin\gamma \qquad \text{(A-242)}$$

$$N_\phi = -\frac{8\, I_m}{jk} \frac{e^{\frac{-jk\ell U_1}{2}}\, e^{\frac{-jk\ell U_2}{2}} \sin\frac{k\ell U_1}{2} \sin\frac{k\ell U_2}{2}}{U_1\, U_2} \sin\gamma\, (\sin\theta \cos\gamma - \cos\phi) \qquad \text{(A-243)}$$

The free-space field intensities are:

$$E_{\theta f} = \frac{j30k\ e^{-jkr}}{r} N_{\theta} \quad \text{(A-244)}$$

$$E_{\phi f} = \frac{j\ 30\ k\ e^{-jkr}}{r} N_{\phi} \quad \text{(A-245)}$$

The attenuation relative to free space is:

$$A = \sqrt{\frac{|E_{\theta}|^2 + |E_{\phi}|^2}{|E_{\theta f}|^2 + |E_{\phi f}|^2}} \quad \text{(A-246)}$$

$$ADB = 20 \log \frac{1}{|A|} \quad \text{(A-247)}$$

The electric field intensities in the diffraction region are:

$$E_{\theta} = \frac{j30k\ e^{-jkd}}{d} (N_{\theta})\ (2\ F_r) \quad \text{(A-248)}$$

$$E_{\phi} = \frac{j30k\ e^{-jkd}}{d} (N_{\phi})\ (2\ F_r) \quad \text{(A-249)}$$

SIDE-LOADED VERTICAL HALF-RHOMBIC

For wire #1:

$$\theta' = \pi/2 - \alpha', \ \phi' = 0, \ H_{s1} = z = s \sin\alpha' \quad \text{(A-250)}$$

$$\cos\psi_1 = \cos\theta \sin\alpha' + \sin\theta \cos\alpha' \cos\phi \quad \text{(A-251)}$$

For wire #2:

$$\theta' = \pi/2 + \alpha, \ \phi' = 0, \ H_{s2} = (\ell - s) \sin\alpha' \quad \text{(A-252)}$$

$$\cos\psi_2 = -\cos\theta \sin\alpha' + \sin\theta \cos\alpha' \cos\phi \quad \text{(A-253)}$$

The current distribution on the two wires is given by:

$$I_1(s) = I_m e^{-jks} \quad \text{(A-254)}$$

$$I_2(s) = I_m e^{-jk\ell} e^{-jks} \quad \text{(A-255)}$$

Following the same approach used in the previous subsections, the final expressions for the components of electric field strength are:

$$E_{\theta 1} = 30 I_m \frac{e^{-jkr}}{r} \left\{ -\cos\alpha' \cos\theta \cos\phi \left[F_1 - R_v F_2 + (1-R_v) F_e F_2 \frac{\sqrt{n^2 - \sin^2\theta}}{n^2 \cos\theta} \left(\sin^2\theta - \frac{\sqrt{n^2 - \sin^2\theta}}{n^2} \cos\theta \right) \right] \right. \quad \text{(A-256)}$$

$$\left. + \sin\alpha' \sin\theta \left[F_1 + R_v F_2 + (1-R_v) F_e F_2 \left(\sin^2\theta - \frac{\sqrt{n^2 - \sin^2\theta}}{n^2} \cos\theta \right) \right] \right\}$$

$$E_{\theta 2} = -30\, I_m \frac{e^{-jkr}}{r} e^{-jk\ell U_1} \Bigg\{ \cos\alpha' \cos\theta \cos\phi \left[F_2 - R_v F_1 e^{-jk2k\ell \sin\alpha' \cos\theta} + (1-R_v)\, F_e F_1 \frac{\sqrt{n^2 - \sin^2\theta}}{n^2 \cos\theta} \right.$$

$$\left. \times \left(\sin^2\theta - \frac{\sqrt{n^2 - \sin^2\theta}}{n^2} \cos\theta\right) e^{-j2k\ell \sin\alpha' \cos\theta} \right] \qquad \text{(A-257)}$$

$$+ \sin\alpha' \sin\theta \left[F_2 + R_v F_1 e^{-j2k\ell \sin\alpha' \cos\theta} \right.$$

$$\left. + (1-R_v)\, F_e F_1 \left(\sin^2\theta - \frac{\sqrt{n^2 - \sin^2\theta}}{n^2} \cos\theta\right) e^{-j2k\ell \sin\alpha' \cos\theta} \right] \Bigg\}$$

$$E_{\phi 1} = -30\, I_m \frac{e^{-jkr}}{r} \cos\alpha' \sin\phi \left[F_1 + R_h F_2 + (1-R_h)\, F_m F_2 \right] \qquad \text{(A-258)}$$

$$E_{\phi 2} = -30\, I_m \frac{e^{-jkr}}{r} \cos\alpha' \sin\phi \left[F_2 e^{-jk\ell U_1} + R_h F_1 e^{-jk\ell U_2} + (1-R_h)\, F_m F_1 e^{-jk\ell U_2} \right] \qquad \text{(A-259)}$$

where

$$U_1 = 1-\cos\psi_1 = 1-\cos\theta \sin\alpha' - \sin\theta \cos\alpha' \cos\phi \qquad \text{(A-260)}$$

$$U_2 = 1-\cos\psi_1 + 2\cos\theta \sin\alpha' = 1-\cos\psi_2$$

$$= 1 + \cos\theta \sin\alpha' - \sin\theta \cos\alpha' \cos\phi \qquad \text{(A-261)}$$

$$F_i = \frac{1 - e^{-jk\ell U_i}}{U_i} \quad , \quad i = 1, 2 \tag{A-262}$$

The total field components become:

$$E_\theta = E_{\theta 1} + E_{\theta 2} = \frac{30\ I_m\ e^{-jkr}}{r}\ F_\theta' \tag{A-263}$$

$$E_\phi = E_{\phi 1} + E_{\phi 2} = -\frac{30\ I_m\ e^{-jkr}}{r}\ F_\phi' \tag{A-264}$$

where

$$\begin{aligned} F_\theta' = -\cos\alpha' \cos\theta \cos\phi \Bigg[& F_1 + F_2\, e^{-jk\ell U_1} - R_v\,(F_2 + F_1\, e^{-jk\ell U_2}) \\ & + (1-R_v)\, F_e\, \frac{\sqrt{n^2 - \sin^2\theta}}{n^2 \cos\theta}\ x\ (\sin^2\theta - \sqrt{n^2 - \sin^2\theta}\cos\theta)\ (F_2 + F_1 e^{-jk\ell U_2}) \Bigg] \\ & + \sin\alpha' \sin\theta \Bigg[F_1 - F_2\, e^{-jk\ell U_1} + R_v\,(F_2 - F_1\, e^{-jk\ell U_2}) \\ & + (1-R_v)\, F_e\, (\sin^2\theta - \sqrt{n^2 - \sin^2\theta}\cos\theta)\ (F_2 - F_1\, e^{-jk\ell U_2}) \Bigg] \end{aligned} \tag{A-265}$$

$$\begin{aligned} F_\phi' = \cos\alpha' \sin\phi \Bigg[& F_1 + F_2\, e^{-jk\ell U_1} + R_h\,(F_2 + F_1\, e^{-jk\ell U_2}) \\ & + (1-R_h)\, F_m\, (F_2 + F_1\, e^{-jk\ell U_2}) \Bigg] \end{aligned} \tag{A-266}$$

The directive gain of the side-terminated vertical half-rhombic antenna is then:

$$g_d = \frac{30\ (|F_\theta'|^2 + |F_\phi'|^2)}{R_{in}} \tag{A-267}$$

where

$$R_{in} = 60 \left(\ell n \frac{\lambda}{2\pi a} + \ell n \sin \alpha' - 0.6\right) \qquad \text{(A-268)}$$

with

a = wire radius

Equation A-268 is exact when the ground is perfectly conducting.

The radiation efficiency is:

$$\eta = -2.3 \text{ dB } (59\%) \qquad \text{(A-269)}$$

The total radiation vectors become:

$$N_\theta = \frac{I_m}{jk}\left[-F_1 (\cos\alpha' \cos\theta \cos\phi - \sin\alpha' \sin\theta)\right] \qquad \text{(A-270)}$$

$$- F_2 e^{-jk\ell U_1} (\cos\alpha' \cos\theta \cos\phi + \sin\alpha' \sin\theta)$$

$$= \frac{I_m}{jk}\left[-\cos\alpha' \cos\theta \cos\phi \,(F_1 + F_2 e^{-jk\ell U_1}) + \sin\alpha' \sin\theta \,(F_1 - F_2 e^{-jk\ell U_1})\right]$$

$$N_\phi = -\frac{I_m}{jk}\left[F_1 + F_2 e^{-jk\ell U_1}\right] \sin\phi \cos\alpha' \qquad \text{(A-271)}$$

The free-space electric field intensities are given by:

$$E_{\theta f} = j30\ k \frac{e^{-jkr}}{r} N_{\theta} \quad \text{(A-272)}$$

$$E_{\phi f} = j30\ k \frac{e^{-jkr}}{r} N_{\phi} \quad \text{(A-273)}$$

The attenuation relative to free space is given by:

$$A = \sqrt{\frac{|E_{\theta}|^2 + |E_{\phi}|^2}{|E_{\theta f}|^2 + |E_{\phi f}|^2}} \quad \text{(A-274)}$$

$$ADB = 20 \log \frac{1}{|A|} \quad \text{(A-275)}$$

The electric field intensities in the diffraction region are:

$$E_{\phi} = j30k \frac{e^{-jkd}}{d} (N_{\theta}) (2\ F_r) \quad \text{(A-276)}$$

$$E_{\phi} = j\ 30\ k \frac{e^{-jkd}}{d} (N_{\phi}) (2\ F_r) \quad \text{(A-277)}$$

HORIZONTAL YAGI-UDA ARRAY

For this antenna:

$$\theta' = \pi/2,\ \phi = 0,\ \alpha' = 0,\ H_s = H,\ s = x,\ \cos\psi = \sin\theta\cos\phi$$

$$I_i(s) = I_{mi} \sin k\,(\ell_i - |x|),\ i = 1,2,\ldots,N \tag{A-278}$$

$$E_{\theta i} = -j60\, I_i \frac{e^{-jkr_i}}{r_i} e^{jkH\cos\theta} \frac{\cos(k\ell\cos\psi) - \cos k\ell_i}{\sin^2\psi} \cos\phi$$

$$\times \left[\cos\theta\,(1-R_v\, e^{-j2kH\cos\theta}) + (1-R_v)\sqrt{\frac{n^2 - \sin^2\theta}{n^2}}\, e^{-j2kH\cos\theta}\, F_e\left(\sin^2\theta - \sqrt{\frac{n^2-\sin^2\theta}{n^2}}\cos\theta\right)\right] \tag{A-279}$$

$$E_{\phi i} = j60\, I_i \frac{e^{-jkr_i}}{r_i} e^{jkH\cos\theta} \frac{\cos(k\ell\cos\psi) - \cos k\ell_i}{\sin^2\psi} \sin\phi$$

$$\times \left[1 + R_h\, e^{-j2kH\cos\theta} + (1-R_h)\, F_m\, e^{-j2kH\cos\theta}\right] \tag{A-280}$$

r_i is the distance between the base of the i^{th} element and the far-field point, which is related to r_1 by:

$$r_i = r_1 - y_i \sin\theta \sin\phi \tag{A-281}$$

where

$$y_1 = 0,\ y_2 = d_1,\ y_3 = d_1 + d_2,\ \ldots\ y_n = \sum_{i=1}^{N-1} d_i \qquad \text{(A-282)}$$

The total field components can be obtained by summing the contributions from all the elements to give:

$$E_\theta = \sum_{i=1}^{N} E_{\theta i} \simeq -j60\,\frac{e^{-jkr_1}}{r_1}\,e^{jkH\cos\theta}\,\frac{\cos\phi}{\sin^2\psi}\left[\cos\theta\,(1-R_v e^{-j2kH\cos\theta}) + (1-R_v)\right.$$
$$\left.\times\,\frac{\sqrt{n^2 - \sin^2\theta}}{n^2}\,e^{-j2kH\cos\theta}\,F_e\left(\sin^2\theta - \frac{\sqrt{n^2 - \sin^2\theta}}{n^2}\cos\theta\right)\right](A_{11} + jB_{11}) \qquad \text{(A-283)}$$

$$E_\phi = \sum_{i=1}^{N} E_{\phi i} \simeq j60\,\frac{e^{-jkr_1}}{r_1}\,e^{jkH\cos\theta}\,\frac{\sin\phi}{\sin^2\psi}\left[1 + R_h e^{-j2kH\cos\theta}\right. \qquad \text{(A-284)}$$
$$\left.+\,(1-R_h)\,F_m e^{-j2kH\cos\theta}\right](A_{11} + jB_{11})$$

where

$$A_{11} + jB_{11} = \sum_{i=1}^{N} I_{mi}\,e^{jk\,y_i\sin\theta\sin\phi}\,[\cos(k\ell_i\cos\psi) - \cos k\ell_i] \qquad \text{(A-285)}$$

The input impedence looking into the feed point of the active element can be determined by considering the circuit relations:

$$\begin{bmatrix} Z_{11} + R_h' Z_{11}' & Z_{12} + R_h' Z_{12}' & \cdots & Z_{1N} + R_h' Z_{1N}' \\ Z_{21} + R_h' Z_{21}' & Z_{22} + R_h' Z_{22}' & \cdots & Z_{2N} + R_h' Z_{2N}' \\ \vdots & & & \vdots \\ Z_{N1} + R_h' Z_{N1}' & Z_{N2} + R_h' Z_{N2}' & \cdots & Z_{NN} + R_h' Z_{NN}' \end{bmatrix} \begin{bmatrix} I_{b1} \\ I_{b2} \\ \vdots \\ I_{bN} \end{bmatrix} = \begin{bmatrix} 0 \\ V_2 \\ \vdots \\ 0 \end{bmatrix} \quad \text{(A-286)}$$

where R_h, the reflection coefficient for horizontal polarization with $\theta = 0°$, is given by:

$$R_h' = \frac{1 - n}{1 + n} = \frac{1 - \frac{k_2}{k}}{1 + \frac{k_2}{k}} = \frac{k - k_2}{k + k_2} \quad \text{(A-287)}$$

and

Z_{ii} = open-circuit self-impedance of the i^{th} real element, calculated by Equation A-289 with $\ell = \ell_i$

Z_{ij} = open-circuit mutual impedance between the i^{th} and j^{th} real elements, calculated by Equation A-290 with $d_{ij} = |y_i - y_j|$

Z_{ii}' = open-circuit mutual impedance between the i^{th} real element and its own image, calculated by Equation A-288 with $\ell = \ell_i$ and $d = 2H$

Z_{ij}' = open-circuit mutual impedance between the i^{th} real element and the image of the j^{th} real element, calculated by Equation A-290 with $d_{ij} = \sqrt{4H^2 + (y_i - y_j)^2}$

$$Z_m = \frac{60}{1 - \cos 2k\ell} \Big[e^{-j2k\ell} [K(U_o) - 2K(U_1)] + e^{j2k\ell} [K(V_o) - 2K(V_1)] + 2 [K(U_o') - K(U_1) - K(V_1)] + 2 K(U_o') (1 + \cos 2k\ell) \Big] \quad \text{(A-288)}$$

where

$$K(x) = Ci(x) - j\,Si(x) = \int_{\infty}^{x} \frac{\cos y}{y}\,dy - j\int_{o}^{x} \frac{\sin y}{y}\,dy \qquad \text{(A-288a)}$$

$$U_o = k\left[\sqrt{d^2 + 4\ell^2} - 2\ell\right] \qquad \text{(A-288b)}$$

$$V_o = k\left[\sqrt{d^2 + 4\ell^2} + 2\ell\right] \qquad \text{(A-288c)}$$

$$U_o' = kd \qquad \text{(A-288d)}$$

$$U_1 = k\left[\sqrt{d^2 + \ell^2} - \ell\right] \qquad \text{(A-288e)}$$

$$V_1 = k\left[\sqrt{d^2 + \ell^2} + \ell\right] \qquad \text{(A-288f)}$$

$$d = 2H \qquad \text{(A-288g)}$$

Equation A-288 is also used to calculate the self impedance if d = a 2, where a is the radius of the dipole, i.e.:

$$Z_{11} = Z_m \Big|_{d = a\sqrt{2}} \qquad \text{(A-289)}$$

Since Equation A-288 is not valid for $k\ell = \pi P$, P = 1, 2, ..., the more exact formulas in Reference 9 should be used. To save computer time, Equation A-288 can be used satisfactorily in most cases.

The mutual impedance between two parallel dipoles of different lengths, referred to the antenna base, is found from:[39]

$$Z_m' = \frac{60}{\cos W_2 - \cos W_1}\left[e^{-jW_1}\,[K(U_o) - K(U_1) - K(U_2)]\right.$$

$$+ e^{jW_1}\,[K(V_o) - K(V_1) - K(V_2)] + e^{-jW_2}\,[K(U_o') - K(U_1) - K(V_2)] \quad \text{(A-290)}$$

$$\left. + e^{jW_2}\,[K(V_o') - K(V_1) - K(U_2)] + 2\,K(W_o)\,(\cos W_1 + \cos W_2)\right]$$

where

$$K(x) = Ci(x) - j\,Si(x) \quad \text{(A-290a)}$$

$$U_o = k\left[\sqrt{d_{ij}^2 + (\ell_i + \ell_j)^2} - (\ell_i + \ell_j)\right] \quad \text{(A-290b)}$$

$$V_o = k\left[\sqrt{d_{ij}^2 + (\ell_i + \ell_j)^2} + (\ell_i + \ell_j)\right] \quad \text{(A-290c)}$$

---

[39] King, R.W.P. and Wu, T.T., "Currents, Charges, and Near Fields of Cylindrical Antennas", Radio Science, Vol. 69D, No. 3, pp. 429-446, March 1965.

$$U_o' = k \left[\sqrt{d_{ij}^2 + (\ell_i - \ell_j)^2} - (\ell_i - \ell_j) \right] \quad \text{(A-290d)}$$

$$V_o' = k \left[\sqrt{d_{ij}^2 + (\ell_i - \ell_j)^2} + (\ell_i - \ell_j) \right] \quad \text{(A-290e)}$$

$$U_1 = k \left[\sqrt{d_{ij}^2 + \ell_i^2} - \ell_i \right] \quad \text{(A-290f)}$$

$$V_1 = k \left[\sqrt{d_{ij}^2 + \ell_i^2} + \ell_i \right] \quad \text{(A-290g)}$$

$$U_2 = k \left[\sqrt{d_{ij}^2 + \ell_j^2} - \ell_j \right] \quad \text{(A-290h)}$$

$$V_2 = k \left[\sqrt{d_{ij}^2 + \ell_j^2} + \ell_j \right] \quad \text{(A-290i)}$$

$$W_1 = k (\ell_i + \ell_j) \quad \text{(A-290j)}$$

$$W_2 = k (\ell_i - \ell_j) \quad \text{(A-290k)}$$

$$W_o = k d_{ij} \quad \text{(A-290l)}$$

d_{ij} = distance between the two elements considered.

It is easy to show that Equation A-288 can be obtained from Equation A-290 by letting $\ell_i = \ell_j = \ell$.

Solving for I_{bi} from Equation A-286, the current maxima can be calculated

from:

$$I_{mi} = \frac{I_{bi}}{\sin k\ell_i} \qquad i = 1, 2, \ldots, N \tag{A-291}$$

The input resistance is given by:

$$R_{in} = \text{Re}\left(\frac{V_2}{I_{b2}}\right) \tag{A-292}$$

Again, the directive gain is found by:

$$g_d = \frac{r_1^2 \left(|E_\theta|^2 + |E_\phi|^2 \right)}{30\, I_{b2}^2\, R_{in}} \tag{A-293}$$

Since I_{b2}, E_θ, and E_ϕ are directly proportional to V_2, V_2 cancels in Equation A-293. E_θ and E_ϕ are given by Equations A-283 and A-284 and R_{in} by Equation A-292. I_{b2} is found in Equation A-286. The radiation efficiency of a Yagi-Uda array is given by:

$$\eta = -1.8 \text{ dB } (65\%) \tag{A-294}$$

The power gain in decibels is given by:

$$G_p = -1.8 + 10 \log_{10} g_d \tag{A-295}$$

The radiation vectors are obtained by summing the contributions from all the elements to give:

$$N_\theta = -\cos\phi\cos\theta \sum_{i=1}^{N} \frac{2I_{mi}}{k} \frac{\cos(k\ell_i\cos\psi) - \cos k\ell_i}{\sin^2\psi} e^{jky_i\sin\theta\sin\phi} \quad \text{(A-296)}$$

$$N_\phi = \sin\phi \sum_{i=1}^{N} \frac{2I_{mi}}{k} \frac{\cos(k\ell_i\cos\psi) - \cos k\ell_i}{\sin^2\psi} e^{jky_i\sin\theta\sin\phi} \quad \text{(A-297)}$$

The free-space field intensities are given by:

$$E_{\theta f} = j30k \frac{e^{-jkr}}{r} N_\theta \quad \text{(A-298)}$$

$$= -\frac{j60\, e^{-jkr}}{r} \frac{\cos\phi\cos\theta}{\sin^2\psi} \sum_{i=1}^{N} I_{mi} e^{jky_i\sin\theta\sin\phi} [\cos(k\ell_i\cos\psi) - \cos k\ell_i]$$

$$E_{\phi f} = \frac{j60e^{-jkr}}{r} \frac{\sin\phi}{\sin^2\psi} \sum_{i=1}^{N} I_{mi} e^{jky_i\sin\theta\sin\phi} \quad \text{(A-299)}$$

$$x\,[\cos(k\ell_i\cos\psi) - \cos k\ell_i]$$

The attenuation relative to free-space is:

$$A = \sqrt{\frac{|E_\theta|^2 + |E_\phi|^2}{|E_{\theta f}|^2 + |E_{\phi f}|^2}} \qquad \text{(A-300)}$$

$$ADB = 20 \log \frac{1}{|A|} \qquad \text{(A-301)}$$

The electric field intensities in the diffraction region are:

$$E_\theta = \frac{-j60\, e^{-jkd}}{d} \frac{\cos\phi \cos\theta}{\sin^2 \psi} \left\{ \sum_{i=1}^{N} I_{mi} e^{jky_i \sin\theta \sin\phi} \right.$$

$$\left. x \left[\cos (k\ell_i \cos\psi) - \cos k\ell_i\right] \right\} (2 F_r) \qquad \text{(A-302)}$$

$$E_\phi = \frac{j60e^{-jkd}}{d} \frac{\sin\phi}{\sin^2 \psi} \left\{ \sum_{i=1}^{N} I_{mi} e^{jky_i \sin\theta \sin\phi} \right.$$

$$\left. x \left[\cos (k\ell_i \cos\psi) - \cos k\ell_i\right] \right\} (2 F_r) \qquad \text{(A-303)}$$

HORIZONTALLY POLARIZED LOG-PERIODIC DIPOLE ARRAY[40]

For this antenna,

$$\alpha' = 0, \quad \theta' = \pi/2, \quad \phi' = 0, \quad s = x, \quad H_s = H_i, \quad \cos\psi = \sin\theta \cos\phi$$

$$I_m \sin k (\ell - s) = I_{mi} \sin k (\ell_1 - |x|) \qquad \text{(A-304)}$$

ψ'' = angle between the far-field point (θ, ϕ) and the array axis.

---

[40] Ma, M.T. and Walters, L.C., Computed Radiation Patterns of Log-Periodic Antennas Over Lossy Plane Ground, ESSA Technical Report IER 54-ITSA 52, Boulder, CO, 1967.

$$\cos\psi'' = \cos\theta \cos\theta'' + \sin\theta \sin\theta'' \sin\phi \qquad \text{(A-305)}$$

The lengths of the dipole elements are related by:

$$\frac{\ell_n}{\ell_{n+1}} = \tau;\ n = 1, 2, \ldots, N-1;\ 0 < \tau < 1 \qquad \text{(A-306)}$$

The spacing between dipole elements is related to the element lengths by:

$$\frac{d_n}{\ell_{n+1}} = (1-\tau)\cot\alpha \qquad \text{(A-307)}$$

$$r_i = r_1 - \left(\sum_{n=1}^{i=1} d_n\right) \cos\psi'' = r_1 - y_i \csc\theta'' \cos\psi''$$

$$i = 1, 2, \ldots, N \qquad \text{(A-308)}$$

$$y_1 = 0$$

$$H_i = H_1 + \left(\sum_{n=1}^{i=1} d_n\right) \cos\theta'' = H_1 + y_i \cot\theta'' \qquad \text{(A-309)}$$

The field components contributed by the i^{th} element are:

$$E_{\theta i} = - \frac{j60 I_{mi} e^{-jkr_i}}{r_i} \frac{\cos(k\ell_i \cos\psi) - \cos k\ell_i}{\sin^2\psi} \cos\phi \quad \text{(A-310)}$$

$$x \left[\cos\theta \left(1 - R_v e^{-j2kH_i \cos\theta}\right) + (1-R_v) \frac{\sqrt{n^2 - \sin^2\theta}}{n^2} F_e \left(\sin^2\theta - \frac{\sqrt{n^2 - \sin^2\theta}}{n^2} \cos\theta\right) e^{-j2kH_1\cos\theta} \right]$$

$$E_{\phi i} = \frac{j60 I_{mi} e^{-jkr_i}}{r_i} \frac{\cos(k\ell_i \cos\psi) - \cos k\ell_i}{\sin^2\psi} \sin\phi \left[1 + R_h e^{-j2kH_i\cos\theta} + (1-R_h) F_m e^{-j2kH_i \cos\theta} \right] \quad \text{(A-311)}$$

Summing the contributions from all the dipole elements gives:

$$E_\theta = - \frac{j60 e^{-jkr_1}}{r_1} \frac{\cos\phi \cos\theta}{\sin^2\psi} S_\theta \quad \text{(A-312)}$$

$$E_\phi = \frac{j60 e^{-jkr_1}}{r_1} \frac{\sin\phi}{\sin^2\psi} S_\phi \quad \text{(A-313)}$$

where

$$S_\theta = \sum_{i=1}^{N} I_{mi} e^{jky_i \csc\theta'' \cos\psi''} \left[\cos(k\ell_i \cos\psi) - \cos k\ell_i\right] \tag{A-314}$$

$$x\left[1 - R_v e^{-j2kH_i \cos\theta} + (1-R_v) e^{-j2kH_i \cos\theta} F_e \frac{\sqrt{n^2 - \sin^2\theta}}{n^2 \cos\theta}\right.$$

$$\left. x\ (\sin^2\theta - \frac{\sqrt{n^2 - \sin^2\theta}}{n^2} \cos\theta)\right]$$

$$S_\phi = \sum_{i=1}^{N} I_{mi} e^{jky_i \csc\theta'' \cos\psi''} \left[\cos(k\ell_i \cos\psi) - \cos k\ell_i\right] \tag{A-315}$$

$$x\left[1 + R_h e^{-j2kH_i \cos\theta} + (1-R_h) F_m e^{-j2kH_i \cos\theta}\right]$$

$$I_{mi} = \frac{I_{bi}}{\sin k\ell_i} \tag{A-316}$$

The directive gain of the array is given by:

$$g_d = \frac{120}{R_{in}} \frac{\cos^2\phi \cos^2\theta\ |S_\theta|^2 + \sin^2\phi\ |S_\phi|^2}{\sin^4\psi} \tag{A-317}$$

Calculation of the input impedance over lossy ground is extremely difficult. The main problem is the determination of the dipole feed-point currents accounting for the effects of lossy ground. Following Reference 8, two different types of ground will be considered separately.

a. For ground with relatively low conductivity, such as sea ice, polar ice cap, or poor ground, the presence of the ground will be ignored for the purpose of determining the dipole feed-point currents. The poor ground is not likely to have a substantial effect on the current distribution. When calculating the input impedance, the imperfect ground effect is taken into

account by adding necessary terms pertaining to the horizontally polarized reflection coefficient.

b. For ground with relatively high conductivity, such as sea water or fresh water, the feed-point currents are determined as if the antenna were above a perfectly conducting ground using R_h to account for the imperfect ground.

Case 1 (Ground with Relatively Low Conductivity)

The matrix of dipole feed-point currents is given by:

$$[I_a] = \{[U] + [Y_f]\ [Z_a]\}^{-1}\ [I] \qquad \text{(A-318)}$$

where

$[U]$ = N X N unit maxtrix

$[I] = [1\ 0\ 0\ \ldots\ 0]^T$

(The current source at the feed point of the shortest dipole is normalized to unity.)

$[Z_a]$ = open-circuit antenna-impedance matrix given by:

$$[Z_a] = \begin{bmatrix} Z_{11a} & Z_{12a} & & Z_{1Na} \\ Z_{21a} & Z_{22a} & \cdots & Z_{2Na} \\ \vdots & & & \vdots \\ Z_{N1a} & Z_{N2a} & \cdots & Z_{NNa} \end{bmatrix} \qquad \text{(A-319)}$$

The main-diagonal terms represent the self-impedance of the dipoles, which can be calculated by Equation A-289. The off-diagonal elements represent the mutual impedances between dipoles. These mutual impedances can be calculated by Equation A-290 with:

$$d_{ij} = \sum_{n=i}^{j=1} d_n .$$

The response voltages appearing at the dipole feed points are found by:

$$[V_a] = [Z_a]\ [I_a] \qquad \text{(A-320)}$$

The input impedance Z_{in} of the entire array is numerically equal to the voltage V_1 across the feed point since the input current has been assumed to be unity. Including the effects of lossy ground:

$$Z_{in}' = V_1 = Z_{11a} I_{1a} + Z_{12a} I_{2a} + \cdots + Z_{1Na} I_{Na}$$

$$+ R_h' \sum_{i=1}^{N} Z_{1\,(N+i)a} I_{ia} = R_{in}' + j X_{in}' \qquad \text{(A-321)}$$

where

$$R_h' = \frac{k - k_2}{k + k_2} \quad (R_h \text{ with } \theta = 0) \qquad \text{(A-322)}$$

$Z_{1(N+i)a}$ = open-circuit mutual impedance between the first (shortest) dipole and the image of the i^{th} dipole.

The mutual impedance can be calculated from Equation A-290 with:

$$dij = \sqrt{4H^2 + \left(\sum_{n=1}^{j-1} d_n\right)^2 + 4H\left(\sum_{n=1}^{j-1} d_n\right)\cos\theta'', \quad d_o = 0} \qquad \text{(A-323)}$$

$[Y_f]$ = short-circuit admittance matrix (N X N) associated with the transmission line feeding the array

$$[Y_f] = \begin{bmatrix} Y_{11f} & Y_{12f} & 0 & \cdots & 0 \\ Y_{21f} & Y_{22f} & Y_{23f} & \cdots & 0 \\ 0 & Y_{32f} & \ddots & \ddots & \vdots \\ \vdots & 0 & \ddots & \ddots & Y_{(N-1)Nf} \\ 0 & 0 & \cdots & Y_{(N-1)Nf} & Y_{NNf} \end{bmatrix} \qquad \text{(A-324)}$$

where

$$Y_{11f} = -jY_o \cot kd_1 \qquad \text{(A-325)}$$

$$Y_{22f} = -jY_o (\cot kd_1 + \cot kd_2) \qquad \text{(A-326)}$$

$$Y_{(N-1)\,(N-1)f} = -j\,Y_o (\cot k\,d_{N-1} + \cot k\,d_{N-2}) \qquad \text{(A-327)}$$

$$Y_{NNf} = Y_T' - j\, Y_o \cot kd_{N-1} \tag{A-328}$$

$$Y_T' = Y_o \frac{\cos kd_N + jY_o Z_T \sin kd_N}{Y_o Z_T \cos kd_N + j \sin kd_N} \tag{A-329}$$

$$Y_{12f} = Y_{21f} = -j\, Y_o \csc kd_1 \tag{A-330}$$

$$Y_{23f} = Y_{32f} = -j\, Y_o \csc kd_2 \tag{A-331}$$

$$Y_{(N-1)Nf} = Y_{N(N-1)f} = -j\, Y_o \csc kd_{N-1} \tag{A-332}$$

Y_o = characteristic admittance of the transmission line

Z_T = termination impedance connected to the last (longest) dipole at a distance $d_n = \ell_n/2$.

Case 2 (Ground with Relatively High Conductivity)

The dipole feed-point current in this case is given by:

$$[I_a'] = \left\{[U] + [Y_f]\,[Z_a] + [Y_f]\,[Z_a']\right\}^{-1} [I]$$

where

$$[Z_a'] = \begin{bmatrix} Z_{1(N+1)a} & Z_{1(N+2)a} & \cdots & Z_{1(2N)a} \\ Z_{2(N+1)a} & Z_{2(N+2)a} & \cdots & Z_{2(2N)a} \\ \cdots & \cdots & \cdots & \cdots \\ Z_{N(N+1)a} & Z_{N(N+2)a} & \cdots & Z_{N(2N)a} \end{bmatrix} \tag{A-334}$$

$[Z_a']$ = open-circuit mutual-impedance matrix between the real dipoles and their images

$Z_{i(N+j)a}$ = open-circuit mutual-impedance between the i^{th} real element and the image of the j^{th} element.

All the mutual impedances can be calculated by Equation A-290 with

$$d_{in} = \left[4 (H + y_i \cot\theta")^2 + \left(\sum_{n=i}^{j=1} d_n\right)^2 + 4 (H + y_i \cot\theta") \left(\sum_{n=1}^{j=1} d_n\right) \cos\theta" \right]^{1/2} \quad \text{(A-335)}$$

With the dipole feed-point currents determined, the input impedance is given by:

$$Z_{in}" = \frac{V_1}{} = Z_{11a} I_{1a}' + Z_{12a} I_{2a}' + \ldots + Z_{1Na} I_{Na}' + R_h' \left[Z_{1(N+1)a} I_{1a}' + Z_{1(N+2)a} I_{2a}' + \ldots + Z_{s(2N)a} I_{Na}' \right] = \sum_{i=1}^{N} (Z_{1ia} + R_h' Z_{1(N+i)a}) I_{ia}' = R_{in}'' + j X_{in}'' \quad \text{(A-336)}$$

The radiation vectors are given by:

$$N_\theta = -\cos\theta \cos\phi \sum_{i=1}^{N} \frac{2 I_{mi}}{k} \frac{\cos (k\ell_i \cos\psi) - \cos k\ell_i}{\sin^2 \psi} e^{jky_i \csc\theta" \cos\psi"} \quad \text{(A-337)}$$

$$N_\phi = \sin\phi \sum_{i=1}^{N} \frac{2\, I_{mi}}{k} \frac{\cos(k\ell_i \cos\psi) - \cos k\ell_i}{\sin^2\psi} e^{jky_i \csc\theta'' \cos\psi''} \quad \text{(A-338)}$$

$$E_{\theta f} = j30k \frac{e^{-jkr}}{r} N_\theta \quad \text{(A-339)}$$

$$E_{\phi f} = j30k \frac{e^{-jkr}}{r} N_\phi \quad \text{(A-340)}$$

The attenuation relative to free space is:

$$A = \frac{\sqrt{\cos^2\theta \cos^2\phi\, |S_\theta|^2 + \sin^2\phi\, |S_\phi|^2}}{|S_f| \sqrt{\cos^2\theta \cos^2\phi + \sin^2\phi}} \quad \text{(A-341)}$$

where

$$S_f = \left[\sum_{i=1}^{N} I_{mi} e^{jky_i \csc\theta'' \cos\psi''} [\cos(k\ell_i \cos\psi) - \cos k\ell_i] \right] \quad \text{(A-342)}$$

The electric field intensities in the diffraction region are:

$$E_\theta = -\frac{j\,60\, e^{-jkd}}{d} \frac{\cos\theta \cos\phi}{\sin^2\psi} (S_f)(2\, F_r) \quad \text{(A-343)}$$

$$E_\phi = \frac{j60\, e^{-jkd}}{d} \frac{\sin\phi}{\sin^2\psi} (S_f)(2\, F_r) \quad \text{(A-344)}$$

VERTICALLY POLARIZED LOG-PERIODIC DIPOLE ARRAY

The lengths of the dipole elements are related by:

$$\frac{\ell_n}{\ell_{n+1}} = \tau;\ n = 1, 2, \ldots, N-1;\ 0 < \tau < 1 \qquad \text{(A-345)}$$

The spacing between the dipole elements is related to the element lengths by:

$$\frac{d_n}{\ell_{n+1}} = \frac{1 - \tau}{\sin(\alpha_2 + \alpha_3) - \tan\alpha_3 \cos(\alpha_2 + \alpha_3)} \qquad \text{(A-346)}$$

The angles α_1, α_2, and α_3 are related by:

$$\frac{\sin\alpha_1}{\cos(\alpha_1 + \alpha_2 + \alpha_3)} = \frac{\sin\alpha_2}{\cos\alpha_3} \qquad \text{(A-347)}$$

The height of the center of the i^{th} element above ground is determined by:

$$H_i = \ell_i \frac{\tan(\alpha_2 + \alpha_3)}{\tan(\alpha_1 + \alpha_2 + \alpha_3) - \tan(\alpha_2 + \alpha_3)} \qquad \text{(A-348)}$$

Since the dipole elements are parallel to the Z-axis, only the θ-component of the field exists. The final expression for the electric field strength is:

$$E_\theta = \frac{j60\, e^{-jkr_1}}{r_1} \frac{A_{12} + jB_{12}}{\sin\theta} \qquad \text{(A-349)}$$

and

$$E_\phi = 0 \tag{A-350}$$

where

$$A_{12} + jB_{12} = \sum_{i=1}^{N} \frac{I_{bi}}{\sin k\ell_i} e^{jkH_i \cos\theta} \left[\cos (k\ell_i \cos\theta) - \cos k\ell_i\right] \tag{A-351}$$

$$\times \left[1+R_v e^{-j2kH_i \cos\theta} + (1-R_v)(\sin^2\theta - \frac{\sqrt{n^2 - \sin^2\theta}}{n^2} \cos\theta) e^{-j2kH_i \cos\theta}\right.$$

$$\left. \times \left[1-j\sqrt{\pi P_e}\, e^{-P_e \sin^2\theta} \operatorname{erfc} (j\sqrt{P_e})\right]\right] e^{jky_i \sec(\alpha_2 + \alpha_3) \cos\psi'}$$

$$\cos\psi' = \cos\theta \sin(\alpha_2 + \alpha_3) + \sin\theta \cos(\alpha_2 + \alpha_3) \sin\phi \tag{A-352}$$

Y_i = y-coordinate of the feed-point of the i^{th} dipole.

ψ' = angle between the far-field point (θ, ϕ) and the array axis $(\theta' = \frac{\pi}{2} - \alpha_2 - \alpha_3, \phi' = \frac{\pi}{2})$.

The short-circuit admittance matrix for the transmission line is given by Equation A-324.

The elements of the open-circuit impedance matrix for the dipoles are given by:

$$[Z_a] = \begin{bmatrix} Z_{11a} & Z_{12a} & \cdots & Z_{1Na} \\ Z_{21a} & Z_{22a} & \cdots & Z_{2Na} \\ \vdots & & & \\ Z_{N1a} & Z_{N2a} & \cdots & Z_{NNa} \end{bmatrix} \quad \text{(A-353)}$$

The mutual impedances, when two dipoles are either arranged in echelon or collinear as shown in Figure A-2 are as follows.[41] The diagonal elements are found by Equation A-20.

For echelon arrangement:

$$\begin{aligned} Z_{ija} = \frac{30}{\cos k(\ell_i - \ell_j) - \cos k(\ell_i + \ell_j)} \{ & e^{-jk(\ell_i - h_{ij})} [K(U_o) - K(U_1)] \\ & + e^{jk(\ell_i - h_{ij})} [K(V_o) - K(V_1)] + e^{-jk(\ell_i + h_{ij})} [K(U_o') - K(U_2)] \\ & + e^{jk(\ell_i + h_{ij})} [K(V_o') - K(V_2)] + e^{-jk(\ell_i - 2\ell_j - h_{ij})} [-K(U_1) + K(U_3)] \\ & + e^{-jk(\ell_i - 2\ell_j - h_{ij})} [-K(V_1) + K(V_3)] + e^{-jk(\ell_i + 2\ell_j + h_{ij})} [-K(U_2) + K(U_4)] \\ & + e^{jk(\ell_i + 2\ell_j + h_{ij})} [-K(V_2) + K(V_4)] + 2 \cos k\ell_i \, e^{-jkh_{ij}} [K(W_2) - K(W_1)] \\ & + 2 \cos k\ell_i \, e^{jkh_{ij}} [K(Y_2) - K(Y_1)] + 2 \cos k\ell_i \, e^{-jk(2\ell_j + h_{ij})} [K(W_2) - K(W_3)] \\ & + 2 \cos k\ell_i \, e^{jk(2\ell_i + h_{ij})} [K(Y_2) - K(Y_3)] \} \end{aligned} \quad \text{(A-354)}$$

---

[41] King, H.E., "Mutual Impedance of Unequal Length Antennas in Echelon," IRE Trans. Antennas and Propagation, Vol. AP-5, No. 3, pp. 306-313, 1957.

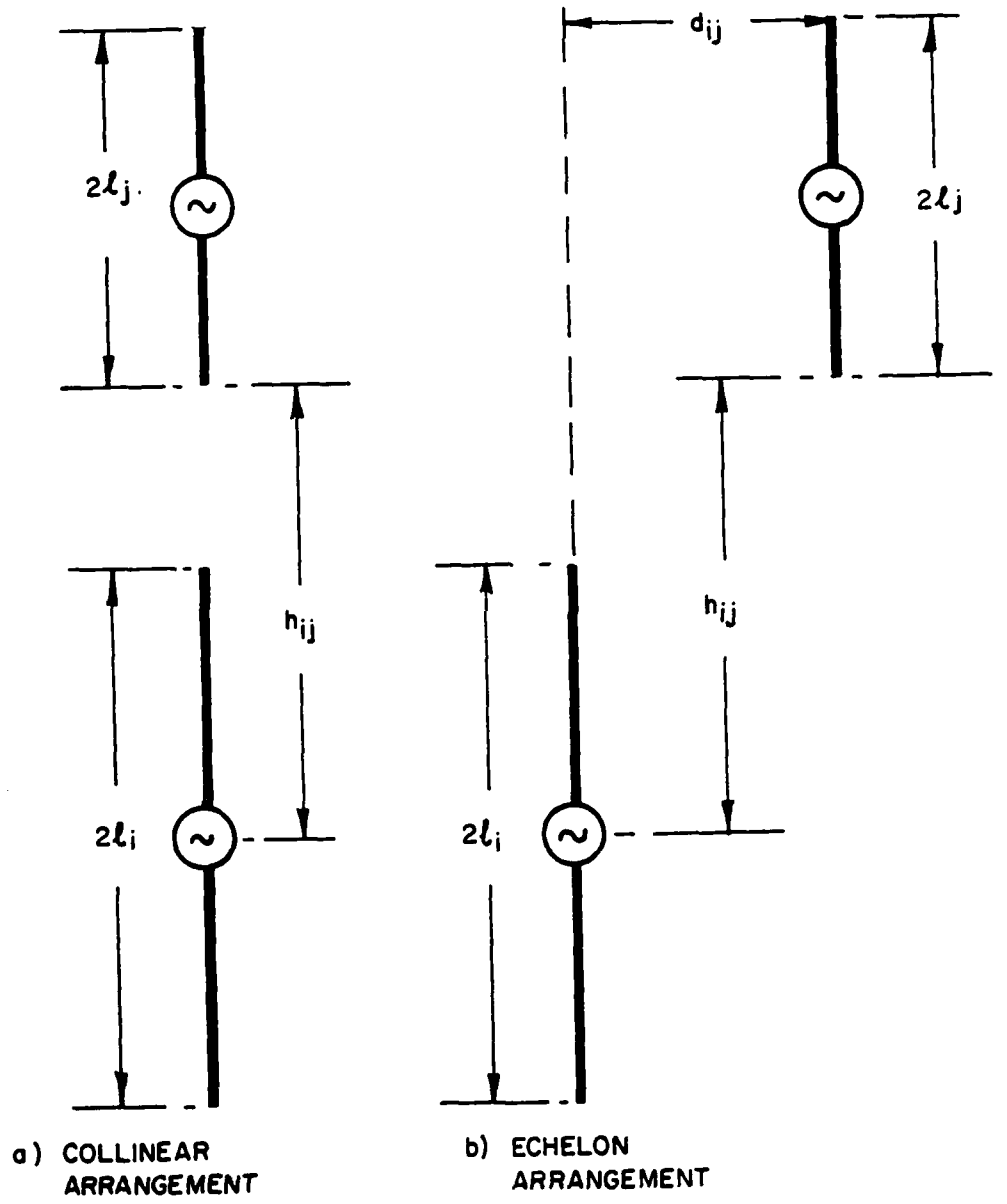

Figure A-2. Two parallel dipoles of arbitrary lengths.

For collinear arrangement:

$$
\begin{aligned}
Z_{ija} = \frac{30}{\cos k(\ell_i-\ell_j) - \cos k(\ell_i+\ell_j)} \Bigg\{ & e^{-jk(\ell_i-h_{ij})} [K(U_o)-K(U_1)] \\
& + e^{jk(\ell_i-h_{ij})} \ln\left[\frac{h_{ij}-\ell_i+\ell_j}{h_{ij}-\ell_i}\right]\Bigg\} \\
& + e^{jk(\ell_i+h_{ij})} [K(V_o')-K(V_2)] + e^{-jk(\ell_i+h_{ij})} \ln\left[\frac{h_{ij}+\ell_i+\ell_j}{h_{ij}+\ell_i}\right] \\
& + e^{-jk(\ell_i-2\ell_j-h_{ij})} [-K(U_1)+K(U_3)] + e^{jk(\ell_i-2\ell_j-h_{ij})} \ln\left[\frac{h_{ij}-\ell_i+\ell_j}{h_{ij}-\ell_i+2\ell_j}\right] \\
& + e^{jk(\ell_i+2\ell_j+h_{ij})} [-K(V_2)+K(V_4)] + e^{-jk(\ell_i+2\ell_j+h_{ij})} \ln\left[\frac{h_{ij}+\ell_i+\ell_j}{h_{ij}+\ell_i+2\ell_j}\right] \\
& + 2\cos k\ell_i\, e^{jkh_{ij}} [-K(Y_1)+K(Y_2)] + 2\cos k\ell_i\, e^{-jkh_{ij}} \ln\left[\frac{h_{ij}}{h_{ij}+\ell_j}\right] \\
& + 2\cos k\ell_i\, e^{jk(2\ell_j+h_{ij})} [K(Y_2)-K(Y_3)] \\
& + 2\cos k\ell_i\, e^{-jk(2\ell_j+h_{ij})} \ln\left[\frac{h_{ij}+2\ell_j}{h_{ij}+\ell_j}\right]
\end{aligned}
\qquad \text{(A-355)}
$$

where

$$U_o = k\left[\sqrt{d_{ij}^2 + (h_{ij}-\ell_i)^2} + (h_{ij}-\ell_i)\right]$$

$$V_o = k\left[\sqrt{d_{ij}^2 + (h_{ij}-\ell_i)^2} - (h_{ij}-\ell_i)\right]$$

$$U_o' = k\left[\sqrt{d_{ij}^2 + (h_{ij}+\ell_i)^2} - (h_{ij}+\ell_i)\right]$$

$$V_o' = k\left[\sqrt{d_{ij}^2 + (h_{ij} + \ell_i)^2} + (h_{ij} + \ell_i)\right]$$

$$U_1 = k\left[\sqrt{d_{ij}^2 + (h_{ij} - \ell_i + \ell_j)^2} + (h_{ij} - \ell_i + \ell_j)\right]$$

$$V_1 = k\left[\sqrt{d_{ij}^2 + (h_{ij} - \ell_i + \ell_j)^2} - (h_{ij} - \ell_i + \ell_j)\right]$$

$$U_2 = k\left[\sqrt{d_{ij}^2 + (h_{ij} + \ell_i + \ell_j)^2} - (h_{ij} + \ell_i + \ell_j)\right]$$

$$V_2 = k\left[\sqrt{d_{ij}^2 + (h_{ij} + \ell_i + \ell_j)^2} + (h_{ij} + \ell_i + \ell_j)\right]$$

$$U_3 = k\left[\sqrt{d_{ij}^2 + (h_{ij} - \ell_i + 2\ell_j)^2} + (h_{ij} - \ell_i + 2\ell_j)\right]$$

$$V_3 = k\left[\sqrt{d_{ij}^2 + (h_{ij} - \ell_i + 2\ell_j)^2} - (h_{ij} - \ell_i + 2\ell_j)\right]$$

$$U_4 = k\left[\sqrt{d_{ij}^2 + (h_{ij} + \ell_i + 2\ell_j)^2} - (h_{ij} + \ell_i + 2\ell_j)\right]$$

$$V_4 = k\left[\sqrt{d_{ij}^2 + (h_{ij} + \ell_i + 2\ell_j)^2} + (h_{ij} + \ell_i + 2\ell_j)\right]$$

$$W_1 = k\left[\sqrt{d_{ij}^2 + h_{ij}^2} - h_{ij}\right]$$

$$Y_1 = k\left[\sqrt{d_{ij}^2 + h_{ij}^2} + h_{ij}\right]$$

$$W_2 = k\left[\sqrt{d_{ij}^2 + (h_{ij} + \ell_j)^2} - (h_{ij} + \ell_j)\right]$$

$$Y_2 = k\left[\sqrt{d_{ij}^2 + (h_{ij} + \ell_j)^2} + (h_{ij} + \ell_j)\right]$$

$$W_3 = k\left[\sqrt{d_{ij}^2 + (h_{ij} + 2\ell_j)^2} - (h_{ij} + 2\ell_j)\right]$$

$$Y_3 = k\left[\sqrt{d_{ij}^2 + (h_{ij} + 2\ell_j)^2} + (h_{ij} + 2\uparrow_j)\right]$$

d_{ij} is the perpendicular distance between the two dipoles, and h_{ij} is the distance measured from the feed point of the i^{th} dipole to the nearest end of the j^{th} dipole.

The mutual impedances between the i^{th} and j^{th} real elements Z_{ija} is calculated from Equation A-354 with:

$$d_{ij} = \left(\sum_{n=i}^{j=1} d_n \right) \cos (\alpha_2 + \alpha_3) \qquad \text{(A-357)}$$

$$h_{ij} = \left(\sum_{n=i}^{j=1} d_n \right) \sin (\alpha_2 + \alpha_3) - \ell_j \qquad \text{(A-358)}$$

For the typical element $Z_{i(N+j)a}$ in Equation A-334, Equation A-354 is used when $i \neq j$ with the same d_{ij} as Equation A-357, and $h_{ij} = H_j + H_i - \ell_j$. When $i = j$, Equation A-355 is used with $h_{ij} = 2H_i - \ell_i$.

The feed-point currents are determined by Equation A-318 if the free-space approximation is applied.

The input impedance for the free-space approximation is found by:

$$Z_{in} = \sum_{i=1}^{N} [Z_{11a} + R_v' Z_{1(N+i)a}] I_{ia} = R_{in} + j X_{in} \qquad \text{(A-359)}$$

where

$$R_v' = \frac{k_2 - k}{k_2 + k} \quad (R_v \text{ with } \theta = 0) \qquad \text{(A-360)}$$

For the perfect-ground approximation, Equation A-333 is used.

The input impedance for the perfect-ground approximation is found by:

$$Z_{in}'' = \sum_{i=1}^{N} [Z_{11a} + R_v' Z_{1(N+i)a}] I_{ia}' = R_{in}'' + j X_{in}'' \qquad \text{(A-361)}$$

The expression for the directive gain for the vertically polarized log-periodic dipole array becomes:

$$g_d = \frac{120}{R_{in}} \frac{A_{12}^2 + B_{12}^2}{\sin^2 \theta} \qquad \text{(A-362)}$$

where R_{in} is given by Equation A-359 for the free-space approximation, and by Equation A-361 for the perfect-ground approximation. $A_{12} + jB_{12}$ is given by Equation A-351.

The radiation vector is given by:

$$N_\theta = \sum_{i=1}^{N} \frac{2 I_{bi}}{\sin k\ell_i} \frac{\cos (k\ell_i \cos\theta) - \cos k\ell_i}{\sin \theta} e^{jky_i \sec(\alpha_2 + \alpha_3) \cos\psi'} \qquad \text{(A-363)}$$

The free-space field intensity is given by:

$$E_{\theta f} = \frac{j60 \, e^{-jkr_1}}{r_1} \sum_{i=1}^{N} \frac{I_{bi}}{\sin k\ell_i} \frac{\cos (k\ell_i \cos\theta) - \cos k\ell_i}{\sin\theta} \times e^{jky_i \sec (\alpha_2 + \alpha_3) \cos\psi'}$$

The attenuation relative to free-space is:

$$A = \frac{|E_\theta|}{|E_{\theta f}|} \qquad \text{(A-365)}$$

$$ADB = 20 \log \frac{1}{|A|} \quad \text{(A-366)}$$

The electric field intensity in the diffraction region is found by:

$$E_\theta = j30k \frac{e^{-jkd}}{d} (N_\theta) (2 F_r) \quad \text{(A-367)}$$

$$E_\phi = 0 \quad \text{(A-368)}$$

CURTAIN ARRAY

For a curtain array:

Z_1 = height of the lowest element above ground
Z_i = height of the i^{th} element on each bay
$Z_i - Z_{i-1}$ = vertical spacing of elements
Y_i = horizontal position of the $(i + n)^{th}$ bay, $Y_o = 0$
$Y_i - Y_{i-1}$ = horizontal spacing of bays (bay separation)
N = number of bays
M = number of elements in each bay
X_1 = reflector spacing
ℓ = half-length of element.

The field components produced by the first bay are:

$$E_{\theta 1} = -j60 I_m \frac{e^{-jkr}}{r} \frac{\cos(k\ell \cos\psi) - \cos k\ell}{\sin^2\psi} \sin\phi (A_{13} + jB_{13}) \quad \text{(A-369)}$$

$$E_{\phi 1} = j60\, I_m \frac{e^{-jkr}}{r} \frac{\cos(k\ell\cos\psi) - \cos k\ell}{\sin^2\psi} \cos\phi\, (A_{14} + jB_{14}) \quad \text{(A-370)}$$

where r is the distance between (Y, Z) = (0, 0) and the far-field point.

$$A_{13}+jB_{13} = \sum_{i=1}^{M} C_i\, e^{jkZ_i(\cos\theta - \cos\theta_o)} \left[\cos\theta\,(1-R_v e^{-j2kZ_i\cos\theta}) + (1-R_v) F_e \frac{\sqrt{n^2 - \sin^2\theta}}{n^2} (\sin^2\theta - \frac{\sqrt{n^2 - \sin^2\theta}}{n^2}\cos\theta)\, e^{-j2kZ_i\cos\theta}\right] \quad \text{(A-371)}$$

$$A_{14}+jB_{14} = \sum_{i=1}^{M} C_i\, e^{jkZ_i(\cos\theta-\cos\theta_o)} \left[1+R_h e^{-j2kZ_i\cos\theta} + (1-R_h) F_m e^{-j2kZ_i\cos\theta}\right] \quad \text{(A-372)}$$

$$\cos\psi = \sin\theta\sin\phi$$

C_i represents the relative amplitude excitation of the i^{th} dipole with $C_1 = 1$, and θ_o is the desired position of the beam maximum.

The array factor for N bays is:

$$S_y = \sum_{n=1}^{N} e^{jky_{n-1}\sin\theta(\sin\phi - \sin\theta_o)} \quad \text{(A-373)}$$

where ϕ_o determines the position of the beam maximum in an azimuthal surface assuming that the amplitude excitations for corresponding elements in each bay are the same.

The array factor resulting from the arrays of the real elements and their images with respect to the screen at $x = -x_1$ is:

$$S_x = 1-e^{-j2kX_1\cos\psi_x} = 2j\, e^{-jkX_1\cos\psi_x} \sin(kX_1\cos\psi_x) \qquad (A-374)$$

where $\cos_{\psi x} = \sin\theta\cos\phi$.

The total field components become:

$$E_{\theta,t} = E_{\theta 1}\, S_x\, S_y \qquad (A-375)$$

$$E_{\phi,t} = E_{\phi 1}\, S_x\, S_y \qquad (A-376)$$

The input resistance of individual elements can be expressed as:

$$R_i^n = \mathrm{Re}\,(Z_i^n),\ i = 1,2,\ldots,M;\ n = 1,2,\ldots,N \qquad (A-377)$$

Where Z_i^n representing the input impedance looking into the i^{th} element of the n^{th} bay can be calculated by considering the following four groups:

First group - open-circuit self or mutual impedances among the real elements themselves. For example, Z_{iM}^{nN} is the mutual impedance between the i^{th} element of the n^{th} bay and the M^{th} element of the N^{th} bay, and Z_{ii}^{nn} is the self-impedance of the i^{th} element of the n^{th} bay.

Second group - open-circuit mutual impedances between the real elements and their imperfect images under the ground. For example Z_{iMp}^{nN} is the mutual impedance between the i^{th} element of the n^{th} bay and the imperfect image of the M^{th} element of the N^{th} bay.

Third group - open-circuit mutual impedances between the real elements and their perfect images with respect to the vertical conducting screen.

Fourth group - Open-circuit mutual impedances between the real elements and the imperfect images of the perfect images behind the vertical conducting screen.

$$
\begin{aligned}
Z_i^n = {} & Z_{i1}^{n1} + Z_{i2}^{n1} + \cdots\cdots Z_{ii}^{n1} + Z_{iM}^{n1} \\
& + Z_{i1}^{n2} + Z_{i2}^{n2} + \cdots\cdots + Z_{ii}^{n2} + \cdots\cdots + Z_{iM}^{n2} \\
& + \cdots\cdots \\
& + Z_{i1}^{nn} + Z_{i2}^{nn} + \cdots\cdots + Z_{ii}^{nn} + \cdots\cdots + Z_{iM}^{nn} \\
& + \cdots\cdots \\
& + Z_{ii}^{nN} + Z_{i2}^{nN} + \cdots\cdots + Z_{ii}^{nN} + \cdots\cdots + Z_{iM}^{nN} \qquad \text{First Group} \\
& + R_h' \left(Z_{i1p}^{n1} + Z_{i2p}^{n1} + \cdots\cdots + Z_{iip}^{n1} + \cdots\cdots Z_{iMP}^{n1}\right. \\
& + \cdots\cdots \\
& + Z_{i1p}^{nn} + Z_{i2p}^{nn} + \cdots\cdots + Z_{iip}^{nn} + \cdots\cdots + Z_{iMP}^{nn} \\
& + \cdots\cdots \\
& \left. + Z_{i1P}^{nN} + Z_{i2P}^{nN} + \cdots\cdots + Z_{iip}^{nN} + \cdots\cdots + Z_{iMP}^{nN}\right) \qquad \text{Second Group} \\
& - \left(Z_{i1d}^{n1} + Z_{i2d}^{n1} + \cdots\cdots + Z_{iid}^{n1} + \cdots\cdots + Z_{iMd}^{n1}\right. \\
& + \cdots\cdots \\
& + Z_{i1d}^{nn} + Z_{i2d}^{nn} + \cdots\cdots + Z_{iid}^{nn} + \cdots\cdots + Z_{iMd}^{nn} \qquad \text{Third Group} \\
& + \cdots\cdots \\
& \left. + Z_{i1d}^{nN} + Z_{i2d}^{nN} + \cdots\cdots + Z_{iid}^{nN} + \cdots\cdots + Z_{iMd}^{nN}\right) \\
& - R_h' \left(Z_{i1t}^{n1} + Z_{i2t}^{n1} + \cdots\cdots + Z_{iit}^{n1} + \cdots\cdots Z_{iMt}^{n1}\right. \\
& + \cdots\cdots \\
& + Z_{i1t}^{nn} + Z_{i2t}^{nn} + \cdots\cdots + Z_{iit}^{nn} + \cdots\cdots + Z_{iMt}^{nn} \qquad \text{Fourth Group} \\
& + \cdots\cdots \\
& \left. + Z_{i1t}^{nN} + Z_{i2t}^{nN} + \cdots\cdots + Z_{iit}^{nN} + \cdots\cdots + Z_{iMt}^{nN}\right) \qquad \text{(A-378)}
\end{aligned}
$$

The total power supplied to the entire system when all the elements are of equal length 2ℓ is:

$$W_{in} = |I_m|^2 \{R_1 + C_2^2 R_2 + \ldots\ldots + C_m^2 R_m + R_1^2 + C_2^2 R_2^2 + \ldots\ldots + C_m^2 R_m^2 + \ldots\ldots + R_1^N + C_2^2 R_2^N + \ldots\ldots + C_m^2 R_m^N\} \sin^2 k\ell \quad \text{(A-379)}$$

$$= |I_m|^2 \sin^2 k\ell \sum_{n=1}^{N} \sum_{i=1}^{M} C_i^2 R_i^n \quad (C_1 = 1)$$

*
C_i = 1 unless otherwise indicated.

The directive gain for the curtain array is:

$$g_d = \frac{480 |S_y|^2 \sin^2(kX_1 \cos\psi_x) [\sin^2\phi (A_{13}^2 + B_{13}^2) + \cos^2\phi (A_{14}^2 + B_{14}^2)]}{\sin^2 k\ell \sum_{n=1}^{N} \sum_{i=1}^{M} C_i^2 R_i^n} \quad \text{(A-380)}$$

$$x \frac{[\cos(k\ell \cos\psi) - \cos k\ell]^2}{\sin^4\psi}$$

The free-space field intensities are:

$$E_{\theta f} = -\frac{j60 I_m e^{-jkr}}{r} \frac{\cos(k\ell \cos\psi) - \cos k\ell}{\sin^2\psi} \sin\phi \cos\theta \quad \text{(A-381)}$$

$$x \sum_{i=1}^{M} C_i e^{jkZ_i (\cos\theta - \cos\theta_o)}] S_x S_y$$

$$E_{\phi f} = \frac{j60\, I_m\, e^{-jkr}}{r} \frac{\cos(k\ell\cos\psi) - \cos k\ell}{\sin^2\psi} \cos\phi \qquad \text{(A-382)}$$

$$\times \left[\sum_{i=1}^{M} C_i\, e^{jkZ_i(\cos\theta - \cos\theta_o)} \right] S_x S_y$$

The attenuation relative to free space is:

$$A = \sqrt{\frac{|E_{\theta t}|^2 + |E_{\phi t}|^2}{|E_{\theta f}|^2 + |E_{\phi f}|^2}} \qquad \text{(A-383)}$$

The electric field intensities in the diffraction region are:

$$E_\theta = -\frac{j60\, I_m\, e^{-jkd}}{d} \frac{\cos(k\ell\cos\psi) - \cos k\ell}{\sin^2\psi} \sin\phi\cos\theta \qquad \text{(A-384)}$$

$$\times \left[\sum_{i=1}^{M} C_i\, e^{jkZ_1(\cos\theta - \cos\theta_o)} \right] S_x S_y \frac{2F}{r}$$

$$E_\phi = \frac{j60\, I_m\, e^{-jkd}}{d} \frac{\cos(k\ell\cos\psi) - \cos k\ell}{\sin^2\psi} \cos\phi \qquad \text{(A-385)}$$

$$\times \left[\sum_{i=1}^{M} C_i\, e^{jkZ_i(\cos\theta - \cos\theta_o)} \right] S_x S_y \frac{2F}{r}$$

SLOPING DOUBLE RHOMBOID

For the sloping double rhomboid:

α = angle between the principal antenna axis and the major rhomboid axis, in degrees

β = angle between the major rhomboid axis and the long leg, in degrees

γ = angle between the major rhomboid axis and the short leg, in degrees

ℓ_1 = short leg length

ℓ_2 = long leg length

H_1 = feed height

H_4 = termination height

α' = angle subtended between the wires and the horizontal plane, in degrees

$$L = \ell_2 \cos(\beta + \alpha) + \ell_1 \cos(\alpha + \gamma) \tag{A-386}$$

$$\cot\alpha' = \frac{\ell_1 \cos(\alpha + \gamma) + \ell_2 \cos(\alpha + \beta)}{H_4 - H_1} \tag{A-387}$$

For wire 1:

$$\theta' = \theta' - \alpha', \quad \phi' = (\pi/2) + \alpha + \gamma$$

$$\cos\psi_1 = \cos\theta \cos((\pi/2) - \alpha') + \sin\theta \sin((\pi/2) - \alpha') \cos(\phi-(\pi/2)-\alpha-\gamma)$$

$$= \cos\theta \sin\alpha' + \sin\theta \cos\alpha' \sin(\phi-\alpha-\gamma) \tag{A-388}$$

For wire 2:

$$\theta' = (\pi/2) - \alpha', \quad \phi' = (\pi/2) + \alpha + \beta$$

$$\cos\psi_2 = \cos\theta \sin\alpha' + \sin\theta \cos\alpha' \sin(\phi-\alpha-\beta) \tag{A-389}$$

For wire 3:

$$\theta' = (\pi/2) - \alpha', \quad \phi' = (\pi/2) - (\alpha+\beta)$$
$$\cos\psi_3 = \cos\theta \sin\alpha' + \sin\theta \cos\alpha' \sin(\phi+\alpha+\beta) \tag{A-390}$$

For wire 4:

$$\theta' = (\pi/2) - \alpha', \quad \phi' = (\pi/2) - (\alpha+\gamma)$$
$$\cos\psi_4 = \cos\theta \sin\alpha' + \sin\theta \cos\alpha' \sin(\phi + \alpha + \gamma) \tag{A-391}$$

The height of the current element above ground for wires 1, 2, 3, and 4 is:

$$H_s = H_1 + s \sin\alpha' \tag{A-392}$$

For wires 6 and 7, it is:

$$H_s = H_2 + s \sin\alpha' \tag{A-393}$$

For wires 5 and 8, it is:

$$H_s = H_3 + s \sin\alpha' \tag{A-394}$$

The current distributions on the wires are given by:

$$I_1(s) = -I_m e^{-jks} \tag{A-395}$$

$$I_3(s) = I_m e^{-jks} \tag{A-396}$$

$$I_8(s) = I_m e^{-jks} e^{-jk\ell_2} \quad \text{First Rhomboid} \tag{A-397}$$

$$I_6(s) = -I_m e^{-jks} e^{-jk\ell_1} \tag{A-398}$$

$$I_2(s) = -I_m e^{-jks} \quad \text{(A-399)}$$

$$I_4(s) = I_m e^{-jks} \quad \text{(A-400)}$$

$$I_7(s) = I_m e^{-jks} e^{-jk\ell_1} \quad \text{Second Rhomboid} \quad \text{(A-401)}$$

$$I_5(s) = -I_m e^{-jks} e^{-jk\ell_2} \quad \text{(A-402)}$$

where

$$H_2 = H_1 + \ell_1 \cos(\alpha+\gamma) \tan\alpha' \quad \text{(A-403)}$$

$$H_3 = H_1 + \ell_2 \cos(\alpha+\gamma) \tan\alpha' \quad \text{(A-404)}$$

The field components are:

$$E_{\theta 1} = 30 I_m \frac{e^{-jkr}}{r} \left\{ \cos\alpha' \cos\theta \sin(\phi-\alpha-\gamma) \left[\frac{1-e^{-jk\ell_1 U_1}}{U_1} - R_v e^{-j2kH_1\cos\theta} \frac{1-e^{-jk\ell_1 U_1'}}{U_1'} \right. \right. \quad \text{(A-405)}$$

$$\left. + (1-R_v) F_e e^{-j2kH_1\cos\theta} \frac{\sqrt{n^2-\sin^2\theta}}{n^2\cos\theta} \left(\sin^2\theta - \frac{\sqrt{n^2-\sin^2\theta}}{n^2}\cos\theta\right) \frac{1-e^{-jk\ell_1 U_1'}}{U_1'} \right]$$

$$- \sin\alpha' \sin\theta \left[\frac{1-e^{-jk\ell_1 U_1}}{U_1} + R_v e^{-j2kH_1\cos\theta} \frac{1-e^{-jk\ell_1 U_1'}}{U_1'} \right.$$

$$\left. \left. + (1-R_v) F_e e^{-j2kH_1\cos\theta} \times \frac{1-e^{-jk\ell_1 U_1'}}{U_1'} \left(\sin^2\theta - \frac{\sqrt{n^2-\sin^2\theta}}{n^2}\cos\theta\right) \right] \right\}$$

$$E_{\theta 3} = -30\, I_m \frac{e^{-jkr}}{r} \left\{ \cos\alpha' \cos\theta \sin(\phi+\alpha+\beta) \left[\frac{1-e^{-jk\ell_2 U_3}}{U_3} - R_v e^{-j2kH_1\cos\theta} \frac{1-e^{-jk\ell_2 U_3'}}{U_3'} \right] \right. \tag{A-406}$$

$$+ (1-R_v) F_e e^{-j2kH_1\cos\theta} \frac{\sqrt{n^2-\sin^2\theta}}{n^2\cos\theta} \left(\sin^2\theta - \frac{\sqrt{n^2-\sin^2\theta}}{n^2}\cos\theta \right) \frac{1-e^{-jk\ell_2 U_3'}}{U_3'} \Bigg]$$

$$+ \sin\alpha' \sin\theta \left[\frac{1-e^{-jk\ell_2 U_3}}{U_3} + R_v e^{-j2kH_1\cos\theta} \frac{1-e^{-jk\ell_2 U_3'}}{U_3'} \right.$$

$$\left. \left. + (1-R_v) F_e e^{-j2kH_1\cos\theta} \frac{1-e^{-jk\ell_2 U_3'}}{U_3'} \left(\sin^2\theta - \frac{\sqrt{n^2-\sin^2\theta}}{n^2}\cos\theta \right) \right] \right\}$$

$$E_{\theta 8} = 30\, I_m \frac{e^{-jkr}}{r} e^{-jk\ell_2 U_3} \left\{ -\cos\alpha' \cos\theta \sin(\phi-\alpha-\gamma) \left[\frac{1-e^{-jk\ell_1 U_1}}{U_1} - \frac{1-e^{-jk\ell_1 U_1'}}{U_1'} R_v e^{-j2kH_3\cos\theta} \right] \right. \tag{A-407}$$

$$+ (1-R_v) F_e e^{-j2kH_3\cos\theta} \frac{1-e^{-jk\ell_1 U_1'}}{U_1'} \frac{\sqrt{n^2-\sin^2\theta}}{n^2\cos\theta} \left(\sin^2\theta - \frac{\sqrt{n^2-\sin^2\theta}}{n^2}\cos\theta \right) \Bigg] + \sin\alpha' \sin\theta$$

$$\times \left[\frac{1-e^{-jk\ell_1 U_1}}{U_1} + \frac{1-e^{-jk\ell_1 U_1'}}{U_1'} R_v e^{-j2kH_3\cos\theta} \right.$$

$$\left. \left. + (1-R_v) F_e e^{-j2kH_3\cos\theta} \frac{1-e^{-jk\ell_1 U_1'}}{U_1'} \left(\sin^2\theta - \frac{\sqrt{n^2-\sin^2\theta}}{n^2}\cos\theta \right) \right] \right\}$$

$$E_{\theta 6} = 30\, I_m \frac{e^{-jkr}}{r} e^{-jk\ell_1 U_1} \left\{ \cos\alpha' \cos\theta \sin(\phi+\alpha+\beta) \left[\frac{1-e^{-jk\ell_2 U_3}}{U_3} \right.\right. \tag{A-408}$$

$$\left. - \frac{1-e^{-jk\ell_2 U_3'}}{U_3'} R_v e^{-j2kH_2\cos\theta} + (1-R_v) \right.$$

$$\times F_e e^{-j2kH_2\cos\theta} \frac{1-e^{-jk\ell_2 U_3'}}{U_3'} \frac{\sqrt{n^2-\sin^2\theta}}{n^2\cos\theta} (\sin^2\theta$$

$$\left. - \frac{\sqrt{n^2-\sin^2\theta}}{n^2} \cos\theta) \right] - \sin\alpha' \sin\theta \left[\frac{1-e^{-jk\ell_2 U_3}}{U_3} \right.$$

$$+ \frac{1-e^{-jk\ell_2 U_3'}}{U_3'} R_v e^{-j2kH_2\cos\theta} + (1-R_v) F_e e^{-j2kH_2\cos\theta} \frac{1-e^{-jk\ell_2 U_3'}}{U_3'}$$

$$\left.\left. \times (\sin^2\theta - \frac{\sqrt{n^2-\sin^2\theta}}{n^2} \cos\theta) \right] \right\}$$

$$E_{\theta 4} = -30\, I_m \frac{e^{-jkr}}{r} \left\{ \cos\alpha' \cos\theta \sin(\phi+\alpha+\gamma) \left[\frac{1-e^{-jk\ell_1 U_4}}{U_4} - \frac{1-e^{-jk\ell_1 U_4'}}{U_4'} \right.\right.$$

$$\times R_v e^{-j2kH_1\cos\theta} + (1-R_v) F_e \tag{A-409}$$

$$\times e^{-j2kH_1\cos\theta} \frac{1-e^{-jk\ell_1 U_4'}}{U_4'} \frac{\sqrt{n^2-\sin^2\theta}}{n^2\cos\theta} (\sin^2\theta$$

$$\left. - \frac{\sqrt{n^2-\sin^2\theta}}{n^2} \cos\theta) \right] + \sin\alpha' \sin\theta \left[\frac{1-e^{-jk\ell_1 U_4}}{U_4} + \frac{1-e^{-jk\ell_1 U_4'}}{U_4'} \right.$$

$$\times R_v e^{-j2kH_1\cos\theta} + (1-R_v) F_e e^{-j2kH_1\cos\theta} \frac{1-e^{-jk\ell_1 U_4'}}{U_4'} (\sin^2\theta$$

$$\left.\left. - \frac{\sqrt{n^2-\sin^2\theta}}{n^2} \cos\theta) \right] \right\}$$

$$E_{\theta 7} = 30\, I_m \frac{e^{-jkr}}{r} e^{-jk\ell_1 U_4} \left\{ -\cos\alpha' \cos\theta \sin(\phi-\alpha-\beta) \left[\frac{1-e^{-jk\ell_2 U_2}}{U_2} \right.\right. \tag{A-410}$$

$$\left. - \frac{1-e^{-jk\ell_2 U_2'}}{U_2'} R_v\, e^{-j2kH_2\cos\theta} + (1-R_v)\, F_e \right.$$

$$\times e^{-j2kH_2\cos\theta} \frac{1-e^{-jk\ell_2 U_2'}}{U_2'} \frac{\sqrt{n^2-\sin^2\theta}}{n^2\cos\theta} (\sin^2\theta$$

$$\left. - \frac{\sqrt{n^2-\sin^2\theta}}{n^2}\cos\theta) \right] + \sin\alpha' \sin\theta \left[\frac{1-e^{-jk\ell_2 U_2}}{U_2} + \frac{1-e^{-jk\ell_2 U_2'}}{U_2'} \right.$$

$$\times R_v\, e^{-j2kH_2\cos\theta} + (1-R_v)\, F_e\, e^{-j2kH_2\cos\theta} \frac{1-e^{-jk\ell_2 U_2'}}{U_2'} (\sin^2\theta$$

$$\left.\left. - \frac{\sqrt{n^2-\sin^2\theta}}{n^2}\cos\theta) \right] \right\}$$

$$E_{\theta 5} = 30\, I_m \frac{e^{-jkr}}{r} e^{-jk\ell_2 U_2} \left\{ \cos\alpha' \cos\theta \sin(\phi+\alpha+\gamma) \left[\frac{1-e^{-jk\ell_1 U_4}}{U_4} \right.\right. \tag{A-411}$$

$$\left. - \frac{1-e^{-jk\ell_1 U_4'}}{U_4'} R_v\, e^{-j2kH_3\cos\theta} + (1-R_v)\, F_e \right.$$

$$\times e^{-j2kH_3\cos\theta} \frac{1-e^{-jk\ell_1 U_4'}}{U_4'} \frac{\sqrt{n^2-\sin^2\theta}}{n^2\cos\theta} (\sin^2\theta - \frac{\sqrt{n^2-\sin^2\theta}}{n^2}\cos\theta) \left. \right]$$

$$- \sin\alpha' \sin\theta \left[\frac{1-e^{-jk\ell_1 U_4}}{U_4} + \frac{1-e^{-jk\ell_1 U_4'}}{U_4'} \times R_v\, e^{-j2kH_3\cos\theta} \right.$$

$$\left.\left. + (1-R_v)\, F_e\, e^{-j2kH_3\cos\theta} \frac{1-e^{-jk\ell_2 U_4'}}{U_4'} (\sin^2\theta - \frac{\sqrt{n^2-\sin^2\theta}}{n^2}\cos\theta) \right] \right\}$$

$$E_{\theta 2} = 30\, I_m \frac{e^{-jkr}}{r} \left\{ \cos\alpha' \cos\theta \sin(\phi-\alpha-\beta) \left[\frac{1-e^{-jk\ell_2 U_2}}{U_2} - \frac{1-e^{-jk\ell_2 U_2'}}{U_2'} R_v\, e^{-j2kH_1\cos\theta} + (1-R_v)\, F_e \right.\right. \quad \text{(A-412)}$$

$$\left. \times e^{-j2kH_1\cos\theta} \frac{\sqrt{n^2-\sin^2\theta}}{n^2\cos\theta} \left(\sin^2\theta - \frac{\sqrt{n^2-\sin^2\theta}}{n^2}\cos\theta\right) \frac{1-e^{-jk\ell_2 U_2'}}{U_2'} \right]$$

$$- \sin\alpha' \sin\theta \left[\frac{1-e^{-jk\ell_2 U_2}}{U_2} + \frac{1-e^{-jk\ell_2 U_2'}}{U_2'} \right.$$

$$\times R_v e^{-j2kH_1\cos\theta} + (1-R_v)\, F_e\, e^{-j2kH_1\cos\theta} \frac{1-e^{-jk\ell_2 U_2'}}{U_2'} \left(\sin^2\theta \right.$$

$$\left.\left. \left. - \frac{\sqrt{n^2-\sin^2\theta}}{n^2}\cos\theta\right) \right] \right\}$$

$$E_{\phi 1} = -30\, I_m \frac{e^{-jkr}}{r} \cos\alpha' \cos(\phi-\alpha-\gamma) \left[\frac{1-e^{-jk\ell_1 U_1}}{U_1} + \frac{1-e^{-jk\ell_1 U_1'}}{U_1'} \right. \quad \text{(A-413)}$$

$$\left. \times R_h\, e^{-j2kH_1\cos\theta} + (1-R_h)\, F_m e^{-j2kH_1\cos\theta} \frac{1-e^{-jk\ell_1 U_1'}}{U_1'} \right]$$

$$E_{\phi 3} = 30\, I_m \frac{e^{-jkr}}{r} \cos\alpha' \cos(\phi+\alpha+\beta) \left[\frac{1-e^{-jk\ell_2 U_3}}{U_3} + \frac{1-e^{-jk\ell_2 U_3'}}{U_3'} \right. \quad \text{(A-414)}$$

$$\left. \times R_h\, e^{-j2kH_1\cos\theta} + (1-R_h)\, F_m e^{-j2kH_1\cos\theta} \frac{1-e^{-jk\ell_2 U_3'}}{U_3'} \right]$$

$$E_{\phi 8} = 30\, I_m \frac{e^{-jkr}}{r} e^{-jk\ell_2 U_3} \cos\alpha' \cos(\phi-\alpha-\gamma) \left[\frac{1-e^{-jk\ell_1 U_1}}{U_1} + \frac{1-e^{-jk\ell_1 U_1'}}{U_1'} \right.$$

$$\left. \times R_h\, e^{-j2kH_3\cos\theta} + (1-R_h)\, F_m e^{-j2kH_3\cos\theta} \frac{1-e^{-jk\ell_1 U_1'}}{U_1'} \right] \quad \text{(A-415)}$$

$$E_{\phi 6} = -30\, I_m \frac{e^{-jkr}}{r} e^{-jk\ell_1 U_1} \cos\alpha' \cos(\phi+\alpha+\beta) \left[\frac{1-e^{-jk\ell_2 U_3}}{U_3} \right. \tag{A-416}$$

$$\left. + \frac{1-e^{-jk\ell_2 U_3'}}{U_3'} R_h e^{-j2kH_2\cos\theta} + (1-R_h) F_m e^{-j2kH_2\cos\theta} \frac{1-e^{-jk\ell_2 U_3'}}{U_3'} \right]$$

$$E_{\phi 2} = -30\, I_m \frac{e^{-jkr}}{r} \cos\alpha' \cos(\phi-\alpha-\beta) \left[\frac{1-e^{-jk\ell_2 U_2}}{U_2} \right. \tag{A-417}$$

$$\left. + \frac{1-e^{-jk\ell_2 U_2'}}{U_2'} R_h e^{-j2kH_1\cos\theta} + (1-R_h) F_m e^{-j2kH_1\cos\theta} \frac{1-e^{-jk\ell_2 U_2'}}{U_2'} \right]$$

$$E_{\phi 4} = 30\, I_m \frac{e^{-jkr}}{r} \cos\alpha' (\phi+\alpha+\gamma) \left[\frac{1-e^{-jk\ell_1 U_4}}{U_4} \right. \tag{A-418}$$

$$+ \frac{1-e^{-jk\ell_1 U_4'}}{U_4'} R_h e^{-j2kH_1\cos\theta}$$

$$\left. + (1-R_h) F_m e^{-j2kH_1\cos\theta} \frac{1-e^{-jk\ell_1 U_4'}}{U_4'} \right]$$

$$E_{\phi 7} = -30\, I_m \frac{e^{-jkr}}{r} e^{-jk\ell_1 U_4} \cos\alpha' \cos(\phi-\alpha-\beta) \left[\frac{1-e^{-jk\ell_2 U_2}}{U_2} \right. \tag{A-419}$$

$$+ \frac{1-e^{-jk\ell_2 U_2'}}{U_2'} R_h e^{-j2kH_2\cos\theta}$$

$$\left. + (1-R_h) F_m e^{-j2kH_2\cos\theta} \frac{1-e^{-jk\ell_2 U_2'}}{U_2'} \right]$$

$$E_{\phi 5} = -30\, I_m \frac{e^{-jkr}}{r} e^{-jk\ell_2 U_2} \cos\alpha' \cos(\phi+\alpha+\gamma) \left[\frac{1-e^{-jk\ell_1 U_4}}{U_4} + \frac{1-e^{-jk\ell_1 U_4'}}{U_4'} R_h\, e^{-j2kH_3\cos\theta} + (1-R_h)\, F_m\, e^{-j2kH_3\cos\theta} \frac{1-e^{-jk\ell_1 U_4'}}{U_4'} \right] \quad \text{(A-420)}$$

$$\cos\psi_1' = -\cos\theta \sin\alpha' + \sin\theta \cos\alpha' \sin(\phi-\alpha-\gamma) \quad \text{(A-421)}$$

$$\cos\psi_2' = -\cos\theta \sin\alpha' + \sin\theta \cos\alpha' \sin(\phi-\alpha-\beta) \quad \text{(A-422)}$$

$$\cos\psi_3' = -\cos\theta \sin\alpha' + \sin\theta \cos\alpha' \sin(\phi+\alpha+\beta) \quad \text{(A-423)}$$

$$\cos\psi_4' = -\cos\theta \sin\alpha' + \sin\theta \cos\alpha' \sin(\phi+\alpha+\gamma) \quad \text{(A-424)}$$

$$U_i = 1-\cos\psi_i,\ i = 1,2,3,4 \quad \text{(A-425)}$$

$$U_i' = 1-\cos\psi_i',\ i=1,\ 2,\ 3,\ 4 \quad \text{(A-426)}$$

The total fields are:

$$E_\theta = \sum_{i=1}^{8} E_{\theta i} \quad \text{(A-427)}$$

$$E_\phi = \sum_{i=1}^{8} E_{\phi 1} \quad \text{(A-428)}$$

The expression for directive gain is:

$$g_d = \frac{r^2 \left(|E_\theta|^2 + |E_\phi|^2\right)}{120\ I_m^{\,2}\ R_{in}} \qquad \text{(A-429)}$$

Since the two rhombics are connected in parallel, the total input current is $2\ I_m\ e^{-jks}$, and R_{in} may be taken as $\frac{600}{2} = 300\Omega$.

The radiation vectors are given by:

$$N_{\theta 1} = \frac{I_m}{jk} \frac{1-e^{-jk\ell_1 U_1}}{U_1} \left[\cos\alpha' \cos\theta \sin(\phi-\alpha-\gamma) - \sin\alpha' \sin\theta\right] \qquad \text{(A-430)}$$

$$N_{\theta 2} = \frac{I_m}{jk} \frac{1-e^{-jk\ell_2 U_2}}{U_2} \left[\cos\alpha' \cos\theta \sin(\phi-\alpha-\beta) - \sin\alpha' \sin\theta\right] \qquad \text{(A-431)}$$

$$N_{\theta 3} = \frac{I_m}{jk} \frac{1-e^{-jk\ell_2 U_3}}{U_3} \left[-\cos\alpha' \cos\theta \sin(\phi+\alpha+\beta) - \sin\alpha' \sin\theta\right] \qquad \text{(A-432)}$$

$$N_{\theta 4} = \frac{I_m}{jk} \frac{1-e^{-jk\ell_1 U_4}}{U_4} \left[-\cos\alpha' \cos\theta \sin(\phi+\alpha+\gamma) - \sin\alpha' \sin\theta\right] \qquad \text{(A-433)}$$

$$N_{\theta 5} = \frac{I_m}{jk} \frac{1-e^{-jk\ell_1 U_4}}{U_4} e^{-jk\ell_2 U_2} \left[\cos\alpha' \cos\theta \sin(\phi+\alpha+\gamma) - \sin\alpha' \sin\theta\right] \qquad \text{(A-434)}$$

$$N_{\theta 6} = \frac{I_m}{jk} \frac{1-e^{-jk\ell_2 U_3}}{U_3} e^{-jk\ell_1 U_1} \left[\cos\alpha' \cos\theta \sin(\phi+\alpha+\gamma) - \sin\alpha' \sin\theta\right] \qquad \text{(A-435)}$$

$$N_{\theta 7} = \frac{I_m}{jk} \frac{1-e^{-jk\ell_2 U_2}}{U_2} e^{-jk\ell_1 U_4} \left[-\cos\alpha' \cos\theta \sin(\phi-\alpha-\beta) + \sin\alpha' \sin\theta\right] \qquad \text{(A-436)}$$

$$N_{\theta 8} = \frac{I_m}{jk} \frac{1-e^{-jk\ell_1 U_1}}{U_1} e^{-jk\ell_2 U_3} [-\cos\alpha' \cos\theta \sin(\phi-\alpha-\gamma) + \sin\alpha' \sin\theta] \quad \text{(A-437)}$$

$$N_{\phi 1} = \frac{-I_m}{jk} \frac{1-e^{-jk\ell_1 U_1}}{U_1} \cos\alpha' \cos(\phi-\alpha-\gamma) \quad \text{(A-438)}$$

$$N_{\phi 2} = \frac{-I_m}{jk} \frac{1-e^{-jk\ell_2 U_2}}{U_2} \cos\alpha' \cos(\phi-\alpha-\beta) \quad \text{(A-439)}$$

$$N_{\phi 3} = \frac{I_m}{jk} \frac{1-e^{-jk\ell_2 U_3}}{U_3} \cos\alpha' \cos(\phi+\alpha+\beta) \quad \text{(A-440)}$$

$$N_{\phi 4} = \frac{I_m}{jk} \frac{1-e^{-jk\ell_1 U_4}}{U_4} \cos\alpha' \cos(\phi+\alpha+\gamma) \quad \text{(A-441)}$$

$$N_{\phi 5} = \frac{-I_m}{jk} \frac{1-e^{-jk\ell_1 U_4}}{U_4} e^{-jk\ell_2 U_2} \cos\alpha' \cos(\phi+\alpha+\gamma) \quad \text{(A-442)}$$

$$N_{\phi 6} = \frac{-I_m}{jk} \frac{1-e^{-jk\ell_2 U_3}}{U_3} e^{-jk\ell_1 U_1} \cos\alpha' \cos(\phi+\alpha+\beta) \quad \text{(A-443)}$$

$$N_{\phi 7} = \frac{I_m}{jk} \frac{1-e^{-jk\ell_2 U_2}}{U_2} e^{-jk\ell_1 U_4} \cos\alpha' \cos(\phi-\alpha-\beta) \quad \text{(A-444)}$$

$$N_{\phi 8} = \frac{I_m}{jk} \frac{1-e^{-jk\ell_1 U_1}}{U_1} e^{-jk\ell_2 U_3} \cos\alpha' \cos(\phi-\alpha-\gamma) \quad \text{(A-445)}$$

The total radiation vectors are:

$$N_\theta = \sum_{i=1}^{8} N_{\theta 1} \tag{A-446}$$

$$N_\phi = \sum_{i=1}^{8} N_{\phi 1} \tag{A-447}$$

The free-space field intensities are given by:

$$E_{\theta f} = \frac{j30ke^{-jkr}}{r} N_\theta \tag{A-448}$$

$$E_{\phi f} = \frac{j30ke^{-jkr}}{r} N_\phi \tag{A-449}$$

The attenuation relative to free space is:

$$A = \sqrt{\frac{|E_\theta|^2 + |E_\phi|^2}{|E_{\theta f}|^2 + |E_{\phi f}|^2}} \tag{A-450}$$

and

$$ADB = 20 \log_{10} \frac{1}{|A|} \tag{A-451}$$

The electric field intensities in the diffraction region are:

$$E_\theta = \frac{j30ke^{-jkd}}{d} (N_\theta) (2 F_r) \tag{A-452}$$

$$E_\phi = \frac{j30ke^{-jkd}}{d} (N_\phi) (2 F_r) \tag{A-453}$$

APPENDIX B

INTEGRALS ENCOUNTERED IN VERTICAL-MONOPOLE CALCULATIONS

In this appendix, the following integral, encountered in vertical-monopole calculations, is evaluated:

$$J_3 = \int_0^{\ell} e^{-jkZ\cos\theta} \sin k(\ell-Z)\; j\sqrt{\pi P_e}\; \exp(-P_e)\; \operatorname{erfc}(j\sqrt{P_e})\; dZ \qquad (B\text{-}1)$$

From King (see Reference 27, pp. 757-758):

$$\frac{1-R_v}{2}\sqrt{\pi P_e}\exp(-P_e)\operatorname{erfc}(j\sqrt{P_e}) = k\sqrt{n^2-\sin^2\theta}\int_0^{\infty} e^{-jkg}\, dZ' \qquad (B\text{-}2)$$

where z' is a variable introduced by Van der Pol (see Reference 17).

and:

$$g = (n^2\cos\theta_r + \sqrt{n^2-\sin^2\theta_r})\,Z' + \frac{n^4 Z'^2}{2r}\sin^2\theta_r \qquad (B\text{-}3)$$

From Equations B-1 and B-2:

$$J_3 = \int_0^{\ell} \sin k(\ell-Z)\, e^{-jkZ\cos\theta}\, \frac{2k\sqrt{n^2-\sin^2\theta}}{j(1-R_v)} \int_0^{\infty} e^{-jkg}\, dZ'\, dZ \qquad (B\text{-}4)$$

where

$$\cos\theta = \frac{h}{r_1} \text{ and } \cos\theta_r = \frac{h+z}{r}$$

$$J_3 = j\frac{2k\sqrt{n^2-\sin^2\theta}}{1-R_v}\int_0^{\ell}\int_0^{\infty} e^{-jk\left(\frac{h}{r}+\frac{n^2Z'}{r}\right)Z}\sin k(\ell-Z) \times \exp\left[-jk\left(Z'\frac{n^2h}{r}+Z'\sqrt{n^2-\sin^2\theta}+\frac{n^4Z^2}{2r}\sin^2\theta\right)\right]dZ'\,dZ \quad \text{(B-5)}$$

Changing the order of integration:

$$J_3 = j\frac{2k\sqrt{n^2-\sin^2\theta}}{1-R_v}\int_0^{\infty}\int_0^{\ell} e^{-jkbZ}\sin k(\ell-Z)\,dZ\; e^{(\alpha^2Z'^2\sin^2\theta+\beta Z')}\,dZ' \quad \text{(B-6)}$$

where

$$b = \frac{h}{r}+\frac{n^2Z'}{r} \quad \text{(B-7)}$$

$$\alpha^2 = -jk\frac{n^4}{2r} \quad \text{(B-8)}$$

$$\beta = -jk\left(\frac{n^2h}{2}+\sqrt{n^2-\sin^2\theta}\right) \quad \text{(B-9)}$$

$$\int_0^{\ell} e^{-jkbZ} \sin k(\ell-Z)\, dZ = \frac{1}{k^2(1-b^2)} \left[e^{-jkb\ell} + jb \sin k\ell - \cos k\ell \right] \qquad \text{(B-10)}$$

Neglecting b^2 since $b^2 << 1$ gives:

$$\int_0^{\ell} e^{-jkbZ} \sin k(\ell-Z)\, dZ = \frac{1}{k} \left[e^{-jkb\ell} + jb \sin k\ell - \cos k\ell \right] \qquad \text{(B-11)}$$

Substituting Equation B-11 into B-6 gives:

$$J_3 = j\frac{2k\sqrt{n^2-\sin^2\theta}}{1-R_v} \int_0^{\infty} \frac{1}{k} \left[e^{-jkb\ell} + jb \sin k\ell - \cos k\ell \right] \exp\left(\alpha^2 Z'^2 \sin^2\theta + \beta Z'\right) dZ' \qquad \text{(B-12)}$$

$$J_3 = j\frac{2\sqrt{n^2-\sin^2\theta}}{1-R_v} e^{-jk\ell\cos\theta} J_{31} + (j\sin k\ell \cos\theta - \cos k\ell) J_{32} + j\frac{n^2}{r} \sin k\ell\, J_{33} \qquad \text{(B-13)}$$

where

$$J_{31} = \int_0^{\infty} \exp\left[\alpha^2 Z'^2 \sin^2\theta + \beta_1 Z'\right] dZ' = j\frac{\sqrt{\pi}}{2\alpha\sin\theta} \exp(-w_1)\, \operatorname{erfc}(j\sqrt{w_1}) \qquad \text{(B-14)}$$

$$J_{32} = \int_0^\infty \exp\left[\alpha^2 z'^2 \sin^2\theta + \beta z'\right] dz' = -j\frac{\sqrt{\pi}}{2\alpha\sin\theta} e^{-w} \operatorname{erfc}(j\sqrt{w}) \quad \text{(B-15)}$$

$$J_{33} = \int_0^\infty z' \exp\left[\alpha^2 z'^2 \sin^2\theta + \beta z'\right] dz' = \frac{-1}{2\alpha^2 \sin^2\theta}\left[1 - j\sqrt{\pi w}\, e^{-w} \operatorname{erfc}(j\sqrt{w})\right] \quad \text{(B-16)}$$

and

$$\beta_1 = \beta - jk\ell\frac{n^2}{r} = -jk\left[\frac{n^2(h+\ell)}{r} + \sqrt{n^2 - \sin^2\theta}\right] \quad \text{(B-17)}$$

$$W_1 = \frac{\beta_1^2}{4\alpha^2 \sin^2\theta} = -\frac{jkr}{2\sin^2\theta}\left[\frac{h+\ell}{r} + \frac{\sqrt{n^2 - \sin^2\theta}}{n^2}\right]^2 \quad \text{(B-18)}$$

$$W = \frac{\beta^2}{4\alpha^2 \sin^2\theta} = -\frac{jkr}{2\sin^2\theta}\left[\frac{h}{r} + \frac{\sqrt{n^2 - \sin^2\theta}}{n^2}\right]^2 \quad \text{(B-19)}$$

Substituting Equations B-14, B-15, and B-16 into B-13 yields:

$$J_3 = \frac{\sqrt{n^2-\sin^2\theta}}{1-R_v}\left[\frac{e^{-jk\ell\cos\theta}}{n^2\sin\theta}\sqrt{\frac{j2\pi r}{k}}\, e^{-w_1}\,\mathrm{erfc}\,(j\sqrt{w_1}) + (j\sin k\ell\cos\theta - \cos k\ell)\right.$$

$$\left. x\,\frac{1}{n^2\sin\theta}\sqrt{\frac{j2\pi r}{k}}\, e^{-w}\,\mathrm{erfc}(j\sqrt{w}) + \frac{n^2\sin k\ell}{r}\frac{j2r}{n^4 k\sin^2\theta}\{1-j\sqrt{\pi w}\, e^{-w}\mathrm{erfc}(j\sqrt{w})\}\right]$$

$$= \frac{\sqrt{n^2-\sin^2\theta}}{n^2(1-R_v)}\left[\frac{e^{-jk\ell\cos\theta}}{\sin\theta}\sqrt{\frac{j2\pi r}{k}}\, e^{-w_1}\,\mathrm{erfc}(j\sqrt{w_1}) + (j\sin k\ell\cos\theta - \cos k\ell)\frac{1}{\sin\theta}\right.$$

$$\left. x\sqrt{\frac{j2\pi r}{k}}\, e^{-w}\,\mathrm{erfc}(j\sqrt{w}) + \frac{j2\sin k\ell}{k\sin^2\theta}\{1-j\sqrt{\pi w}\, e^{-w}\,\mathrm{erfc}\,(j\sqrt{w})\}\right] \quad \text{(B-20)}$$

Since $W_1 = W = P_e$:

$$J_3 = \frac{\sqrt{n^2-\sin^2\theta}}{n^2(1-R_v)}\left\{\sqrt{\frac{j2\pi r}{k}}\, e^{-P_e}\,\mathrm{erfc}(j\sqrt{P_e})\right. \quad \text{(B-21)}$$

$$\left.\left[\frac{\{\cos(k\ell\cos\theta) - \cos k\ell\} - j\,\{\sin(k\ell\cos\theta) - \sin(k\ell\cos\theta)\}}{\sin\theta}\right] + \frac{j2F_e\sin k\ell}{k\sin^2\theta}\right\}$$

APPENDIX C

INTEGRALS ENCOUNTERED IN VERTICAL-DIPOLE CALCULATIONS

In this appendix, the following two integrals encountered in elevated-vertical-dipole calculations are evaluated:

$$J_3 = \int_{Z_o-\ell}^{Z_o} e^{-jkZ\cos\theta} \sin k(\ell-Z_o+Z) \left[1-j\sqrt{\pi P_e}\, e^{-P_e}\, \mathrm{erfc}\,(j\sqrt{P_e})\right] dZ \quad (C-1)$$

$$J_e' = \int_{Z_o}^{Z_o+\ell} e^{-jkZ\cos\theta} \sin k(\ell+Z_o-Z) \left[1-j\sqrt{\pi P_e}\, e^{-P_e}\, \mathrm{erfc}\,(j\sqrt{P_e})\right] dZ \quad (C-2)$$

The first parts of the integrals are straightforward. The second part of J_3 is:

$$J_{31} = \int_{Z_o-\ell}^{Z_o} e^{-jkZ\cos\theta} \sin k(\ell-Z_o+Z)\; j\sqrt{\pi P_e}\, e^{-P_e}\, \mathrm{erfc}\,(j\sqrt{P_e})\, dZ \quad (C-3)$$

Following the same techniques as those used in APPENDIX B:

$$J_{31} = j\frac{2k\sqrt{n^2-\sin^2\theta}}{1-R_v} \int_o^\infty \int_{Z_o-\ell}^{Z_o} e^{-jkbZ} \sin k(\ell-Z_o+Z)\, dZ \exp\{\alpha^2 Z'^2 \sin^2\theta + \beta Z'\}\, dZ' \quad (C-4)$$

where b, α^2, and β are given by Equations B-7, B-8, and B-9, respectively.

$$\int_{Z_o-\ell}^{Z_o} e^{-jkbZ} \sin k(\ell - Z_o + Z)\, dZ = \frac{e^{-jkb(Z_o-\ell)} - e^{-jkbZ_o}(\cos k\ell + jb \sin k\ell)}{k(1-b^2)} \quad (C\text{-}5)$$

$$= \frac{1}{k}\left[e^{-jkb(Z_o-\ell)} - e^{-jkbZ_o}(\cos k\ell + jb \sin k\ell)\right]$$

Substituting Equation C-5 into C-4 yields:

$$J_{31} = j\frac{2\sqrt{n^2-\sin^2\theta}}{1-R_v}\int_o^\infty \{e^{-jkb(Z_o-\ell)} - e^{-jkbZ_o}(\cos k\ell + jb \sin k\ell)\} \quad (C\text{-}6)$$

$$x \quad \exp\{\alpha^2 Z'^2 \sin^2\theta + \beta Z'\}\, dZ'$$

$$J_{31} = j\frac{2\sqrt{n^2-\sin^2\theta}}{1-R_v} e^{-jkZ_o\cos\theta} e^{jk\ell\cos\theta} J_{311} \quad (C\text{-}7)$$

$$-(\cos k\ell + j\cos\theta \sin k\ell)\, J_{312} - j\frac{n^2}{r}\sin k\ell\, J_{313}$$

where

$$J_{311} = \int_o^\infty \exp(\alpha^2 Z'^2 \sin^2\theta + \beta_2 Z')dZ' = -j\frac{\pi}{2\alpha\sin\theta} e^{-W_2^2} \operatorname{erfc}(j\, W_2) \quad (C\text{-}8)$$

$$J_{312} = \int_o^\infty \exp\left(\alpha^2 z'^2 \sin^2\theta + \beta_3 z'\right) dz' = -j\frac{\sqrt{\pi}}{2\alpha\sin\theta} e^{-W_3} \operatorname{erfc}\left(j\sqrt{W_3}\right) \quad \text{(C-9)}$$

$$J_{313} = \int_o^\infty z' \exp\left(\alpha^2 z'^2 \sin^2\theta + \beta_3 z'\right) dz'$$

$$= \frac{-1}{2\alpha^2 \sin^2\theta}\left[1 - j\sqrt{\pi w_3}\, e^{-w_3} \operatorname{erfc}\left(j\sqrt{w_3}\right)\right] \quad \text{(C-10)}$$

$$\beta_2 = \beta - jk\frac{n^2}{r}(z_o - \ell) = -jk\left[\frac{n^2(h+z_o-\ell)}{r} + \sqrt{n^2-\sin^2\theta}\right] \quad \text{(C-11)}$$

$$\beta_3 = \beta - jk\frac{n^2}{r} z_o = -jk\left[\frac{n^2(h+z_o)}{r} + \sqrt{n^2-\sin^2\theta}\right] \quad \text{(C-12)}$$

$$W_2 = \frac{\beta_2^2}{4\alpha^2\sin^2\theta} = -j\frac{kr}{2\sin^2\theta}\left[\frac{h+z_o-\ell}{r} + \frac{\sqrt{n^2-\sin^2\theta}}{n^2}\right]^2 \quad \text{(C-13)}$$

$$W_3 = \frac{\beta_3^2}{4\alpha^2\sin^2\theta} = -j\frac{kr}{2\sin^2\theta}\left[\frac{h+z_o}{r} + \frac{\sqrt{n^2-\sin^2\theta}}{n^2}\right]^2 \quad \text{(C-14)}$$

The second part of Equation C-2 is:

$$J_{31}' = \int_{Z_o}^{Z_o+\ell} e^{-jkZ\cos\theta} \sin k(\ell+Z_o-Z)\; j\sqrt{\pi P_e}\; e^{-P_e}\, \mathrm{erfc}\,(j\sqrt{P_e})\, dZ \quad \text{(C-15)}$$

Following the same procedure as that used to evaluate Equation C-3:

$$J_{31}' = \frac{2\sqrt{n^2-\sin^2\theta}}{1-R_v} e^{-jkZ_o\cos\theta}\, e^{-jk\ell\cos\theta}\, J_{311}' - (\cos k\ell - j\cos\theta \sin k\ell)\, J_{312} + j\frac{n^2}{r}\sin k\ell\, J_{313} \quad \text{(C-16)}$$

where

$$J_{311}' = \int_0^{\infty} \exp(\alpha^2 Z'^2 \sin^2\theta + \beta_4 Z') = -j\frac{\sqrt{\pi}}{2\alpha\sin\theta}\, e^{-W_4}\, \mathrm{erfc}\,(j\sqrt{W_4}) \quad \text{(C-17)}$$

$$\beta_4 = \beta - jk\frac{n^2}{r}(Z_o+\ell) = -jk\left[\frac{n^2(h+Z_o+\ell)}{r} + \sqrt{n^2-\sin^2\theta}\right] \quad \text{(C-18)}$$

$$W_4 = \frac{\beta_4^2}{4\alpha^2\sin^2\theta} = -j\frac{kr}{2\sin^2\theta}\left[\frac{h+Z_o+\ell}{r} + \sqrt{\frac{n^2-\sin^2\theta}{n^2}}\right]^2 \quad \text{(C-19)}$$

$$J_{31} + J_{31}' = j \frac{2\sqrt{n^2-\sin^2\theta}}{1-R_v} e^{-jkZ_o\cos\theta} \times \left[e^{-jkZ_o\cos\theta} J_{311} + e^{-jk\ell\cos\theta} J_{311}' - 2 J_{312} \cos k\ell \right] \quad (C\text{-}20)$$

Since:

$$W_2 = W_3 = W_4 = P_3$$

and

$$J_{311} = J_{311}' = J_{312}$$

$$J_{31} + J_{31}' = j \frac{2\sqrt{n^2-\sin^2\theta}}{1-R_v} e^{-jkZ_o\cos\theta} J_{311} \left[2\cos(k\ell\cos\theta) - 2\cos k\ell \right]$$

$$= \frac{2\sqrt{n^2-\sin^2\theta}}{1-R_v} e^{-jkZ_o\cos\theta} \frac{\sqrt{\pi}}{\alpha\sin\theta} e^{-P_e} \operatorname{erfc}(j\sqrt{P_e}) \{\cos(k\ell\cos\theta) - \cos k\ell\} \quad (C\text{-}21)$$

$$J_{31} + J_{31}' = \frac{2\sqrt{n^2-\sin^2\theta}}{n^2(1-R_v)} e^{-jkZ_o\cos\theta} \sqrt{\frac{j2\pi r}{k}} e^{-P_e} \operatorname{erfc}(j\sqrt{P_e}) \frac{\cos(k\ell\cos\theta)-\cos k\ell}{\sin\theta} \quad (C\text{-}22)$$

$$J_3+J_3' = \frac{2\,e^{-jkZ_o\cos\theta}}{k\sin^2\theta}\{\cos(k\ell\cos\theta)-\cos k\ell\} - \frac{2e^{-jkZ_o\cos\theta}}{1-R_v}\frac{\sqrt{n^2-\sin^2\theta}}{n^2}\sqrt{\frac{j2\pi r}{k}} \times e^{-P_e}\,\mathrm{erfc}\,(j\sqrt{P_e})\;\frac{\cos(k\ell\cos\theta)-\cos k\ell}{\sin\theta} \quad \text{(C-23)}$$

Equation C-23 can be simplified further to yield:

$$J_3+J_3' = \frac{2e^{-jkZ_o\cos\theta}}{k\sin^2\theta}\{\cos(k\ell\cos\theta)-\cos k\ell\}-\cos k\ell\} \times \left[1-\frac{\sin\theta}{1-R_v}\frac{\sqrt{n^2-\sin^2\theta}}{n^2}\sqrt{j2\pi kr}\;e^{-P_e}\,\mathrm{erfc}\,(j\sqrt{P_e})\right] \quad \text{(C-24)}$$

$$= \frac{2e^{-jkZ_o\cos\theta}}{k}\;\frac{\cos(k\ell\cos\theta)-\cos k\ell}{\sin^2\theta} \times \left[1-j\sqrt{\pi P_e}\sin^2\theta\; e^{-P_e}\,\mathrm{erfc}\,(j\sqrt{P_e})\right]$$

APPENDIX D

FORMULAS FOR CALCULATING FIELD STRENGTH OVER SPHERICAL EARTH WITHIN THE RADIO HORIZON

The formulas presented in APPENDIX A are for calculating field strength and gain over planar earth and over spherical earth in the diffraction region beyond the radio horizon. The formulas presented in this appendix are for calculating field strength over spherical earth within the radio horizon.

Within the radio horizon, the effects of spherical earth are taken into account by use of the divergence factor. Only the direct and ground-reflected contributions to the fields are considered in this formulation, because the surface wave is negligible when the feed points of the antennas are at least several wavelengths above the surface of the earth.

The quantities in the following equations are described in Section 5 and in APPENDIX A. The appropriate formulas for calculating directive gain from the following equations are given in TABLE 2 of Section 5 which also provides expressions for the radiation efficiency.

HORIZONTAL DIPOLE

$$E_\theta = -j60\, I_m \frac{\cos(k\ell\cos\psi)-\cos k\ell}{\sin^2\psi} \cos\phi\, \cos\theta \left(\frac{e^{-jkR_d}}{R_d} - R_v\, \alpha_{div} \frac{e^{-jkR_r}}{R_r}\right) \quad (D\text{-}1)$$

$$E_\phi = j60 I_m \frac{\cos(k\ell\, \cos\psi) - \cos k\ell}{\sin^2\psi} \sin\phi \left(\frac{e^{-jkR_d}}{R_d} + R_h\, \alpha_{div} \frac{e^{-jkR_r}}{R_r}\right) \quad (D\text{-}2)$$

VERTICAL MONOPOLE

$$E_\theta = j30\, I_m \left[\frac{e^{-jkR_d}}{R_d} \frac{A_2 + jB_2}{\sin\theta} + R_v\, \alpha_{div} \frac{e^{-jkR_r}}{R_r} \frac{A_2 - jB_2}{\sin\theta} \right] \quad \text{(D-3)}$$

$$E_\phi = 0 \quad \text{(D-4)}$$

VERTICAL MONOPOLE WITH RADIAL-WIRE GROUND SCREEN

$$E_\theta = j30\, I_m \left[\frac{e^{-jkR_d}}{R_d} \frac{A_2 + jB_2}{\sin\theta} + R_v\, \alpha_{div} \frac{e^{-jkR_r}}{R_r} \frac{A_2 - jB_2}{\sin\theta} \right] x\ (GSCF) \quad \text{(D-5)}$$

$$GSCF = - \frac{\eta \sin\theta \int_0^{ka} \left[e^{-j\sqrt{x^2 + k^2 \ell^2}} - e^{-jx} \cos k\ell \right] J_1(x\sin\theta)\, dx}{120\pi \sin k\ell \left[\cos(k\ell \cos\theta) - \cos k\ell \right]} \quad \text{(D-6)}$$

$$E_\phi = 0 \quad \text{(D-7)}$$

ELEVATED VERTICAL DIPOLE

$$E_\theta = j60\, I_m \frac{\cos(k\ell\cos\theta) - \cos k\ell}{\sin\theta}\left[\frac{e^{-jkR_d}}{R_d} + R_v\,\alpha_{div}\,\frac{e^{-jkR_r}}{R_r}\right] \qquad \text{(D-8)}$$

$$E_\phi = 0 \qquad \text{(D-9)}$$

INVERTED-L

$$E_{\theta,v} = j30\, I_m\left[\frac{e^{-jkR_d}}{R_d}\,\frac{A_4+jB_4}{\sin\theta} + R_v\,\alpha_{div}\,\frac{e^{-jkR_r}}{R_r}\,\frac{A_4 - jB_4}{\sin\theta}\right] \qquad \text{(D-10)}$$

$$E_{\phi,v} = 0 \qquad \text{(D-11)}$$

$$E_{\theta,h} = -j30\, I_m \frac{A_5+jB_5}{\sin^2\psi_h'}\cos\theta\,\sin\phi\left[\frac{e^{-jkR_d}}{R_d} - R_v\,\alpha_{div}\,\frac{e^{-jkR_r}}{R_r}\right] \qquad \text{(D-12)}$$

$$E_{\phi,h} = j30\, I_m \frac{A_5+jB_5}{\sin^2\psi_h'}\cos\phi\left[\frac{e^{-jkR_d}}{R_d} + R_h\,\alpha_{div}\,\frac{e^{-jkR_r}}{R_r}\right] \qquad \text{(D-13)}$$

ARBITRARILY TILTED DIPOLE

$$E_\theta = -j60\, I_m \frac{e^{-jkR_d}}{R_d} \frac{\cos(k\ell\cos\psi) - \cos k\ell}{\sin^2\psi} (\cos\alpha' \sin\phi \cos\theta - \sin\alpha' \sin\theta) \quad \text{(D-14)}$$
$$-R_v\, \alpha_{div} \frac{e^{-jkR_r}}{R_r} \frac{\cos(k\ell\cos\psi) - \cos k\ell}{\sin^2\psi} (\cos\alpha' \sin\phi \cos\theta + \sin\alpha' \sin\theta)$$

$$E_\phi = j60\, I_m \cos\alpha' \cos\phi \left[\frac{e^{-jkR_d}}{R_d} \frac{\cos(k\ell\cos\psi) - \cos k\ell}{} \right. \quad \text{(D-15)}$$
$$\left. + R_h\, \alpha_{div} \frac{e^{-jkR_r}}{R_r} \frac{\cos(k\ell\cos\psi') - \cos k\ell}{\sin^2\psi'} \right]$$

SLOPING LONG-WIRE

$$E_\theta = -j30\, I_m \frac{e^{-jkR_d}}{R_d} \frac{A_6 + jB_6}{\sin^2\psi} (\cos\alpha' \sin\phi \cos\theta - \sin\alpha' \sin\theta) \quad \text{(D-16)}$$
$$-R_v\, \alpha_{div} \frac{e^{-jkR_r}}{R_r} \frac{A_\eta + jB_\eta}{\sin^2\psi'} (\cos\alpha' \sin\phi \cos\theta + \sin\alpha' \sin\theta)$$

$$E_\phi = j30\, I_m \cos\alpha' \cos\phi \left[\frac{e^{-jkR_d}}{R_d} \frac{A_6+jB_6}{\sin^2\psi} + R_h\, \alpha_{div} \frac{e^{-jkR_r}}{R_r} \frac{A_\eta+jB_\eta}{\sin^2\psi'} \right] \quad \text{(D-17)}$$

TERMINATED SLOPING-V

$$E_{\theta 1} = 30\, I_m \left\{ \cos\alpha' \cos\theta \cos(\phi-\beta') \left[\frac{e^{-jkR_d}}{R_d} \frac{1-e^{-jk\ell U_1}}{U_1} - R_v\, \alpha_{div} \frac{e^{-jkR_r}}{R_r} \right.\right.$$
$$\left. \times \frac{1-e^{-jk\ell U_3}}{U_3} \right] - \sin\alpha' \sin\theta \left[\frac{e^{-jkR_d}}{R_d} \frac{1-e^{-jk\ell U_1}}{U_1} \right. \qquad \text{(D-18)}$$
$$\left.\left. + R_v\, \alpha_{div} \frac{e^{-jkR_r}}{R_r} \frac{1-e^{-jk\ell U_3}}{U_3} \right] \right\}$$

$$E_{\theta 2} = -30\, I_m \left\{ \cos\alpha' \cos\theta \cos(\phi+\beta') \left[\frac{e^{-jkR_d}}{R_d} \frac{1-e^{-jk\ell U_2}}{U_2} \right.\right.$$
$$\left. - R_v\, \alpha_{div} \frac{e^{-jkR_r}}{R_r} \frac{1-e^{-jk\ell U_4}}{U_4} \right] - \sin\alpha' \sin\theta \qquad \text{(D-19)}$$
$$\left.\left. \times \left[\frac{e^{-jkR_d}}{R_d} \frac{1-e^{-jk\ell U_2}}{U_2} + R_v\, \alpha_{div} \frac{e^{-jkR_r}}{R_r} \frac{1-e^{-jk\ell U_4}}{U_4} \right] \right\}$$

$$E_{\phi 1} = 30\, I_m \cos\alpha' \sin(\phi-\beta') \left[\frac{e^{-jkR_d}}{R_d} \frac{1-e^{-jk\ell U_1}}{U_1} \right.$$
$$\left. + R_h\, \alpha_{div} \frac{e^{-jkR_r}}{R_r} \frac{1-e^{-jk\ell U_3}}{U_3} \right] \qquad \text{(D-20)}$$

$$E_{\phi 2} = -30\, I_m \cos\alpha' \sin(\phi+\beta') \left[\frac{e^{-jkR_d}}{R_d} \frac{1-e^{-jk\ell U_2}}{U_2} + R_h\, \alpha_{div} \frac{e^{-jkR_r}}{R_r} \frac{1-e^{-jk\ell U_4}}{U_4} \right] \quad \text{(D-21)}$$

$$E_\theta = E_{\theta 1} + E_{\theta 2} \quad \text{(D-22)}$$

$$E_\phi = E_{\phi 1} + E_{\phi 2} \quad \text{(D-23)}$$

TERMINATED SLOPING RHOMBIC

The total field components are given by:

$$E_\theta = E_{\theta 1} + E_{\theta 2} + E_{\theta 3} + E_{\theta 4} \quad \text{(D-24)}$$

and

$$E_\phi = E_{\phi 1} + E_{\phi 2} + E_{\phi 3} + E_{\phi 4} \quad \text{(D-25)}$$

where $E_{\theta 1}$, $E_{\theta 2}$, $E_{\phi 1}$, and $E_{\phi 2}$ are given by Equations D-18, D-19, D-20, and D-21, respectively, and:

$$E_{\theta 3} = 30\, I_m\, e^{-jk\ell U_2} \left\{ -\cos\alpha' \cos\theta \cos(\phi-\beta') \left[\frac{e^{-jkR_d}}{R_d} \frac{1-e^{-jk\ell U_1}}{U_1} - R_v\, \alpha_{div}\, e^{-j2kH_1\cos\theta} \frac{e^{-jkR_r}}{R_r} \frac{1-e^{-jk\ell U_3}}{U_3} \right] + \sin\alpha' \sin\theta \left[\frac{e^{-jkR_d}}{R_d} \frac{1-e^{-jk\ell U_1}}{U_1} + R_v\, \alpha_{div}\, e^{-j2kH_1\cos\theta} \frac{e^{-jkR_r}}{R_r} \frac{1-e^{-jk\ell U_3}}{U_3} \right] \right\} \quad \text{(D-26)}$$

$$E_{\theta 4} = 30\, I_m\, e^{-jkU_1} \left\{ \cos\alpha' \cos\theta \cos(\phi+\beta') \left[\frac{e^{-jkR_d}}{R_d} \frac{1-e^{-jk\ell U_2}}{U_2} - R_v\, \alpha_{div}\, e^{-j2kH_1\cos\theta} \frac{e^{-jkR_r}}{R_r} \frac{1-e^{-jk\ell U_4}}{U_4} \right] - \sin\alpha' \sin\theta \left[\frac{e^{-jkR_d}}{R_d} \frac{1-e^{-jk\ell U_2}}{U_2} + R_v\, \alpha_{div}\, e^{-j2kH_1\cos\theta} \frac{e^{-jkR_r}}{R_r} \frac{1-e^{-jk\ell U_4}}{U_4} \right] \right\} \quad \text{(D-27)}$$

$$E_{\phi 3} = -30\, I_m\, e^{-jk\ell U_2} \cos\alpha' \sin(\phi-\beta') \left[\frac{e^{-jkR_d}}{R_d} \frac{1-e^{-jk\ell U_1}}{U_1} + R_h\, \alpha_{div}\, e^{-j2kH_1\cos\theta} \frac{e^{-jkR_r}}{R_r} \frac{1-e^{-jk\ell U_3}}{U_3} \right] \quad \text{(D-28)}$$

$$E_{\phi 4} = 30\, I_m e^{-jk\ell U_1} \cos\alpha' \sin(\phi+\beta') \left[\frac{e^{-jkR_d}}{R_d} \frac{1-e^{-jk\ell U_2}}{U_2} + R_h\, \alpha_{div}\, e^{-j2kH_1\cos\theta} \frac{e^{-jkR_r}}{R_r} \frac{1-e^{-jk\ell U_4}}{U_4} \right] \quad (D\text{-}29)$$

TERMINATED HORIZONTAL RHOMBIC

$$E_{\theta 1} = 30\, I_m \frac{1-e^{-jk\ell U_1}}{U_1} \cos\theta \cos(\phi-\gamma) \left[\frac{e^{-jkR_d}}{R_d} - R_v\, \alpha_{div} \frac{e^{-jkR_r}}{R_r} \right] \quad (D\text{-}30)$$

$$E_{\theta 2} = -30\, I_m \frac{1-e^{-jk\ell U_2}}{U_2} \cos\theta \cos(\phi+\gamma) \left[\frac{e^{-jkR_d}}{R_d} - R_v\, \alpha_{div} \frac{e^{-jkR_r}}{R_r} \right] \quad (D\text{-}31)$$

$$E_{\theta 3} = -30\, I_m \frac{1-e^{-jk\ell U_1}}{U_1} e^{-jk\ell U_2} \cos\theta \cos(\phi-\gamma) \left[\frac{e^{-jkR_d}}{R_d} - R_v\, \alpha_{div} \frac{e^{-jkR_r}}{R_r} \right] \quad (D\text{-}32)$$

$$E_{\theta 4} = 30\, I_m \frac{1-e^{-jk\ell U_2}}{U_2} e^{-jk\ell U_1} \cos\theta \cos(\phi+\gamma) \left[\frac{e^{-jkR_d}}{R_d} - R_v\, \alpha_{div} \frac{e^{-jkR_r}}{R_r} \right] \quad (D\text{-}33)$$

$$E_{\phi 1} = 30\, I_m \frac{1-e^{-jk\ell U_1}}{U_1} \sin(\phi-\gamma) \left[\frac{e^{-jkR_d}}{R_d} + R_h\, \alpha_{div} \frac{e^{-jkR_r}}{R_r}\right] \quad \text{(D-34)}$$

$$E_{\phi 2} = -30\, I_m \frac{1-e^{-jk\ell U_2}}{U_2} \sin(\phi+\gamma) \left[\frac{e^{-jkR_d}}{R_d} + R_h\, \alpha_{div} \frac{e^{-jkR_r}}{R_r}\right] \quad \text{(D-35)}$$

$$E_{\phi 3} = -30\, I_m \frac{1-e^{-jk\ell U_1}}{U_1} e^{-jk\ell U_2} \sin(\phi-\gamma) \left[\frac{e^{-jkR_d}}{R_d} + R_h\, \alpha_{div} \frac{e^{-jkR_r}}{R_r}\right] \quad \text{(D-36)}$$

$$E_{\phi 4} = 30\, I_m \frac{1-e^{-jk\ell U_2}}{U_2} e^{-jk\ell U_1} \sin(\phi+\gamma) \left[\frac{e^{-jkR_d}}{R_d} + R_h\, \alpha_{div} \frac{e^{-jkR_r}}{R_r}\right] \quad \text{(D-37)}$$

$$E_\theta = \sum_{i=1}^{4} E_{\theta i} \quad \text{(D-38)}$$

$$E_\phi = \sum_{i=1}^{4} E_{\phi 1} \quad \text{(D-39)}$$

SIDE-LOADED VERTICAL HALF-RHOMBIC

$$E_\theta = 30\, I_m \left[-\cos\alpha' \cos\theta \cos\phi \left\{ (F_1 + F_2 e^{-jk\ell U_1}) \frac{e^{-jkR_d}}{R_d} - R_v \alpha_{div} (F_2 + F_1 e^{-jk\ell U_2}) \frac{e^{-jkR_r}}{R_r} \right\} \right. \quad \text{(D-40)}$$

$$\left. + \sin\alpha' \sin\theta \left\{ F_1 - F_2 e^{-jk\ell U_1} \frac{e^{-jkR_d}}{R_d} + R_v \alpha_{div} \left(F_2 - F_1 e^{-jk\ell U_2} \right) \frac{e^{-jkR_r}}{R_r} \right\} \right]$$

$$E_\phi = -30\, I_m \cos\alpha' \sin\phi \left[(F_1 + F_2 e^{-jk\ell U_1}) \frac{e^{-jkR_d}}{R_d} + R_h \alpha_{div} (F_2 + F_1 e^{-jk\ell U_2}) \frac{e^{-jkR_r}}{R_r} \right] \quad \text{(D-41)}$$

HORIZONTAL YAGI-UDA ARRAY

$$E_\theta = j60 \frac{\cos\theta \cos\phi}{2} \left[\frac{e^{-jkR_d}}{R_d} \right] \quad \text{(D-42)}$$

$$\sin\psi$$

$$- R_v \alpha_{div} \frac{e^{-jkR_r}}{R_r} \left[\sum_{i=1}^{N} I_{mi} e^{jkY_i \sin\theta \sin\phi} \right] \times \left\{ \cos(k\ell_i \cos\psi) - \cos k\ell_i \right\}$$

$$E_\phi = j60 \frac{\sin\phi}{\sin^2\psi} \left[\frac{e^{-jkR_d}}{R_d} + R_h \alpha_{div} \frac{e^{-jkR_r}}{R_r} \right] \left[\sum_{i=1}^{N} I_{mi} e^{jkY_i \sin\theta \sin\phi} \right] \times \{ \cos(k\ell_i \cos\psi) - \cos k\ell_i \} \quad \text{(D-43)}$$

HORIZONTALLY POLARIZED LOG-PERIODIC DIPOLE ARRAY

$$E_\theta = -j60 \frac{\cos\theta \cos\phi}{\sin^2\psi} \left[\sum_{i=1}^{N} I_{mi} e^{jkY_i \csc\theta'' \cos\psi''} \{\cos(k\ell_i \cos\psi) - \cos k\ell_i\} \right] \times \left[\frac{e^{-jkR_d}}{R_d} - \frac{e^{-jkR_r}}{R_r} R_v \alpha_{div} e^{-j2k(H_i - H_1)\cos\theta} \right] \quad \text{(D-44)}$$

$$E_\phi = j60 \frac{\sin\phi}{\sin^2\psi} \sum_{i=1}^{N} \left[I_{mi} e^{jkY_i \csc\theta'' \cos\psi''} \{\cos(k\ell_i \cos\psi) - \cos k\ell_i\} \right] \times \left\{ \frac{e^{-jkR_d}}{R_d} + \frac{e^{-jkR_r}}{R_r} R_h \alpha_{div} e^{-j2k(H_i - H_1)\cos\theta} \right\} \quad \text{(D-45)}$$

VERTICALLY POLARIZED LOG-PERIODIC DIPOLE ARRAY

$$E_\theta = \frac{j60}{\sin\theta}\left[\sum_{i=1}^{N} \frac{I_{bi}}{\sin k\ell_i} e^{jk(H_i - H_1)\cos\theta} \{\cos(k\ell_i \cos\theta) - \cos k\ell_i\}\right.$$

(D-46)

$$\times e^{jkY_i \sec(\alpha_2 + \alpha_3)\cos\psi'} \left\{\frac{e^{-jkR_d}}{R_d}\right.$$

$$\left.\left. + \frac{e^{-jkR_r}}{R_r} R_v \alpha_{div} e^{-j2k(H_i - H_1)\cos\theta}\right\}\right]$$

$$E_\phi = 0 \qquad \text{(D-47)}$$

CURTAIN ARRAY

$$E_\theta = -j60\, I_m \frac{\cos(k\ell\cos\psi) - \cos k\ell}{\sin^2\psi} \sin\phi \sum_{i=1}^{M} C_i e^{jkZ_i(\cos\theta - \cos\theta_o)}$$

(D-48)

$$\times \cos\theta \left[\frac{e^{-jkR_d}}{R_d} - \frac{e^{-jkR_r}}{R_r} R_v \alpha_{div} e^{-j2kZ_i\cos\theta}\right] S_x S_y$$

$$E_\phi = j60\, I_m \frac{\cos(k\ell\cos\psi)-\cos k\ell}{\sin^2\psi}\cos\phi \sum_{i=1}^{M} C_i\, e^{jkZ_i(\cos\theta-\cos\theta_o)} \quad \text{(D-49)}$$

$$\times \left[\frac{e^{-jkR_d}}{R_d} + \frac{e^{-jkR_r}}{R_r} \times R_h\, \alpha_{div}\, e^{-j2kZ_i\cos\theta}\right] S_x S_y$$

SLOPING DOUBLE RHOMBOID

$$E_{\theta 1} = 30\, I_m \left[\cos\alpha' \cos\theta \sin(\phi-\alpha-\gamma)\left\{\frac{1-e^{-jk\ell_1 U_1}}{U_1}\frac{e^{-jkR_d}}{R_d} - R_v\, \alpha_{div}\frac{1-e^{-jk\ell_1 U_1'}}{U_1'}\frac{e^{-jkR_r}}{R_r}\right\}\right. \quad \text{(D-50)}$$

$$\left. - \sin\alpha' \sin\theta \left\{\frac{1-e^{-jk\ell_1 U_1}}{U_1}\frac{e^{-jkR_d}}{R_d} + R_v\, \alpha_{div}\frac{1-e^{-jk\ell_1 U_1'}}{U_1'}\frac{e^{-jkR_r}}{R_r}\right\}\right]$$

$$E_{\theta 3} = -30\, I_m \left[\cos\alpha' \cos\theta \sin(\phi+\alpha+\beta) \left\{\frac{1-e^{-jk\ell_2 U_3}}{U_3} \frac{e^{-jkR_d}}{R_d} - R_v\, \alpha_{div} \frac{1-e^{-jk\ell_2 U_3'}}{U_3'} \frac{e^{-jkR_r}}{R_r}\right\}\right. \quad \text{(D-51)}$$

$$\left. + \sin\alpha' \sin\theta \left\{\frac{1-e^{-jk\ell_2 U_3}}{U_3} \frac{e^{-jkR_d}}{R_d} + R_v\, \alpha_{div} \frac{1-e^{-jk\ell_2 U_3'}}{U_3'} \frac{e^{-jkR_r}}{R_r}\right\}\right]$$

$$E_{\theta 8} = 30\, I_m\, e^{-jk\ell_2 U_3} \left[-\cos\alpha' \cos\theta \sin(\phi-\alpha-\gamma) \left\{\frac{1-e^{-jk\ell_1 U_1}}{U_1} \frac{e^{-jkR_d}}{R_d} - R_v \alpha_{div} \frac{1-e^{-jk\ell_1 U_1'}}{U_1'} \frac{e^{-jkR_r}}{R_r} \times e^{-j2k\,(H_3-H_1)\cos\theta}\right\}\right. \quad \text{(D-52)}$$

$$\left. + \sin\alpha' \sin\theta \left\{\frac{1-e^{-jk\ell_1 U_1}}{U_1} \frac{e^{-jkR_d}}{R_d} + R_v\, \alpha_{div} \frac{1-e^{-jk\ell_1 U_1'}}{U_1'} \frac{e^{-jkR_r}}{R_r} e^{-j2k\,(H_3-H_1)\cos\theta}\right\}\right]$$

$$E_{\theta 6} = 30\, I_m\, e^{-jk\ell_1 U_1} \left[\cos\alpha' \cos\theta \sin(\phi+\alpha+\beta) \left\{ \frac{1-e^{-jk\ell_2 U_3}}{U_3} \frac{e^{-jkR_d}}{R_d} - R_v\, \alpha_{div} \frac{1-e^{-jk\ell_2 U_3'}}{U_3'} \frac{e^{-jkR_r}}{R_r} e^{-j2k(H_2-H_1)\cos\theta} \right\} \right. \tag{D-53}$$

$$\left. - \sin\alpha' \sin\theta \left\{ \frac{1-e^{-jk\ell_2 U_3}}{U_3} \frac{e^{-jkR_d}}{R_d} + R_v\, \alpha_{div} \frac{1-e^{-jk\ell_2 U_3'}}{U_3'} \frac{e^{-jkR_r}}{R_r} e^{-j2k(H_2-H_1)\cos\theta} \right\} \right]$$

$$E_{\theta 4} = -30\, I_m \left[\cos\alpha' \cos\theta \sin(\phi+\alpha+\gamma) \left\{ \frac{1-e^{-jk\ell_1 U_4}}{U_4} \frac{e^{-jkR_d}}{R_d} - R_v\, \alpha_{div} \frac{1-e^{-jk\ell_1 U_4'}}{U_4'} \frac{e^{-jkR_r}}{R_r} \right\} \right. \tag{D-54}$$

$$\left. + \sin\alpha' \sin\theta \left\{ \frac{1-e^{-jk\ell_1 U_4}}{U_4} \frac{e^{-jkR_d}}{R_d} + R_v\, \alpha_{div} \frac{1-e^{-jk\ell_1 U_4'}}{U_4'} \frac{e^{-jkR_r}}{R_r} \right\} \right]$$

$$E_{\theta 7} = 30\, I_m\, e^{-jk\ell_1 U_4} \left[-\cos\alpha' \cos\theta \sin(\phi-\alpha-\beta) \left\{ \frac{1-e^{-jk\ell_2 U_2}}{U_2} \frac{e^{-jkR_d}}{R_d} - R_v\, \alpha_{div} \frac{1-e^{-jk\ell_2 U_2'}}{U_2'} \frac{e^{-jkR_r}}{R_r} e^{-j2k(H_2-H_1)\cos\theta} \right\} \right. \quad \text{(D-55)}$$

$$\left. + \sin\alpha' \sin\theta \left\{ \frac{1-e^{-jk\ell_2 U_2}}{U_2} \frac{e^{-jkR_d}}{R_d} + R_v\, \alpha_{div} \frac{1-e^{-jk\ell_2 U_2'}}{U_2'} \frac{e^{-jkR_r}}{R_r} e^{-j2k(H_2-H_1)\cos\theta} \right\} \right]$$

$$E_{\theta 5}' = 30\, I_m\, e^{-jk\ell_2 U_2} \cos\alpha' \cos\theta \sin(\phi+\alpha+\gamma) \left\{ \frac{1-e^{-jk\ell_1 U_4}}{U_4} \frac{e^{-jkR_d}}{R_d} - R_v\, \alpha_{div} \frac{1-e^{-jk\ell_1 U_4'}}{U_4'} \frac{e^{-jkR_r}}{R_r} e^{-j2k(H_3-H_1)\cos\theta} \right\} \quad \text{(D-56)}$$

$$\left. - \sin\alpha' \sin\theta \left\{ \frac{1-e^{-jk\ell_1 U_4}}{U_4} \frac{e^{-jkR_d}}{R_d} + R_v\, \alpha_{div} \frac{1-e^{-jk\ell_1 U_4}}{U_4'} \frac{e^{-jkR_r}}{R_r} e^{-j2k(H_3-H_1)\cos\theta} \right\} \right]$$

$$E_{\theta 2} = 30\, I_m \left[\cos\alpha' \cos\theta \sin(\phi-\alpha-\beta) \left\{ \frac{1-e^{-jk\ell_2 U_2}}{U_2} \frac{e^{-jkR_d}}{R_d} - R_v\, \alpha_{div} \frac{1-e^{-jk\ell_2 U_2'}}{U_2'} \frac{e^{-jkR_r}}{R_r} \right\} - \sin\alpha' \sin\theta \left\{ \frac{1-e^{-jk\ell_2 U_2}}{U_2} \frac{e^{-jkR_d}}{R_d} + R_v\, \alpha_{div} \frac{1-e^{-jk\ell_2 U_2'}}{U_2'} \frac{e^{-jkR_r}}{R_r} \right\} \right] \quad \text{(D-57)}$$

$$E_{\phi 1} = -30\, I_m \cos\alpha' \cos(\phi-\alpha-\gamma) \left[\frac{1-e^{-jk\ell_1 U_1}}{U_1} \frac{e^{-jkR_d}}{R_d} + R_h\, \alpha_{div} \frac{1-e^{-jk\ell_1 U_1'}}{U_1'} \frac{e^{-jkR_r}}{R_r} \right] \quad \text{(D-58)}$$

$$E_{\phi 3} = 30\, I_m \cos\alpha' \cos(\phi+\alpha+\beta) \left[\frac{1-e^{-jk\ell_2 U_3}}{U_3} \frac{e^{-jkR_d}}{R_d} + R_h\, \alpha_{div} \frac{1-e^{-jk\ell_2 U_3'}}{U_3'} \frac{e^{-jkR_r}}{R_r} \right] \quad \text{(D-59)}$$

$$E_{\phi 8} = 30\, I_m e^{-jk\ell_2 U_3} \cos\alpha' \cos(\phi-\alpha-\gamma) \left[\frac{1-e^{-jk\ell_1 U_1}}{U_1} \frac{e^{-jkR_d}}{R_d} + R_h\, \alpha_{div} \frac{1-e^{-jk\ell_1 U_1'}}{U_1'} \frac{e^{-jkR_r}}{R_r} e^{-j2k(H_3-H_1)\cos\theta} \right] \quad \text{(D-60)}$$

$$E_{\phi 6} = -30\, I_m e^{-jk\ell_1 U_1} \cos\alpha' \cos(\phi+\alpha+\beta) \left[\frac{1-e^{-jk\ell_2 U_3}}{U_3} \frac{e^{-jkR_d}}{R_d} + R_h\, \alpha_{div} \frac{1-e^{-jk\ell_2 U_3'}}{U_3'} \frac{e^{-jkR_r}}{R_r} e^{-j2k(H_2-H_1)\cos\theta} \right] \quad \text{(D-61)}$$

$$E_{\phi 2} = -30\, I_m \cos\alpha' \cos(\phi-\alpha-\beta) \left[\frac{1-e^{-jk\ell_2 U_2}}{U_2} \frac{e^{-jkR_d}}{R_d} + R_h\, \alpha_{div} \frac{1-e^{-jk\ell_2 U_2'}}{U_2'} \frac{e^{-jkR_r}}{R_r} \right] \quad \text{(D-62)}$$

$$E_{\phi 4} = 30\, I_m \cos\alpha' \cos(\phi+\alpha+\gamma) \left[\frac{1-e^{-jk\ell_1 U_4}}{U_4} \frac{e^{-jkR_d}}{R_d} + R_h\, \alpha_{div} \frac{1-e^{-jk\ell_1 U_4'}}{U_4'} \frac{e^{-jkR_r}}{R_r} \right] \quad \text{(D-63)}$$

$$E_{\phi 7} = 30\, I_m e^{-jk\ell_1 U_4} \cos\alpha' \cos(\phi-\alpha-\beta) \left[\frac{1-e^{-jk\ell_2 U_2}}{U_2} \frac{e^{-jkR_d}}{R_d} + R_h\, \alpha_{div} \frac{1-e^{-jk\ell_2 U_2'}}{U_2'} \frac{e^{-jkR_r}}{R_r} e^{-j2k(H_2-H_1)\cos\theta} \right] \quad \text{(D-64)}$$

AD-A102 622 IIT RESEARCH INST ANNAPOLIS MD F/G 20/14
APACK, A COMBINED ANTENNA AND PROPAGATION MODEL.(U)
JUL 81 S CHANG, H C MADDOCKS F19628-80-C-0042
UNCLASSIFIED ESD-TR-80-102 NL

4 OF 5
AD A
102622

END
DATE FILMED
9-81
DTIC

$$E_{\phi 5} = -30\, I_m e^{-jk\ell_2 U_2} \cos\alpha' \cos(\phi+\alpha+\beta) \left[\frac{1-e^{-jk\ell_1 U_4}}{U_4} \frac{e^{-jkR_d}}{R_d} + R_h\, \alpha_{div} \frac{1-e^{-jk\ell_1 U_4'}}{U_4'} \frac{e^{-jkR_r}}{R_r} e^{-j2k(H_3-H_1)\cos\theta} \right] \quad \text{(D-65)}$$

$$E_\theta = \sum_{i=1}^{8} E_{\theta i} \quad \text{(D-66)}$$

$$E_\phi = \sum_{i=1}^{8} E_{\phi i} \quad \text{(D-67)}$$

REFERENCES

1. Barghausen, A.F., Finney, J.W., Proctor, L.L., and Schultz, L.D., Predicting Long-Term Operational Parameters of High-Frequency SKYWAVE Telecommunication Systems, ESSA Technical Report ERL 110-ITS-78, Institute for Telecommunication Science, Boulder, CO, May 1969.

2. Burke, G. and Poggio, A., Numerical Electromagnetic Code (NEC) -- Method of Moments, Part I: Program Description - Theory, Part II: Program Description - Code, and Part III: User's Guide, Technical Document 116, Naval Ocean Systems Center, San Diego, CA, 18 July 1977 (revised 2 January 1980).

3. Meidenbauer, R., Chang, S., and Duncan, M., A Status Report on the Integrated Propagation System (IPS), ECAC-TN-78-023, Electromagnetic Compatibility Analysis Center, Annapolis, MD, October 1978.

4. Maiuzzo, M.A. and Frazier, W.E., A Theoretical Ground Wave Propagation Model - Nλ Model, ESD-TR-68-315, Electromagnetic Compatibility Analysis Center, Annapolis, MD, December 1968.

5. Banos, A., Jr., Dipole Radiation in the Presence of a Conducting Half-Space, Pergamon Press, Oxford, England, 1966.

6. Weeks, W.L., Antenna Engineering, McGraw-Hill, New York, NY, 1968.

7. Sommerfeld, A., "Uber die Ausbreitung der Wellen in der drahtlosen Telegraphic," Ann. Physik, Vol. 28, 1909, pp. 665-736.

8. Sommerfeld, A., "Uber die Ausbreitung der Wellen in der drahtlosen Telegraphic," Ann. Physik, Vol. 81, 1926, pp. 1135-1153.

9. Sommerfeld, A., Partial Differential Equations, Academic Press, New York, NY, 1949.

10. Norton, K.A., "The Propagation of Radio Waves Over the Surface of the Earth and in the Atmosphere": Part I, Proc. IRE, Vol. 24, October 1936, pp. 1369-1389; Part II, Proc. IRE, Vol. 25, September 1937, pp. 1203-1236.

11. Kuebler, W. and Snyder, S., The Sommerfeld Integral, Its Computer Evaluation and Application to Near Field Problems, ECAC-TN-75-002, Electromagnetic Compatibility Analysis Center, Annapolis, MD, February 1975.

12. Laitenen, P., Linear Communication Antennas, Technical Report No. 7, U.S. Army Signal Radio Propagation Agency, Fort Monmouth, NJ, 1959.

13. Ma, M.T. and Walters, L.C., Power Gains for Antennas Over Lossy Plane Ground, Technical Report ERL 104-ITS 74, Institute for Telecommunication Sciences, Boulder, CO, 1969.

References (Continued)

14. Ma, M.T., Theory and Application of Antenna Arrays, Wiley Interscience, New York, NY, 1974.

15. Pocklington, H.E., "Electrical Oscillations in Wires," Comb. Phil. Soc. Proc., 25 October 1897, pp. 324-332.

16. Schelkunoff, S.A. and Friis, H.T., Antennas, Theory and Practices, John Wiley and Sons, New York, NY, 1952.

17. Bremmer, H., Terrestrial Radio Waves, Elsevier Publishing Co., New York, NY, 1949.

18. Norton, K.A., "The Calculation of Ground Wave Field Intensity Over a Finitely Conducting Spherical Earth," Proc. IRE, Vol. 29, No. 12, December 1941, pp. 623-639.

19. Foster, D., "Radiation from Rhombic Antenna," Proc. IRE, Vol. 25 No. 10, October 1937, pp. 1327-1353.

20. Schelkunoff, S.A., "A General Radiation Formula," Proc. IRE, Vol. 27, No. 10, October 1939, pp. 660-666.

21. Van der Pol, B. and Bremmer, H., "The Diffraction of Electromagnetic Waves from an Electrical Point Source Round a Finitely Conducting Sphere," Phil. Mag.: Ser. 7, 24, 1937, pp. 141-176 and 825-864; 25, 1938, pp. 817-834; and 26, 1939, pp. 261-275.

22. Fock, V.A., Electromagnetic Diffraction and Propagation Problems, Pergamon Press, New York, NY, 1965.

23. Johler, J.R., Kellar, W.J., and Walters, L.C., Phase of the Low Radio-Frequency Ground Wave, National Bureau of Standards Circular 573, National Bureau of Standards, Boulder, CO, 26 June 1956.

24. Kuebler, W., Ground Wave Electric Field Intensity Formulas for Linear Antennas, ECAC-TN-74-11, Electromagnetic Compatibility Analysis Center, Annapolis, MD, June 1974.

25. Rice, P.L., Longley, A.G., Norton, K.A., and Barsis, A.P., Transmission Loss Predictions for Tropospheric Communication Circuits, NBS Technical Note 101, Vols. I and II, National Bureau of Standards, Boulder, CO, 1967.

26. International Radio Consultative Committee (CCIR), Recommendations and Reports of the CCIR, 1978, Propagation in Non-Ionized Media, Vol. V, XIVth Plenary Assembly, Kyoto, Japan, 1978.

References (Continued)

27. King, R.W.P., The Theory of Linear Antennas, Harvard University Press, Cambridge, MA, 1956.

28. Sommerfeld, A. and Renner, F., "Strahlungsenergie und Erdabsorption bei Dipolantennen," Ann. Physik, Vol. 41, pp. 1-36, 1942.

29. Kuebler, W. and Karwath, A., Program RENNER: Normalized Radiation Resistance of a Hertzian Dipole over Arbitrary Ground, ECAC-TN-75-024, Electromagnetic Compatibility Analysis Center, Annapolis, MD, January 1976.

30. Wait, J.R. and Pope, W.A., "The Characteristics of a Vertical Antenna With a Radial Conductor Ground System," Appl. Sci. Res., Section B.4, 1954, pp. 177-185.

31. Wait, J.R. and Surtees, W.J., "Impedance of a Top-loaded Antenna of Arbitrary Length Over a Circular Grounded Screen," J. Appl. Physics, Vol. 25, 1954, pp. 553-555.

32. Wait, J.R., "Effect of the Ground Screen on the Field Radiated from a Monopole," IRE Trans. Antennas and Propagation, Vol. AP-4, No. 2, 1956, pp. 179-181.

33. Maley, S.W. and King, R.J., "The Impedance of a Monopole Antenna With a Circular Conducting-Disk Ground System on the Surface of a Lossy Half-space," J. Research NBS, 65D (Radio Propagation) No. 2, 1961, pp. 183-188.

34. Jordon, E.C. and Balmain, K.G., Electromagnetic Waves and Radiating Systems, Prentice Hall, Englewood Cliffs, NJ, 1968.

35. Ramo, S., Whinnery, J.R., and Van Duzer, T., Fields and Waves in Communication Electronics, John Wiley and Sons, New York, NY, 1965.

36. Baker, H.C. and LaGrone, A.H., "Digital Computation of the Mutual Impedance Between Thin Dipoles," IRE Trans. Antennas and Propagation, Vol. AP-10, No. 2, pp. 172-178, March 1962.

37. Bruce, E., "Developments in Short-Wave Directional Antennas," Proc. IRE, Vol. 19, No. 8, pp. 1406-1433, August 1931.

38. Bruce, E., Beck, A.C. and Lowry, L.R., "Horizontal Rhombic Antennas," Proc. IRE, Vol. 23, No. 1, pp. 24-46, January 1935.

39. King, R.W.P. and Wu, T.T., "Currents, Charges, and Near Fields of Cylindrical Antennas", Radio Science, Vol. 69D, No. 3, pp. 429-446, March 1965.

References (Continued)

40. Ma, M.T. and Walters, L.C., Computed Radiation Patterns of Log-Periodic Antennas Over Lossy Plane Ground, ESSA Technical Report IER 54-ITSA 52, Boulder, CO, 1967.

41. King, H.E., "Mutual Impedance of Unequal Length Antennas in Echelon," IRE Trans. Antennas and Propagation, Vol. AP-5, No. 3, pp. 306-313, 1957.

DISTRIBUTION LIST FOR
APACK, A COMBINED ANTENNA
AND PROPAGATION MODEL
ESD-TR-80-102

External	Copies
Air Force	
HQ USAF/FMO Washington, DC 20330	1
HQ RADC/RBC Griffiss AFB, NY 13441	1
HQ AFCC/XOPR Scott AFB, IL 62225	1
HQ PACAF/DCOF Hickam AFB, HI 96258	1
HQ USAFE/DCONJ APO New York 09012	1
HQ AFEWC/ESTS/SAT San Antonio, TX 78243	1
HQ EIC/EIEUS Oklahoma City AFS, OK 73145	1
HQ TAWC/OA Eglin AFB, FL 32542	1
HQ ESC/SD San Antonio, TX 78243	1
HQ ESD/DCJP Hanscom AFB, MA 01731	4
RADC/DCCT Griffiss AFB, NY 13441	1
USAFT AWC/EWC Attn: J. H. Smith, Jr. Eglin AFB, IL 32541	1

DISTRIBUTION LIST FOR
ESD-TR-80-102 (continued)

Army

USATECOM 1
Attn: DRSTE-AD-A (D. Pritchard)
Aberdeen Proving Ground, MD 21005

CDR, USATECOM 1
Attn: DRSTE-EL (L. Doughty)
Aberdeen Proving Ground, MD 21005

USAAMSAA 1
Attn: (H. Dubin)
Aberdeen Proving Ground, MD 21005

CDR USARRADCOM 1
Attn: DRCPM-ADG-E (Christenson)
Picatinny Arsenel
Dover, NJ 07801

Commander 1
US Army Signal Center & Fort Gordon
Attn: ATZHCD-SD (H. Siemen)
Fort Gordon, GA 30905

CDR, USAEPG 1
Attn: STEEP-MT-M
Fort Huachuca, AZ 85613

CDR, USACEEIA 1
Attn: CCC-EMEO (Mr. H. Merkel)
Fort Huachuca, AZ 85613

CDR, USACORADCOM 1
Attn: DRCPM-TDS-PL (H. Bahr, J. Lioy)
Fort Monmouth, NJ 07703

Director 1
US Army Combat Surveillance
and Target ACQ Lab
Attn: DELECS-R (Longinotti)
Fort Monmouth, NJ 07703

CDR, USAERADCOM 1
Attn: DRDCO-COM-RF-2 (P. Sass)
Fort Monmouth, NJ 07703

DISTRIBUTION LIST FOR
ESD-TR-80-102 (Continued)

Army (Continued)

CDR, USACORADCOM 1
Attn: DRDCO-COM-RY-3 (P. Major)
Fort Monmouth, NJ 07703

CDR, USACORADCOM 1
Attn: DRDCO-COM-RY-5 (W. Kessleman)
Fort Monmouth, NJ 07703

CDR, UACORADCOM 1
Attn: DRDCO-SEI-A (S. Segner)
Fort Monmouth, NJ 07703

Director Signal Warfare Lab 1
Attn: DELSW-PS (Dr. F. Williams)
Vint Hill Farms Station
Warrenton, VA 22186

ASD/XRE 1
Mr. E. G. Barthel
Wright-Patterson AFB, OH 45433

DoD Army Frequency Coordinator 1
Attn: Mr. G. Hungate
WSMR, NM 88002

Navy

Chief of Naval Operations (OP-941F) 1
Navy Department
Washington, DC 20350

Special Projects

Director 1
Defense Communications Agency
Attn: Code 225
Washington, DC 20305

Director 2
National Security Agency
Attn: W36/Mr. V. McConnell
Ft. George G. Meade, MD 20755

DISTRIBUTION LIST FOR
ESD-TR-80-102 (Continued)

Special Projects (Continued)

Department of Transportation 1
Federal Aviation Administration
Attn: ARD-450
NASSIF Bldg, Room 7223
400 7th St. SW
Washington, DC 20590

National Aeronautics & 1
Space Administration
Goodard Space Flight Center
Attn: Code 801/Jim Scott
Greenbelt, MD 20771

Commander in Chief 1
U.S. Readiness Command
Attn: RCJ6-T
MacDill AFB, FL 33608

National Telecommunications & 1
Information Admin.
Attn: Stan Cohn
1325 G. St., NW
Washington, DC 20005

DCEC 1
Attn: (R 410)
1860 Wiehle Avenue
Reston, VA 22090

Rapid Deployment Agency 1
Attn: RDJ6-E (Maj. Champagne)
MacDill AFB, FL 33608

Dr. Sooyoung Chang 2
Mitre Corp.
W763
1820 Dolly Madison Boulevard
McLean, VA 22102

Dr. Hugh C. Maddocks 2
Mitre Corp.
W769
1820 Dolly Madison Boulevard
McLean, VA 22102

DISTRIBUTION LIST FOR
ESD-TR-80-102 (Continued)

Defense Technical Information Center Cameron Station Alexandria, VA 22314	12
AFGL (SULR) Hanscom AFB, MA 01731	2
Air University Library Maxwell AFB, AL 36112	1

Internal

CA	2
CF	1
CJ	1
CN	1
XM/J. Janoski	2
SM-1	1
SMDL	10
SMA/D. Baran	1
SMA/D. Madison	1
SMAD/R. Albus	1
SMAD/B. Campbell	1
SMAD/R. Meidenbauer	1
SMAD/K. O'Haver	1
SMAD/H. Riggins	35
SMAD/W. Stuart	1
SMAM/M. Weissberger	1

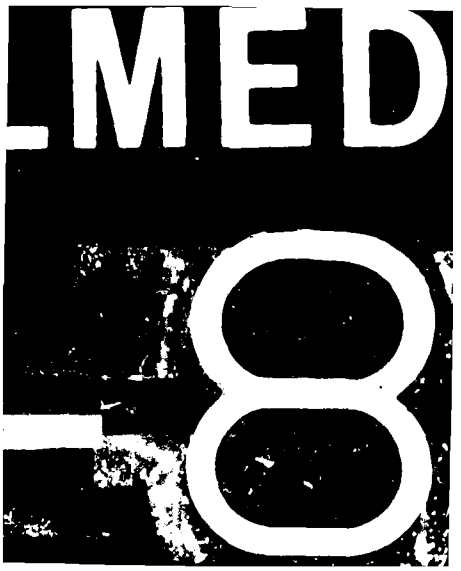
LMED
8

AD-A102 622 IIT RESEARCH INST ANNAPOLIS MD F/G 20/14
APACK, A COMBINED ANTENNA AND PROPAGATION MODEL.(U)
JUL 81 S CHANG, H C MADDOCKS F1962A-80-C-0042
UNCLASSIFIED ESD-TR-80-102 NL

END
DATE FILMED
12-81
DTIC

SUPPLEMENTARY

INFORMATION

AD-A102 682

DEPARTMENT OF THE ARMY
U. S. ARMY COMMUNICATIONS COMMAND
FORT HUACHUCA, ARIZONA 85613

CCC-EMEO-PED

SUBJECT: Calculation of Antenna Power Gain

Director
Electromagnetic Compatibility
Analysis Center, North Severn
ATTN: XM
Annapolis, Maryland 21402

1. Reference is made to IIT Research Institute Report Number ESD-TR-80-102, July 1981, subject: APACK, A Combined Antenna and Propagation Model.

2. Section seven of the referenced report makes comparisons between the antenna gains predicted by the accessible antenna package (APACK) manufacturer's data, ERL 110-ITS-78 (SKYWAVE), M.T. MA, and the Numerical Electromagnetic Code (NEC). Several disagreements and unsolved problems were encountered in this section and our comments are attached as an inclosure.

3. If additional work is performed of this type, it is recommended that the accuracy of the calculated power gains be determined for each antenna as well as the differences between computer programs. Since antenna design is a responsibility of this Agency, any information concerning accuracy of computer programs would be appreciated.

FOR THE COMMANDER:

Miles A. Merkel

1 Incl
as

MILES A. MERKEL
Chief, Electromagnetics Engineering Office

RECOMMENDED CHANGES TO PUBLICATIONS AND BLANK FORMS

For use of this form, see AR 310-1; the proponent agency is the US Army Adjutant General Center.

Use Part II (reverse) for Repair Parts and Special Tool Lists (RPSTL) and Supply Catalogs/Supply Manuals (SC SM).

DATE

TO: (Forward to proponent of publication or form) (Include ZIP Code)
Director, ECAC, North Severn
ATTN: XM
Annapolis, Maryland 21402

FROM: (Activity and location) (Include ZIP Code)
Commander
USACEEIA
ATTN: CCC-EMEO-PED
Fort Huachuca, Arizona 85613

PART I - ALL PUBLICATIONS (EXCEPT RPSTL AND SC SM) AND BLANK FORMS

PUBLICATION FORM NUMBER	DATE	TITLE
IIT Research Institute Report Number ESD-TR-80-102	July 1981	APACK, A Combined Antenna and Propagation Model

ITEM NO.	PAGE NO.	PARAGRAPH	LINE NO.*	FIGURE NO.	TABLE NO.	RECOMMENDED CHANGES AND REASON (Exact wording of recommended change must be given)
1	83	2	5			STATEMENT: "In most cases, there is reasonable agreement between APACK predictions and the NEC predictions." COMMENT: In many cases there is no reasonable agreement between any two antenna gain predictions (see 2, 3, 4, 6, and 8).
2	84	3	8			STATEMENT: "The reason for the higher gains perdicted by NEC has not been determined." COMMENT: The reason for the differences in antenna gain should be determined and the most correct method available should be specified by this report.
3	84	4	3			STATEMENT: "The difference between the APACK predictions and the NEC predictions. . . approach 7 dB near the zenith." COMMENT: Same comment as Item No. 2.
4	92	3	2			STATEMENT: "Since comparisons of APACK predictions with other data for both horizontal and vertical orientations indicated reasonable agreement, comparisons. . ." COMMENT: This statement conflicts with Statement at Item 3.
5	92	2	5			STATEMENT: "The reason for the high value of gain predicted by NEC at 30 MHz, as compared with the APACK and SKYWAVE values, has not been explained." COMMENT: Same as Item No. 2.
6	92	4	1			STATEMENT: ". . . both APACK and SKYWAVE predict lower gains than NEC." COMMENT: Same as Item No. 2

*Reference to line numbers within the paragraph or subparagraph.

TYPED NAME, GRADE OR TITLE	TELEPHONE EXCHANGE AUTOVON, PLUS EXTENSION	SIGNATURE
EDWIN F. BRAMEL Electronics Engineer	(602) 538-6779 AV 879-6779	Edwin F Bramel

DA FORM 1 FEB 74 2028

REPLACES DA FORM 2028 1 DEC 68 WHICH WILL BE USED.

RECOMMENDED CHANGES TO PUBLICATIONS AND BLANK FORMS

For use of this form, see AR 310-1; the proponent agency is the US Army Adjutant General Center.

Use Part II (reverse) for Repair Parts and Special Tool Lists (RPSTL) and Supply Catalogs Supply Manuals (SC SM).

DATE

TO: (Forward to proponent of publication or form) (Include ZIP Code)

FROM: (Activity and location) (Include ZIP Code)

PART I - ALL PUBLICATIONS (EXCEPT RPSTL AND SC SM) AND BLANK FORMS

PUBLICATION FORM NUMBER	DATE	TITLE
IIT Research Institute Report Number ESD-TR-80-102	July 1981	APACK, A Combined Antenna and Propagation Model

ITEM NO.	PAGE NO.	PARA-GRAPH	LINE NO.*	FIGURE NO.	TABLE NO.	RECOMMENDED CHANGES AND REASON (Exact wording of recommended change must be given)
7	103	5	1			STATEMENT: "Figures 41, 42, and 43 show comparisons between APACK, NEC, and manufacturer's data for the. . ." COMMENT: See Item 8.
8	110, 111, & 112			41, 42, & 43		COMMENT: These figures refer to skywave, not NEC like Item 7. No values were given for the antenna parameters used. The reason for the differences in antenna gain should be determined and the most correct method available should be specified by this report.
9.						COMMENT: The latest available antenna gain programs from NTIA-ITS were not considered, i.e., IONCAP, SETCOM.

*Reference to line numbers within the paragraph or subparagraph.

TYPED NAME, GRADE OR TITLE	TELEPHONE EXCHANGE AUTOVON, PLUS EXTENSION	SIGNATURE
EDWIN F. BRAMEL Electronics Engineer	(602) 538-6779 AV 879-6779	Edwin F Bramel

DA FORM 1 FEB 74 2028

REPLACES DA FORM 2028, 1 DEC 68, WHICH WILL BE USED.